

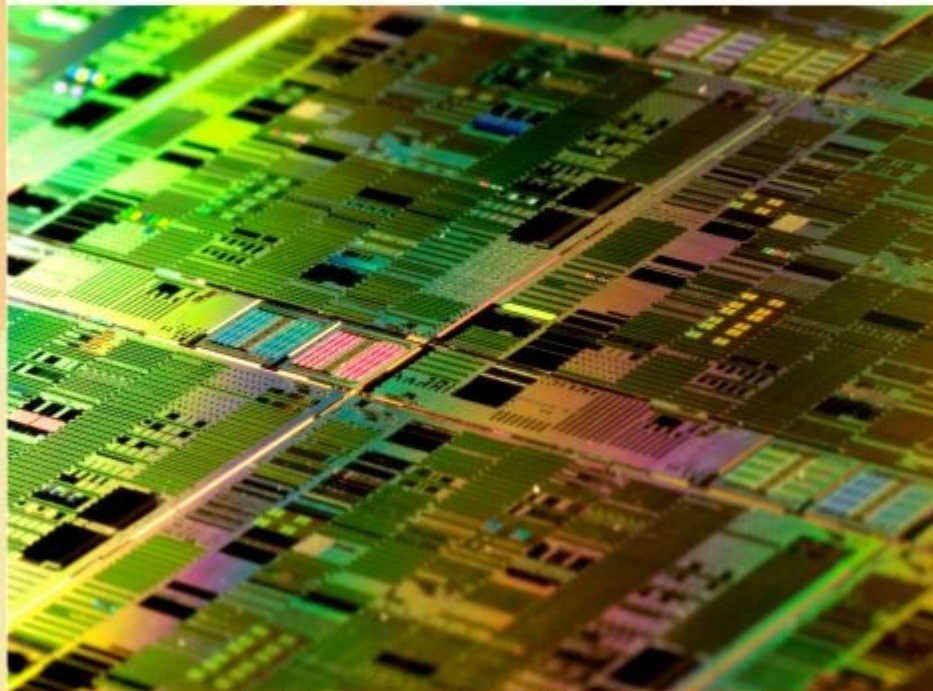


INSTITUTO POLITÉCNICO NACIONAL
"LA TÉCNICA AL SERVICIO DE LA PATRIA"



6° CONGRESO INTERNACIONAL TENDENCIAS TECNOLÓGICAS EN COMPUTACIÓN 2010

18 AL 22 DE OCTUBRE



CENTRO DE INNOVACIÓN Y DESARROLLO TECNOLÓGICO EN CÓMPUTO

"Unidad Profesional Adolfo López Mateos", Av. Juan de Dios Bátiz s/n, casi esq. Miguel Othón de Mendizábal, Edificio CIDETEC.
Colonia Nueva Industrial Vallejo,
Delegación Gustavo A. Madero, C.P 07700, México D.F.
Tel. 5729-6000 ext.52538 email: cidetec@ipn.mx

www.cidetec.ipn.mx

www.ipn.mx

www.sep.gob.mx



MÉXICO 2010

GOBIERNO
FEDERAL

SEP



MEMORIAS

Index / índice

<i>Performance of the Graphic Processing Unit for general purpose.</i>	6
<i>Aproximación numérica de funciones oscilantes usando redes neuronales artificiales supervisadas.....</i>	16
<i>Computer Worms and Their Typing</i>	17
<i>P2P Networking Strategies to Support Massive Online Multiuser Virtual Environments.....</i>	22
<i>DVRMedia2 Virtual Reality Advanced Editor For Crowded Worlds Simulations.....</i>	29
<i>Evaluation of the behavior of carbon steel pipes used for drinking water supply using digital image processing.....</i>	37
<i>Soft real time Simulation of a DC motor considering Power Losses</i>	42
<i>Optimization of machining strategy for merging CAD-CAM-CNC-oriented manufacturing of complex parts.....</i>	51
<i>Researching and design of solar module maximum power capturing technique using microcontroller.....</i>	57
<i>Signals acquisition and processing for corrosion control in carbon steel pipelines used for potable water supply.....</i>	61
<i>IMPLEMENTATION OF A QPSK MODULATOR TO DVB-S TRANSMITTER through FPGA</i>	65
<i>An Arrival Times Model for Real Time Tasks Using a Cellular Automaton.....</i>	72
<i>Estimating the Fundamental Tone of continuous voice in real-time</i>	78
<i>Implementing free software on computer equipment frequently an option for reducing electricity consumption.....</i>	83
<i>Three Dimensional hair model by means particles using Blender</i>	88
<i>Digit recognition using Static Hidden Markov Models and Vector Quantization for Nahuatl language.....</i>	95
<i>Speech recognition based in Vector Quantization in a virtual environment.....</i>	102
<i>Spatially Photoluminescence of InAs/InGaAs quantum dots.....</i>	108
<i>Automatización y supervisión de un proceso neumático usando herramientas alternativas aplicadas al aprendizaje y la enseñanza</i>	111
<i>Diseño de una Antena Concentradora de Señal para Laptop.....</i>	119
<i>Classification of diabetic retinopathy using digital image treatment, HU moments and associative memories.....</i>	126

<i>Implementación de la Huella digital para el encendido de automóvil.....</i>	<i>131</i>
<i>ITS</i>	
<i>Intelligent Transport Systems</i>	
<i>Sistemas Inteligentes de Transporte.....</i>	<i>137</i>
<i>CINEMATICA Y DINÁMICA DE LA MARCHA HUMANA.....</i>	<i>143</i>

HISTORIA DEL CIDETEC

Los orígenes del CIDETEC se remontan al período de 1981 a 1996, cuando se pone en marcha el proyecto de autoequipamiento en Materia de Cómputo, como resultado de la inquietud de un investigador de la sección de graduados de UPIICSA, el entonces Maestro en Ciencias, Miguel Lindig Bos.

En 1987, se crea el Centro de Investigación Tecnológica en Computación (CINTEC), con la finalidad de desarrollar el proyecto de autoequipamiento ya mencionado. Un año después, para cumplir con los objetivos de educación e investigación en Ingeniería de Cómputo, el Consejo General Consultivo del IPN aprueba el programa de Maestría en Ingeniería de Cómputo, que se mantiene adscrito al CINTEC hasta 1996.

En ese año, como parte de los esfuerzos del Instituto por fortalecer sus cuadros tecnológicos, se forma el Centro de Investigación en Computación (CIC), con grupos académicos provenientes del CINTEC y CENAC.

Al año siguiente, 1997, el CINTEC evoluciona, dando paso al CIDETEC, teniendo como objetivos primordiales: consolidar la infraestructura de cómputo institucional y aprovechar las ventajas tecnológicas para incidir en los procesos productivos, sin dejar de lado la educación profesionalizante en sus diferentes modalidades. Como consecuencia de esto, en 2004 se le autoriza un nuevo programa de Maestría en Tecnología de Cómputo.



Edificio CIDETEC

Es importante hacer notar que desde sus primeras etapas, hasta el año 2006, el CIDETEC carece de instalaciones propias, utilizando para sus funciones un espacio facilitado por la UPIICSA, en su Sección de Estudios de Posgrado; por ello, el CIDETEC agradece a la Unidad Profesional Interdisciplinaria de Ingeniería y Ciencias Sociales y Administrativas, el apoyo brindado a lo largo de esos años.

Coincidiendo con su decimo aniversario, en enero de 2007 el CIDETEC recibe sus instalaciones, un nuevo edificio de diseño funcional, adecuado a sus necesidades y actividades, ubicado en el corredor de cómputo de la Unidad Profesional Adolfo López Mateos en Zacatenco.



Inauguración de las Instalaciones. Abril de 2008

OBJETIVO

El Centro de Innovación y Desarrollo Tecnológico en Cómputo, tiene como objetivo formar maestros en Tecnología de Cómputo con amplios conocimientos teóricos y prácticos de la computación para desempeñar tareas de investigación y transferencia de tecnología, construyendo soluciones de calidad sustentables y pertinentes para los sectores sociales y productivos en los ámbitos regional, nacional e internacional.

Realizar investigaciones y desarrollos tecnológicos en el área de tecnología de cómputo, pertinentes a las necesidades del país y acorde con los planes institucionales, nacionales y estatales de desarrollo.

Misión

El Centro de Innovación y Desarrollo Tecnológico en Cómputo es una unidad académica de nivel posgrado, dependiente del IPN, dedicada a formar y capacitar profesionales de excelencia en el área de la Ingeniería de Cómputo en particular y la Computación en lo general, con un alto grado de competitividad científico-tecnológica, a fin de responder a las necesidades existentes en los sectores social y productivo del país, a través de las actividades académicas del Centro y su interacción con proyectos de investigación y desarrollo tecnológico.

Visión

Ser un Centro innovador, que forma profesionales e investigadores de alto nivel, y cuyas funciones de docencia, investigación y desarrollo tecnológico impacten primordialmente en nuestro país, con presencia y alcance internacional.

Contar con un capital humano de excelencia, actualizado y dinámico, vinculado con los sectores académico, social y productivo.

Que los procesos formativos, de investigación y de desarrollo tecnológico sean pertinentes y cumplan con normas internacionales de calidad; que sus programas cuenten con acreditación y sus egresados sean reconocidos ampliamente por su preparación y competitividad.

En el CIDETEC, la academia y la investigación estarán estrechamente vinculados, de tal forma que los avances científicos y tecnológicos sean difundidos y aprovechados oportunamente por la sociedad.

Performance of the Graphic Processing Unit for general purpose.

1 J. Antonio Álvarez, 1Gustavo Martínez Romero, 2 Elizabeth Acosta Gonzalez.

1 IPN México ,Centro de Investigación e Innovación Tecnológica, Cerrada de Cecati S/N. Col. Santa Catarina Azcapotzalco México D. F. CP:02250
jaalvarez@ipn.mx, egustavo2000@yahoo.com.mx.

2 IPN México-UPIICSA,Sección de Estudios de posgradoAv. Té 950. Colonia Granjas México, México D. F.
egonzagar@ipn.mx

ABSTRACT

A computer graphics card is an additional peripheral that enhances the performance of rendered graphics. Recently, there has been an increasing interest in general purpose computation on graphics hardware. The ability to work independently alongside the CPU as a coprocessor is interesting but not motivating enough to learn how to apply problems to the graphics domain. This paper analyzes the overall architecture of the GPU and its performance.

Keywords: GPU architecture, Computer graphics card, GPU performance, CPU alternative.

1. INTRODUCTION

Commodity graphics hardware has evolved tremendously over the last years – it started with basic polygon rendering via 3dfx's Voodoo Graphics in 1996, and continued with custom vertex manipulation four years later, the graphics processing unit (GPU) now has improved to a full-grown graphics-driven processing architecture with a speed-performance approx. 750 times higher than a decade before (1996: 50 b/s, 2006: 36,8 b/s).

This makes the GPU evolving much faster than the CPU, which became approx. 50 times faster in the same period (1996: 66 SPECfp2000, 2006: 3010 SPECfp2000) [1]. Figure 1.1 shows the GPU performance over the last ten years and how the gap to the CPU increases.

Experts believe that this evolution will continue for at least the next five years [2,3].

New graphics hardware architectures are being developed with technologies that allow more generic computation. GPGPU (general-purpose computation on GPUs) became very important and started a new area related to computer graphics research. This leads to a new paradigm, where the CPU (central processing unit) does not need to compute every

However, not every kind of algorithm can be allocated for the GPU (graphics processing unit) but

only those that can be reduced to a stream based process. Besides, even if a problem is adequate for GPU processing, there can be cases where using the GPU to solve such problems is not worthy, because the latency generated by memory manipulation on the GPU can be too high, severely degrading application performance.

non-graphics application issue.[5,6,7].

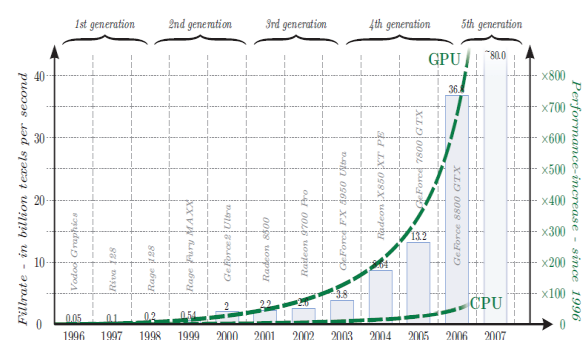


Fig. 1.1. The performance-increase of computer graphics hardware over the last decade . The green trend line shows that the GPU doubles its speed-performance every 13 months (i.e. GPU of 2006 are approx. 750 times faster than GPUs of 1996). In contrast, the performance of the CPU doubles only every 22 months [1].

Many mathematics and physics simulation problems can be formulated as stream based

processes, making it possible to distribute them naturally between the CPU and the GPU. This may be extremely useful when real time processing is required or when performance is critical. However, this approach is not always the most appropriate for a process that can be potentially solved using graphics hardware. There are many factors that must be considered before deciding if the process must allocate the CPU or the GPU.

Some of these factors may be fixed and some may depend on the process status.

A correct process distribution management is important for two reasons:

- It is desired that both the GPU and the CPU have similar process load, avoiding the cases where one is overloaded and the other is fully idle;
- It is convenient to distribute processes considering which architecture will be more efficient for that kind of problem.

2. THE COMPUTER GRAPHICS CARD

A computer graphics card is an additional peripheral that enhances the performance of rendered graphics. The card mainly consists of a graphical processing unit (GPU), memory, and a digital/analog converter and connections to and from the graphics card. Most applications on a computer requires some type of graphics to be displayed. The information is processed from the application to the central processing unit(CPU) which is then sent to the specialized graphics accelerator for quicker processing. After undergoing the transformation of computer code, the data is then sent to a monitor to be displayed. Figure 2.1 shows the general flow diagram of Graphics Card.

Originally, computers were once all text based and did not come with a Graphical User Interface (GUI) that consumers have grown accustomed to. As computer technology has advanced, graphics has become an important part in the way humans interact with computers and the demand for graphic oriented

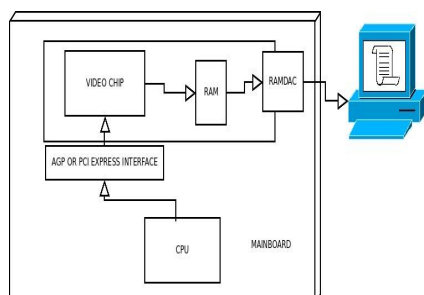


Fig. 2.1. General Flow Diagram of Graphics Card.

Most computer chips are produced as silicon chips. A silicon chip is composed of thousands of transistors, which are in turn composed of three layers of conducting material, mainly silicon, forming a “sandwich” design. The layer might contain either a positive or negative type of silicon. With a difference in electrical charge, and allowance to accept and receive electrons, transistors are used as switches. Current cannot pass through a transistor because of the diode effect. Diodes are devices that block current going in one direction while allowing the opposite direction of the current to flow. This is very important as it can keep sensitive electronics safe from a reverse charge.

computing has called for the need of specialized graphical processing. This is when the age of graphical accelerated cards began.

3. GPU DESING

The GPU , The processor accelerates graphical processing while taking the CPU’s workload, which is used to process every instruction code for the computer. Since graphical processing units are devoted to processing graphics, the processing of advanced graphical algorithms and coding are accelerated compared to the regular CPU, that is illustrated in the figure 3.1.

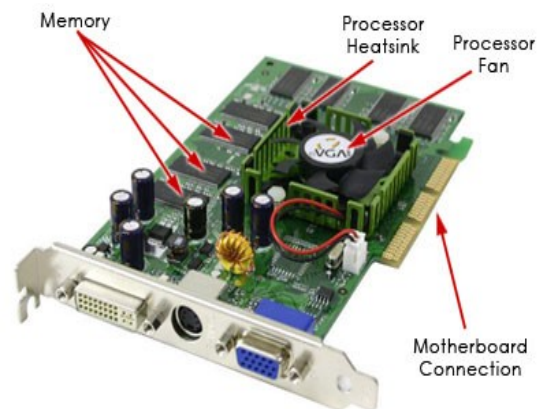


Fig. 3.1. Basic Layout of Graphics Card

Originally, computers were once all text based and did not come with a Graphical User Interface

2.1 Pipelined Architecture

A pipelined architecture is the standard procedure for processors as it breaks down a large task into smaller individual grouped tasks.[4] When a set of instructions are transferred to the GPU the GPU then breaks up the instructions and sends the broken up instructions to other areas of the graphics card specifically designed for decoding and completing a set of instructions. These pathways are called stages.

The more stages the graphics card has, the faster it can process information as the information can be broken down into smaller pieces while many stages work on a difficult instruction, that is illustrated in the figure 3.1.1.

Pipeline Process : Stage 1

The pipeline process starts with an "Application/Scene" stage, also known as the workload-reduction trick. This stage is devoted to deciding which particular object will be rendered in the three dimensional(3D) environment. The way that 3D environments are created is through a Cartesian Coordinate Systems (an x, y, and z axis) in which objects are placed to create a scene. Scenes can have multiple angles to view them, in which they are created by reference points (cameras). The view space is determined by objects and angles depending on how the creator programmed the scene. The first process of the graphics pipeline is to only render and produce the images of the view space and to skip over unnecessary instructions that will not be displayed even if it was processed. This system allows the graphics card to produce scenes and graphics efficiently.

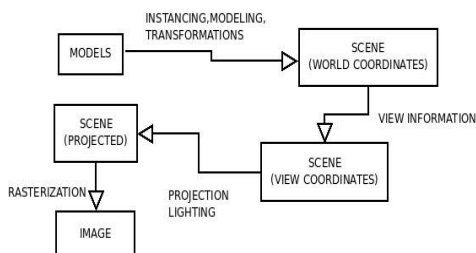


Fig. 3.1.1 The Graphic Pipeline

There are also factors that involve in processing the image efficiently, mainly the Level of Detail (LOD). An objects distance to the reference point of the view camera has an effect on the object's LOD. Some objects are assigned multiple resolution settings (the quality of image that is determined by the number of triangles that composes the object) in which the closer object might receive a higher resolution, while the same object farther away might be at a lower resolution to reduce the workload of the graphics card.

Pipeline Process : Stage 2

The second stage involves the scene's geometry. Objects mainly get moved from frame to frame to give an illusion that the object is moving in a real time setting. Objects can both be moved and manipulated in a scene depending on the application in which it is running. This manipulation of objects is generally called transformation. The objects can be stretched, skewed, moved or moved about an axis, or scaled differently. It is in the second stage of

processing that the objects in the environment are altered.

Geometric lightning also occurs in the second stage after the objects are in their proper place, and once the figures receive their shape through the geometric transform process. Different types of lightning, depending on the application being run, will be processed to give the graphics a realistic appearance.

After the lightning is calculated the scene needs to get rid of unnecessary triangles that are only partially shown through the view space. This process is similar to the process which occurs in the first stage and also includes the process of "clipping." "Clipping is the operation to discard only the parts of triangles that in some way partially or fully fall outside the view volume".

Pipeline Process : Stage 3

The third stage implies an algorithm called the digital differential analyzer (DDA) which calculates the position of each part of all the triangles, and determines if the triangles are connected to other triangles. This process is done by computing the slope of each triangle's edge in hope to improve the quality of the image being produced and by allowing more detailed information to be assigned to the triangles. Sometimes when two triangles are touching, or even overlapping each other, a rough pixel "stair-step" occurs in which the edges between the two triangles create non realistic images of edges extruded surfaces that would not normally occur.

Another thing that occurs in the triangle setup phase is the assignment of color and depth values for each pixel. Since the edges of the triangles were calculated, the color and depth values may be interpolated using each triangle's vertex vales of color and depth. Along with the color and depth, the texture coordinates of each pixel is also interpolated in which they will be processed in the fourth stage.

Pipeline Process : Stage 4

The last stage of the pipeline is considered the rendering / rasterization stage. "To fill the frame buffer the drawing primitives are subdivided into pixels, a process known as scan-conversion or rasterization" (Schneider, Benyt-Olaf, pg 245). After all the processes of computing location, color, geometric values, etc., this last stage puts it all together and produces the 3D environment onto a 2D screen.

After the triangle setup is completed in the third stage, the next step is to provide shading values. Shading values are similar to the color and depth values contained in stage 3 and add the finishing touches on the scene. There are three common shading methods: Flat, Gouraud, and Phong shading.

Flat Shading - operates per triangle and provides a quick render of the scene that does not involve extensive computations. This type of shading does not produce a high quality image.

Gouraud Shading - operates per vertex of the triangles. Compared to flat shading, Gouraud shading produces a higher quality image while sacrificing render speed. Because of Gouraud shading takes the lighting values of each vertex of the triangle and interpolates the values across the surface of the triangle, the object will appear smoother and not as rigid as flat shading.

Phong Shading - operates per pixel and is the most computation demanding shading process compared to flat and Gouraud shading. Phong shading incorporates the Gouraud Shading idea of taking the average shading of the vertices and also implies its own process that includes other triangle's shading as well. This makes the object blend together easier for more complex designs and results in a higher quality image making it more realistic.

3.2 Memory

Random Access Memory (RAM) assists the graphics card process information. RAM is composed of transistors and memory cells that are arranged in a row and column grid that allows data to be stored and accessed quickly. New technology yielded the Double Data-Rate Synchronous Dynamic Random Access Memory (DDR SDRAM, commonly referred to as DDR), and the DDR2 RAM modules. These types of RAM modules are economically beneficial as they have higher efficiency, cost less, and have a higher potential for improvement.

The memory cells of the RAM can read either the number 1 or 0, which changes due to the capacitor change in gain or loss of electrons. Dynamic memory has a slight flaw, the capacitors have a natural electron leak and are drained of electrons every few milliseconds. To solve this problem, the CPU or the memory controller has to recharge all of the capacitors holding a 1 before they discharge. That

is why RAM refreshes thousands of times per second. Memory cells have their own special support infrastructure of circuits that enables it to identify each row and column in the memory cell, keeping track of the refresh sequence, reading and restoring signals from a cell, and telling a cell if it should take a charge or not. Figure 3.2.1 shows the The General flow chart of Gouraud/Phong shading .

The memory of the graphics card (VRAM) is controlled by the GPU that stores data in specialized video memory storage space. This storage space operates by the use of common storage space but is especially reserved for graphical processing. The memory operates along with the GPU to produce quick instructions and processing that the graphics card can accomplish. VRAM is necessary to keep the entire screen image in memory. The CPU sends instructions to the video card which undergoes the graphical process and eventually is able to be displayed on a screen.

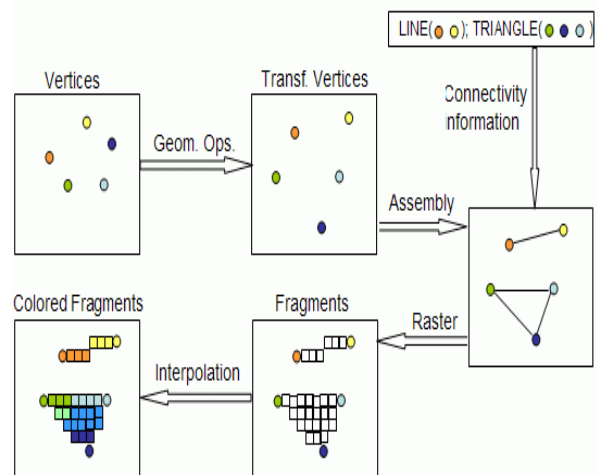


Fig. 3.2.1. General flow chart of Gouraud/Phong shading

3.3 Connections

Computer Bus Connector - the graphics card itself is connected directly to the motherboard either through an Accelerated Graphics Port (AGP) or a Peripheral Component Interconnect Express (PCIe) slot.

Recently PCIe has replaced the AGP in becoming the quickest method to transfer information between an additional device and the computer. "A connection between a PCIe device and the system is known as a 'link' and this link is built around a dedicated, bi-directional, serial (1-bit), point-to-point connection known as a 'lane'".

This allows the GPU and CPU to interact with one another at high speeds to process different instructions. Because of the PCIe high bandwidth there can be up to 32 “lanes.” The links and lanes that is illustrated in the figure 3.3.1.

4 Performance

How much faster can one make applications run by using GPU? , the answer is: it depends. It depends on the nature of the application itself, and what you using as the basis for comparison, for example, code that is single-core or multi-core, or optimized or not. Given some approximation of expected performance, one can evaluate other considerations such as the effort to port, price/performance, performance/watt, and performance/space. [1]

4.1 Configuration

The configuration tested is:

- OPTIPLEX GX-360 – 1U Intel server with one of the two processors installed. This server contains one 2.66GHz E5430 quad-core processor and 16GB of memory.
- Nvidia Geforce 8600 GTS
- The Nvidia Geforce 8600 GTS connects to the OPTIPLEX GX-360 via 16x PCIe slot.
- The OPTIPLEX GX-360 is running Ubuntu 9.04. CUDA 1.1 is installed.

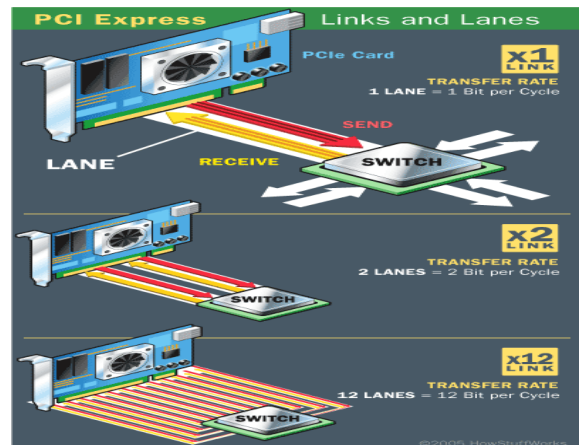


Fig 3.3.1: Overview of PCIe capabilities .

4.2 Benchmarks

Four benchmarks have been ported to the Nvidia Geforce 8600 GTS so far:

- 1.matmatmul – matrix matrix multiply
- 2.FFT – One and two dimensional FFT benchmark
- 3.bandwidthTest – tests bandwidth for writing to and reading from the card
- 4.Monte Carlo Black-Scholes

4.2.1 Matmatmul (matrix matrix multiply) Benchmark.

This benchmark computes $C = A*B + C$, where A, B, and C are matrices. It is run for a range of dimensions from 100 to 10000. In all cases the matrices are dimensioned as square matrices. Thus, it is testing a subset of the functionality of the BLAS SGEMM and DGEMM routines.[8].

Only the single precision version of matmatmul was run, since Nvidia Geforce does not support double precision. The Nvidia CUDA SDK includes a cublas library that provides a subset of the blas library functions. The cublasSgemm function was used to implement this benchmark on Nvidia Geforce. The cublas library includes functions to copy data from the host to the card and copy results back from the card to the host, and these were also used for all tests. Thus, no board-side code needs to be written or compiled to use these cublas functions, but C code needs to be written to make the CUDA and cublas calls to:

1. Select which Nvidia Geforce card to use
2. Copy input data from the host to the card
3. Calculate the result by calling cublasSgemm
4. Copy the results back to the host

This sequence is straightforward to code in C and does not require any knowledge of optimizing board-side code. The benchmark is illustrated in the figure 4.2.1.

In addition to the cublasSgemm included in the CUDA 1.1 SDK, we tested a tuned version of a sgemm sent to us by Nvidia. Comments in the code say that it was written at UC Berkeley. Note that sources for the cublas library are available from the Nvidia web-site. This version runs faster than the cublasSgemm function. It implements a subset of sgemm options and only accepts array-size parameters that are certain multiples of powers of 2. While all multiples of 64 can be used, some array dimensions can be multiples of 4 or 16. Some results for this function are included.

The bottom two curves show the performance measured using SGEMM in the Intel MKL library with one or four cores of the processor. The MKL library implementation of SGEMM should be considered highly optimized code that has been tuned carefully by experts. This implementation also allows SGEMM to use multiple threads under the control of the environment variable OMP_NUM_THREADS, so it is code that has already been modified to take advantage of multiple cores.

The next line shows the performance using cublasSgemm from the CUDA 1.1 library. This measurement of Gflops/second includes the time needed to copy data to and from the GPU card. Note that there are some significant peaks in the results at certain array sizes. The next line (cublasSgemm N*64) uses the same code but uses only array sizes that are multiple of 64. The top line shows the performance of the CUDA SGEMM that has been tuned for a subset of SGEMM arguments.

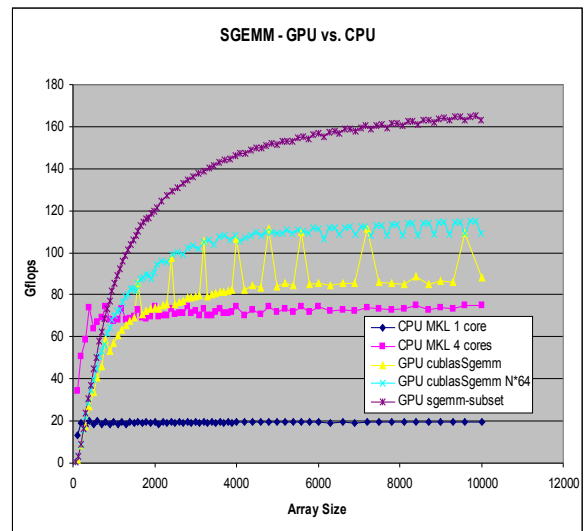
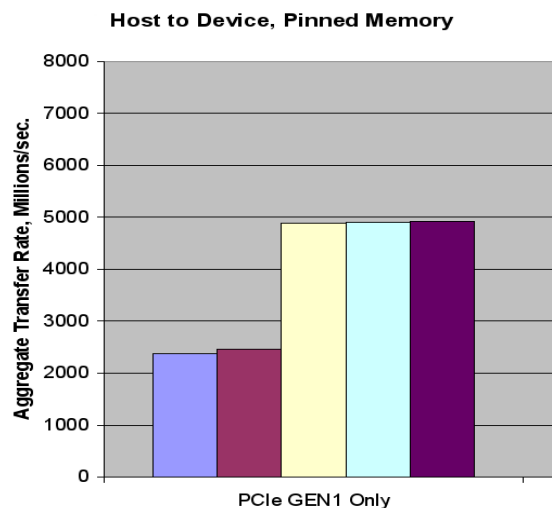


Fig 4.2.1 Shows the Gigaflops/second measured for a single-precision matrix-matrix-multiply

4.2.2 Bandwidth Tests



This benchmark is an HP test tool used to evaluate the data transfer characteristics of multiple GPGPUs on different system platforms. It is based on the original "bandwidthTest" example contained in the NVIDIA CUDA SDK. There are four basic transfer types provided, device to host, host to device, device to device, and read after write. The transfer type, length of transfer, host memory buffer type (pinned or paged) can be selected on a per GPGPU basis, and any of the available GPGPUs may be selected in a test, providing a wide variety of test cases that can be performed.

The bandwidth tests whose results are shown below were conducted using the OPTIPLEX GX-360 system platform configured with an NVIDIA Geforce 8600 GTS. The 8600 GTS is connected to the OPTIPLEX GX-360 via PCIe x16 interface.

Bandwidth tests were conducted using data transfer sizes from 1,000,000 to 100,000,000 bytes in increments of 1,000,000 bytes. The transfer rate of a 50,000,000 byte transfer was selected to display in the graphs. Transfer types of host to device and device to host, using both pinned and paged host memory buffers are presented.

The software used to conduct these tests consists of NVIDIA CUDA SDK and TOOLKIT version 1.1, NVIDIA Driver for Linux with CUDA (171.05) and Linux Ubuntu 9.04. The benchmarks are illustrated in the figure 4.2.2.1 and 4.2.2.2

Overall, these are impressive I/O rates, with transfers from device to host reaching a maximum of about 3GB/sec, showing that these GPU devices and host OPTIPLEX GX-360 are utilizing the available PCIe 16x bandwidth.

4.2.3 1D FFT and 2D FFT

These benchmarks compute the discrete Fourier transform (DFT) using the fast Fourier transform (FFT) algorithm in one and two dimensions. The 1D FFT is performed for sizes varying in size from 2^1 to 2^{20} . The 2D FFT is performed for sizes varying from 2^2 to 2^{12} in each dimension.

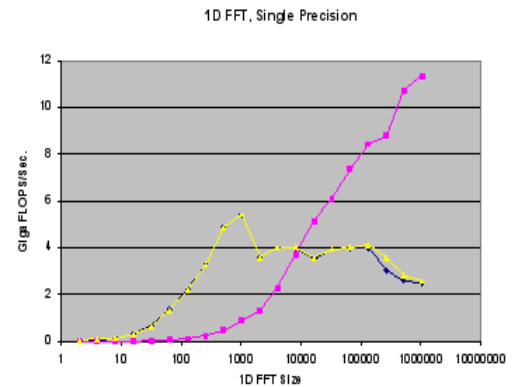
Only the single precision version of FFT benchmarks was run, since 8600 GTS Nvidia Geforce does not support double precision floating point. The NVIDIA CUDA SDK includes a cufft library that provides APIs for 1D, 2D, and 3D real and complex FFTs. The cufft library provides a programming interface that is similar to the well known FFTW open source software package.

Fig. 4.2.2.1 Hows the measured transfer rate, Host to device

To use the cufft library, one first creates a plan that defines the size, number of dimensions, and type of FFT to be performed, real to real, complex to complex, etc.

As cufft library does not include functions to copy data to/from the GPGPU, the cudaMemcpy function is used for this purpose. Once the data has been

moved to the GPGPU, the FFT is performed by calling the cufftExecC2C function. This then performs a complex to complex FFT.



Device to Host, Pinned Memory

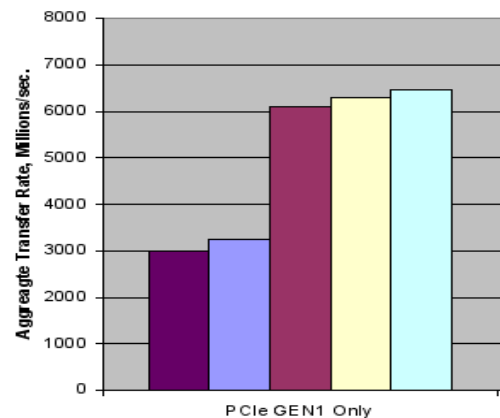


Fig. 4.2.2.2 Hows the measured transfer rate, Device to Host

The benchmark consists of a timed loop that performs two FFTs, one forward and one inverse. The results of the inverse transform are compared to the input data to the forward transform and tested for accuracy as they should be same. Unlike Intel's MKL library, the cufft library does not offer the ability to scale the result of an FFT.

In order to do the comparison the results of the inverse transform are scaled by the reciprocal of the transform size using a small CUDA kernel written as part of this benchmark. Thus the timed portion of the benchmark looks like this:

1. Create the FFT plan
2. Copy input data from the host to the Nvidia Geforce GPGPU

3. Calculate the forward FFT
4. Calculate the inverse FFT
5. Scale the results
6. Copy the results from the Nvidia Geforce GPGPU to the host
7. Destroy the FFT plan

In order to provide accurate timing, smaller FFTs may be performed up to a 100 or a 1000 times before the execution time is calculated. Larger transform sizes may be performed a few as 1 or 10 times. The benchmarks are illustrated in the figure 4.2.3.1 and 4.2.3.2.

Fig. 4.2.3.1 Shows the Gigaflops/sec. measured for 1D complex-to-complex forward and inverse FFT. The lines on the graph represent results for a single core OPTIPLEX GX-360

These results only show an advantage to FFT on the GPU vs. CPU for large sizes. However, this does not take into consideration that a real application would perform some computations on the GPU between the forward and inverse FFT. It should also be noted that forward transforms can be considerably faster than inverse transforms on the GPGPU. We have measured speeds that are up to 3 times as fast for forward transforms when compared to inverse transforms for larger problem dataset sizes.

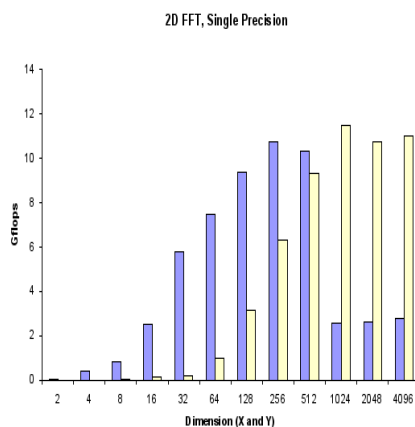
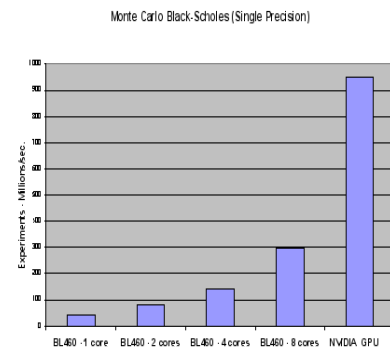


Fig. 4.2.3.2 Show the Gigaflops/sec measured results for 2D complex-to-complex forward and inverse FFT. The bars on the graph represent results for a single core. The results shown are only for square transform sizes, this was done for sake of simplicity of the graph.

4.3.3 Monte Carlo Black-Scholes

This benchmark is an evaluation of European Stock Option Pricing using a Monte Carlo simulation of the Black-Scholes equation. The benchmark evaluates only a single stock option, from 1 to 256 million times, each evaluation is referred to as an experiment. An experiment consists of a draw from the random number generator, an evaluation of the equation, and a sum of the option price and sum of the square of the option price. This benchmark was chosen for its very high computational density and minimal amount of input/output data.[9].

The benchmark uses a Hammersley sequence to generate a uniform random number sequence. This is then transformed to a normal distribution using a polar form Box-Muller transform. This method of generating random numbers was chosen for its ability to be implemented in a highly parallel form. In both implementations of the benchmark, for multi-core CPUs and the GPGPU, the same random number sequence is generated.



In the multi-core CPU version of the benchmark parallelism is achieved through the use of OpenMP pragmas and setting the OMP_NUM_THREADS environment variable to specify the number of threads to be used in the simulation. In the GPGPU version, a CUDA kernel was developed to execute on the GPGPU. The GPGPU operates as a coprocessor to the host system and is capable of executing a very high number of threads in parallel. The number of threads used in the simulation is determined at runtime, when the kernel is launched. For this benchmark, 4096 threads were used.

The benchmark as implemented on the NVIDIA GPGPU generates an array of partial sums of the option price and the square of the option price. Each partial sum is generated by a single thread running on the GPGPU. At the end of the simulation, the array is transferred to the host and the CPU generates the final sums and option pricing.

Only a single precision version of the benchmark was run, as the 8600 GTS only supports single precision floating point format.

The Black-Scholes NVIDIA GPU results shown below were conducted using the OPTIPLEX GX-360 system platform configured with an NVIDIA 8600 GTS. The CPU results are from running the benchmark on a BL460c server blade. The BL460c is a dual-socket quad-core 3.0GHz Intel Xenon based platform. The software used to conduct NVIDIA 8600 GTS test consists of NVIDIA CUDA SDK and TOOLKIT version 1.1, NVIDIA Driver for Linux with CUDA (171.05) and Linux Ubuntu 9.04.

The software used to conduct the CPU based test consists of the Intel C++ compiler for Linux, Intel Math Kernel Library for Linux and Linux Ubuntu 9.04. The benchmark is illustrated in the figure 4.2.3.1

The results for the NVIDIA GPGPU demonstrate the computational capability of the GPGPU, providing a 23X increase when compared to a single CPU core and a 3X increase for an 8-core platform. In addition to the execution time of the benchmark on the GPGPU, results include all of the necessary overhead operations to allocate memory on the GPGPU and host, transfer of parameters and the execution kernel to the GPGPU, transfer of the results from the GPGPU to the host, and final calculations on the host. [2] In this benchmark, the overhead items are essentially fixed for each simulation and have an effect on the results that can be achieved for a given simulation size. For example, in a simulation with 4 million experiments the GPGPU results are 12X that of a single-core CPU result; with 16 million experiments one sees 19X that of a single-core CPU result. Simulations with larger numbers of experiments rapidly approach the maximum observed.

Fig. 4.2.3. Shows the results of the Monte Carlo Black-Scholes simulation in millions of experiments per second. The data points shown are for the maximum results achieved over the course of simulations containing 1 to 256 million experiments. For the CPU results, one sees a near linear scaling over 1 to 8 CPU cores. This is an expected result given the highly parallel nature of the benchmark.

5 Conclusion

As applications demand more processing power, graphic cards will continue to advance in technology to meet these demands. The world of graphics, either through movies, games, or regular software applications, is a huge industry that is pushing graphical processing to its limits. Graphical pipelines are annual being added to newer models of graphic cards to increase processing speeds. Also, with the added potential of processing graphics,

displays such as monitors, projectors, or even televisions will be affected by the graphic cards to meet the demand of displaying higher quality images. Graphical technology has increased exponentially since the first computers were invented and will continue to do so meeting the demands for more life-like graphics in applications.

A number of things have been learned thus far in our investigations:

- A GPU can deliver 10x the single-precision Gflops of CPU core, but a wide range of speedups can be stated for a given problem. It is important to describe the conditions of both the GPU and CPU execution of the computation.
- In making comparisons to CPU performance, it is important to note if the GPU performance includes the time to transfer data to and from the GPU board.
- CUDA BLAS and FFT libraries provide optimized GPU implementations of these functions, and do not require expertise in optimizing code for the GPU. However, applications will likely require some user-written GPU code to be used in combination with calls to these libraries.
- FFT on the GPU outperforms the CPU, but only if the transform size is sufficiently large. Smaller sizes may be a win depending on the other computations to be carried out on the data prior transferring the data back to host memory. Using pinned verses paged memory buffers may also be a win depending on transfer sizes. Also, batching of 1D transforms needs to be considered, these are likely to be effective over many transforms. A key to achieving good acceleration is to have a high ratio of computation to data movement.
- Applications that require little data transfer, have long computation times, and are readily adapted to use parallelism such as Monte Carlo Black-Scholes show impressive speed-ups compared to optimized multi-core implementations.
- The addition of additional interfaces to the overall benchmark framework to accommodate the features of accelerators is clearly a beneficial endeavor. For instance, allowing a particular accelerator to allocate memory using a mechanism optimal for that accelerator is likely to provide an improved result.

Future investigations will include an analysis of the effect of competition between GPU's for I/O

bandwidth. Comparisons to CPU performance using up to 8 cores will also be done. The results will be extended to include AMD FireStream 9170, which we have just begun to test.

References

- [1] J. L. SPEC CPU2000: measuring CPU performance in the new millennium. *IEEE Computer*, 33(7):28-35, 2000.
- [2] D. Kirk. The future: programmable GPUs & cinematic computing. Presentation at WinHEC'03, 2003. On line available at http://developer.nvidia.com/object/cg_tutorial_teaching.html.
- [3] W. R. Mark. Future visualization platform. Panel Presentation at IEEE Visualization (VIS'04), 2004. On line available at <http://wwwcs1.csres.utexas.edu/users/billmark/talks>.
- [4] J. Lengyel, M. Reichert, B. R. Donald, and D. P. Greenberg. Real-time robot motion planning using rasterizing computer graphics hardware. In *Computer Graphics (SIGGRAPH'90 Proceedings)*, volume 24, pages 327-335, August 1990.
- [5] G. Kedem and Y. Ishihara. Brute force attack on UNIX passwords with SIMD computer. In *USENIX Security Symposium (SECURITY'99 Proceedings)*, pages 93-98, August 1999.
- [6] K. E. Hof III, T. Culver, J. Keyser, M. Lin, and D. Manocha. Fast computation of generalized Voronoi diagrams using graphics hardware. In *Computer Graphics (SIGGRAPH'99 Proceedings)*, pages 277-286, July 1999.
- [7] P. Kipfer, M. Segal, and R. Westermann. UberFlow: A GPU-based particle engine. In *ACM SIGGRAPH/Eurographics Workshop on Graphics Hardware (EGGH'04 Pro-ceedings)*, pages 115-122, 2004.
- [8] E. S. Larsen and D. McAllister. Fast matrix multiplies using graphics hardware. In *High Performance Networking and Computing (SC'01 Proceedings)*, November 2001.
- [9] T. Jansen, B. von Rymon-Lipinski, N. Hanssen, and E. Keeve. Fourier Volume Rendering on the GPU using a Split-Stream-FFT. In *Vision, Modeling, and Visualization (VMV'04 Proceedings)*, November 2004.

Ricard L. Burden, J. Douglas Faires (1983),
Numerical Analysis, Seventh Edition

Aproximación numérica de funciones oscilantes usando redes neuronales artificiales supervisadas

Sandoval-Solís, María de Lourdes, Chaman-García,
 Iván Christhofer

Facultad de Ciencias de la Computación

Benemérita Universidad Autónoma de Puebla

RESUMEN

En este trabajo se presenta una arquitectura de Red Neuronal Artificial Supervisada (RNAS) de tres capas, la cual es vectorial y su función de activación es una matriz. Esta RNAS, con nodos equidistantes, nos permite obtener una matriz simétrica y definida positiva, que es nuestra función de activación. Para entrenar la red se utiliza los métodos de Gradientes Conjugados y Newton. Utilizando la RNAS anteriormente descrita, se aproximan numéricamente funciones muy oscilantes con singularidades a una combinación lineal de funciones coseno.

Se prueba la metodología a funciones como:

$$f(x) = \sin(mx), f(x) = \frac{\cos((2m+1)x)}{\cos(x)}, f(x) = x \tan(x), f(x) = \sin(m \cot(x)) \sin(2x)$$

con $m=5,10,50,100$

Referencia

Chaman García, Iván Christhofer (2010), *Integración Numérica con Redes Neuronales*, Tesis, Benemérita Universidad Autónoma de Puebla

Zeng Zhe-Zhao Wang Yao-Nan Wen Hui (2006), *Numerical Integration Based on a Neural Network Algorithm*, Computing in Science & Engineering; Jul/Aug, Vol 8 Issue 4, pp. 42-48 7

David E. Luenbeger (1989) , *Linear and nonlinear programming*, Addison-wesleyIberoamericana

Computer Worms and Their Typing

Jesús Audelo, Miguel Melendez, Antonio Solís
National Polytechnic Institute, Culhuacan ESIME
Section of Graduate Studies and Research
Santa Ana Avenue San Francisco 1000 Colonia
Culhuacan CP 04 430
Tel: 56242000 Ext. 73206
E-mail: jaudelo@ipn.mx

Abstract. There is malicious code that spreads it without requiring any assistance or human intervention, this code is better known as worm and is capable of causing the most destructive attacks against computer networks. Worms can cause widespread faults, may be just a computer or a network effect, which is why it is of great relevance and the impact it can cause can be decisive in the functioning of an entire system. One of the most important stages of the worms that use to locate their targets and begin its spread is scanning, allowing them to locate potential targets.

1 Introduction

It is important to note that at the stage of scanning the attacker tries to find various ways to break into a system that has set as its goal. The attacker seeks to discover even more of the systems like operating system being used, what services are running. Based on the facts that the attacker has gathered, he or she tried a strategy to launch an attack.

Considering some of the research [1] [2], [3], we classify the different types of scan that is regularly used by the so-called malicious code such as viruses, but we focus on the more dangerous worms. We begin by mentioning the most basic scans and then mentioned the most sophisticated.

The way the worms commonly classified is shown in Fig 1.

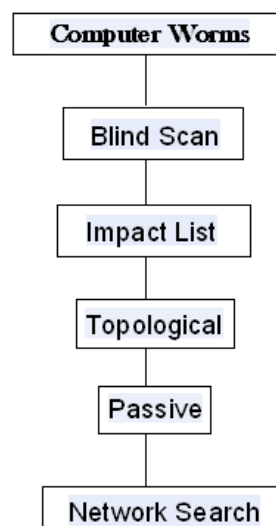


Fig 1. Classification of worms.

Therefore we propose a classification of scans forming two branches, which we call blind scans and scans not blind.

1.1 Development

Within the blind scans are the most basic scans, in which malicious code is not a priority on their objectives, and the scans are not blind, which have a high priority and may even have very specific objectives.

Within the blind scans that we classify as three types in particular, which are: sequential, random and permutation scanning [4]. Most scans are based on the opportunity, so they are much more prone to failure because it has a high error rate of connection. Many worms use this type of blind scans, but because they are the most common and basic systems based on anomaly detection are designed to capture these worms. Such worms are easy to implement and spread rapidly but are not very accurate. One of the main limitations of blind scan is that its effectiveness is now more limited because to find their targets have to scan the entire IPv4 address space within the broad range of Internet.

Therefore we call such scans are not blind effective on average much higher than blind scans [5], because these features include in their information that allows them to disperse more effectively and accurately, without spending part of their resources in pursuit of their aims, these worms are called routing, as part of its features include such information that is contained in its code routing tables, which allow you to have specific targets or at least narrows your search range

thus making it more effective, these worms often use information that provides the protocol BGP (Border Gateway Protocol) and the routing tables which gives this cut its spectrum scanning and may attack systems in particular, from a specific geographical location or an Internet service provider.

The blind scan just testing involves a set of directions in order to detect vulnerable computers. There are two simple ways to scan, one that is in sequence and the way they operate is through a block of addresses using a set of these in an orderly manner and the other is random in which they try to rule out addresses from a block pseudo-random samples.

Because this type of scan is very simple dispersal strategy is very common, these two forms of scanning are used by worms and worms self that require a timer or those based on activation. These kinds of scans are usually much more effective doing your scans locally. This may seem a limiting factor in the spread of the worm, not so much because it has access internally to the barriers that can be implemented within a network as it can be a firewall.

One way in which the scans are more optimal is the permutation, this type of scan is very effective for the worm to perform a search in a distributed manner, allowing you to know when it has infected most computers on the network.

The most effective way of optimizing the search or collection of information from vulnerable computers, is a scan with a limited bandwidth, a clear example of this type of scan is the worm Redi Code [5], which carries out limited exploration routines by the latency of the connection requests rather than by the performance of the requests can be sent.

We can see that the scope of this class of worm, will depend on many factors as can be the number of vulnerable computers within the reach of its scanning range. So I can take some time to locate his victims through a blind scan, if your code included within a more sophisticated scanning system.

Then there are the scans are not blind, as is the one with a previously generated list of objectives. In this list, the attacker in advance and collected information on potential victims vulnerable enough, so really this increases considerably the efficiency of propagation of a worm, which is called flash worm [4,6]. It is possible that this type of worm or complicated as the biggest effort is to obtain the list of objectives, but it is still possible to make a relatively small number of targets from public lists of easy access in case you want to achieve greater range of objectives it is necessary to consider an exhaustive search within search the compilation of a comprehensive database. As you can notice the scan code is independent of the worm code itself [7], this would imply that such scans may also be added to other codes of some worms.

Externally generated target list, this is generated independently as they can be a metasever (is considered a metasever to a central manager for the dispersion of web resources, much like a database), which is an intermediate in the worm which is responsible for providing the information it needs to spread, well this is still active so that remains to receive information from other active servers. The worms that rely on some metasever in the first instance we ask for information to determine new targets. This type of worm collects information through online services [8], especially games, in which the participant can be anywhere in the world, providing information on metasever, even when the population is relatively little, there a metasever who is making requests to find vulnerable computers. Estas técnicas pueden ser utilizadas para hacer que los gusanos sean más rápidos atacando servidores web.

Internal target lists, since many applications have information about other teams, they can provide information on the vulnerabilities of certain services, thus generating a list, which can be used to develop a topological worm, allowing This local information searches to locate new potential victims deciphering the local topology. This can be very fast, depending on which equipment is connected, especially if the route to access it to one of them is shorter, the propagation speed is raised [7]. These can be difficult to detect because although the worm itself is an anomaly, the traffic it generates generated appears to be normal communication between systems.

Passive worms, these are characterized by not having to search for equipment that could be potential victims, however this awaits patiently for the victim comes into contact with him, this behavior makes him a worm turn slow but very cautious and which produces no abnormal pattern in network traffic in your target discovery stage. As these worms is slow but effective because it leverages the normal behavior of the user to find new victims.

The above description describes most of worms that we have called blind, because of the way in which these worms perform scans to collect information about potential victims or targets. Now we describe the main characteristics of the worms are not blind, which thus call for its way of obtaining information about their objectives.

Worms do not have the characteristic blind contain detailed information of their potential victims, in these worms have worms known as routing, which implement advanced techniques to make their attacks [5], these worms greatly increase their speed of propagation, removing empty addresses within its scan range [9], to achieve this is based on information obtained from the BGP (Border Gateway Protocol), routable address. This allows the worm to spread three times faster than a traditional worm [9]. Moreover this type of worm is not only faster but also more dangerous, since information provided by the

BGP protocol, allows routing worm drive and precise attacks that can be identified more specific objectives, as can be a country, a company, an Internet service provider or an Autonomous System (AS) without causing any collateral damage to other targets. This is very important because they can carry out attacks aimed purely destructive potentially damaging, or more important to companies jeopardize the security of a country to be able to direct it specifically to this. Also compared to traditional worms routing worm can cause severe congestion in the Internet back-bone because they have specific information on the routes to follow to be delivered to a destination. Moreover, it is difficult to quickly detect a routing worm, it is not possible to distinguish illegal scans of irregular or regular connections we have with normal traffic.

Considering all the information that gets the worm routing of IP addresses, not only can greatly increase the speed of propagation, but that can be deployed for specific attacks, which in turn can result in obtaining information on vulnerable computers within the selection of specific attacks.

Therefore it is logical routing worms spread more effectively and faster than conventional worms. So we determined that all the worms performing conventional scans the entire spectrum of IP addresses, using either method are in our classification of blind worms, and all the worms that use privileged information such as BGP routing tables are within of our classification of worms not blind.

Using the model-McKendrick Kerrmack infection [10], to study the spread of worms and compare the speed with which worms spread blind to sighted people.

The model assumes that each host resides in one of two states: susceptible or infectious. The classic model of infection for a finite population is [10]:

$$\frac{dI_t}{dt} = \beta I_t [N - I_t]$$

Equation 1. Infection Model Kerrmack-McKendrick.

Which use the analytical solution:

$$I_t = \frac{I_0 N}{I_0 + (N - I_0)e^{-\beta N t}}$$

Equation 2. Kerrmack-McKendrick analytical expression.

Whereas infection rate according to Zou et al [11]:

$$\alpha = \eta \frac{N}{n}$$

Equation 3.A infection.

Analysis for the Code Red worm [5], Fig 2 shows the time Code Red worm spread of the traditional way.

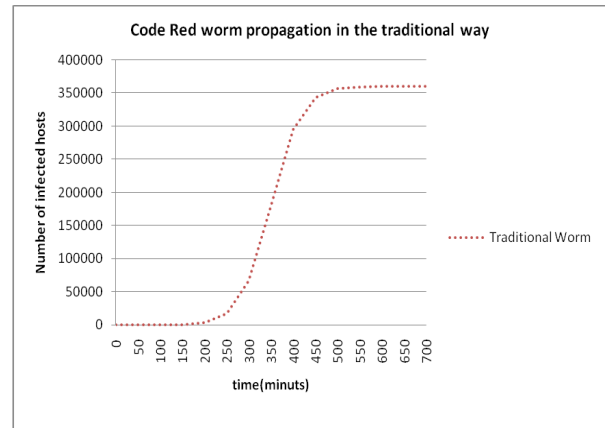


Fig 2. Graphic spread of Code Red worm in the traditional manner.

Analysis for the Code Red worm routing Class Fig. 3.

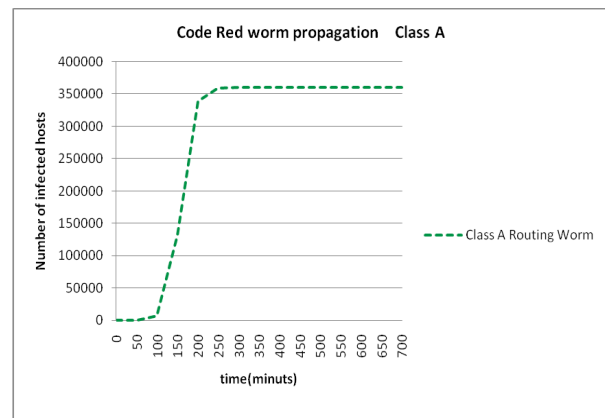


Fig 3. Graphic Code Red worm propagation Class A.

Analysis for BGP routing worm Code Red Fig.4.

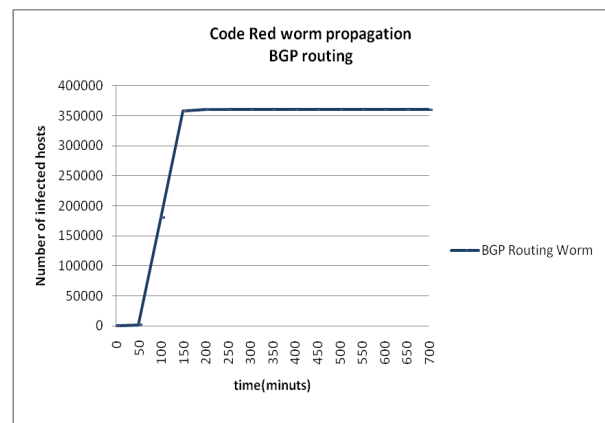


Fig 4. Worm propagation Grafica BGP routing Code Red.

From the graphs above we can conclude the efficiency of the worms are not blind to the blind worms, as shown in Figure 5.

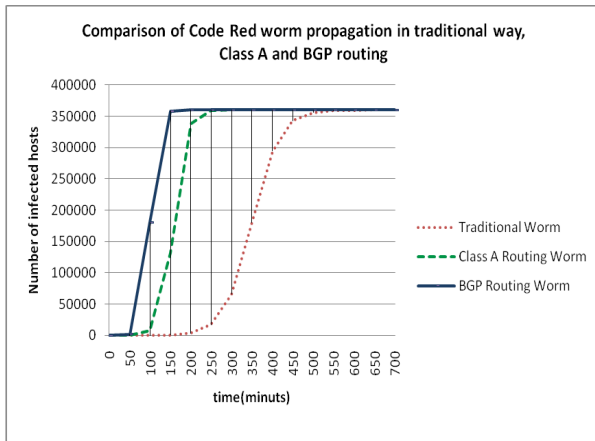


Fig 5. Comparative table between worms of the types: traditional, class A and BGP, and their speed of propagation.

Analysis for the Slammer worm in Figure 6 shows the propagation time of the Slammer worm in a traditional manner for the same model.

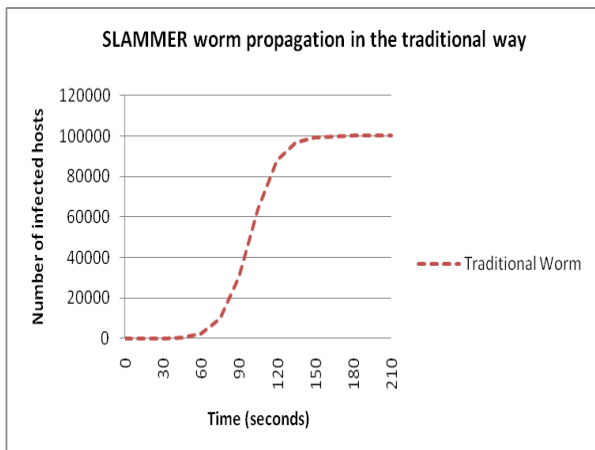


Figure 6. Grafica Slammer worm propagation in the traditional manner.

Analysis for the Slammer routing worm Class Fig. 7.

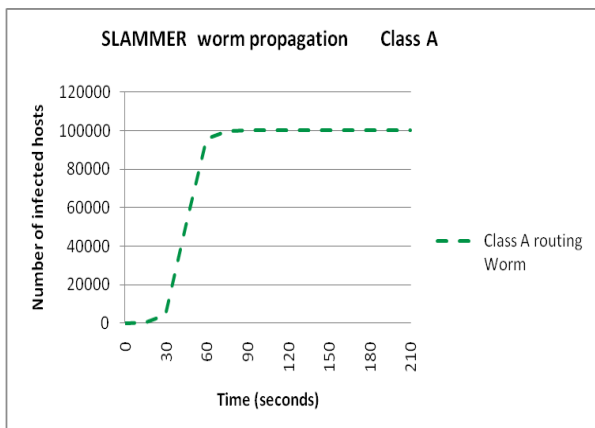


Figure 7. Grafica Slammer worm propagation Class A.

Analysis for BGP routing Slammer worm Fig.8.

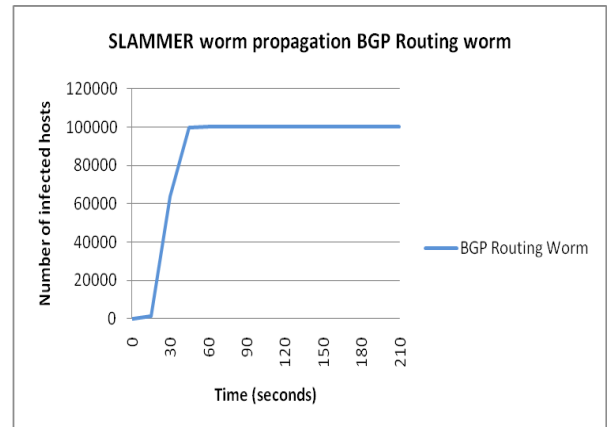


Figure 8. Propagation Graph BGP routing Slammer worm.

From the graphs above we can conclude the efficiency of the worms are not blind to the blind worms, as shown in Figure 9.

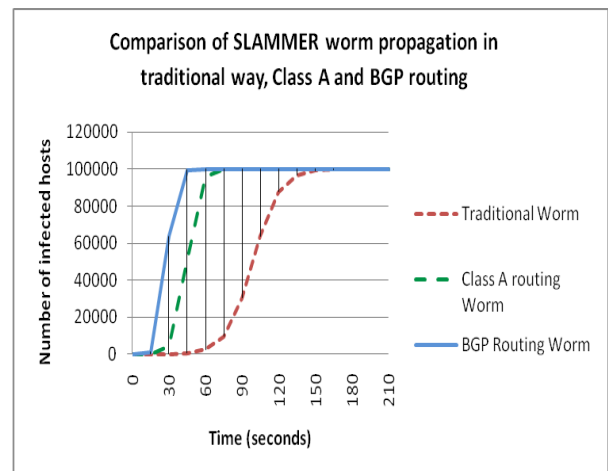


Fig 9 Comparison table between worms of two types: traditional, class A and BGP, and their speed of propagation.

2 Conclusions

The monitoring of the documents consulted and mathematical model evaluation performed in different types of worms indicate that the definition can be called as the blind and blind worms, in addition to efficiency and imminent danger of worms is not blind with respect to the blind worms, because the information they have these attacks to establish a specific way, making it very efficient and difficult to detect.

References

- [1] Cliff Changchun Zou*, Don Towsley†, Weibo Gong, Department of Electrical & Computer Engineering, Department of Computer Science Univ. Massachusetts, Amherst. *On the Performance of Internet Worm Scanning Strategies.*

-
- [2] Zesheng Chen and Chuanyi Ji School of Electrical & Computer Engineering Georgia Institute of Technology, Atlanta, Georgia 30332 *Optimal worm-scanning method using vulnerable-host distributions.*
- [3] Zesheng Chen, Chao Chen, Communications, 2008. ICC '08. IEEE International Conference. *A Closed-Form Expression for Static Worm-Scanning Strategies.*
- [4] Pele Li, Mehdi Salour, and Xiao Su, San Jose State University. *A Survey of Internet Worm Detection and Containment.* 1st Quarter 2008 Volume 10, No. 1.
- [5] Cliff C. Zou, Don Towsley, Weibo Gong, Songlin Cai, University of Massachusetts, Amherst MA 01003. *Routing Worm: A Fast, Selective Attack Worm based on IP Address Information.*
- [6] D. M. S. Staniford, V. Paxson, and N. Weaver. *The Top Speed of Flash Worm.* Proc. ACM WORM '04, 2004.
- [7] V. P. N. Weaver, S. Staniford, and R. Cunningham, *A Taxonomy of Computer Worms.* Proc. ACM WORM '03, 2003.
- [8] Gamespy, Gamespy Arcade, <http://www.gamespyarcade.com>
- [9] Cliff C. Zou, Don Towsly, Weibo Gong, Songlin Cai, University of Massachusetts, Amherst MA 01003. *Advanced RoutingWorm and ItsSecurity Challenges.*
- [10] D.J. Daley and J. Gani. *Epidemic Modelling: An Introduction.* Cambridge University Press, 1999.
- [11] Cliff C. Zou, Lixin Gao, Weibo Gong, and Don Towsley. *Monitoring and Early Warning for Internet Worms.* In 10th ACM Conference on Computer and Communication Security (CCS'03), Oct. 27-31, Washington DC, USA, 2003.

P2P Networking Strategies to Support Massive Online Multiuser Virtual Environments

Student: Martha Patricia Martinez-Vargas¹, Director:
Victor M. Larios-Rosillo¹
Co-Director: Patrice Torguet²

¹ University of Guadalajara, CUCEA, Department of
Information Systems
Periferico Norte 899, Los Belenes
45130 Zapopan, Jalisco, Mexico
{mmartinez, [vmarios](mailto:vmarios@ucea.udg.mx)}@ucea.udg.mx¹, torguet@irit.fr²

Massively Multiuser Virtual Environments (MMVE) technologies offer an interesting support for collaborative activities to communities and private or governmental organizations with geographically distant users. Such organizations or communities can collaborate in richer interactive environments sharing and modifying information over the network or running collaborative simulations or training sessions. This project proposes a distributed architecture in order to support massively multiuser virtual environments and collaborative actions among communities of users. One strategy is to support better the user's interactions based on peer to peer (P2P) networking technologies. To get that support, the virtual worlds are divided in regions; by creating partitions of the network representing the online user connections to manage their interactions in each region. One of the main original contributions of this work are the integration of a P2P library based on Voronoi diagrams as a strategy to connect users as peers and create dynamic network connections to improve the connectivity among users with potential interactions. A problem that could be present in this architecture is that each peer or user contributes to the system and some of them must have more responsibilities to manage regions and the dynamic network connections and then, some problems could be present to identify region leaders, to update concurrent interactions and to define how to create and update replicas in the

P2P network by a VoroCast delivery technique. The social impact of this project is reflected in virtual environments applications focus in educational institutions or business. Offering learning or even simulation experiences for large communities (more than a thousand users simultaneously) and scalability issues.

Keywords: Distributed Virtual Reality, P2P Networks, Massive Online Multiuser Virtual Environments, VAST, VoroCast, Scalability.

1. Context and State of the art

The Massively Multiuser Virtual Environments over networks like the Internet are growing in an exponential order. Thus, a problem of scalability is present and new efforts to solve it are driving to use P2P networks. In such; any member can support the system with its own resources avoiding bottle necks of centralized systems as decreasing network bandwidth and processing overload in servers to support thousands of users. Also, P2P can improve the fault tolerance of the system because all the peers share the system state and can replace a failing peer in contrast with common centralized client-server solutions. However, the cost in development of an adapted P2P architecture for Distributer Virtual Environments (DVE) offer many challenges to coordinate all the peers, to keep the coherence of the system and to support the high interactivity demanded for the DVE.

1.1 Massive Multiuser Environment

In recent years, the Massively Multiuser Virtual Environments (MMVEs) have been more popular among communities of users over the Internet reporting the support of thousands of concurrent users. Some of such applications are related to electronic commerce, the video-games industry, collaborative remote medicine training and virtual training for governmental of private organizations with geographical constraints for the participant members. Some examples of such applications can involve expert users of different disciplines in a collaborative environment in order to optimize human, and material resources to reach organizational goals [9] [5].

1

2

As relevant examples of MMVEs we can talk about EverQuest with 2,500 concurrent users in one world, Eve Online and Second Life with peaks of 45,000 concurrent users. Other relevant application under this context is the China's World of Warcraft, that during the year 2008, reported a peak of 1 million concurrent users [1] (even though each server currently manages only about 5,000 concurrent players). On the other hand, this kind of applications has the challenge to increase the scalability of its system and hence find an appropriate architecture and strategies to support massive concurrent users peaks. In order to support MMVEs, current client-server applications have to increase their resources arriving to limits that are not costly effective as well as not feasible solutions. Under this context our proposal is based on the P2P architecture filtering strategies as an approach to contribute in the development of MMVEs.

1.2 P2P Architecture

In Peer-to-Peer (P2P) architecture each node or peer of the network contribute to the overall system with its own computer resources such as: bandwidth (offering its network support to communicate with close peers), storage space (reserving memory and hard disk for distributed databases to keep the system coherence), and computer power (balancing the processing requirements among the participant peers and distributing computations). From this point of view, if more peers participate in the system, then for some cases, more resources as processing, memory and network connectivity are available. However, as the number of P2P participants is increased, the coordination complexity becomes an issue as well as other problems related to data consistency and real time interactivity among distant peers. Some of such problems are the main topic of this work were some strategies are suggested to offer a solution for the specific context of massive multiuser shared virtual environments.

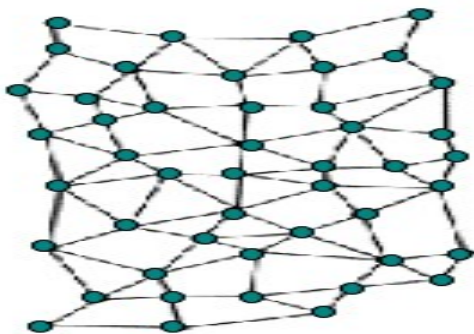


Fig. 1 A Peer-to-Peer Network

The figure 1 shows an example of a P2P network, where the users have direct connection among peers and have the two roles: 1) client to request data updates and 2) server to send data. The database is distributed and replicated on the peers to increase fault tolerance and data accessibility. The advantage of this architecture as told before, is the absence of a central fail point. It means that, if one of the peers goes down, then the system is not affected on its execution which is based and relayed over the rest of the available connected active peers.

2 Problem description

The current problem that we are interested is to solve the scalability problem in MMVE using P2P architecture. Focus in how to support a growing number of users until thousands leading them to have a good communication over the network to offer a highly interactive environment. Another related problem that we are interested in is to support a distributed environment populated with many 3D object where users can change their state, as examples buildings, trees, and accessories of a room in the virtual world. From these two main problems we can identify some related issues to keep in the system as the persistency of the state of the system among the users. Finally, this work is more related to the networking support; the algorithms to update and distribute the state of the 3D objects. Later this work will be integrated another work, in the direction of a distributed database to keep persistence of objects states in virtual environment. In the next sections are present more details about the specific problems introduced in this paragraph.

2.1 System Scalability

System scalability is the ability to handle in the application architecture a growing number of users and managed objects in the virtual environment simultaneously in the system. Usually this is related to number to simultaneous users [18]. Hence, the system should exhibit the ability to optimize the use of available resources depending on the amount of virtual objects to manage in the virtual world (buildings, accessories, special devices) and the number of users connected. The grade of scalability can be determined by several factors as for example, bandwidth, processor capabilities and rendering speeds [9]. Without a scalable architecture, if the system increases its users and managed objects drastically, it can become broken or behave not stable

resulting in poor interaction among participants seen as system failures [19].

2.2 Persistency

Making an object persistent in a virtual world means that defined attributes and setting of the object are stored in a database to have all the time their last state to show to other participants able to interact. It means that when users are entering in the virtual world, they get the last update about the state of all the objects in the virtual world including other users avatars. Persistent objects are organized in persistent object stores, which store their state on disk. Ordinarily, persistent objects store organize a large numbers of persistent objects stored in a database or in a disk awaiting their use and to be active [15]. On each user access the environment must save the last state, with the aim of having a persistently environment [19]. The persistency demands the right allocation of resources with planning and organization by the application [21].

2.3 Interactivity

The interactivity is the degree of communication and interaction among users, by the communication medium and with messages. Actually, there are three dimensions of interactivity; active control, two-way communication and synchronicity. The active control is characterized by voluntary action. Two-way communication is the capacity of mutual communication among users. Synchronicity is the grade in which the users input into a communication and they receive simultaneously the response. System without a good level of interaction could be stressful for the users [20].

2.4 System Integration

In figure 2 displays the architecture with details. This application could be executed on any platform, because it is developed in Java and the Virtual Machine offers heterogeneous support. One of the main contributions of this work is the integration of all the communication support for 3D environments to a simple user interface showing the 3D worlds. The 3D user interface allows the interaction. This project is based on the jMonkey (jME³) 3D graphics engine [8]. All the communication support is adapted

³ jME (jMonkey Engine) is an open source framework developed in Java and created to deal with high performance Open GL graphics and providing all the necessary tools for 3D games development.

to the 3D interface, which demands special care in the threads and security considerations. Other parallel works are developing in details others aspects of the user interface such as objects and avatars editors.

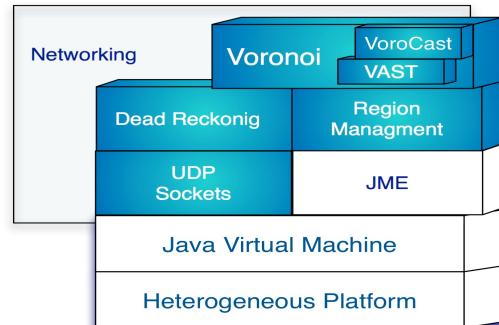


Fig. 2 General Architecture

The networking module contains, UDP socket to update the data of the 3D environment.

With the goal to reduce the network traffic, the strategy is to divide the virtual world in regions to generate network traffic only in the region where the event happened and not in the whole environment.

The Voronoi diagram strategy is implemented to apply filtering in the communication scheme by dividing the virtual world in cells. VAST⁴ is a network library to support a DVR with P2P architecture and has the principles of Voronoi diagrams. In the subsection 3.1 are more details about Voronoi diagrams.

3 Methodology

With the purpose of reducing the messages in communications and get a scalable system, we are implementing diverse strategies, such as Voronoi-VAST a technique, which is currently using only in simulations, not in a real implementation. VAST use the Area of Interest (AOI), which is integrated by the users and their neighbors to send data, but the messages are only transmit to its AOI. However the messages must be transmitted to all region users, and this could be possible by VoroCast. Another strategy

⁴ Voronoi-based Adaptive Scalable Transfer, <http://vast.sourceforge.net/>

is dead reckoning technique to simulate the path of remote object and reduce data sent. Region manager is an additional strategy that divides the world in regions with the aim of supporting by many peers. jME is the engine that allows the development of the 3D interface. Finally is the Network support.

3.1 Voronoi-VAST

The Voronoi diagram is a mathematic algorithm that dynamically divides the virtual world into a number of cells; those cells generate the Voronoi diagram, and they are managed by network peers with consistency control [4]. In the figure 3 are shown the image of the Voronoi diagram integration, the image was taken of the Netlogo library. VAST helps to implement Voronoi. With this library it is possible to create the AOI (Area of Interest) for peers and manage them. This strategy theoretically reduces the communication but was not implemented in a real networked virtual environment. Our challenge was to implement VAST in this kind of applications.

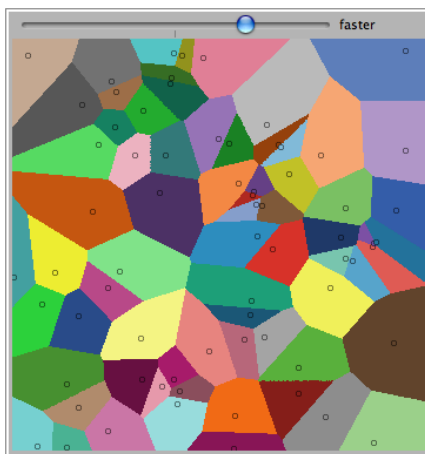


Fig. 3 A Voronoi diagram integration

VAST is a network library to support scalable P2P virtual environment. This library has a mathematic algorithm that find neighboring peers to update. VAST provides two simple functions; a peer may join in the P2P network, and a visibility radius of AOI in the virtual environment. VAST is only tested in simulations, but not in real MMVE that is the goal of this work. In the figure 4 is shown the AOI of the user 1 and theirs neighbors that integrate it. This AOI is dynamic in a fixed time a user can be a neighbor to update. Examples of these users are in the figure 4, as blue circle without red point.

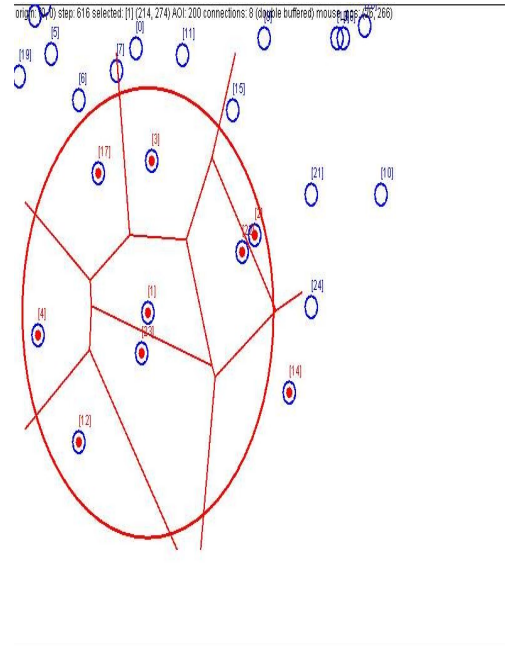


Fig. 4 VAST Area of Interest / VAST integration of dynamic Area of Interest

An area of interest is illustrated in the figure 5, in which a user has interactions with its neighbors, creating the AOI. In the AOI users send updates only to the neighbors surrounding him. This AOI is dynamic in relation to neighbors and their interaction in fixed time [13]. This technique sends data and reduces the consumption of bandwidth. Another strategy is VoroCast, a technique to strew data to all users of the region.

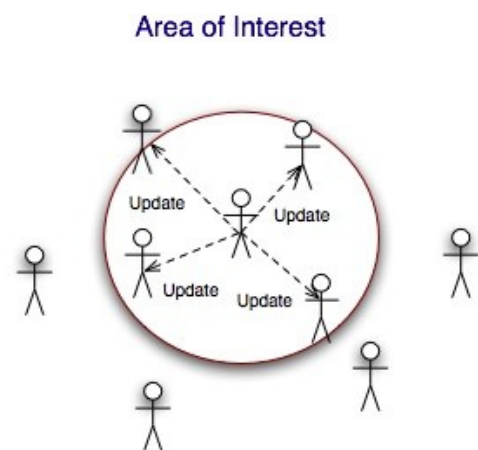


Fig. 5 An Area of Interest

3.2 VoroCast and FiboCast diffusion strategies

There are two forwarding AOI-cast designs as VoroCast and FiboCast with the objective of reduce the bandwidth consumption. VoroCast is a kind of AOI-cast scheme, with the goal of enhancing the AOI scalability of P2P. VoroCast implements the Voronoi diagram to organize the AOI neighbors, and constructs a spanning tree across the AOI over the neighbors. VoroCast propagates messages to all the neighbors in the same AOI [18]. The figure 6 points up the VoroCast technique where a user interacts with its neighbors and the neighbors transmit messages to their neighbors. Transmitting the message only to all the user of the AOI. Another diffusion strategy is FiboCast.

FiboCast is an extension of VoroCast, and it is focus in the users change, the messages are sending to nearest and clearest users, by Fibonacci sequences, adjusting dynamically the messages range in the sequence (e.g., 0, 1, 1, 2, 3, 5, 8...) based on the sum of the two previous numbers, with this two fields are added to messages; the current hop count and a maximal hop count. The AOI neighbors receive the updates by their hop counts from the original node and with the Fibonacci sequences in a round robin way. In each forwarding messages, the hop count increment and it is sent until reach the maximal hop count [17]. VoroCast and FiboCast make an important reduction in bandwidth consumption, in order to provide better AOI scalability. But there are other strategies whereas dead reckoning offers a good deal to decrease message over peers.

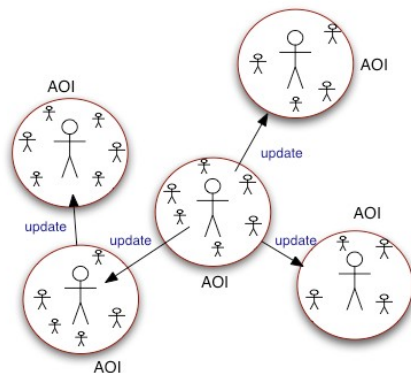


Fig. 6 VoroCast diffusion strategy

3.3 Dead Reckoning

Dead Reckoning is a technique that allows predicting and estimating the current state of a real object in order to reduce the sent data. An example of dead reckoning is shown in the figure 7, where the local avatar has a trajectory with many messages to send. With this technique is able to make a prediction of the trajectory of the real model, in order to reduce the data to send, the messages are only send when there is a change in the trajectory. The main idea is to transmit the update packets less frequently, in order to make an approximation of the real trajectory object and reduce also the consumption of bandwidth [9]. An additional strategy is a region manager, another way to manage and support the virtual world.

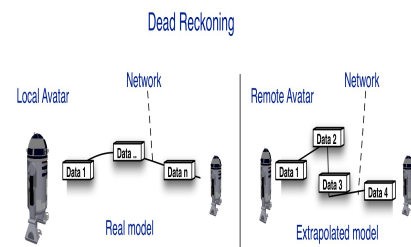


Fig. 7 Dead Reckoning Techniques

3.4 Region Manager

The virtual world is divided in hexagonal regions for better management, in the figure 8 is shown the virtual world in region decompositions. One region is management by a super peer; each super peer manages the 3D world and also the user interactions. When the super peer fails down another peer can replace it, and takes its role using leader election with distributed algorithms. With the object to have a safe environment, and easier support to the world [15]. A further tactic is the use of JME to develop the 3D interface.



Fig. 8 Region Manager Strategies

3.5 JME Integration

The 3D interface is development with the jMonkey Engine (JME), a 3D game engine. This engine allows operating the capacities of video games such as, scene visualizations, graphic representations, manipulation of cameras, illumination and the manipulation of dispositive among others. In the figure 9 is shown a 3D interface with an avatar interacting in the virtual world as part of the first prototype. The avatar interactions must be transmitted by network support.

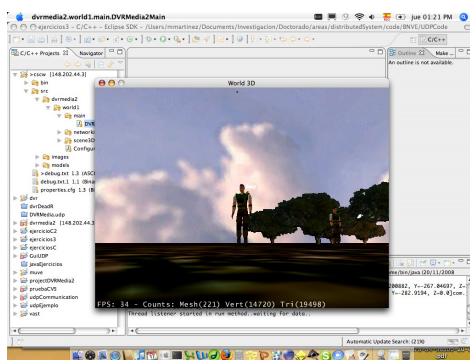


Fig. 9 JME Integration

4 Perspectives

After the integration of the 3D interface with VAST, we now need to debug this integration and measure the communication generated. Test the performance of the system in a cluster. Submit a paper in international congress.

4.1 Massive Test over a cluster

Test the system over a cluster with several nodes, and hundred and thousand of users. Besides make a test with multitudes of artificial avatars.

4.2 Simulations for P2P massive environments

The simulations for P2P with massive environment could be possible by the strategies before mentioned. Voronoi-Vast implementation, VoroCast technique, dead reckoning technique, the region manager, 3D interface with JME and Network support by protocols UDP, several libraries and a VPN for the firsts test.

4.3 Migrating from decentralized system to distributed P2P architecture

To have a pure P2P scheme is too complex, but in the progress of this work, the role of the super peer is going to be reduced with the idea to give more task to the peers. The fault tolerance is an important aspect in security.

4.4 Fault tolerance

In the security of the system the fault tolerance is an important aspect. For example when a peer fail down, other peers have the ability to take the turn of the expired peer and the system continue working without problem. To have a persistent environment data could be stored in a database.

4.5 System coherence (DB support)

To facilitate the persistence of the virtual environment the databases play an important role. The integration of the system with databases is the subject of another PhD thesis. However in future the database is going to be distributed.

5 Concluding remarks

This paper presented strategies for MMVE applications, with a P2P architecture and filtering techniques, with the aim to solve the problem of scalability and uses interaction. Nevertheless bring many challenges to research.

The principal contributions of this work are; the implementation of VAST because it does not have a real implementation only a simulation, dead reckoning with several concurrent users.

Acknowledgement to:



Bibliography

- H. Shun-Yun.: Spatial Publish Subscribe, IEEE Virtual Reality workshop MMVE'09, March, 2009.
- P. Morillo et all.: Providing Full Awareness to Distributed Virtual Environments Based on Peer-to-Peer Architectures, Springer-Verlag, 2006.
- Web page, VAST. <http://vast.sourceforge.net/>, June 2009.
- H. Shun-Yun, Chang Shao-Chen and Jiang Jehn-Ruey.: Voronoi State Management for Peer-to-Peer Massively Multiplayer Online Games, IEEE, 2008.
- M.P. Martinez, V.M. Larios.: DVRMedia2 P2P Networking Strategies to Support Massive Online Multiuser Virtual Environments, PhD Internal Report, University of Guadalajara, CUCEA, Department of Information Systems, December 2008.
- J. Jehn-Ruey et all.: Scalable AOI-cast for Peer-to-Peer Networked Virtual Environments, 2008.
- D. Frey et all.: Solipsis: A Decentralized Architecture for Virtual Environments, MMVE 2008, The 1st International Workshop on Massively Multiuser Virtual Environments at IEEE Virtual Reality.
- Bleedcrimson designs "JMonkey Engine" <http://jmonkeyengine.com/>, Jun 2009.
- Zyda, S. S., Zyda, M.: Networked Virtual Environments: Design and Implementation, Addison-Wesley, ACM Press, 1999, ISBN: 0-201-32557-8.
- P. Torguet: NetworkedVEs, University of Paul Sabatier, IRIT, VORTEX, July 2008.
- Torki, S., Torguet, P., and Sanza, C.: Adaptive Classifier System-Based Dead Reckoning, IPT-EGVE Symposium, 2007.
- Tanenbaum, S., and Van Steen, M.: Distributed Systems Principles and Paradigms, Alan Apt, 2002, ISBN 0-13-088893-1.
- Chen, A., and Muntz, R. R.: Peer Clustering: A Hybrid Approach to Distributed Virtual Environments, The 5th Workshop on Network & System Support for Games, Netgames'06, ACM, 2006.
- Ye, M., and Cheng, L.: System-performance modeling for massively multiplayer online role-playing games, IBM Systems Journal, 2006.
- Coulouris G., Dollomore J., and T. Kindberg.: Distributed System Concept and Desing. Fourth edition, ISBN: 0-321-26354-5, AddisonWesley, 2005.
- Wooldridge, M.: An Introduction to MultiAgent Systems, ISBN 0-471-4969 I-X, August 2002.
- Jehn-Ruey J. et all.: Scalable AOI-cast for Peer-to-Peer Networked Virtual Environments, 2008.
- Shun-Yun H., and Guan-Ming L.: Scalable Peer-to-Peer Networked Virtual Environment, ACM, SIGCOMM'04 Workshops, 1-58113-942-X, 2004.
- Liu Yuping, and L. J. Shrum.: What is interactivity and is it always such a good thing? Implication of definition, person, and situation for the influence of interactivity on advertising effectiveness, Journal of Advertising, 2002.
- Souad EL MERHEBI.: La gestion d'effet : méthode de filtrage dans les environnements virtuels distribués MÉMOIRE, PhDThesis, Université Paul Sabatier - Toulouse 3 École Doctorale Informatique et Télécommunications.

DVRMedia2 Virtual Reality Advanced Editor For Crowded Worlds Simulations

Martha Elena Zavala Villa
Victor Manuel Larios Rosillo
CUCEA Universidad de Guadalajara
Periférico Norte 799 Modulo L-304
Los Belenes, Zapopan Jalisco. México
TEL:(013)3770-3430, Fax:(013)3770-3353
{martha_ezv, vmlarios}@cucea.udg.mx

Hervé Luga
VORTEX-IRIT University Toulouse I,
2 rue du Doyen-Gabriel-Marty 31042
Toulouse France
herve.luga@univ-tlse1.fr

Abstract. In this work, it is proposed a Heterogeneous Crowd Generation (HCG) system for the development and management of synthetic humanoid character creation that allows the user to build and share heterogeneous crowds in virtual spaces. Its main objective is to define the development and management mechanisms required for the generation of heterogeneous humanoid crowds in an autonomous way. This is achieved by the MakeHuman project software integration, which creates realistic 3D meshes humanoids, and resulting in a list of parameters that make it unique at the character. And the use of Genetic Algorithms (GA), solve the creation of realistic characters for virtual humanoid crowds based in the optimal parameter list, and a Distance Function to obtain the physical differences for each character. There are two important aspects to control in the development of crowds, are the physical and the behavioral attributes of each humanoid. These two sets of controlled aspects will allow generation of thousands of humanoids with a heterogeneous distribution, previously parameterized. The impact of this research is the possibility to use virtual reality technology for humanoid crowd simulations, without the complexity required to manually model artificial heterogeneous populations. Other researchers could benefit from this application and the portability of the system since is developed in Java and Python.

Keywords: Heterogeneous Crowd Generation, Character Creation, Crowd Simulations, Genetic Algorithms, And Humanoid Generation.

1 Introduction.

The avatar representation is an important aspect of virtual environments, because it allows a 3D humanoid user appearance and interaction inside the virtual worlds.

To obtain a realistic avatar appearance, it is necessary to consider many human aspects, like muscular movement simulation, morphological characteristics of the human body, and hundreds of parameters linked to the character and appearance [1].

An example of this can be seen in the movie "AVATAR" directed by James Cameron. This film managed thousands of virtual characters but the characters did not look real enough. To solve this problem, the movie team used the "Computer Generated Imagery (CGI)" system, that obtains in high precision the details of actor's facial interpretations, and translates them onto the virtual characters in the movie [2]. The principles of more realistic and heterogeneous avatar generations are explained in the following sections.

1.1 Avatar modeling.

The avatar permits the user to navigate and interact in VE applications [3].

It is not simple to generate realistic avatars, because the human body is a very sophisticated structure with complex internal and external organization, and contains hierarchy of levels.

It is possible to use many 3D representation programs to generate a virtual humanoid forms [1]. The problem with the most of the available software, are the necessary requirements for the installation and the time that takes to learn to use it. It is

important to mention that the software is not always difficult to use, but to obtain specific results a lot of effort and time may be required [4].

If users with less or no knowledge about 3D software access to a website dedicated to the generation of virtual characters, it could be easy for them to generate an avatar, because it is only needed to modify the appearance of the software furnishing of an avatar model. With the help of the software menus, it is easy to make changes on the morphology of the avatar, to achieve the desired appearance [5].

The time required to generate a virtual character, differs according to the application, and abilities of each user. The main contribution of this work is the generation of crowds consisting of thousands of heterogeneous humanoids, with minimal user intervention, and with an automatic creation through a simple parameters variation using genetic algorithms.

1.2 Crowd Simulations.

The crowd representations simulate the movement of a large number of avatars to observe their collective behavior, interaction and reaction. Simulating crowds, offers considerable advantages in the study of many different areas. It help us to simplify processes, to set goals and limits based in the crowd reaction behavior [6].

Currently, this kind of simulations is used to study the crowd motion in real-time, complex crowd behavior, dynamic interaction among people, like training in emergency cases and evacuation simulations [7].

An example of crowd generation systems can be seen in development tool called "*Crowdbrush*" used for managing scenes with a multitude of avatars [8]. Such a tool, allows users to load into a virtual

environments hundreds of synthetic characters in real time. Another example is the "*Dryad*" tool [9] used to generate hundreds of trees in virtual environments.

Other examples related to crowd simulations are environments with realistic artificial crowds, and which are popular in the video game industry like: Civilization II, Alpha Centauri, Warcraft, Rise of Nations, Catan, Age of Empires among others [10] [11].

In applications such as training software, crowds can be used to construct simulations for emergency responses to awareness situations. This kind of systems uses the attributes of virtual environments and crowd simulations to study a human behavior, to simulate evacuations, earthquake, natural disasters, and social problems involving massive amount of users [12], [13].

This paper pretends to study how to generate crowd populations of artificial humanoids with help of the Genetic Algorithms and with marked differences between the characters within the population. The use of Genetic Algorithms will be explained below.

1.3 Genetic Algorithms.

The Genetic Algorithms (*GA*) is a technique used to find and approximate to the optimal solutions that imitates the genetic biologic evolution as a strategy to solve problems.

The GA provide a set of potential problem solutions, coded in some way and a measure called "*fitness function*" that allows quantitative assessment of each candidate solution with the aim of improving the GA and the random generator [14].

The techniques of using the GA have been improved over the years. In 1965 Ingo Rechenberg of the Berlin Technical University, introduced a programming that imitate the biological evolution like strategy to solve problems [15].

John Holland in 1962 works with adaptive systems and proposes the mutation and crossover. J. Fogel, A Owens and M Walsh in 1966 programmed machine that by the random mutation chose the best solution to continue [16][17].

The hypothesis of this paper, is based on use of such algorithms to generate a heterogeneous humanoid crowd population by using operators of mutation and crossover, and obtain the best parameters to conform our new crowd generation at large scale and in an efficient way.

2 Problem definition.

Virtual environments allow to the user the generation and the control of movements of their own avatar representation [18]. Currently the avatar could be generated in automatic way by using software or some graphical user interfaces (GUI). Not all of these systems allow saving and exporting the avatar models [19].

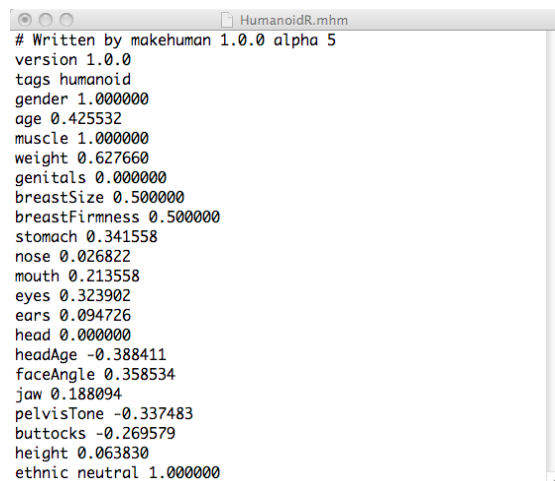
With usual software it is possible to create humanoids that are later possible to copy and multiply to generate a crowd. But the real problem to solve in this research work is that the crowds consist of multiples of the same avatar models and that is not good for the crowd simulation, because every humanoid in the crowd will be clone of the first model [20].

The main problem is to generate a crowd simulation of hundreds of synthetic heterogeneous humanoids at a large scale in an efficient an automated way and with totally random individuals distribution in its physical appearance and behavioral characteristics.

2.1 Avatar description.

To generate a virtual human, it is necessary to include some morphological characteristics and some algorithms to simulate the avatar in a more realistic way [19].

In addition it is required to have a list of parameters that represent the avatar physical appearance such as: age, sex, muscular thickness, body shape, facial characteristics, among others. An example of this can be observed in the figure 1 that shows a list of parameters resulting to generate a humanoid in the software MakeHuman.



```
# Written by makehuman 1.0.0 alpha 5
version 1.0.0
tags humanoid
gender 1.000000
age 0.425532
muscle 1.000000
weight 0.627660
genitals 0.000000
breastSize 0.500000
breastFirmness 0.500000
stomach 0.341558
nose 0.026822
mouth 0.213558
eyes 0.323902
ears 0.094726
head 0.000000
headAge -0.388411
faceAngle 0.358534
jaw 0.188094
pelvisTone -0.337483
buttocks -0.269579
height 0.063830
ethnic neutral 1.000000
```

Fig. 1. MakeHuman avatar parameters.

In some virtual environments, the avatar could be generated by a very intuitive graphical user interface as in Second Life [21], or Poser [22]. The user should only choose among offered options of the avatar's physical appearance and accessories as tattoos, glasses, jewelry, caps, etc.

However, the physical appearance of the avatars population is not the only problem to solve. The bigger problem is to achieve heterogeneous crowd to obtain totally random individuals. There exist ways to generate virtual crowds like: using agents [12], overlaying pre-captured crowd images onto the background image [23], with commodity graphics hardware [24], etc.

But these are not well suited for the generation of a huge numbers of characters that form a big crowd, because they generate homogeneous crowds. What is really needed to generate is a multitude to simulate a crowd with as much variety as possible. Therefore, we look for the generation of physically different humanoids in a crowd in an automatic way, as a main proposal to solve in this research paper.

2.2 Automatic avatar generation.

To automate the avatar generation, it is necessary to define the physical characteristics for the avatars representation. For example, to generate humanoids in the contemporaneous software as in the MakeHuman project [25], it is necessary to define all the facial aspects and physical appearances for the character.

All the changes generated in the MakeHuman avatar, are possible to adjust while interacting trough the GUI. The application may generate a new avatar

based on the user request, and will save a file with a list of parameters like shown in figure 2.



Fig. 2. MakeHuman software for the modeling of three-dimensional human characters.

When the user manipulates the MakeHuman widgets they can to modify the character. The interface and all the changes that the character may have can be seen in the figure 2. Internally the MakeHuman application uses a significant number of characteristics that are molding and shaping the new unique character.

As a result, MakeHuman generates a list of modified parameters giving them values between 0% and 100% and transforming the parameters to obtain floating values. As shown in figure 3, the transformation from male to female sex cannot be the same as that for the weight value, and these changes are represented in the figure 3 with the transformed curve[1].

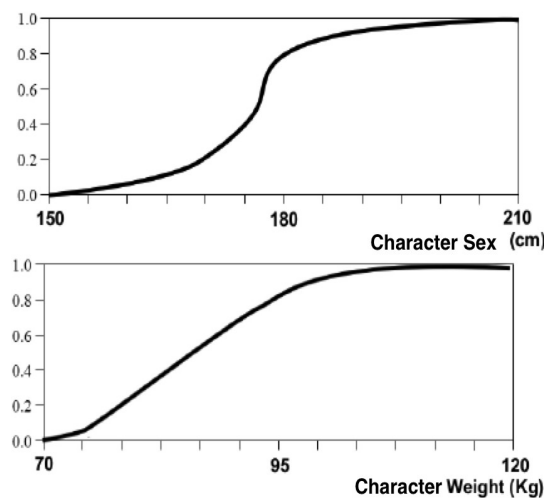


Fig. 3. Suffering transformation humanoid parameters through the MakeHuman GUI.

To obtain a heterogeneous crowd, we needed to generate a seed. And for create the seed; it is necessary to define the list of parameters that will guide the population for the future humanoid crowd generations. The seed will be generated with the help of the MakeHuman project. Selecting and modifying the parameters that will be key pieces if the seed.

Next, with the help of the Genetic Algorithms we will mix the seed parameters to obtain a heterogeneous crowd with humanoids totally random. Once the heterogeneity is achieved, there may be some of the humanoids in the crowd that are physically similar, but not completely clones.

After establishing the key parameters for the generation of the crowd, each ones becomes in a modifiable parameter for the genetic algorithms. The GA provides a set of potential parameter solutions, and by the measurement called "*fitness function*", evaluates each possible parameter solution, with the objective to improve it, and randomly generating a new potential parameter solution. In the figure 4 can be seen the workflow required to generate a humanoid crowd.

Once obtained an optimal solution chosen by the "*fitness*", the Distance Function (*DF*) is calculated based in the parameters ranges that the humanoid could take. The *DF* is calculated to obtain a really distance among the parameters of a set.

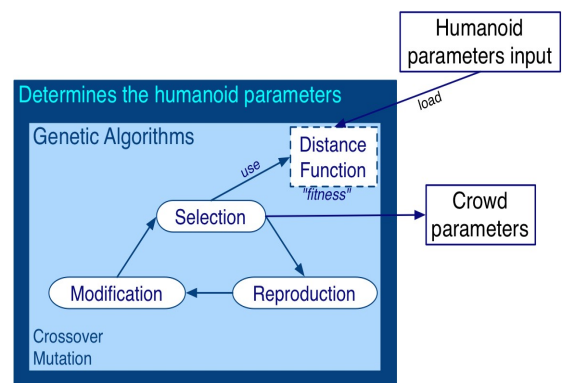


Fig. 4. Workflow for generate humanoid crowd using Genetic Algorithms.

One problem to solve is settling or obtaining a perfect fitness function. With only one perfect solution, to avoid that all the avatars will be clones of the parameters provided by the users. To avoid this and allows the diversity in the crowd, we choose to do further processing in the distance function as shown in the figure 5.

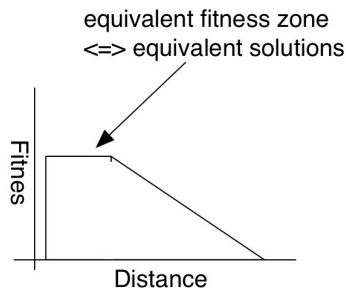


Fig. 5. Distance function equivalent solutions

The DF measures the distance between the avatar parameters (*proposed by the user*) and the solution parameters (*proposed by the "fitness"*) based on the following formula:

$$\text{distance} = \sqrt{\sum_{i=0} (X[i] - Y[i])^2}$$

Where: The distance between the two points can be expressed in terms of parameters like this:

$$\text{distance} = \sqrt{\sum_{i=0} (X_1 \text{ gender} - X_2 \text{ gender})^2 + (Y_1 \text{ age} - Y_2 \text{ age})^2}$$

$X[l_i]$ represent the x humanoid parameters.

$Y[l_i]$ represent the y humanoid parameters.

For example, to determine the age and sex parameters to generate the new humanoid crowd, the user provides values such these:

```
Enter the gender of
humanoid 1: 0.2
Enter the gender of
humanoid 2: 0.5
Enter the age of humanoid
1: 0.34
Enter the age of humanoid
2: 0.50
```

Once obtained the values, the distance is calculated:

```
distance += (X1[0.2]-
X2[0.5])^2*(Y1[0.34]-Y2[0.50])^2
The distance between the two
points is: 0.639999999997
```

Which means that exist a distance of 0.64 among the main humanoid parameters, selected by the GA "fitness", and the target parameters selected by the user to conform the crowd. The algorithm will stop when stopping criteria will be reached.

2.3 Obtained results.

Based on this, it is possible to testing and creates humanoid crowds with different physical characteristics.

For example: following the steps mentioned throughout this article, to generate a heterogeneous human crowd, it is necessary:

- 1 Define a list of parameters to form the base for the crowd,
- 2 Define how many avatars the genetic algorithm will generate, and
- 3 Mix the parameters to obtain the humanoid crowd heterogeneity

Following these steps, the HCG system will generate a heterogeneous crowd over a period of time equivalent to the number of characters and to change parameters as can be seen in the figure 6.

The use and completion of these steps will affect the generation of population and could be generate significant changes in the parameters of each individual in the population.

Before to use the HCG system the parameters list for generate a new population was initialized in a specific value. And when the genetic algorithm is used to generate a population these generate a crowd with significant modifications in the parameter list as shown in the next three figures.

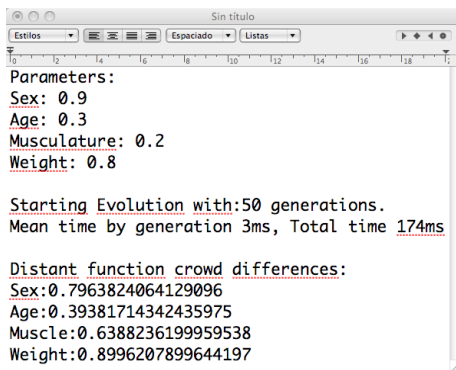


Fig. 6. HGC parameter modification

In the figure 7, at the beginning the Age parameter was specified in one. Once the GA fitness selection and the distance function are applied, the Age parameter changes, generating a crowd population with mixed ages.

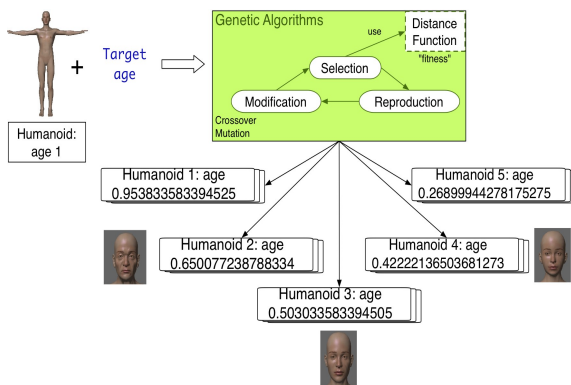


Fig. 7. Heterogeneous age for the crowd, obtained through the HGC system.

In similar form the gender parameter is changed between men and women through the HGC system like shown in the figure 8. At the beginning the data input was the humanoid gender and its value was 0.9. Once activated the HGC system generates a new variation in the crowd.

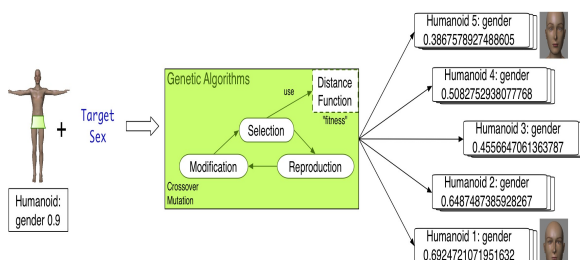


Fig. 8. The Sex parameter changed by the HGC system.

Other example could be observed in the figure 9 with the weight parameter, which is calculated in 0.5 at the beginning and it changes ranging from 0.3 to 0.7.

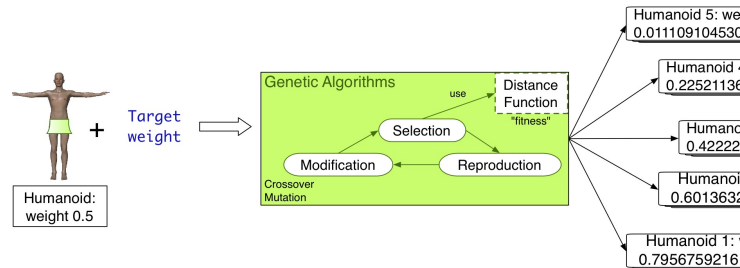


Fig. 9. Oscillation in the weight parameter for the crowd.

It is important to measure the timing required to generate a humanoid crowd with specific number of characters and the time that takes the computer for generates the population.

These tests were conducted for populations that provide from one to a million of virtual characters and the results can be observed in the graph shown in the figure 10. The computer in which was held the test, is a MacBook Pro Intel Core Duo @2.4GHz with 4GB RAM, a JVM 1.6.017 and OSX 10.6.3.

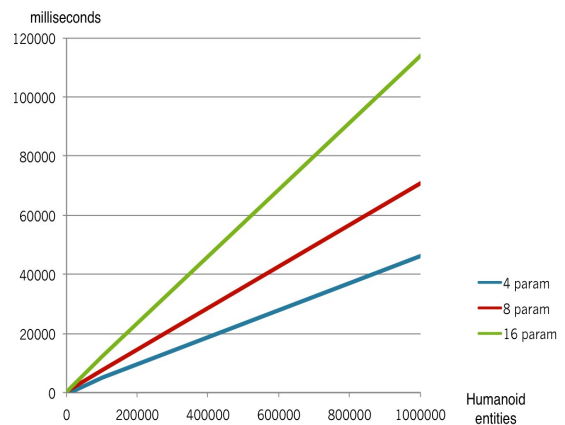


Fig. 10. Crowd generation in periods of time and measuring the parameters variations.

Measure the crowd generation in time, allows distributing the available computation time spatially and temporally according to the user's point of view. The time series show the maximum and minimum values for generate a million of virtual humanoids in two minutes maximum. Which is really fast for a common machine.

We know and consider that the 3d meshes and textures humanoids, can increase the time and load in

the computer. So for future testing's is meant relate this tests in Intel super computing lab.

3 Concluding remarks and perspectives.

With the help of the HCG, which is based on genetic algorithms, the humanoid crowd will be generated with a minimal user intervention. Based in the results of HCG, it is possible to generate the 3D avatar representation in MakeHuman application. Then it is possible to export the 3D humanoids in collada3 format and avatars could be inserted into virtual platforms.

In future work, an interface needs to be developed, to facilitate the user intervention in generating the humanoid crowds. Once the 3D humanoids are obtained, the GUI will be integrated and the production chain to generate crowds of thousands of humanoids is observed in the figure 11. The dotted boxes are under development because it requires programming in python scripts.

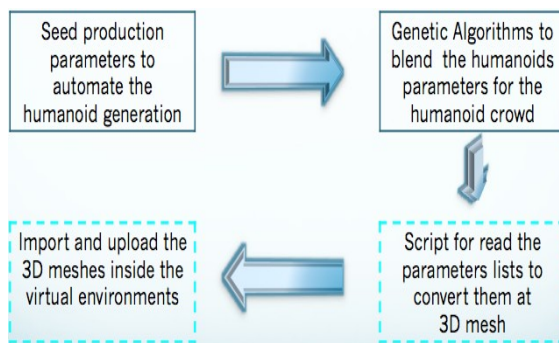


Fig 11. The production chain to generate thousands of heterogeneous humanoids.

Another aspect to develop is the humanoid behavioral attributes, to obtain diversity of reactions in the virtual world. The objective is that each avatar is able to generate its own path planning in the environment to reach their goal or objective position, avoiding collisions with other objects and humanoids represented in the virtual world.

Currently many researchers are working in the generation of virtual populations, but they are focused in different methods and involved in different aspects of the populations like:

- Diverse populations taking particular importance in the character body parts and behavior [11].
- Crowd generation using Artificial Intelligence frameworks to generate animations of virtual avatars and intelligent behavior reactions [26].
- Crowd simulations of humanoids in real time using virtual agents and representing simple behaviors [27].

The HCG system will be used to simulate a humanoid crowd in a stadium for the 2011 Pan American Games. This will be done for the improvement of the security at the 2011 Pan American Games.

4 Acknowledgments.

We want to acknowledge the CONACYT, for the PhD scholarship support, the COECYTJAL, for the equipment donation and mobility, and INTEL, for providing the cluster for testing. Also, we acknowledge the IRT in Toulouse France, for all their collaboration and contribution for this research. We thank to the Information Systems Department from CUCEA University of Guadalajara, for all their support, and finally to the PhD program for all their attention, and specifically to everyone related with this work. Thank you all very much.

References.

1. Bastioni, Manuel and Re, Simone and Misra, Shakti "Ideas and methods for modeling 3D human figures: the principal algorithms used by MakeHuman and their implementation in a new approach to parametric modeling", Compute '08: Proceedings of the 1st Bangalore annual Compute conference.

2. FOX "AVATAR" <http://www.avatarmovie.com/> 2009.
3. Christina K. Bolas "Avatar Personas of Second Life". 2008.
4. Blender, "Blender Material Nodes" <http://www.blender.org/development/release-logs/blender-242/blender-material-nodes/>, 2010
5. Kent Brilliant, "Building a digital human", 2003. ISBN: 1-58450-285-1. Charles River Media. Graphics Series.
6. Diego Gutiérrez, Bernard Frischer, Eva Cerezo, Ana Gómez, Francisco Seron, "AI and virtual crowds: Populating the Colosseum", 2007. Journal of cultural Heritage. Science Direct.
7. Adrien Treuille, Seth Cooper, Zoran Popovic "Continuum Crowds", 2006 ACM Transactions on Graphics SIGGRAPH.
8. Pablo de Heras, Ciechomski and Daniel Thalmann, "Crowdbrush: Interactive Authoring of Real-time Crowd Scenes". Eurographics ACM SIGGRAPH Symposium on Computer Animation 2004.
9. Jerry Talton, Daniel Gibson, Pat Hanrahan, Vladlen Koltun "Collaborative Mapping of a Parametric Design Space". Stanford University, Computer Science Technical Report, CSTR 2008-01, <http://dryad.stanford.edu/> Jan 2008.
10. Joseph Sapp IGDA "Annual Report 2006", <http://www.igda.org/annualreport2006>
11. Rachel McDonnell, Michéal Larkin, Benjamín Hernández, Isaac Rudomin, Carol O'Sullivan, "Eye-catching Crowds: Saliency based Selective Variation". SIGGRAPH 2007 New Orleans. <http://www.siggraph.org/s2009/>
12. Ameya Shendarkar, Karthik Vasudevan, Seungho Lee, Young-Jun Son, "Crowd Simulation for Emergency Response using BDI Agent Based on Virtual Reality". Simulation Conference, 2006. WSC 06. Proceedings of the Winter. ISBN: 1-4244-0500-9
13. Branislav Ulicny, and Daniel Thalmann, "Crowd simulation for interactive virtual environments and VR training systems", 2001 Springer-Verlag.
14. A.E. Eiben and J.E. Smith. "What is an Evolutionary Algorithm". Introduction to Evolutionary Computing, Chapter 2. - 2nd printing, 2007, ISBN: 978-3-540-40184-1 Series: Springer, Natural Computing Series.
15. Ingo Rechenberg "Evolutionary Strategies for Technical Innovation", 1965
16. John H. Holland "Outline for a Logical Theory of Adaptive Systems" 1962 J. ACM.
17. Fogel L. J., Owens, A. J., and Walsh M. J., "Artificial Intelligence through Simulated Evolution". 1966.
18. Peter Small, "Editing & saving appearance in Second Life", <http://www.sl-adventures.com/village/editingAppearanceInSL.html> 2008.
19. Andreas Volz, Rainer Blum, Sascha Häberling, Karim Khakzar "Automatic, Body Measurements Based Generation of Individual Avatars Using Highly Adjustable Linear Transformation". HCI International 2007 ISBN: 978-3-540-73318-8.
20. Bleedcrimson designs "Jmonkey Engine" <http://jmonkeyengine.com/> Apr 27, 2008.
21. Linden Research, Inc "Second Life", <http://secondlife.com/whatis/pricing.php>, Jun 2009.
22. Smith Micro Inc "Poser 8". <http://poser8.smithmicro.com/index.html>
23. Dong-Gyu Park, Sang-Hyun Park, Hoon-Hee Lee and Hwan-Gue Cho. "An automatic crowd generation system using image processing techniques" Department of Computer Science, Pusan National University, Kum-Jung Ku, Pusan, 609-735, South Korea 2000. Sciencedirect.
24. Kasap, Mustafa and Magnenat-Thalmann, Nadia, "Modeling individual animated virtual humans for crowds". SIGGRAPH Asia '08: ACM SIGGRAPH ASIA 2008. <http://doi.acm.org/10.1145/1508044.1508098>
25. MHteam, "Make Human". <http://www.makehuman.org/> 2001-2009
26. Andres Iglesias, Francisco Luengo "AI Framework for Decision Modeling in Behavioral Animation of Virtual Avatars", 2007 Springer-Verlag Berlin Heidelberg 2007.
27. Julien Pettre, Pablo de Heras Ciechomski, Jonathan Maïm, Barbara Yersin, Jean-Paul Laumond and Daniel Thalmann. "Real-time navigating crowds: scalable simulation and rendering". Comp. Anim. Virtual Worlds 2006; 17: 445-455. Published online in Wiley InterScience.

Evaluation of the behavior of carbon steel pipes used for drinking water supply using digital image processing

A.S. Díaz Fergadiz Roldán^{*}, E. Bolaños Rodríguez^{*}, L.R. Coello Galindo^{*}, E. M. Felipe Riverón⁺, y R. I. Calva Fernández²

^{*}Escuela Superior de Tizayuca, Universidad Autónoma del Estado de Hidalgo, Km 2.5 Carretera Federal Tizayuca-Pachuca. C.P. 43800, Tizayuca, Hidalgo. México.

[±]Centro de Investigación en Computación, Instituto Politécnico Nacional. Av. Juan de Dios Bátiz, esq. Miguel Othón de Mendizábal, Col. Nueva Industrial Vallejo, Del. Gustavo A. Madero. C.P. 07738, México, DF.

e-mail {ana_fergadiz@yahoo.com, bola7112@yahoo.com.mx, rocoello77@hotmail.com, edgardo@cic.ipn.mx, calfer_chio@hotmail.com}

Abstract.

On this work we are evaluating steel pipeline (SAE1080) used for conducting drinking water in Hidalgo, Mexico. We are using the digital micro photos processing technique, with the help of a scanning electron microscope from pipeline with or without damages.

The principal conclusions obtained from this investigation show the appearance of silicon in greater amounts than in reports generated on this type of steel, so the pipeline register superficial cracks that cause failures in the supplying system of drinking water.

Keywords: pipeline evaluation, SAE 1018 carbon steel, drinking water, digital image processing.

Introduction

The steel pipeline behavior evaluations used for the drinking water supplying are very important because of the failures that could appear and cause several health troubles among the population when the contamination of the vital liquid is possible, as well as the loss of money and infrastructure [12].

From a previous study by [3], from the point of view of corrosion of this system is obtained as a result, that the medium (drinking water) is not the cause of the material failure (steel), so it is necessary to consider the steel obtaining

process because of the presence of some chemical elements, such as silicon, in greater amounts than the allowable which can cause superficial cracks in the pipeline besides the health damages [5].

Silicon is used as an alloy element with steel. The fused steel is deoxidized and then added the most popular steel has less than 0.03% of silicon. The silicon-steel alloy that contains between 2.5 and 4% of silicon is used for the electric transformer core fabrication, because of the alloy presents low hysteresis features. The duriron alloy contains 15% of silicon, this alloy is hard, fragile and corrosion resistant, so is used in equipments that operate in chemical corrosion environments. The silicon is a copper, bronze and brass alloy element, too [10]. The steel classification includes carbon steel alloy, stainless steel, tool steels and low alloy steel. The carbon steel alloys contain several amounts of carbon and less than 1.65% of manganese, 0.60% of silicon and 0.60% of copper [2].

Sometimes carbon steel alloy one protected with zinc clad to in it is corrosion resistant properties and called as galvanized steel.

The steel alloys contain vanadium and molybdenum, as well as bigger amounts of manganese, silicon and copper than the carbon steel alloys. The stainless steel contains chromium and nickel. The tool steel contains tungsten, molybdenum and other elements that give more hardness and durability.

Low alloy steels (very resistant) have less alloy elements and its resistance is obtained from a special treatment in the mill obtaining [2].

So the purpose of this investigation is: to evaluate the steel pipeline (SAE 1018) behavior used to drinking water supplying with the digital micro photos processing of the interior surfaces

tool, with scanning electron microscope and detect the system failures.

Development

2.1. Background

Several investigations from this topic have studied fluids in pipelines as well as hydrocarbon. There are some precedents of the scanning electron microscopy using for the study of microbial corrosion in SAE 1080 steel from PEMEX [8].

Also exist on investigation projects from National Polytechnic Institute (IPN) with the help of the Michoacán's University at San Nicolas de Hidalgo, Morelia, Technological Institute of Superior Studies of Monterrey (ITESM) in order to look for control and reducing strategies for Mexican and Russian gas and oil pipelines failure for this purpose a new method includes the Kinetic theory to determinate the useful and residual life of these systems and the using of a X-Ray, microanalysis linked to another set of techniques for obtaining results [11].

Research work related to drinking water have focused on finding alternative supply of the vital liquid for human consumption, environmentally friendly, as reported by [6], which describes the production of an environmental good at lake Chapala drinking water supply to the City of Guadalajara, Jalisco, Mexico, through a simulation analysis with a network model.

After a revision of several scientists and technical investigations, we have not found the use of digital images processing technique to detect the silicon presence in steel pipelines that helps to find structural damages in drinking water pipeline systems.

2.2. Materials and Methods

With a scanning electronic microscope three 2 cm by 2 cm damaged specimens made from SAE 1018 steel have been studied as well as three undamaged specimens. The damaged specimen's images (figure 1, 2 y 3) were analyzed with a scanning electronic microscope, XL30 TMP New Look Model, PHILIPS trademark. With the purpose of determinate the quantity of silicon in the carbon steel alloy pipelines, we followed the X-ray analysis principles of the specimens after an electronic bombardment, and all this let us identify the existing elements and their concentration [9]. This chemical element appears as white irregular boundaries inclusions, deposited in several layers.

The 1, 2 and 3 images taken from damaged material and the 4 image of undamaged material analysis is made through a thresholding procedure [4], to show the silicon existence through the clearest images, and then quantify the surface percentage affected by this element. If an image do not show silicon existence (figure 4), it will show a zero value of surface with silicon.

Figure 1. Sample 1 shows a microphotograph inside the damaged carbon steel pipe SAE1018

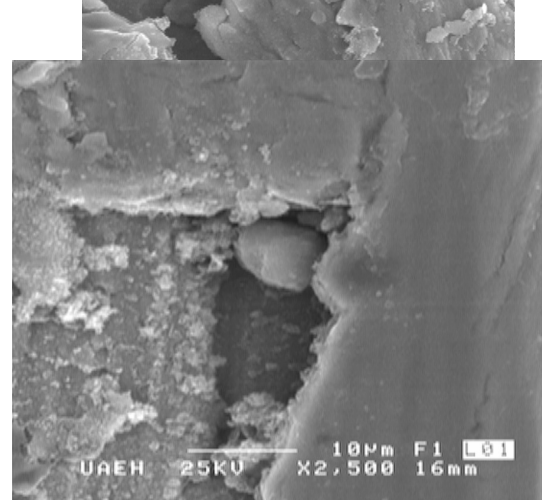


Figure 2. Sample 2 shows a microphotograph inside the damaged carbon steel pipe SAE1018

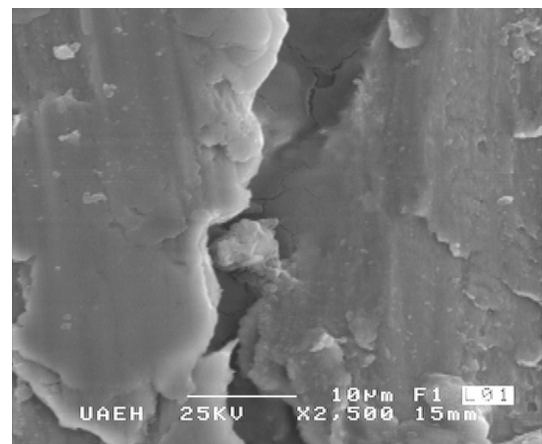


Figure 3. Sample 3 shows a microphotograph inside the damaged carbon steel pipe SAE1018

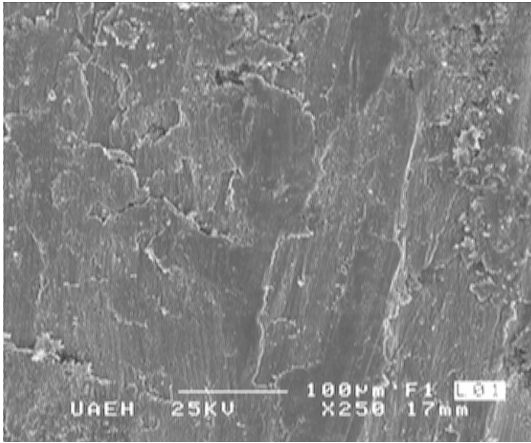


Figure 4. Sample 4 shows a microphotograph inside the undamaged carbon steel pipe SAE1018

Results and Discussion

On table 1, we show the results after the damaged samples images analysis taken with the scanning electron microscope and the X-ray microanalysis expressed in percentage by the amount of the elements contained in the alloy.

Table 1. SAE 1018 carbon steel alloy chemical composition with surface cracks

Element	% of weight
Iron (Fe)	79
Carbon (C)	0.15
Zinc (Zn)	5
Silicon (Si)	15
Manganese (Mn)	0.70

You can see that the silicon concentration on damaged carbon steel alloy specimens is greater than the normal amount of this type of steel [14]. This irregular silicon concentration is probably related to the homogenization time since the material still in a state foundry during the steelmaking process, which has prevented the distribution of silicon, is the same throughout the matrix material.

Table 2, shows the average results obtained after the undamaged SAE 1018 carbon steel specimens, X-ray microanalysis.

Table 2. SAE 1018 carbon steel alloy chemical composition without surface cracks.

Element	% of weight
Iron (Fe)	93.6
Carbon (C)	0.15
Zinc (Zn)	5
Silicon (Si)	0.35
Manganese (Mn)	0.70

Undamaged specimens show an average chemical composition of the alloy elements, expressed in parts by weight of each element and that are reported on NMX-B-324-2006 [7] Mexican regulation and in SAE-J403-2000 [13] and ASTM-A-510-2003 international regulations [1], so we can conclude that in this case our specimens have the quality features required.

Below are the processed images and three samples of damaged pipelines (Figures 5, 6 and 7) and the undamaged one (figure 8). The images have been size reduced by a cut view on their upper levels because of possible mistakes appearance in later calculations when white characters in the micro photos are showed. We have called it reduced images.

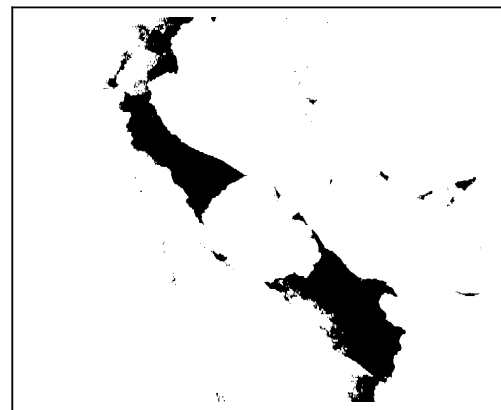


Figure 5. Microphotograph a sample 1 processed inside the damaged carbon steel pipe SAE1018

It's important to note that the measurements over the micro photos have been made considering the pixel area of the segmented surfaces, without the consideration of possible thickening of the silicon inclusions along the time in these pipelines.



Figure 6. Microphotograph of sample 2 processed inside the damaged carbon steel pipe SAE 1018



Figure 7. Microphotograph of sample 3 processed inside the damaged carbon steel pipe SAE 1018



Figure 8. Microphotograph of the sample processed without damage inside the carbon steel pipe SAE 1018

In accordance with the digital micro photos scale of 10 μm that is equivalent to 5.25 cm – measured with a 96 pixels per inch resolution screen- we calculated that the micro photos

resolution is of 20 pixels per micro inches. The average width of the cut images is 48.6 micro inches that are equivalent to 972 pixels of width. The average height of the cut images is 32 micro inches that are equivalent to 640 pixels of height. So the results is a maximum area of 622 080 pixels that are equivalent to 1555 micro inches. But the total amount of pixels of each cut image was exactly measured and we show them in table 3. The average percentage of inclusions in the three damaged images is 92.30 % that is so appreciable. In the three undamaged pipelines without silicon inclusions (figure 8) the average percentage of silicon is of 0.16 % and it is insignificant. The image analysis results are showed on table 3.

Table 3. Results of measurements of the area with deposits of silicon

Number	1	2	3	4
Condition	damage	damage	damage	undamaged
Size (px)	534, 612	532, 208	536 703	529, 840
Without inclusions area (px black)	47,909	37,350	38, 099	528, 942
number of independent inclusions	37	61	86	132
Inclusions area (px white)	486,703	494,858	498,604	898
Total parts by percentage (%)	91.03	92.98	92.90	0.17

In samples of the damaged pipes shows that the inclusions are distributed more or less evenly on the inside of the pipe, which shows that the problem is not casual or accidental, but that has been created by its own structural characteristics the material that the pipe has been manufactured.

Conclusions

After the test of carbon steel alloy pipelines used for drinking water supplying, some structural damages have been detected in the

SAE 1018 carbon steel used to fabricate these pipelines, these troubles are the consequence of silicon inclusions in the internal surfaces that then produce cracks and failures.

In accordance with the thresholding procedure used to extract the clearest images, we can quantify the percentage of silicon contained in the different surfaces of the specimens.

In summary, the high concentrations of silicon in SAE 1018 carbon steel alloy pipelines are the cause of several failures and cracks found in this type of pipelines.

Acknowledgments

The authors express their gratitude to the Teacher Enhancement Program for the financial support granted for the development of this research through project PROMEP UAEH-PTC-455 entitled: Process Monitoring System in the chemical industry, and Dr. Juan Hernández Avila of the Institute of Basic Sciences and Engineering (ICBI) of the Hidalgo's State University (UAEH), for their support in obtaining digital images using and testing taking from scanning electron microscopy.

References

- [1] ASTM-A-510-2003 Standard. *Specification for general requirement for wire rods and course round wire, carbon steel*.
- [2] D.W. Callister. *Materials Science and Engineering. An Introduction*. 5th. Edition. Department of Metallurgical Engineering. University of Utah. John Wiley & Sons, Inc., 1999, 8195 pp.
- [3] E. Bolaños, L.D. López, M.A. Veloz, V.E. Reyes y G.Y. Vega. *Evaluación del comportamiento de un acero al carbono utilizado en tuberías para agua potable mediante espectroscopia de impedancia electroquímica y microscopía electrónica de barrido. Memorias en extenso del XXV congreso de la Sociedad Mexicana de Electroquímica y 3rd Meeting of the Mexican Section ECS*, Zacatecas, México. 2010, pp. 593-599.
- [4] E. Felipe R., D. Suárez H. *Thresholding Method based on the Hmax and Hmin Morphological Operators, Series Research in Computer Science: Advances in Artificial Intelligence: Algorithms and Applications*, Grigori Sidoreov (Ed.), Vol. 40, CIC-IPN, 2008, pp. 83-94.
- [5] F. Rico. *La enorme importancia de la calidad del agua en la salud* [en línea], 23 de marzo de 2008 [citado en 20 de mayo de 2008]. Disponible para

world Wide Web:
http://www.dsalud.com/numero50_3.htm

[6] H.E. Bravo, J.C. Castro y M.A. Gutiérrez. *Producción de un bien medioambiental en el lago de Chapala y abastecimiento de agua potable en la ciudad de Guadalajara: un análisis de simulación con un modelo de redes. Ingeniería hidráulica en México*. Vol. XXIII, núm. 2, abril-junio de 2008, pp. 135-146.

[7] NMX-B-324-CANACERO-2006, norma de la industria Siderúrgica-composición química de los aceros al carbono- Especificaciones y métodos de prueba.

[8] O. Medina, Ortiza., V.H. Jacobo y R. Schouwenaars. *Corrosión microbiológica en aceros de bajo carbono. Ingeniería, investigación y tecnología*. Vol X, núm. 1, enero-marzo de 2009, pp. 9-19.

[9] OXFORD INSTRUMENT MICROANALYSIS GROUP. *Link Isis operator's Guide*. Oxford Instruments (UK) Limited Microanalysis Group. Vol. I, England, UK, 1997, pp. 1-14.

[10] P.L. Mangonon. *Ciencia de los Materiales. Selección y diseño*. México. Pearson Educación, Vol. 1, 2008, 824 pp.

[11] P. Tamayo. *Estrategias para controlar y reducir desperfectos en los sistemas de gasoductos y oleoductos mexicanos rusos* [en línea], primavera de 2005 [citado el 20 de agosto de 2005]. Disponible para World Wide Web:
[http://www.cuid.edu.mx/primavera_2005/presentacion es/IPN_Virtual_Internet_Tamyo.pdf](http://www.cuid.edu.mx/primavera_2005/presentacion/es/IPN_Virtual_Internet_Tamyo.pdf).

[12] R.S. Treseder. *NACE Corrosion Engineers Reference Book*. 2th. Edition, Houston. NACE International, 1991, 233 pp.

[13] SAE-J403-2000 Standard. Chemical composition of SAE carbon steels.

[14] V. Fernández. Tesis de Maestría. *Departamento de Ciencia de los Materiales e Ingeniería Metalúrgica*, Universidad Politécnica de Cataluña. 2004.

Soft real time Simulation of a DC motor considering Power Losses

J. S. Valdez Martínez¹, P. Guevara López², G. Delgado Reyes³

Abstract. This paper presents the modeling and simulation of a Series Wound DC Motor, in real time with their characteristic parameters and their mechanical, electrical and magnetic losses. This simulation was elaborated in Soft Real Time with SIMULINK, because the operating system is sharing the CPU time's. In addition, the simulation was compared with another one [Val09] where the model is linear, first order and with stationary parameters. Finally were obtained graphics from the implementation of system simulation.

Keywords - Simulation, losses, DC motor, Soft Real Time.

I. INTRODUCTION

A real-time system (STR), is that system which is related with the physical world and based on what surrounds it, may emit a series of correct answers, which are provided within established time intervals [MG09].

According to [MGC07] the Soft real-time systems are those where the response times are always in synchrony with the environment dynamics in all intervals of evolution and in certain sense of probability.

A physical system must have the following criteria to be simulated in real time: real processes interaction, issue of correct answers, synchrony with the processes, a convergence error bounded by a predefined value and the recursive expression to follow the dynamics of the process.

Due to the mentioned characteristics, in the case of a physical system (A DC motor), approximate results can be obtained by measuring the system's parameters. And they can be applied in the quality control testing development of DC motors without having to expose a real Electric Motor to destructive tests.

You can also apply for teaching purposes because the students could measure and supervise Electric Motor performance graphically [GVL09].

^{1,2,3} Escuela Superior de Ingeniería Mecánica y Eléctrica, Unidad Culhuacán – IPN, México D.F.

² Centro de Investigación en Ciencia Aplicada y Tecnología Avanzada – IPN, México D.F.

Teléfono (55) 57296000 Ext. 73250 E-mail:

jvaldezmtz@yahoo.com.mx

II. DEVELOPMENT UNIT

2.1 DC motor Fundamentals. The Electric model used is show in Figure 2 [Gue99].

Figure 1. Electromechanical circuit of DC motor series field Units (see Appendix)

Where were obtained the following equations:

$$\dot{\omega}(t) = \frac{ki(t)}{RJ} Ea - \omega(t) \left[\frac{b}{J} + \frac{k^2 i^2(t)}{RJ} \right] \quad (1)$$

$$i_a(\tau) = \frac{ea}{R + k\omega(\tau)} \quad (2)$$

$$T(\tau) = ki_a(\tau) \quad (3)$$

$$P_m(\tau) = \omega(\tau) * T(\tau) \quad (4)$$

$$P_e(\tau) = ea * i_a(\tau) \quad (5)$$

$$P_p(\tau) = P(\tau)_e - P_m(\tau) \quad (6)$$

$$\eta(\tau) = \frac{P_m(\tau)}{P_e(\tau)} \quad (7)$$

Within the DC motor components (The magnetic mechanical and electrical sections) energy is exchanged (From electrical energy to magnetic energy and vice versa) and in these exchange mechanisms, there are the following power losses.

- Mechanical Power Losses: Losses by friction (in the slip bearings and Brushes) and ventilation.
- Magnetical Power losses: Eddy current losses.
- Electric Power Loss: Losses by Joule effect.

And their mathematical representation are based on [Var82].

Friction Power losses in the slip bearings P_{RC} .

$$P_{RC} = 0.52 d_g l_g \sqrt{V_g^3} \quad (8)$$

$$d_g = 2.84 \sqrt{\frac{P_m}{n}} \quad (9)$$

$$l_g = 2.5 d_g \quad (10)$$

$$V_g = \frac{\pi n d_g}{6000} \quad (11)$$

Brush friction power losses P_{RE} .

$$P_{RE} = 9.81 \mu_e P S_e V_{col} \quad (12)$$

And:

$$V_{col} = \frac{\pi D_{col} n}{6000} \quad (13)$$

Ventilation Power losses P_V .

$$P_V = 1.1 V \cdot V_V^2 \quad (14)$$

Being V the amount of air in $[m^3/s]$, needed for machine's cooling and is determined by:

$$V = \frac{\sum \text{Pérdidas transformadas en calor}}{1000 t_e} \quad (15)$$

The temperature rise t_e of the cooling air passing through the machine, is given in $^{\circ}C$ (may be the increase of temperature in a time interval). The peripheral speed of the cooler fan V_V , is calculated by:

$$V_V = \frac{\pi D_V n}{6000} \quad (16)$$

Where D_V is the cooler fan diameter in $[cm]$.

Eddy current Power losses P_f .

$$P_f = \frac{w^2 [ea]^2}{12 \rho (NA)^2} \quad (17)$$

Where the cross-sectional area of the nucleus A is set considering the stacking factor. ρ is the resistivity of the material in $[\Omega \cdot mm^2/m]$, N is the number of turns of the winding and w is the width of the blade in $[m]$.

Armature copper Power loss (Joule effect).

$$P_{cu} = R i_a^2 \quad (18)$$

And based on these measurements, was developed in [Val09] a simulator, according to the features previously mentioned, it can be categorized as fast simulator (Simulation is NOT in Real Time). The Graphic interface Simulator's is shown below:

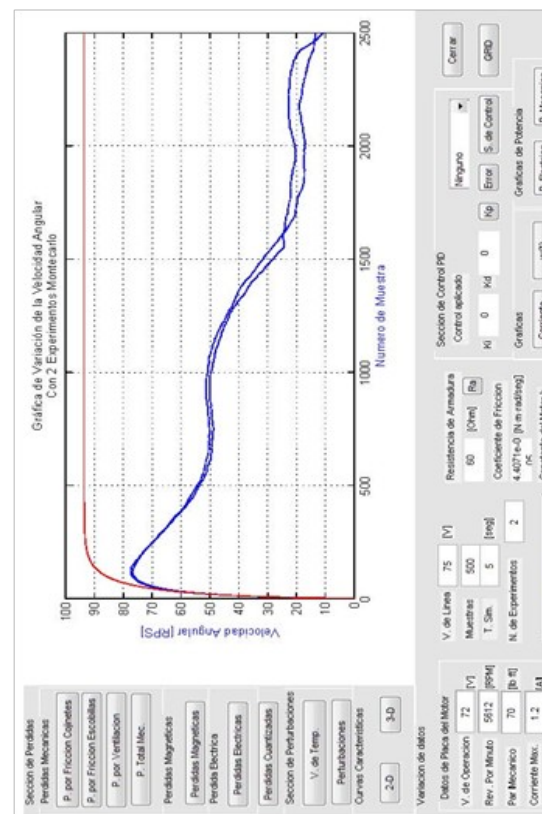


Figure 2. Graphical User Interface [Val09]. You can see two curves: ideal angular speed (color) and velocity perturbations ideal

Initially, the simulator provides the facility to graph the system parameters: the angular velocity, electric current, the electric motor efficiency and the estimation of temperature caused by the addition of disturbance (Added in the simulator model), deterministic (a Mechanical load that slows the motor) and/or non-deterministic (as may be the electric line noise or the internal noise)

2.2 A Electric Motor Soft Real Time Simulation considering Electrical, Mechanical and Magnetic losses.

According to [BK08], a simulator can be considered to work in real-time, must have the following characteristics:

- Deterministic response to disruptions
- Communication between processes
- High-precision timers
- Interrupt Handling

A real-time system provides to the user: **synchronization services** (The external real time with the Operative system time), **capture and interruption treatment** (it is a mechanism that is responsible for capturing interrupts when occur, and advise models or tasks that interest them such disruption is already present), **file management** (It is required because of depending on the system's behavior, sometimes is needed to get data or view data) and **measurement of real time** because in the Mathematical models, should know the actual time to do certain actions (Task).

In SIMULINK is possible to generate the asynchronous interruptions services (Warnings) to the Operating System with Async IRQ Source block.

To manage files, SIMULINK has a number of blocks that allows observe the system's behavior (with a Digital Oscilloscope) and is possible to save digital information obtained in Digital SINKS.

To the deterministic response to disruptions, in SIMULINK there are blocks that help to get information from external data (as well as interruptions), and there are blocks that help to give certain response to the outside, using data acquisition cards.

Then, the minimum time constraints (based on taking digital filtering according to [Gue01]) are the following:

- 1) The extraction and release of information observable and synchronized with the time evolution of the process by considering the sampling criteria [Nyq28].
- 2) Correct answers and bounded in time according to the time constraints of the dynamic system.

3) Ability to express recursively using models obtained from discretization methods (eg finite differences)

4) The value of convergence is bounded within a finite interval on which it is oscillating.

The mathematical model representing a DC motor series field is (1) discretized (expressed recursively) is:

$$\omega(t) = \frac{\beta \zeta + \omega(t - \zeta)}{1 + C \zeta}; i_a(t) = \frac{\gamma}{1 + F} \quad (19)$$

Where:

$$C = \frac{Rb + k^2 i_a^2(t)}{RJ}, \quad \beta = \frac{k i_a(t) ea}{RJ} \quad (20)$$

And:

$$F = \frac{k \omega(t)}{R}, \quad \gamma = \frac{ea}{R} \quad (21)$$

Entering the equation into machine code, we obtain the following program.

Table 1. MATLAB program (to determine execution times)

```

for MC=1:experimentos
for ejec=1:ejecuciones
    omega(MC,1)=0;
    tic;
    for n=1:1000
        F(MC,n)=(k*omega(MC,n))/R;
        ia(MC,n)=gamma/(1+F(MC,n));
        C(MC,n)=(R*b+k*k*ia(MC,n)*ia(MC,n))/(R*J);
        beta(MC,n)=(k*ia(MC,n)*eao)/(R*J);
        omega(MC,n+1)=(xi*beta(MC,n)
+omega(MC,n))/(1+xi*C(MC,n));
    end
    tiempodeejecucion(MC,ejec)=toc;
end
end
for tt=1:ejecuciones
    ejecucionMontecarlo(tt)=sum(tiempodeejecucion(:,tt))/numel(tiempodeejecucion(:,tt));
end

```

And these are the graphs:

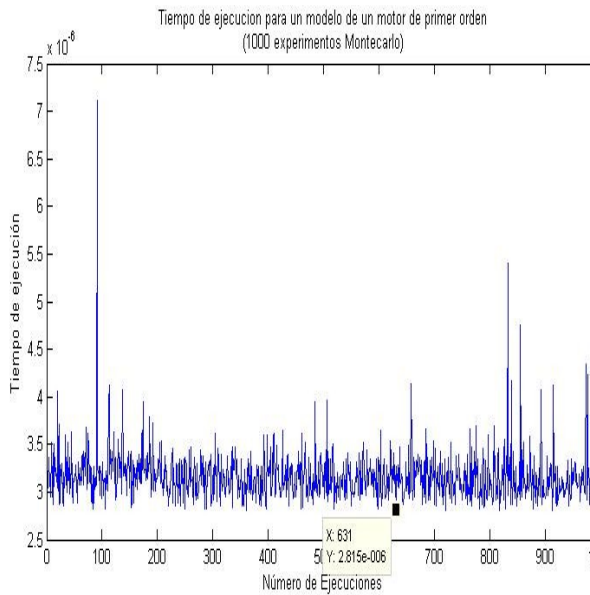


Figure 3. Graph corresponding to 1000 Monte Carlo experiments.
(Average Value 2.815e-006 sec.)

And using the block diagram in Figure 4, were obtained the time execution's (In a Oscilloscope).

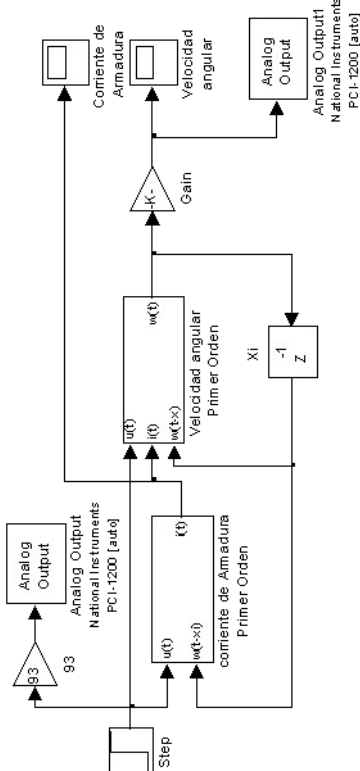


Figure 4. Block diagram in SIMULINK

And the time execution is:

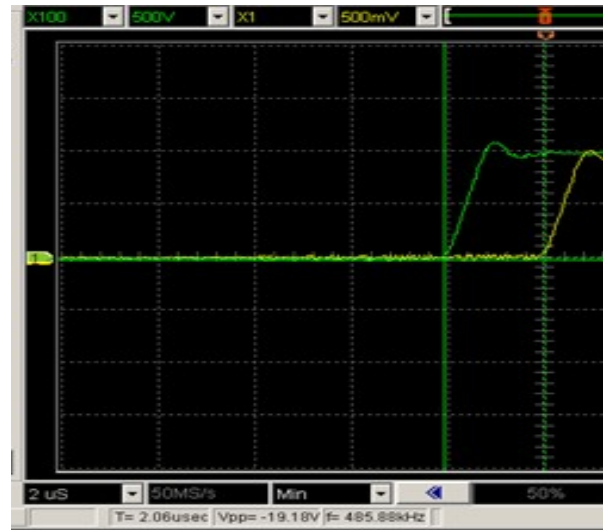


Figure 5. Time execution using an Acquisition Card NI PCI-1200
(Time execution 2.06e-006 sec.)

The time execution obtained using the Acquisition Card NI PCI-1200, is approximated to the values calculated by the MATLAB program. But not all the execution time values are equal, it is because to the processes which are working together and the same time that the MATLAB program, are sharing the CPU's resources with all of them and with this the Operating System is considered like a **Soft Real - Time System**.

And based on equation (1), is made a block diagram in SIMULINK (See Appendix 2), from where we obtain the following graphics:

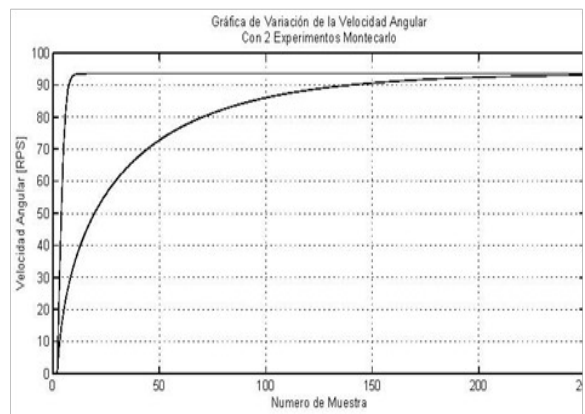


Figure 6. Angular speed[Val09]

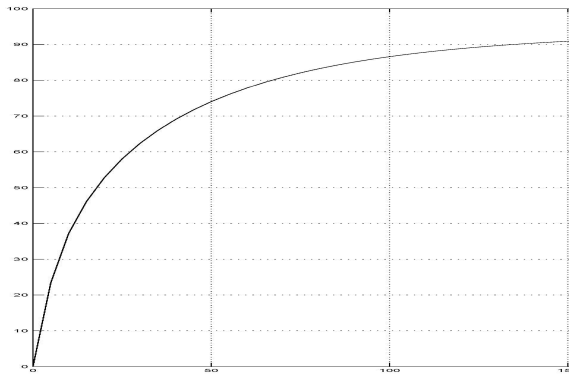


Figure 7. Angular speed (Soft real time simulation)

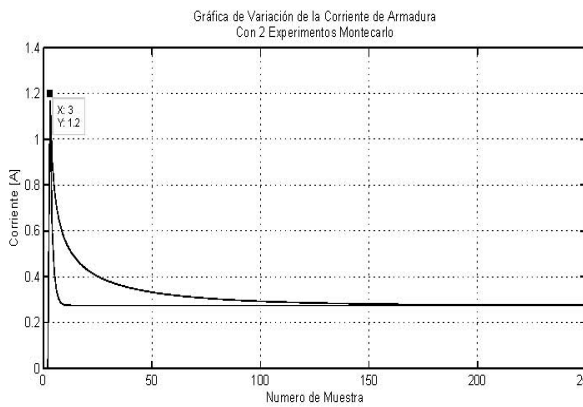


Figure 8. Electric Current Motor [Val09]

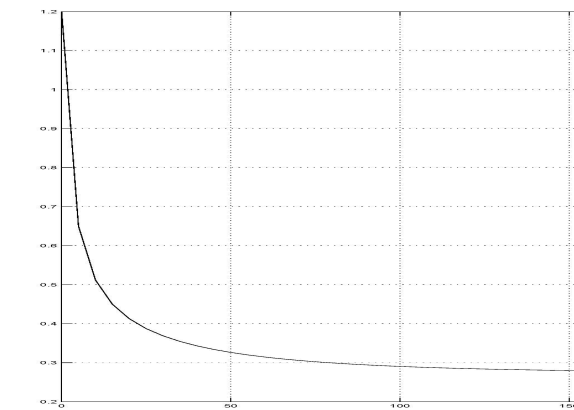


Figure 9. Electric Current Motor (Soft real time simulation)

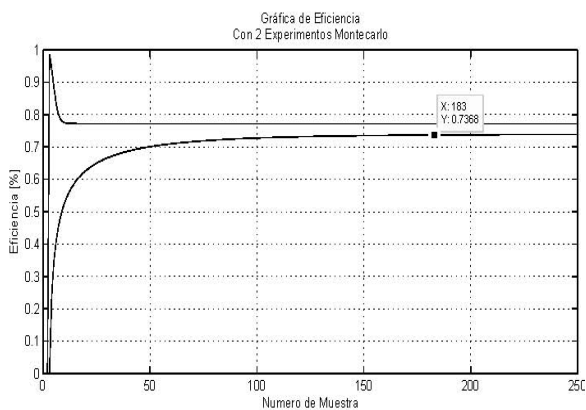


Figure 10. Efficiency [Val09]

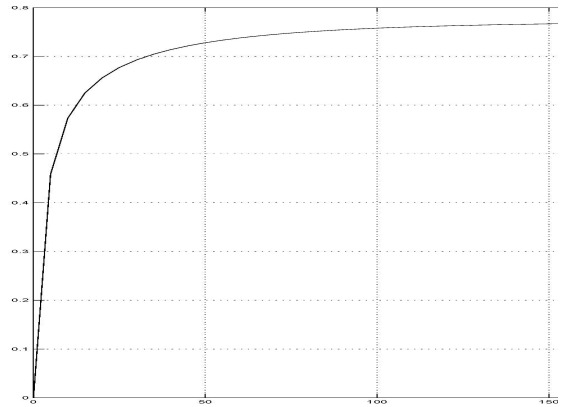


Figure 11. Efficiency (Soft real time simulation)

In a heuristic way, one can say that both systems coincide. And the Power losses have the following graphics:

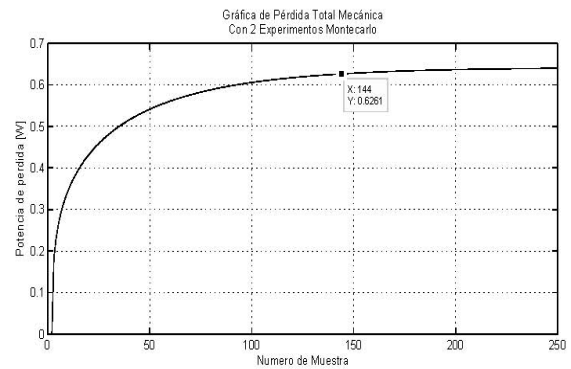


Figure 12. Mechanical Total Power losses

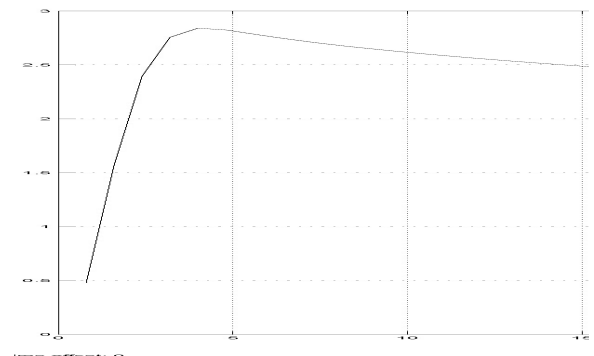


Figure 12. Mechanical Total Power losses (Soft real time simulation)

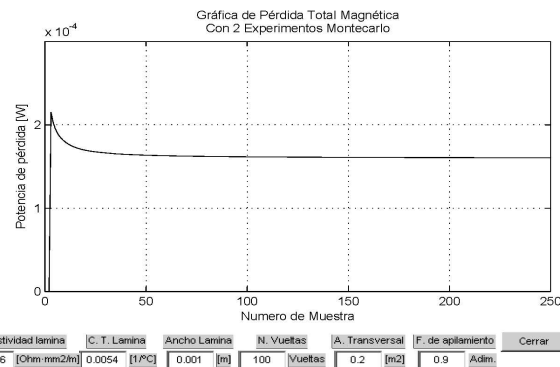


Figure 13. Magnetic Power losses [Val09]

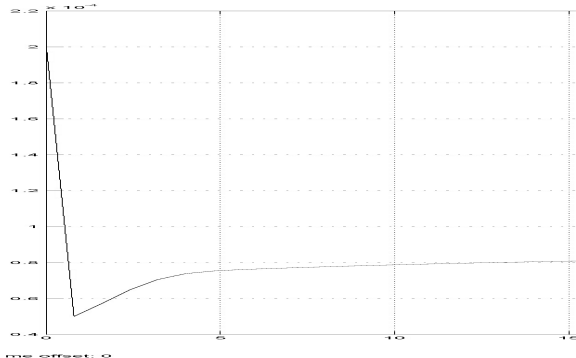


Figure 14. Magnetic Power losses (Soft real time simulation)

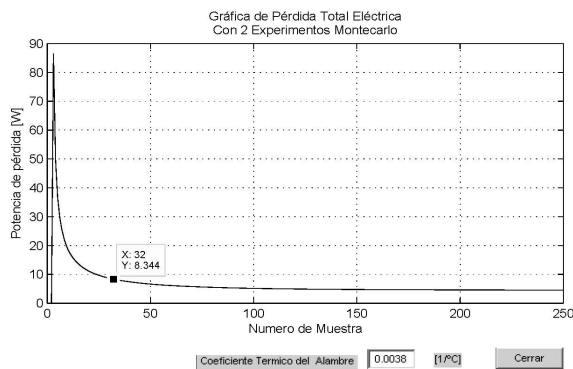


Figure 15. Electric Power Losses [Val09]

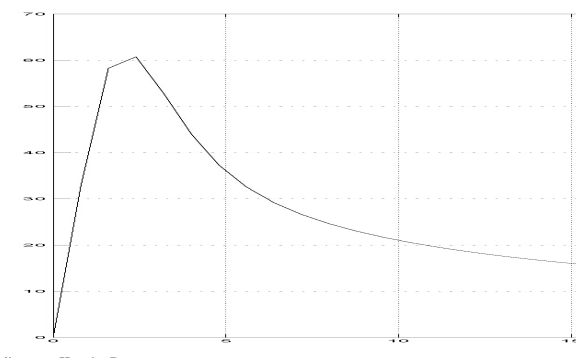


Figure 16. Electric Power Losses (Soft real time simulation)

III. CONCLUSIONS

There are striking differences between the simulator [Val09] and the Soft Real time Simulation. Their nature "fast", in [Val09] is not a good approximation, since the initial values system's was set and they are considered throughout the entire simulation and as such can not be regarded as a good simulation.

In particular for this work, the execution times of the Electric Motor algorithm tends to be very alternative (according to the figures observed) how the computing environment WINDOWS is multitasking can not give all system resources (both hardware and software) to the simulation. But this Electric Motor algorithm can be discretized (using Finite Differences) and can be expressed in recursive form (Depending on the previous state) and with this is possible to simulate in Real-time.

The power losses were characterized in the simulation but we can see that tend to vary from the original, this is because not all the mathematical models of the losses do not have the same convergence time, so in a period of time, the mathematical approximation should to have the same value.

IV. BIBLIOGRAPHY

[Val09]. Valdez Martínez J. S.

"Modelado discreto, Simulación, y Control de un Motor de Corriente Continua Tipo Serie Considerando: Pérdidas Mecánicas, Eléctricas y Magnéticas".

Tesis de Maestría, CICATA Legaria, México.

[MG03] Medel Juárez J. J. y Guevara López P.

"Introducción a los sistemas en tiempo real"

IPN

[MGC07] Medel Juárez J. J. Guevara López P. y Cruz López D.
"Temas Selectos de Sistemas en tiempo Real"

IPN

[GVL09] Guevara López P. Valdez Martínez J. S. y López E.

"Un Prototipo Virtual para la Enseñanza del Funcionamiento del Motor de Corriente Continua"

Congreso Internacional de Innovación Educativa, México

[Gue99] Guevara López P.

"Control de motores de corriente continua con capacidad de telecontrol y tele monitoreo".

Tesis de Maestría, CIC IPN México

[Var82] Vargas Prudente P.

"Problemas Resueltos de máquinas Sincronas: Conversión de Energía II"

IPN, 1982

[BK08] Bergero F. y Kofman E.
 "Desarrollo de un simulador de sistemas híbridos en tiempo real".
 XXI Congreso Argentino de Control Automático, Argentina

[Gue04] Guevara López P.
 "Filtrado Digital en Tiempo Real: Análisis Computacional para Estimación de Parámetros en Sistemas Estocásticos Lineales Estacionarios".
 Tesis de Doctorado, CIC IPN México

[Nyq28] Nyquist H.
 "Certain Topics in Telegraph Transmission Theory".
 AIEE Transactions, EUA.

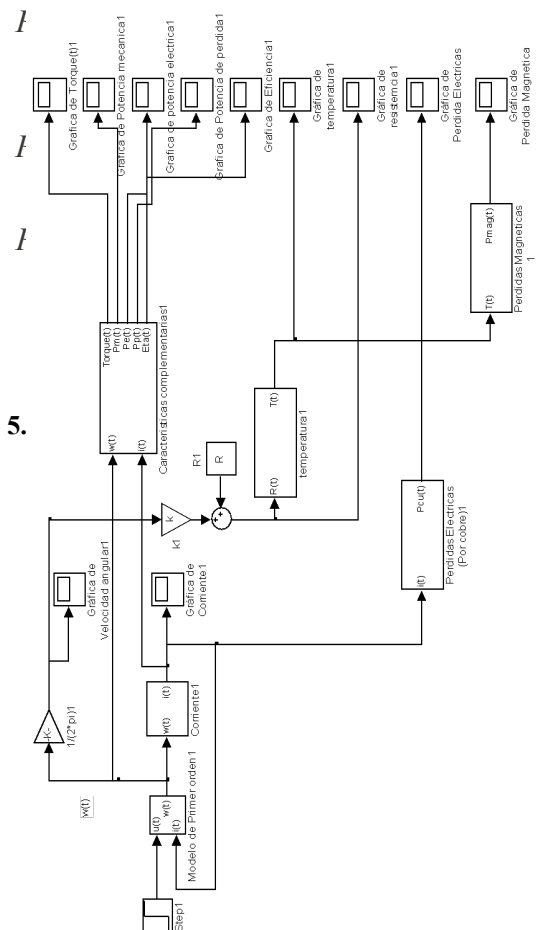
V. APPENDIX

5.1 Units

Symbol	Meaning	Units
$\omega(\tau)$	Angular Velocity	<i>rad/s</i>
<i>ea</i>	Voltage	<i>volts</i>
$i(\tau)$	Armature current	<i>Ampers</i>
$R(\tau)$	Total resistance	<i>Ohms</i>
$T(\tau)$	Torque	<i>N m</i>
$J(\tau)$	Moment of Inertia	<i>Kgm²</i>
<i>b</i>	Coefficient of viscous friction	<i>Nm/rad/seg</i>
ξ	Simulation sampling interval	<i>seconds</i>
τ	Time index of sampling	Non dimensional
<i>k</i>	Motor Constant	Non dimensional
$P_m(\tau)$	Mechanical power	<i>watts</i>
$P_e(\tau)$	Electrical power	<i>watts</i>
$P_p(\tau)$	Total loss power	<i>watts</i>

$\eta(\tau)$	Efficiency	Non dimensional
V_g	Peripheral speed	<i>[m/s]</i>
l_g	Length	<i>[cm]</i>
d_g	Diameter	<i>[cm]</i>
<i>n</i>	Speed	<i>[RPM]</i>
P_{RC}	Friction losses in the slip bearings	<i>watts</i>
μ_e	Brushes friction coefficient	Non dimensional

P	Specific Brush pressure	<i>Kg/cm²</i>
S_e	Brushes friction surface	<i>[cm²]</i>
V_{col}	Collector peripheral speed	<i>[m/s]</i>
D_{col}	Collector diameter	<i>[cm]</i>
P_{MR}	Mechanical losses	<i>watts</i>



Optimization of machining strategy for merging CAD-CAM-CNC-oriented manufacturing of complex parts

Eduardo Alejandro Ramírez-Yáñez ¹, Agustín Cruz-Contreras ¹, Domitilo Libreros ²

¹Departamento de Ingeniería Electrónica, CIITEC-IPN, México D.F., México

²Departamento de Ingeniería Eléctrica, SEPI-ESIME-IPN, México D.F., México

Teléfono (55) 5729-6000 ext.64346 Fax (55)5561-7536 E-mail: eramirezy0901@ipn.mx

Abstract

The purpose of this study is to develop a simple system for computer-aided manufacturing (CAM) for complex parts such as injection molding, reliefs, busts, and etcetera. Go directly to the computer-assisted drawing (CAD) to an automated machine at least three axes emulating a computer numerical control, without the need to go through the codes G & M and not have at our disposal a CNC machine, which avoid the human intervention to correct failures of CAM. For this, the machining strategy to take is to scan in addition that all time the machine takes into account the dimensions of the material block or yew, for getting the final feature, and its geometry, whose surface is constructed with a set of triangles and get stereolithography format (stl)

1.-INTRODUCTION

Today there are sophisticated tools that facilitate the manufacturing process, such as CAD / CAM / CNC, however, there is still a need for the intervention of a specialist to correct certain operations and instructions that computers do not satisfactorily resolved, this because in the programming of CNC's, only indicates the path that tool should describes, and certain parameters like feed rate, but the machine is unaware that the geometry of the piece, i.e. not "know" how is running the piece, and therefore errors of operation, as the collision of the tool to get from one point to another or machining errors, which is where the operator intervention.

In the case of complex parts manufacturing such as plastic injection molds, there are two ways to do it. First is through code, but it really is not very viable, to describe the tool path in order to create the desired shape, is tedious and tiring, because you have to simulate, review the code to correct and repeat these operations until reaching the desired piece, so this option is very unreliable.

However, to make this less tedious part of programming, there are many software that performs this operation to describe the path you should follow the tool and greatly facilitate the programmer's work, from the virtual drawing, but it is still necessary the intervention of a specialist to debug the program, also to parameter changes as tool size and the cutting speed, once finished the program correction, the file is sent to the CNC machine for machining.

The emergence of CAD and CAM were consequences of the need to facilitate the operation of computer numerical control machines, as do complex parts involving a large number of lines of programming in a specific language, it was essential to create programs indirectly in a more friendly and made the drawing and interpretation it to finally translate the language of G & M codes and perform the relevant manufacturing.

The close relationship between the CAD-CAM-CNC has created a very powerful tool to create almost any type of piece that seems more complex. And in this work is intended to achieve a merger integrates these three technologies to further facilitate the process of machining of complex parts without the intervention of a specialist.

2. - The CAD computer aided design

The manufacturing process begins with the drawing of the part, which includes at least two views (front and top), auxiliary, isometric and cuts views, if they are necessary, with their respective dimensions and annotations that completely define the features of the model to be produced.

Currently, there are drawing and design software specialized, which reduces the execution time and facilitate changes and updates to the dimensions and annotations. As you can see the part or parts in three-dimensional virtual reality models, observe it from different angles and even be able to do simulations of movement, fracture analysis, torsion, bending, etc..

Once the drawing is sent to the production department to manufacture the part, either with conventional machines or numerical control, if the last does not have CAD / CAM, there need to be specialized operators for each type manufacturing technology. In the case of CNC's, it must make a program which describes the tool trajectory.

3. - The CNC computer numerical control

The CNC machines are useful for manufacturing processes in medium scale and complex parts with precision. For management, it is necessary to make a specialized program where is indicated the tool path, feed rate, cutting depth, speed tool or workpiece rotation, and the development of routines, where the movement is cyclical, and this saves a few code lines.

With CNC's, even turning or router, and with combination of both, it can say that it is possible to manufacture any type of part, however, while more complex piece to manufacture, programming then becomes more long and tedious, since it depends heavily on the skill programmer to decide the strategy for machining process optimization, debug the program and review the possible faults that might exist with the tool trajectory, being given only possible account in the respective simulation, which is why CNC machines themselves have the primary disadvantage.

4. - CAM computer aided manufacturing

In the same manner as with the drawing, the CNC programming process for manufacturing can be simplified to a few minutes using the computer, implementing the so-called CAM, which the software interprets the drawing and programming performed using the G & M codes, and later, the programmer revise the lines and make changes to the possible faults and errors using simulation, and finally, implement the CNC and manufacturing.

Despite the great reduction of programming time, although there remains the need to debug the program, since it is not efficient translation. This is because the driver only knows how to make the piece through the G code axis motion, but does not know the geometry of it, coupled with that given their increasing complexity, manufacturers make their own extensions and especially that information is passed to the CNC controller is limited, affecting the development of advanced machining systems last generation

5.- The standard for the exchange of product model data STEP-NC.

Due to the problem of CAM software, the ISO "International Standards Organization" has recently developed a new standard for communication of CAM systems and CNC, STEP-NC [14], composed of two new rules: one, the ISO 14 649 [7] developed by the ISO TC184/SC1, where it defines a new model of high-level information for data exchange between CAM systems and CNC systems. The other rule arose from adaptation of ISO 14 649 into the methodology ISO STEP 10 303 (Standard for the Exchange of Product Data Models) [8], which has recently resulted in the publication of a new sub-part of the standard: ISO STEP AP-238 [2] [3] [4] [9].

In STEPNC as well tell the machine tool movements and technological information, they were informed the geometry of the construction characteristics

("features"). With this new technology will be a standards-based integration of CAD / CAM / CNC [10] [15] [11] as well as the development of more intelligent controllers [16]. Although STEPNC contemplated and geometry of the part for manufacturing, there will be an intervention by man, since there is a range of machining strategies designed to make it faster manufacturing. Added to which is subject to a numerical control machine, which in general terms, it is still unattainable for most manufacturing companies.

6 .- machining strategy for merging CAD-CAM-CNC.

The purpose of this study is to develop a simple system for computer aided manufacturing, without the need to have at our disposal a CNC machine, which avoids the intervention of human hands to correct failures of CAM, not create the intermediate step of G & M codes.

The proposed system consists of software - hardware and mechanism, where the first is responsible for the interpretation of virtual 3D drawing made in the CAD, the part to manufacture by scan machining strategy, is sliced 3D drawing on a number of 2D images was subsequently performed for image processing, that through hardware, the movements become relevant engines for the manufacture of the part, and which also takes into account the geometry of the part manufacturing process, Figure 1.

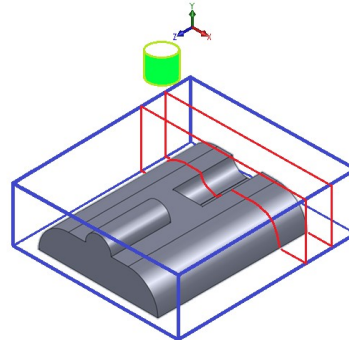


Figure 1.Part to make slicing the block

One way to know the geometry of the part, is using the STL format (Stereolithography), occupied by the 3D printer, where the surface of the solid generated by the CAD, is formed from a finite set of triangles (Figure 2), where it can get the location of each of its three vertices and the vector of the plane formed, information can be displayed in ASCII or binary code, so it is possible to determine the three-dimensional geometry where each triangle is located in space.

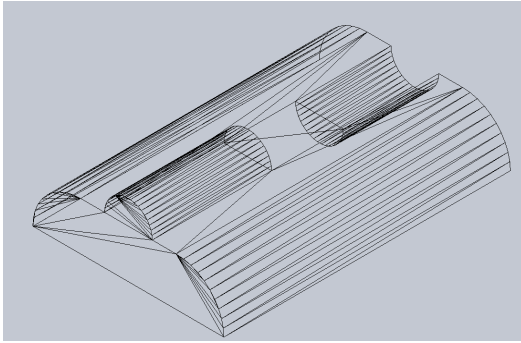


Figure 2. Stl file piece consists of 224 triangles.

Added to this, to facilitate the manufacturing process and mentioned above, the machining strategy is the scan, it means, if we observe the block to plot on top in the XZ plane, the cutting tool is positioned in the upper left corner, then moves the starting point to the right horizontally, the x-axis, once it gets to the other end of the piece, the tool moves down the z axis, being the amount of displacement equal to the size of the diameter of the tool, then the tool moves to the left and goes down again, this operation is repeated until the end, Figure 3.

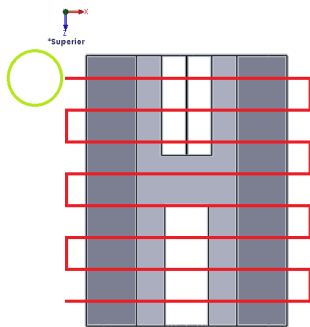


Figure 3. Top view, XZ plane.

Remember that the part has been sectioned into multiple slices, corresponding the slice width with the tool diameter, if you take the first slice and seen it in the XY plane, we have a profile or contour of the piece and as three areas around the contour of the part, 1, 2 and 3, as shown in Figure 4, the horizontal movement of the tool which could be seen in the XZ plane, in XY plane its motion is in x, y axes, because the tool, in general, follows the contours of the piece.

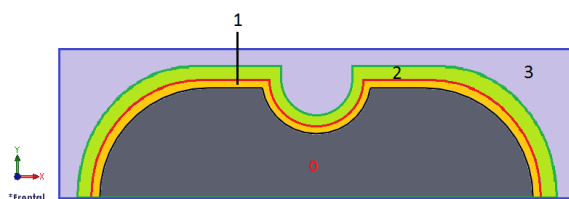


Figure 4. Front view of the first slice.

In the machining process, there are three stages,

carried out by a variety of basic and sophisticated strategies, such steps are: roughing, semi-finishing and finishing, and for each there are a number of parameters to be considered as block material to manufacture, shape, diameter, length and material of the cutting tool, cutting depth, speed and timing.

For roughing, the tool, usually robust, moves horizontally with a certain depth of cut (y_1), along the x-axis and through the area 3 until it to detect the area 2 and its trajectory changes and follows the contour until it is again in the same depth of cut (y_1), and continuous movement horizontally to find, either, again with other area 2 or leave the area 3, it means, block out a considerable distance, and later advance on the z-axis to the next slice and repeat the above procedure, Figure 5.

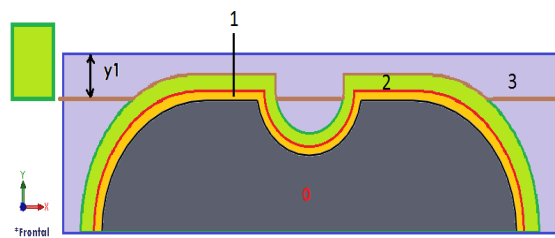


Figure 5. Firts cutting slice

Once finished with all the slices with the same depth of cut (y_1), repeat the process, where you can start over and do the scanning path in reverse, or start from the point of origin, the only unlike the cutting depth changes to a (y_2), occupying the absolute system, i.e. the depth of cut quantities are accumulated, the size remains the same, $y_2 = y_1 + y_1$. As shown in Figure 6.

It can be seen that there is in the semicircle, a part of area 3, that is because the machine knows the size of the cutter and the current geometry of the part, and according to the restrictions of roughing it is not possible cutting that area. In this way, you avoid the intervention of human hands to correct that possible error. Added to this, in the routes where it follows the contour profile and there is no material, it is possible to increase the feed rate to reduce machining time.

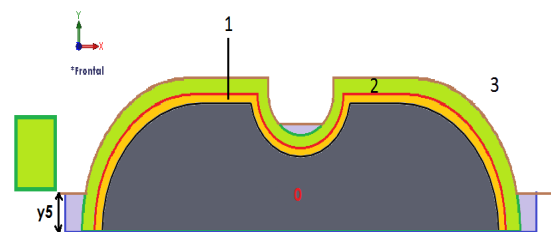


Figure 6. Corte roughing number 5

Once finished the roughing stage, it continues with the semi-finished, occupying a smaller tool, and considering the necessary changes to the same

parameters, obviously, the size of the slice is smaller, and their number increases.

It proceed with the transaction, now it knows that the area 3, as a whole no longer exists, so that the tool is positioned near the area 2 and start to move horizontally, with a depth of cutting (y_i) until meets the area 1 and changes its shape along its path until it leaves the area 1 and return to 2, the same procedure as in the rough.

In the case of area 2 crosses through 3, keep its speed, since there is still material that was not removed above and will continue its horizontal path until the end, Figure 7. At the end with this slice, advancing to the next and the operation is repeated until the end of the piece and the different depths of cut.

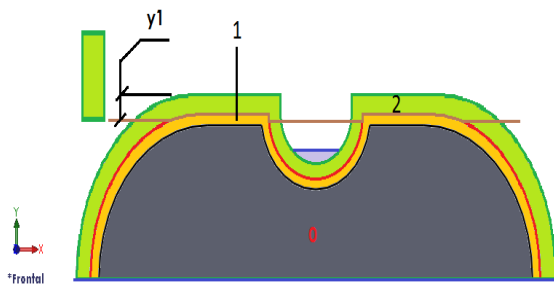


Figure 7. Proceso roughing

Finally, we reach the stage of completion, with a thin cutting tool and rounded tip, or straight, as appropriate, and necessary modifications to the parameters. The trajectory in this operation is to completely follow the contour of the part of each slice and moves to the next to finish and get a piece with a fine finish. Plus it's possible to change the way of slicing the piece, that is, rather than transverse slices, are longitudinal, this in order to give a better finish to the piece, Figure 8.

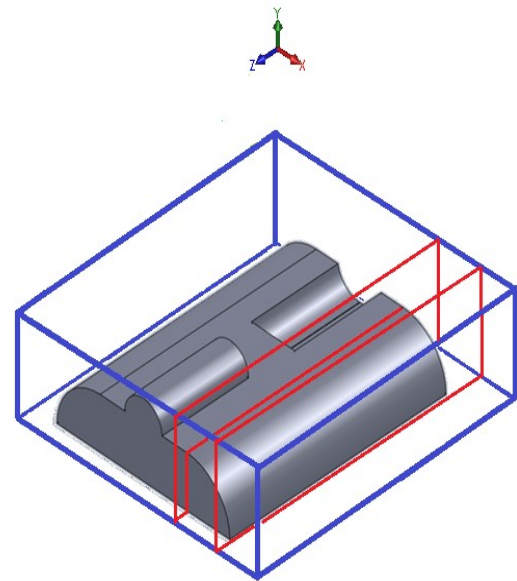


Figure 8. Changes of slices position.

The proposed method of the machining process has been worked only on one side of the block (the top), this indicates that the machine has three degrees of freedom, and that for some parts is enough to manufacture, but for others it you need to operate in the other faces that can be up five, because the bottom is intended to be the basis and subject to the workbench. To accomplish work in the other four remaining sides, it is necessary to add two degrees of freedom to facilitate the development of pieces like the one shown in Figure 9.

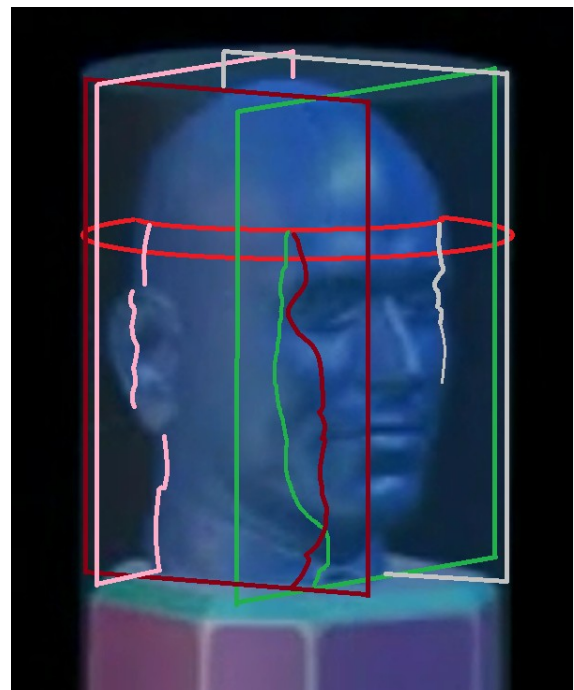
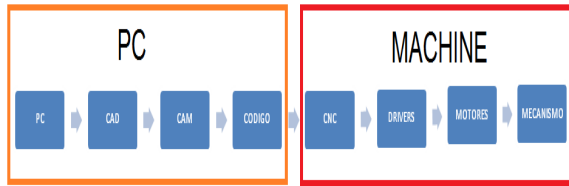
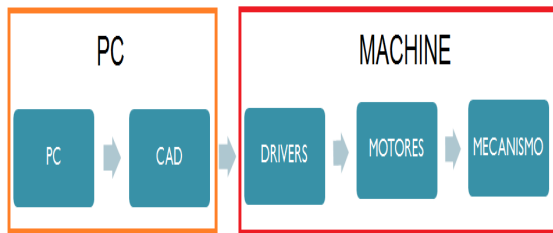


Figure 9. Five faces for operation

The CAD / CAM / CNC using the following procedure to manufacture a piece:



And the proposed procedure is as follows:



The machine to use is currently being built, the mechanism has three degrees of freedom, the spindles are packed and are moved by step motors, which will be connected to the PC through their respective drivers, Figure 10.

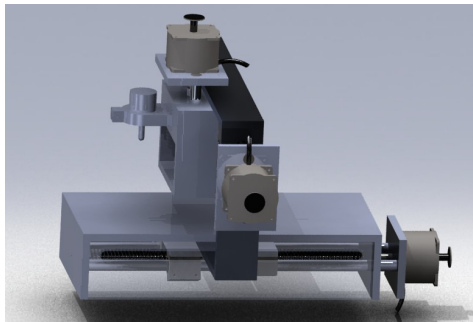


Figure 10. Modeling of three axes machine

This methodology is intended to make parts for plastic injection molds, metal sculptures, engraved in 2D, cutting board, and even for 3D printers.

Conclusions

It is possible to produce complex parts in a conventional machine would be impossible, with the direct path of CAD to the automatic 3-axis, that means not having to build a program G and M code, either manually or by software, and without need for a CNC machine. With a technology that avoids the intervention of a specialist and without investing too much money

References

[1] Albert M. (2000). STEP NC - The End of GCodes? Modern Machine Shop, July 2002, 70-80

[2] Hardwick, M., Loffredo, D. (2001). STEP into NC. Manufacturing Engineering, 126, 38-50.

[3] Hardwick, M. (2004). On STEP-NC and the complexities of product data integration. *ACM/ASME Transactions on Computer and Information in Science Engineering*, 4, 60-67.

[4] Hardwick, M., Loffredo, D. (2006). Lessons learned implementing STEP-NC AP-238. *International Journal of Computer Integrated Manufacturing*, 19(6), 523-533.

[5] IMS (2001). IMS Project 97006 (STEP-NC). STEP_NC STEP-compliant data Interface for

Numerical Controls. On-line, Acc. Feb. 2007: http://www.ims.org/projects/project_info/step_nc.html.

[6] ISO (1982). Numerical Control of Machines — ISO 6983-1, 1982. Numerical Control of Machines — Program Format and Definition of Address Words — Part 1 Program Format and Definition of Address Words — Part 1: Data format for positioning, line motion and contouring control systems, ISO TC 184/SC 1, Geneva, Switzerland. [1]

[7] ISO (2000). International Organization for Estándarization, ISO/DIS 14649-10, 2000. Industrial automation systems and integration – Physical device control. Data model for computerized numerical controllers. General process data. ISO TC 184/SC1, Geneva, Switzerland. [2]

[8] ISO (1994). ISO 10303-1:1994. Industrial automation systems and integration – Product data representation and exchange – Part 1: overview and fundamentals principles. ISO TC 184/SC 4, Geneva, Switzerland. [3]

[9] ISO (2002). ISO 10303-238:2002. Industrial automation systems and integration - Product

data representation and exchange – Part 238: application protocol: application interpreted model for computerized numerical controllers. ISO TC 184/SC 4, Geneva, Switzerland. [4]

[10] OMAC (2005). STEP-NC Pilot Demonstration. OMAC STEP-NC Working Group Meeting, Disponible Online, Accedido en Febrero 2007: www.isd.mel.nist.gov/projects/stepnc/omacorlando-2005/pilot-scenario.pdf.

[11] STEP Tools (2006). ST-Developer on line manuals. On-line. Accedido February 2007: http://www.steptools.com/Support/stdev_docs/.

[12] Suh, S.H., Cho, J.H., Hong H.D. (2002). On the architecture of intelligent STEP-compliant CNC.

International Journal of Computer Integrated Manufacturing, 15 (6), 168-177.

[13] Weck, M., Wolf, J., Kristis, D. (2001). STEPNC: the STEP compliant NC programming interface: evaluation and improvement of the modern

interface. *International IMS Forum*. Ascona , Switzerland.

[14] Xu, X.W. (2006). Realization of STEP-NC enabled machining. *Robotics and Computer-*

Integrated Manufacturing, 22 (2), 144-153. [5]

[15] Xu, X.W. He, Q., (2004), Striving for a total integration of CAD, CAPP, CAM and CNC. *Robotics and Computer-Integrated Manufacturing*, 20(2), 101-9.

[16] Xu, X.W. Newman, S.T., (2006). Making CNC machine tools more open, interoperable and intelligent – a review of the technologies. *Computers in Industry*, 57 (2), 141-52.

[17] A. Sokolov, J. Richard, V.K Nguyen, I. Stroud, W. Maeder P. Xirouchakis. (2006) Algorithms and an extended STEP-NC-compliant data model for wire electro discharge machining based on 3D representation. *International Journal of Computer Integrated Manufacturing*, 19 (6).

[18] I. Stroud, P. Xirouchakis. (2006). Strategy features for communicating aesthetic shapes for

manufacturing. *International Journal of Computer Integrated Manufacturing*, 19 (6).

Researching and design of solar module maximum power capturing technique using microcontroller

Jaime Vega Pérez, Ma. Guadalupe Calderas Patiño*, Jaime Vega García**

Escuela Superior de Ingeniería Mecánica y Eléctrica Ticoman del I. P. N.

ABSTRACT

An alternative technique for the capture of the maximum power from a photovoltaic module (PV) is reported, by sweeping of PV module current-voltage curve, using a capacitor and an electronic switch connected in serial to reflect variable capacitive impedance. The technique is verified with the electronic circuit that captures and processes the current-voltage signals using a microcontroller (PIC) to determine the maximum power and controls the charging and discharging capacitive impedance. Experimental results indicated the electronics prototype designed works rightly.

Objective

Researching and design an electronic circuit to detect the maximum power point of a photovoltaic module.

1 Introduction

The PV generator is an electronic device that converts visible light into direct current electricity, its current generated describes a exponential law [1], and its value increase with the level of light intensity incident on device area and its conversion is efficient, the common PV modules located in the market are made of mono crystalline silicon, its efficient order is of 15 -16% and polycrystalline silicon which has an efficiently of order of 10 but is cheaper than mono crystalline cell. The voltage generated follows a logarithmic law [1] so its value is more permanent, the order of .56 V to a unitary cell in open circuit conditions to low sunstroke of mornings and afternoons.

Due to the cell is an element of low power, to activate an electric equipment was necessary to make an photovoltaic module (PV) which has 32 to 36 cells connected in serial, depending on the manufacturer so that the voltage is increased, the module was designed to charge a car battery [2] so its nominal voltage is self regulated from 11 to 16 V, the current depends on cell size, for a cell of 5 inches of diameter in silicon mono-crystalline is about 3.4 A, for a polycrystalline wafer silicon of 10 x 10 cm is about

Av. Ticoman 600, San José Ticoman, México D. F., 07340, México,
57.29.60.00 ext.
jvegap@ipn.mx

*Secretaria de Investigación y posgrado del I. P. N., México D.F., México

**Escuela Superior de Ingeniería Mecánica y Eléctrica Zacatenco, México D: F., México

2.6 A and the power depends on the module size. PV modules have a wide application in marginalized rural areas where don't have conventional power, for this reason is required electronic circuits of signaling and control to improve the functionality of installed systems.

Due to the output electrical power of the cells or modules change depending on the level of light and decreases by the temperature increase, and its electrical power is maximum only in a minimum margin of its current – voltage curve [3]. When the solar system was designed, the nominal power reported on the manufacturer handbook is selected, but this is measured at 25 °C and 1000W/m² of incident light on PV module, but in real condition working, the temperature of the module increases up to 1.75 times the ambient temperature [1], and the light level is variable, this causes electrical uncoupling between the electrical equipment that we are working with the PV module, because the lighting level and temperature are changing, then a shift in the maximum power point is caused, which results power loss. So, for this reason, it is very important to detect the maximum power point, because it is an important data for the engineer who designs the solar system.

2. Proposal measurement technique

A sweeping technique of the current-voltage curve of the generator is proposed, using the capacitive electrical device coupling to the PV module, to achieve the analog scanning of the I-V curve and detect the maximum power point, without loss energy by dissipation, and so to eliminate the power dissipation of the module in the measurement process, it is coupled to the PV generator a capacitive impedance (Fig 1) whose magnitude changes from 0 to the order of 20 K Ω , This capacitor will be charged by PV module current through an electrical switch (I_1), which is controlled by an electronic circuit using a micro controller (PIC) that detects the maximum power point. It is designed on base the property of self-regulation of the PV module, and the capacitor property to present variable impedance. When the charging process starts, the PV module is placed in

the short-circuit condition, after the value of the capacitor impedance increases during the charging process, crossing the characteristic current – voltage curve of the generator to put into the open circuit condition through the maximum point (Fig. 1).

The sweeping of the I-V curve of the PV module is obtained, previously it must be safe that the capacitor is discharged when the process starts, the switch open and the PV module is in open circuit condition, when the circuit is closed, the capacitor in an instant presents impedance 0 to the module, so the PV module supplies the maximum current (I_{sc}) for the point of short circuit.

As the capacitor charge, increases the impedance that reflects to the module, this reduces the current and increases the voltage (Fig. 2), while samples from current and voltage are captured by the electronics circuit, when it reaches the maximum power point opens the switch. After the capacitor is discharged into a battery and starting the process again.

3. Electronic circuit

The circuit is basically integrated by an sensing stage with a capacitor of 4700 micro Farads, a Mosfet transistor and a resistor of .1 Ohm for the current sampling, by amplifier stages for the current-voltage signals using operational amplifiers of instrumentation, in this case was used the circuit CA308, a microcontroller integrated circuit through a controller interfaces periferic (PIC), using the 74F187 of Microchip, an driven stage and a display stage, we have a block diagram of the power measurer (Fig. 3).

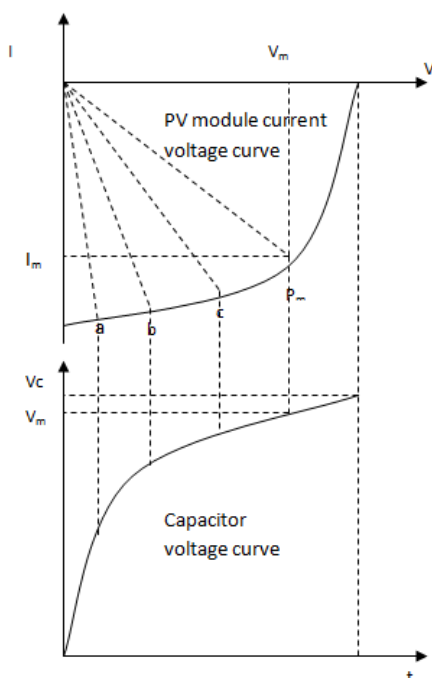


Fig. 1 PV module current-voltage curve and capacitor voltage curve

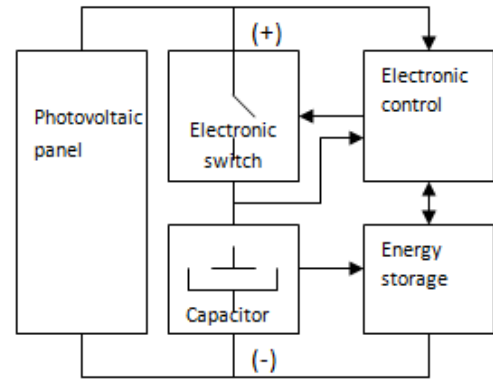


Fig. 2 Block diagram of the capacitive impedance connected to PV module

We can see that all electronic system works on base of a microcontroller, which is programmed to send at the begin a high voltage pulse to activate the switch S2, and the capacitor C is discharge, after sends a high voltage pulse to close the switch S1 and the charge process of the capacitor C is started, immediately its digital – analog converter transforms the analog current and voltage samples to digital samples and makes the product, after reads the next pair of samples and determinates the power, after the last power value is compared with the previous power until finds the maximum power point, in this instant the microcontroller sends a low pulse and the switch S1 is turned off after the information is displayed, the electrical energy storage into the capacitor is discharged toward the battery and the process starts again.

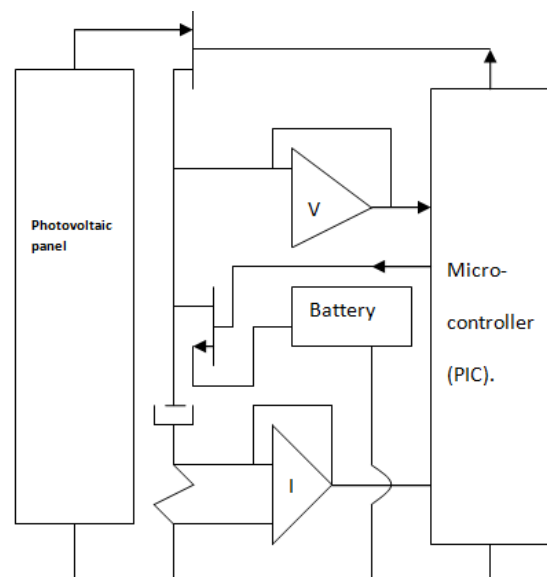


Fig. 3 Block diagram of the control electronic circuit

4. Software design

A Software in assembler language was designed (Fig. 4) in order to activate the microcontroller (PIC), for this, the initial conditions and the labels of the microcontroller were delimited, the input – outputs ports were configured to activate the switches, also the analogical converter was configured by 3 analogical buss, 2 pins of output ports were able to activate the switch. The measurement process start when the microcontroller sends a high voltage pulse to B switch an then the capacitor is discharged, after the converter is activated to read current-voltage samples, the PV module power (P_i) is made the current voltage product and is stored, the next current-voltage pair samples is read and the product P_{n+1} is calculated, the values of P_i with P_{n+1} are compares, if P_i is less than P_{n+1} the microcontroller must access others samples, but if P_i is greater than P_{n+1} then the information is displayed, after the microcontroller waits 0.001s and start the process again.

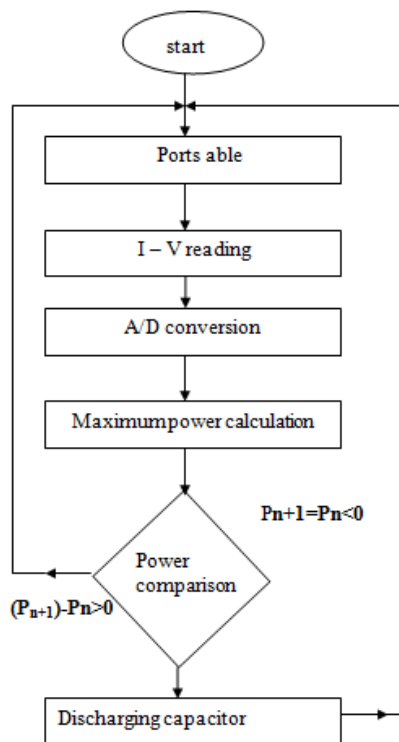


Fig. 4 Flow diagram of the microcontroller program

5. Implementation

Were used amplifier stages using operational amplifiers of instrumentation of low noise, offset voltage, and drift voltage were designed, selected the circuit MC1420, for sensing the current signal was used a factor amplification of 50, and for the voltage an attenuation factor of 0.5, driver stages were

implemented using general purpose transistors, also it was used the microcontroller 16F678, which has an analog digital converter (A/D), this has an resolution of 10 bits, has a pulse modulation and works with a wide frequency rate, up to 500 MHz. The microcontroller was programmed using a computer and also Microchip software, to simulate the correct working. The clock operation frequency of the microcontroller was 500 MHz.

6. Experimental results

To verify the correct operation of the circuit were made previous measurements of waveforms at the outputs of the amplification stages, the voltage pulses at 2 outputs microcontroller and the capacitor voltage, the signal waveforms are shown. (Fig. 5).

Also was made previous measurements of current (I_m) and voltage (V_m) at outputs of amplifiers and power (P_m) indicated in the display of the circuit, were taken different insulation levels, and with a temperature of module of 25°C, see Table 1.

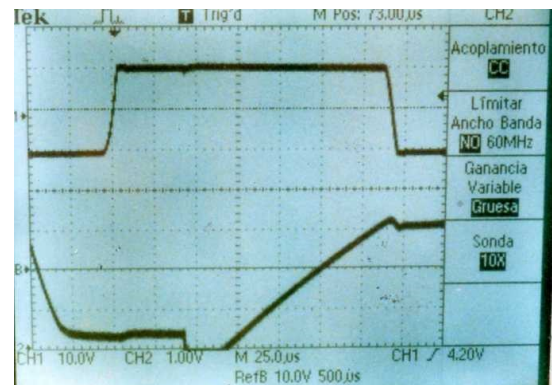


Fig. 5 Experimental waveforms

Light level (W/m^2)	Maximum power (W)	Current (A)	Voltage (V)
935	17.6	1.12	15.36
790	14.45	1.01	14.17
710	14.55	0.9	13.58
615	9.98	0.75	12.74
500	9.92	0.74	11.42
410	6.51	0.62	10.13

Table 1. Experimental results about measurements maximum power

7. Conclusions

The measurement of the maximum power of the solar module, through the sweeping of its current voltage curve, using an external capacitor and control electronics circuit, to change the electrical impedance to the module is right, because the power dissipation is reduced.

The electronic circuit is considerably reduced with the use of the microcontroller, and its working form is more sure, because its behavior is based on a computer program, and although the prototype was designed for low power, measurements was made with 20 W, the power rate can be modified with the same technique of measurement and control logical.

As future work, it will be necessary to take more measurements and electrical test to improve the designed electronic circuit, and also the electronic circuit for power transfer will be developed.

Acknowledgements

The authors are grateful to the project of SIP –IPN No. 20100500 for the financial support.

References

- [1] Vega P. Jaime “Method of design of photovoltaic systems, a proposal”, MA thesis, PESTIC IPN, México 1998. Pp.72-79, 86-88.
- [2] Alan R. Miller. “Improved photovoltaic battery chargers for lower maintenance and higher efficiency”, IEEE Photovoltaic Specialists Conference proceedings, pp. 400-404, 1982.
- [3] Vega Perez J., and Volodymyr Ponomaryov. “Photovoltaic module maximum power detection electronic circuit”. Journal of Telecommunications and Radio engineering, ISSN 0040-2508, Begell House, Inc. Vol. 56, No. 1, 2001, pp. 126-134.
- [4] Millman Jacob, “Microelectronics Digital an Analog Circuits and System”, McGraw Hill, 1979.
- [5] Stout David and Kaufman Milton. “Handbook of Operational Amplifier Circuit Design”. McGraw Hill, 1976.

Signals acquisition and processing for corrosion control in carbon steel pipelines used for potable water supply

Technical Area: Signals Processing.

Abstract

This work deals with the monitoring of physical variables influencing the corrosion process suffered by SAE 1018 carbon steel pipelines used for potable water supply in a region of Hidalgo State, Mexico, by means of a data acquisition card (DAQ) from four sensors: conductivity, pH, chloride concentration, and temperature, and supported by a graphical user interface through LabVIEW 9.0. The obtained main results show the potable water is not the cause of the possible faults or cracking in the carbon steel pipelines.

Key Words: Carbon steel SAE 1018; Signals digital processing; Potable water.

Introduction

Corrosion phenomenon is a deterioration process suffered by metallic materials and their alloys in presence of an aggressive medium through chemical or electrochemical reactions [4], which generates considerable economic, material, environmental and human losses if the system is not controlled [2],[8].

Metallic material at contact with watery solutions (potable water) constitutes an environment that fundamentally is associated with corrosion problems due to the medium's ionic conductivity, reason why generally occurs an electrochemical-type corrosive attack. Among the main factors influencing the corrosion phenomena, whose presence causes whole or partial loss of material, are the pH and oxidizer mediums that frequently are powerful accelerators of the process or sometimes could retard the deterioration due to rust formation on surface or oxygen layers absorption that turn it resistant against chemical attacks and temperature [1].

In this way, it is necessary to take into account techniques that facilitate the obtaining of real time information about the physical variables behavior, such as water's ionic conductivity, pH, chloride concentration, and

H. Lara-Ordaz¹, E. Bolaños-Rodríguez², J.M. Ramírez-Hernández³, J. Bautista-López⁴, G.Y. Vega-Cano⁵, E. Flores-García⁶
^{1, 2, 3, 4, 5, 6}Escuela Superior de Tizayuca, Universidad Autónoma del Estado de Hidalgo, Km 2.5 Carretera Federal Tizayuca-Pachuca, C.P. 43800, Tizayuca, Hidalgo, México.
Correo-e: 1herbertlara@hotmail.com, 2bola7112@yahoo.com.mx, 3jose_manuel1704@hotmail.com, 4jobaulo@yahoo.com.mx, 5gaby@uaeh.edu.mx, 6etizayuca@gmail.com

temperature. The necessity of signals digital processing has great importance in our days, so that, it is very important to acquire data of signals coming from outside, generally from transducers located in different systems of production and/or manufacturing, through cards connected to the computer. Nowadays, processing via computer and visualization of data acquisition via software are essential in the monitoring and operation of control systems, which due to their complexity level and necessity could be required, providing of an interaction between the user and the system.

The main objective in this work is to monitor the corrosion suffered by SAE 1018 carbon steel pipelines used for potable water supply, by using DAQ the four sensors: conductivity, pH, chloride concentration, and temperature; supported by a graphical user interface developed (GUI) through Lab VIEW, in order to detect and predict faults in the system.

2. Development

2.1 Background Research

In the world of the electronic and the scope of monitorized of variables including in the control system.

Today in common observe a computer show the data acquisition by specific purpose software. In this way the monitorized of system includes multiple variables in accordance with study case, between some common like pressure, conductivity, pH, concentration, temperature, level, spending, humidity, among other.

Measurement Engineering should be highlighted signals captured by sensors that help control certain process. So the signals acquired are based on electrical measurements without differentiating are continuous or discrete, are all considered analog signals, for example to acquire a temperature through a thermocouple should measure a voltage drop or a current flowing through the bimetallic joint. If this electrical signal is referred to a distant site, the voltage or current measured is probably not exactly the value, because the electrical

conductor offers some resistance and that affect the measured value, to compensate this difference should be in waypoints or elements that maintain the value of the signal, this type of analog signal is easily affected by external means to induce noise.

Today is imposed conversion of the analog signal into digital analog converters that must be located close to the sensor or primary element measuring, then this digital signal can be sent without suffering many alterations. [3]

When increase the rate of data acquisition and the advantages of silicon technologies, large amounts of data must be transferred to the PC for processing. These transfers are handled by the data bus connecting the device to the PC memory. However, the rate at which data transfer occurs is often the bottleneck in measurements, and is the main reason that many instruments have incorporated expensive memory on the card. [6]

The type of data acquisition system, analog or digital depends on the use of recorded data. In general, analog data systems are used when required bandwidth or inaccuracy can be tolerated. Digital systems are applied when the physical process under study has a little variation (narrow bandwidth) and when this needs a high accuracy and low cost per channel. Digital systems vary in complexity from single-channel systems for measuring and recording voltage automatic systems to multiple channels, which measure a large number of input parameters, compare them with respect to predetermined conditions or established limits, are to perform calculations and make decisions about the input signal. Digital systems are generally more complex than analog, both in terms of volume and complexity of the input data can be handle [9]

The variables involved in the control systems are manifested as analog signals, preserving this nature, is difficult to process them by today's digital devices, to solve this problem made use of digital processing, using current electronic systems, thus it is possible make a monitorized of different variables that denote the behavior of systems and provide elements for decision making process. This point is the importance of the work presented, the aim is to provide a base system that is capable of acquiring data from external signals from various sensors, which in the productive sector can be found in different sections of a system manufacturing, digital processing through a DAQ and provide a friendly environment for the submission of information by software through the computer, as shown in Figure 1.

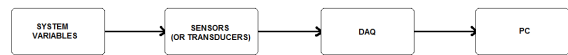


Figure 1. Esquematic diagram for data acquisition.

2.2 Materials and Methods

The carbon steel pipelines SAE 1018, have the next composition, expressed in percent of weight; iron (93.6%), carbon (0.15) zinc (5%), silicon (0.35) manganese (0.70) inter alia.

This work was develop using a NI USB-6229 M Series card, this card has 32 input channels, resolution of 16 bits and velocity of 250 KS/s.

The software used was LabVIEW 2009 from National Instruments.

The method employs in the acquisition of dates of the physical variables involve in this work consist in measurement values through of adecuated sensors for each specific case; the sensors provides an electrical signal output measure that provides information that denoted the behavior of the variables monitorized.

The electrical signals provides from sensors are connected to input channels in the DAQ and an already communication through of a GUI developed in LabVIEW, it shows the values taked of the input variables. The obtained record lets the visualization in numerical form or behavior graphical of the variables in question conductivity, pH, concentration of clorures and temperature.

Were obtained 672 samples, each one is taked by hour the 24 of day in a period by four weeks for each variable.

The data history is generated in the computer connected at DAQ through VI (virtuals instruments) configure to save values by hour.

3. Results and Discussion

The results obtained referring to conductivity variable is displayed in the figure 2. The behavior average from data for this variable takes a value of 76.1 mS/cm and a standard deviation close to 0.3 mS/cm, what evidence low dispersion and the concentration of dissolved calcium salts, carbonates, sulfates and phosphates are high, this favors the presence a passive layer on the carbon steel pipelines in

the system what inhibits the corrosion process.

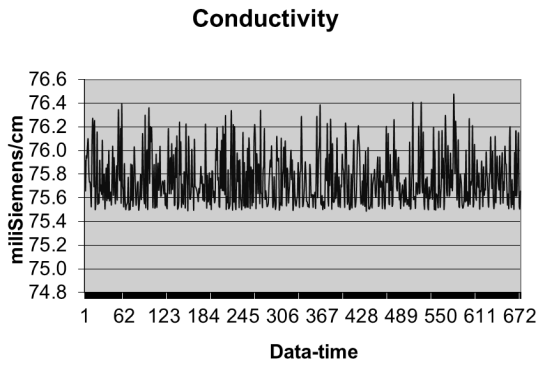


Figure 2. Behavior of Conductivity.

The figure 3 show the tendency of pH variable; can be seen the average is 7.1 and a standard deviation of 0.4, this value is considered minimum variation and it is match with reference [7] where indicated neutral pH or close neutral, the carbon steel is immune.

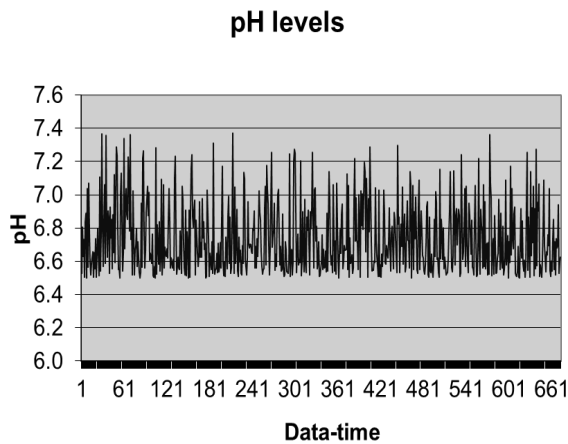


Figure 3. Behavior of pH.

The case of variable or chloride concentration factor, the average result in 6 mg/L, standard deviation 0.4 mg/L; the dispersion is not much and this means than in the presence of chloride ions in the environment, their effect in the corrosive process is obstructed by passive layer of salt forms, this result is evidence by visual inspection than there is not manifestation of bites on the surface in the pipelines. Show figure 4.

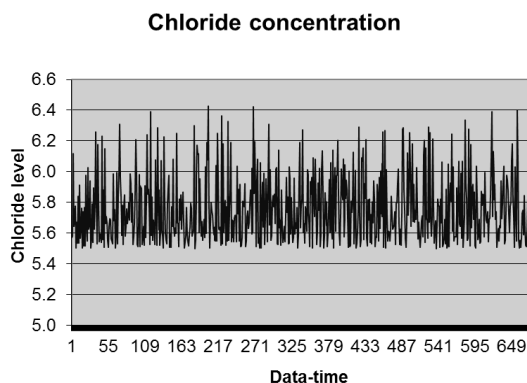


Figure 4. Behavior of Concentration chloride.

The figure 5 show the behavior of temperature variable, the average is 24.5°C, the standard deviation about 1.5°C, the system functions in environment temperature and this operations conditions have not any influence in the corrosion velocity of carbon steel SAE 1018.

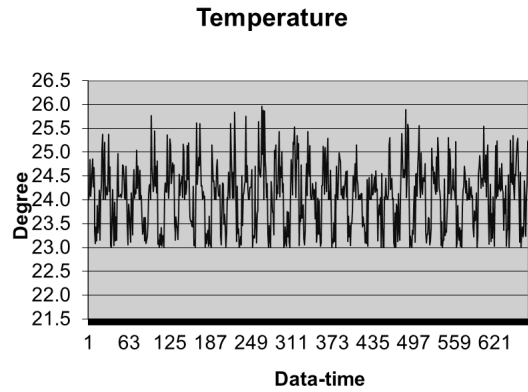


Figure 5. Behavior of Temperature.

4. Conclusion

The results obtained by acquisition card about four parameters by four sensors: conductivity, pH, chloride concentration and temperature and GUI display from LabVIEW allow us to predict: The operation under existing conditions in the monitoring periodic, the environment or potable water does not cause of failure, steel cracking and other signs of corrosion than could happen in the carbon steel SAE 1018 used in supply potable water from Hidalgo region studied.

Acknowledgment

This work can be made by financial support from project PROMEP UAEH-PTC-455 monitoring system to process in chemical industry.

References

- [1] E. Bolaños, L.D. López, M.A Veloz, V.E. Reyes, G.Y. Vega. *Evaluación del comportamiento de un acero al carbono utilizado en tuberías para agua potable mediante espectroscopia de impedancia electroquímica y microscopia electrónica de barrido. Memorias en extenso del XXV Congreso de la Sociedad Mexicana de Electroquímica y 3rd Meeting of the Mexican Section ECS, Zacatecas, México, mayo-junio de 2010, pp.593-599.*
- [2] F. Rico. 23 de marzo de 2008, *La enorme importancia de la calidad del agua en la salud*, 20 de mayo de 2008, http://www.dsalud.com/numero50_3.htm.
- [3] M. Guzmán. 20 de abril de 2008. *TEC ofrecerá nueva carrera de Ingeniería Mecatrónica*. 25 de mayo de 2009,

<http://www.tec.ac.cr/sitios/Vicerrectoria/vie/Documents/InvestigaTEC/investigaTEC%20N%C2%BA6.pdf>.

[4] M. Morcillo, S. Feliú, J.M. Bastidas, *Electrochemical studies of lithium intercalation in $Zr_xTi_{(1-x)}$* , *Rev. Iberoamericana de Corrosión y Protección*, 14, No. 2, Madrid, 1983, pp. 367-379.

[5] M. Pourbaix, *Lecciones de Corrosión Electroquímica*, 1ra. Edición, Instituto Español de Corrosión y Protección, Madrid, 1987.

[6] National Instruments. 20 de abril de 2010, *Introducción a PCI Express*, 28 de mayo de 2010, <http://zone.ni.com/devzone/cda/tut/p/id/5926#toc1>.

[7] P. L. Mangonon, *Ciencia de los Materiales. Selección y diseño*, Pearson Educación, Vol. 1, México DF, 2001.

[8] R.S. Treseder, *NACE Corrosion Engineers Reference Book*, 2nd edition, NACE International, Houston, 1991.

[9] William D. Cooper, Albert D. Helfrick, *Instrumentación Electrónica Moderna y Técnicas de Medición*, Editorial Pearson, Prentice Hall, 1^a Edición, New Jersey, 1991.

IMPLEMENTATION OF A QPSK MODULATOR TO DVB-S TRANSMITTER THROUGH FPGA

Abstract - The QPSK modulation has been implemented using analog methods with acceptable results. But now with the development of tools for both software and hardware for digital signal processing is possible to consider the implementation of a QPSK modulator using devices such as are the FPGA, whose characteristics make it possible in data processing at high frequencies. This article tries to explain the method by which QPSK modulator was implemented on FPGA for use in a DVB-S transmitter.

Key words — **Modulation, QPSK, FPGA, DVB-s.**

David Vázquez Álvarez, Hernández Grande Miguel Ángel, Luna Ponce Rubén.
Departamento de ingeniería en Comunicaciones y Electrónica
ESIME Zacatenco IPN, México, D.F., México.
Teléfono: (55) 57296000 Ext. 54553. E-mail: dvazqueza@ipn.mx

1. Introduction

DVB-S is a member of the family for the DVB Digital Video Broadcasting, is defined as the European standard as EN 300 421. In particular, this specifies the type of modulation (QPSK) and channel coding systems used for standard TV and HDTV, to be used as primary or secondary distribution. Table 1 shows some characteristics of the main DVB standards.

<i>DVB standard</i>		<i>DVB-S</i>	<i>DVB-C</i>	<i>DVB-T</i>
A/D	Codificación fuente	MPEG-2	MPEG-2	MPEG-2
Digital encoder	RS	204,188	204,188	204,188
	Entrelazado	12 bytes	12 bytes	12 bytes
	Convolutcional	½	½	½
D/A	Filtrado	Nyquist	Nyquist	Nyquist
	Modulador	QPSK	QAM	OFDM

Table 1. Characteristics about the DVB standards [1].

As you can see, the property in these standards differ is the type of modulator.

DVB-S is intended to provide direct television services known as DTH (Direct-To-Home) decoder device IRD (Integrated Receiver Decoder) as well as collective antenna systems. DVB-S is suitable for use in different bandwidths of the transponder and is compatible compression format MPEG-2 television services.

DVB-S transmitter consists of several blocks as shown in Figure 1.

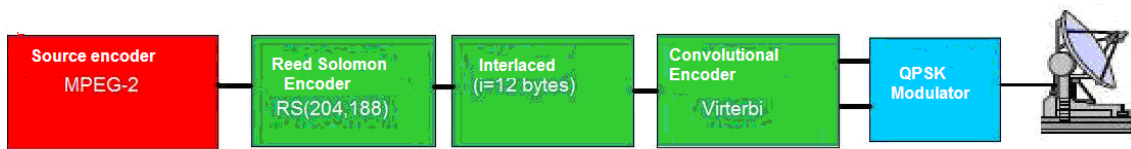


Figure 1. Stages of a QPSK transmitter.

The aim of this paper is to show how the QPSK modulator was implemented in FPGA as part of the proposed DVB-S transmitter [2].

2. QPSK Modulation

The phase modulation is a version of frequency modulation in which the phase of the carrier wave is modulated to encode bits of digital information in each phase change.

With QPSK modulation are four possible output phases, for a single carrier frequency. Because there are four different output phases, there must be four different input conditions. Since the digital input to a QPSK modulator is a binary signal, it takes more than a single bit of input. With two bits, there are four possible conditions: 00, 01, 10 and 11. Consequently, with QPSK, binary input data are combined in groups of two bits is generated by one of four possible input stages.

In essence, a QPSK modulator are two modulators, BPSK, combined in parallel.

Phase	Data
45°	00
135°	01
225°	11
315°	10

Table 2. Correspondence between phases and data.

With QPSK, since the input data are divided into two channels, the bit rate on channel I or Q channel is equal to half the input data rate ($f_b / 2$). Consequently, the fundamental frequency, the higher is present in the data input to the balanced modulator, I, or Q, is equal to one quarter of the input data rate (half of $f_b / 2$: $f_b / 4$) [3].

3. QPSK Simulation in MATLAB



Figure 2. Outline the operation of Xilinx System Generator tool [4].

Our goal is to implement a QPSK modulator using FPGA. QPSK modulator design was developed using the Xilinx System Generator tool platform with Matlab / Simulink as shown in Figure 3. The prototype is shown in Figure 3, which consists of blocks to process information and to obtain the modulated signal. It is possible, using the Xilinx System Generator tool to verify the design behavior using measurement

instruments that Simulink provides. But before this is important to know that both Simulink and MATLAB handle different types of format for the management of information and consequently it is necessary to block called gateways that are provided by Xilinx System Generator whose function is precisely that there is compatibility between the blocks Xilinx System Generator and Simulink.

For the modulator to work is important to provide signals such as: Clock sync source of information and two sinusoidal signals in quadrature one over the other.

These signals were generated using Simulink blocks such as Scope's for displaying the signals (Figure 4), adders, constant, and a clock source and a generator to simulate the binary Bernoulli source.

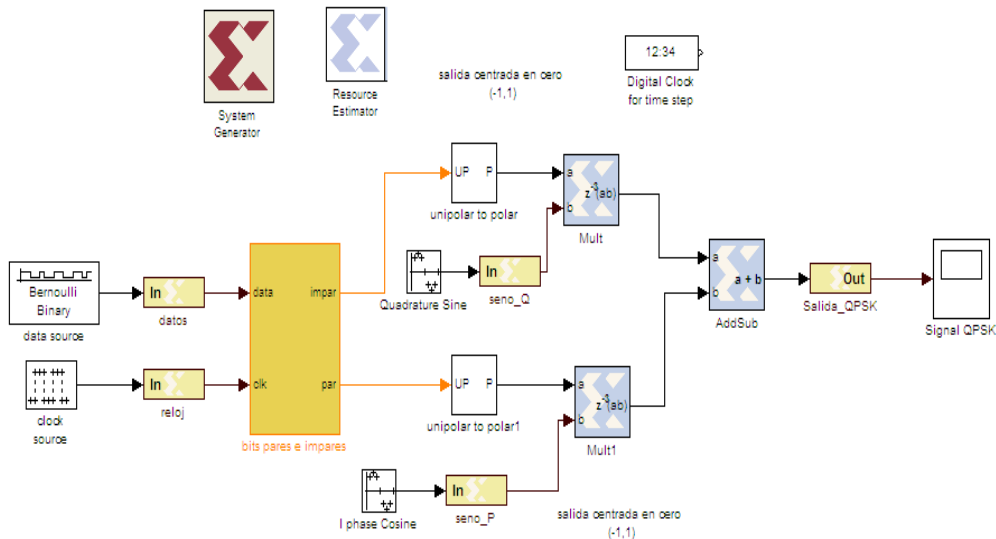


Figure 3. Implementation of Xilinx System Generator modulator in Simulink platform.

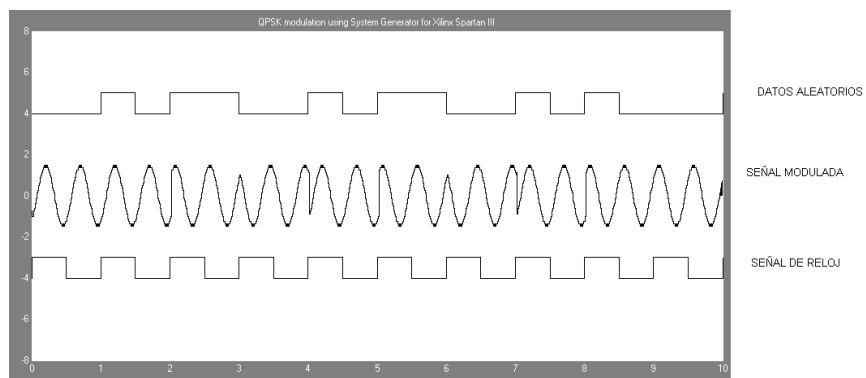


Figure 4. Results obtained in Simulink simulation where you can see the model performance.

4. Implementation

Once created and verified the design, we proceeded to the generation of HDL code from Simulink model. The code generated by Xilinx System Generator will be processed by the Development Environment for Xilinx ISE which is responsible for making the code verification and to generate the file for recording the FPGA.

All locations (physical points for connections) input and output of the modulator must be defined during design or during revision Simulik in ISE.

The necessary signals are described below:

4.1 Source of information.

For the module to work correctly requires the clock signal and the signal source, which will be emulated by a PIC microcontroller [5].

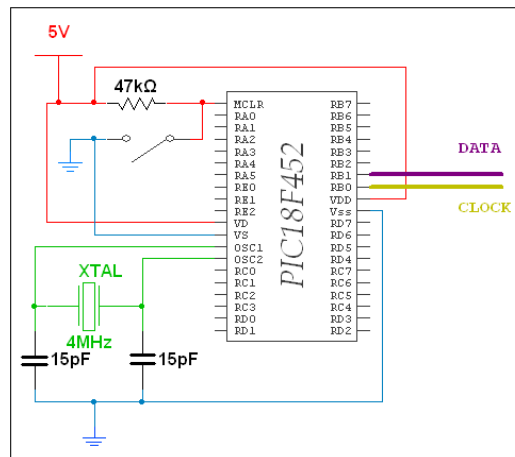


Figure 5. Signal generator circuit and the clock source.

The chart above shows the circuit used to implement the source of information and the clock signal which should have a sync frequency.

The microcontroller deliver two signals for Port B (bit 0 and bit 1). This was programmed in C18, and the generated program is aimed at generating a random bit which simulates a source of information, which as you know their behavior is random. Additionally aims to generate a clock pulse which is synchronized with the signal information.

```
while (1) {

    Delay10TCYx(n);
    PORTBbits.RB0 = !clock;

    if(random()<=1){PORTBbits.RB1 = 1;}
    else{PORTBbits.RB1 = 0;}

}
```

}

The above snippet is responsible for the generation of clock signals and information.

4.2 Outside oscillators

The QPSK modulator needs two sinusoidal signals, which must be 180° out of phase with respect to each other, in this case the modulator requires that these have digital signals, for this reason these were generated by a microcontroller.

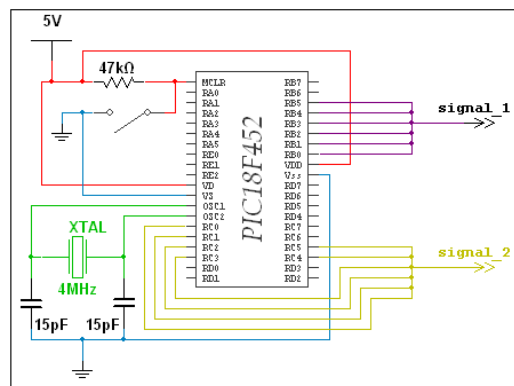


Figure 6. Digital oscillating circuit.

In the figure above shows the circuit implemented to generate sinusoidal signals. The microcontroller deliver two six-bit buses (one for each signal) which are coupled to the FPGA using a special format called 6-bit fixed point. Each signal is delivered to the modulator via port b and c respectively.

For the generation of the code was necessary to sample and quantize the period of a sine wave, which we generated a sequence of 6-bit code, finally the sequence was adapted to fixed-point format for compatibility with the modulator.

4.3 Encoder and digital/ analogical converter.

Once the signal was modulated is necessary to process the signal by a conversion from digital to analog format. Before carrying out the digital to analog conversion is necessary to couple the signal into six-bit fixed point format accepted by the converter circuit using an encoder.

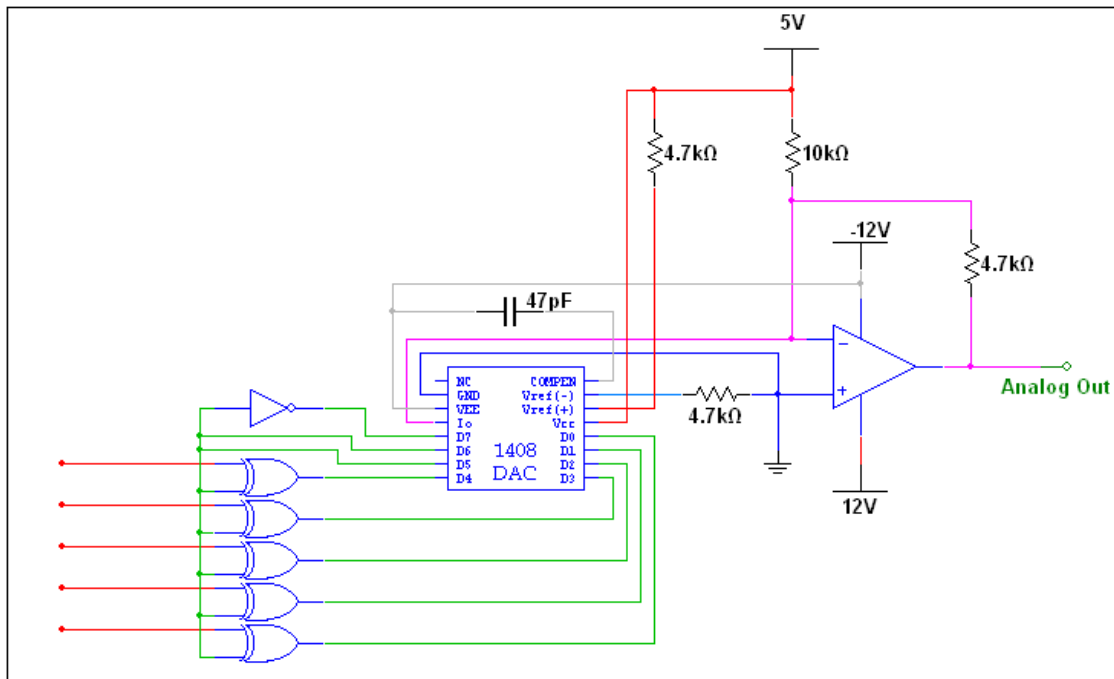


Figure 8. Digital-analog converter.

The encoder will provide a code 8-bit format accepted by the converter, so that later this do the conversion. In this case, use a converter circuit with a resolution of eight bits which eventually will result in the modulated analog signal [7] [11].

4.4 Modulator

The modulator was implemented on an FPGA development board SPARTAN 3. The signals are connected physically to the card according to the assigned locations during the design. We must remember that as mentioned in the chapter on simulation, the format accepted by the blocks of Xilinx is the fixed point, and therefore the signals are represented by buses will have to have this format so they can be correctly interpreted by the FPGA. This detail is provided to program the microcontrollers and the encoder of the D / A, so it was not necessary adjustments in hardware.

5. Tests and results

The final design of Figure 8 was implemented on Spartan 3 development board, which was recorded once our design was verified. Subsequently connected input signals and the converter D / A. The results of the FPGA were compared with results obtained with the Simulink tool of Matlab.

Figure 8. Shows the results of tests on the implementation. What you see in Figure 8 is the QPSK modulated carrier for repetitive data entry. The check was to observe the signal shown in the output of the D / A on the oscilloscope and compare it with the simulation in Simulink. The results were very similar.

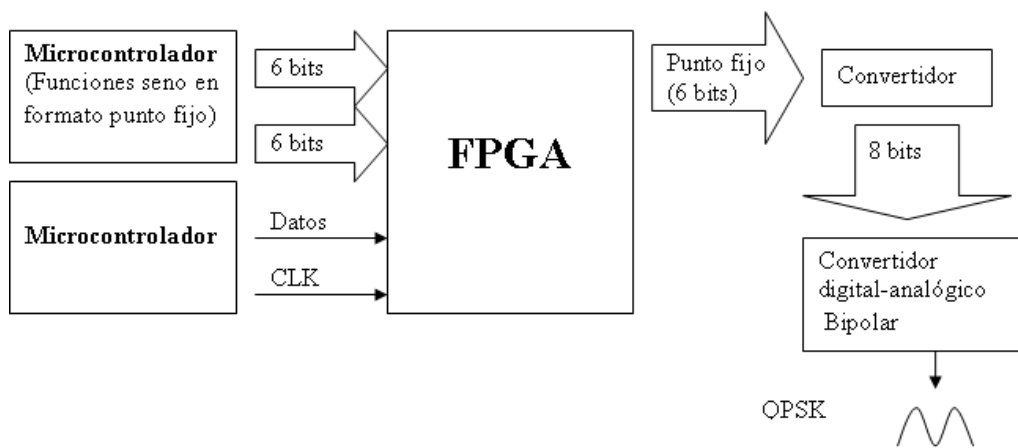


Figure 9. QPSK modulator.

6. Conclusion

This paper discusses the implementation of a QPSK modulator with FPGA as part of the proposed DVB-S transmitter on FPGA. Process simulation and programming in VHDL for FPGA synthesis work properly. It is currently working on the optimization of the D / A so it can provide better resolution of the modulated signal output, further tests are being done for integration with DVB-S transmitter completely.

References

1. ETSI World Class Standards
<http://www.etsi.org/WebSite/Technologies/DVBS.aspx>. 10-Aug-10
2. Communication Systems 4Th Edition
Simon Haykin With Solutions Manual,
Pag. 349, año 2001.
3. FPGA and CPLD Solutions from Xilinx,
Inc. <http://www.xilinx.com/>, August 13,
2010
4. VHDL: Programming by Example,
[Douglas L. Perry](#), Pag 102.
5. Microcontroladores: fundamentos y aplicaciones con PIC, Ramón Pallás Areny. Año 2008. Pág. 78.
6. [Wayne Tomasi](#) – 2003 Sistemas de comunicación, Pág. 220.
7. Adquisición y distribución de señales, Ramón Pallás Areny, Pág. 263, Año 1998.
8. FPGA prototyping by VHDL examples: Xilinx Spartan-3, Pong P. Chu.
9. Sistemas electrónicos digitales, Enrique Mandado y Yago Mandado. Año 2008. Pág. 122.

An Arrival Times Model for Real Time Tasks Using a Cellular Automaton

Topics: Computational Systems, Real-time Systems

P. Guevara-López, D. Cruz-Pérez, J. J. Medel J

Graduate Studies and Research Department, ESIME-IPN, Av. Santa Ana 1000, C.P. 04430, Mexico D.F.

Phone (55) 57296000 ext. 73250 E-mail: pguevara@prodigy.net.mx, dcruzp@hotmail.com,
jjmedelj@yahoo.com.mx

Abstract — *Two mayor problems in Real-time Systems (RTS) are tracing and reconstructing tasks behavior and this is why arrival, execution and finalizing times are needed. In recent papers the hypothesis was that the set of Arrival Times Tasks is known a priori; but there are no models that describe this and the Real-behavior is unknown. In this paper a dynamical model is proposed in order to describe Arrival Times using a Cellular Automaton. With this model it is possible to represent Arrival Times of Periodic Real-time Tasks including its Jitter and consider them as stable complex systems, without using differential equations, non linear systems, queue or stochastic theory.*

Keywords — Real-time, task, arrival time, cellular automata, model.

Introduction

Real-time Systems (RTS) are present in our daily life, in almost everything that surrounds human beings; in avionics, trains, automobiles, T.V., microwave ovens, cellular phones, digital telephone and, interconnection equipment. These are indispensable to assure quality and security in many industrial processes elements and for guaranteeing energy generation, transmission and distribution. In this context, the correct RTS function will depend on the knowledge of the RTS behavior, proving the importance of modeling and theoretical representation.

Modeling many physical systems like electrical, electronic and RTS commonly is based on methods and mathematical expressions such as differential equations, integrals and state variables. Alternative methods are Neural Networks and Fuzzy Logic. System procedures for digitalization allow numerical analysis of models. Cellular automaton are ideal Tasks.

Real-time Tasks

A Real-time System (RTS) is a system that interacts in a bounded environment with known dynamics related to its incomes, outcomes and temporal constraints, in order to maintain a good operation in accordance with basic concepts like stability and controllability. Its three basic considerations are: a) Interacting with the real world, b) Output of correct answers and, c) Obeying temporal constraints.

Frequently RTS are implemented in digital computers with Real-time Operating Systems (RTOS) that comply with POSIX standards and are formed with Real-time Tasks. These are executable programs that are saved in the memory with temporal constraints and an identifier.

A Real-time Task (RTT) is an Executable Entity or Job J_i characterized by an Arrival Time and a Temporal Constraint and formed by a Set of Instances $J_i = \{j_{i,k}\}$, $i, k \in Z_+$. An Instance $j_{i,k}$ is a Job Unit, described as $j_{i,k} = (l_{i,k}, C_{i,k}, d_{i,k})$, $i, k \in Z_+$, $l_{i,k}$ is the Arrival Time of each Instance, $C_{i,k}$ is the Execution Time and, $d_{i,k}$ is the Dead Line of each Instance. When only one Job is treated the index i can be avoided. The absolute Arrival Time l_k of an Instance with index k of a RTT J_i is defined as the time when an Instance asks for processor attention related to the temporal reference origin. Inter Arrival Time or Relative Arrival Time π_k of an Instance with index k of a RTT J_i is defined as the time in which the Instance asks for processor attention related to the Absolute Arrival Time of the Instance with index $k-1$: $p_k = m[l_k, l_{k-1})$

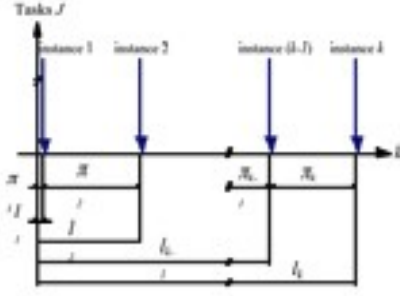


Fig. 1. Absolute Arrival l_k and Relative π_k times for a RTT J with k Instances.

Periodic Real-time Tasks ((PRTT) are activated (released) regularly in almost constant time periods with a small variation or Jitter. Sporadic Real-time Tasks (SRTT) are those tasks with a Release Time that can be represented by a function. Non Periodic Real Time Tasks (NPRTT) are those tasks with Release Times that cannot be represented by a Stochastic function activated randomly (including the Jitter).

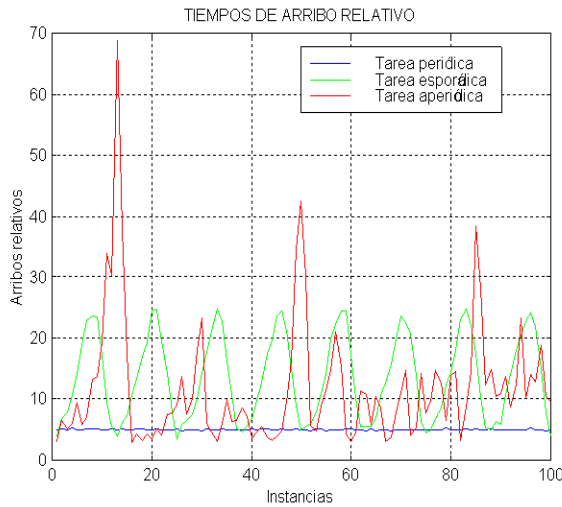


Fig. 2. Inter Arrival Times or Relative Arrival Times for a Periodic, Sporadic and Non Periodic RTTs.

Real-time Tasks: State of the art

In [1] RTT was classified in accordance to time constraints, considering Arrival Times, Deadlines and Execution Times and classifies tasks as Periodic or Non Periodic agreeing with temporal constraints with respect to its Deadlines. Consequently the Job characterizes a task with two states: its Arrival and Execution Times. Where $\tau_1, \tau_2, \dots, \tau_m$, indicating

m Periodic Tasks with period T_1, T_2, \dots, T_m and Execution Times respectively.

In [2] a RTT was defined by the pair (Φ, P) , where Φ is a Set of Execution Times (ϕ_1, ϕ_2, \dots) , and P is the Minimal Time of Separation and is assumed as their Deadlines.

In [3] a Sporadic RTT was defined where the Execution Times had a stochastic variation and its Distribution Function is known.

In [4] Non Periodic Tasks was described as τ_i (from the set of Non Periodic Tasks $T = \{\tau_1, \tau_2, \dots, \tau_N\}$) considering its Arrival Time R_i , Absolute Deadline D_i , Worst Execution Time C_i , Execution Variable e_i denotes the Processing Time for τ_i at any moment, the variable w_i the Last Begin Time of τ_i , that is a function of Present Time "t" and value e_i , Minor Arrival Time $est(i)$, Mayor Arrival Time $lst(i)$. For Critical Sporadic Tasks the Ready Time was assumed equal to the Arrival Time.

In [5] Periodic RTT was described as released in regular periods of time while a Sporadic Task arrived in arbitrary periods of time with a minimum well known value. A task T was described by (c, p) where: a) c is the Maximum Execution Time, b) p is the Minimum Time Interval between task invocation bounded by T . If T is Periodic p means a constant interval between invocations. Considering that T is a sporadic p , specifying the Minimum Interval defined by Nyquists concepts. For Periodic Tasks t_k is the invocation k of task T then: 1) the invocation $(k+1)$ occurs in $t_{k+1} = t_k + p$, 2) execution of invocation k of task T must begin after t_k and must be finished before $t_k + p$. For Sporadic Tasks, if t_k is the time for the k -th invocation of task T then: 1) the $(k+1)$ invocation happens after the $t_k + p$, therefore $t_{k+1} \geq t_k + p$, b) The Execution k -th of task T must begin after t_k and must be completed before $t_k + p$.

In [6], 1) Arrival Time for k -th Periodic Instance was given by

$$r_i(k) = r_i(k-1) + T_i; \quad (1)$$

2) Deadline for k -th Periodic Instance was given by:

$$d_i(k) = r_i(k) + T_i; \quad (2)$$

Considering Deadlines equal to the Inter Arrival Period for Periodic Tasks: a) All tasks $\tau_i: i=1, \dots, n$ had Hard Deadlines, a constant period T_i and a Maximum Execution Time C_i , that is considered known and could be obtained with a static analysis from the code, b) All Periodic Tasks were activated simultaneously in time $t=0$; for example, the first Instance of each Periodic Task had an Arrival Time $r_i(0)=0$, c); the Arrival Time for the k -th Periodic Instance was given by (1), d) Deadline for k -th Periodic Instance was given by (2). For Periodic Tasks it considered: 1) All Periodic Tasks $J_i: i=1, \dots, m$ have no Deadlines; 2) The Maximum Arrival Time of each Non Periodic Task was unknown; 3) The Worst Execution Time of each Non Periodic Task was considered known at its Arrival Time.

In [7] Queue Theory was proposed for describing Arrival Time for Real-time Tasks, supposing that the system had an attention Queue and allocated priorities.

In [8] an ARMA model was proposed for characterizing Dynamic Arrival Times in RTT. The model was:

$$l_k = l_{k-1} + \pi_k, \quad (3)$$

$$l_k = a_k (\pi_{k-1} - w_{k-1}) + u_k + w_k, \quad (4)$$

Whereas internal and external noises ω_k^1 and ω_k^2 rely on the computing system and the environment respectively, they were not correlated. Internal dynamics described by x_k allows the parameter a_k and internal noise ω_k^1 modeled the Real-time Tasks. Execution Times and Deadlines were considered constants.

In [9] and [10] an Arrival Time Model for RTT based on an ARMA model was proposed: a) Periodic, b) Non Periodic and, c) Sporadic Tasks. A First Order, Time Variant and Non Stationary Linear System were proposed, considering Jitter and external perturbations uncorrelated and obeying Normal Distribution. The Jitter was bounded by a known interval.

Absolute Arrival Time l_k of an Instance with index k of a RTT J_i was described recursively by:

$$l_k = l_{k-1} + \pi_k, \quad (5)$$

The Inter Arrival Time π_k of an Instance was given by:

$$\pi_k = a_k (\pi_{k-1} - w_{k-1}) + u_k + w_k, \quad (6)$$

Where:

a_k : System parameters,

w_k : External perturbations to the processor, represented through a random variable with Gaussian Distribution,

u_k : Inter Arrival Reference Time.

Cellular Automaton

In modeling complex systems where it is not convenient to apply conventional mathematical techniques, for example chemical, biological, evolutionary, electrical and genetic computational systems, three options were taken in account

- Achieving a continuous model (in those systems that were analogous),
- Using differences methods (with inherent problems in digitalization),
- Modeling using Cellular Automaton.

A Cellular Automaton (CA) is a discrete dynamical model formed by a set of cells that have random behavior in a given dimension. These systems are mapped in a Discrete Time Space. The cells that form the automaton interact with its neighbors using a Set of Transition Rules that were previously established.

Formally, cellular automaton is a 4-tuple of the form $A = (L, Q, u, f)$ evolving a $d \in \mathbf{Z}_+$ dimension.

Where:

L is a Lattice,

$Q = \{x_{ij}, \dots, n: d\}$ is the set of each cell-state,

u is the relationship with its neighbors and

f is the transition function.

The cellular automata have three parts:

- A discrete lattice (L) is the system cell arrangement,
- A neighborhood (r) is the cells in the vicinity of the cell-state. The behavior of the automaton depends on the vicinities and dictates how it will evolved through time,
- The transition rules (f) are local transition functions as for example: the transition function cell-state or transition table cell-state. A function f can be described by a formula or by a transition function of the form $u(x)^t \Rightarrow x^{t+1}$, or simply by a cell-state transition table.

An example of a Cellular automaton with a Lattice of 2 dimensions ($2D$) with 50 cells, 70 evolutions and $r=4$, a transition function c_0 considering "rule 30" as shown in fig. 3.

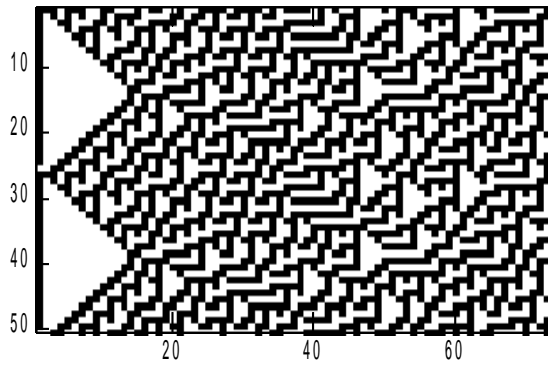


Fig. 3. Cellular automaton with 50 cells, 70 evolutions and 30 rules.

RTT arrival time modeling with cellular automaton

An alternative is the study of Arrival Times by Fuzzy Cellular automaton. It is possible to describe its complex dynamics, eliminating the use of non linear differential equations and superior order with Space State and its Stability Analysis. The proposed model only characterizes Arrival Times for a single task. In the case of Multiple Concurrent or Semi Parallel Tasks a bank of automaton or a bigger dimension automaton is required, in other words, nD with $2 < n$.

The model for Arrival Time behavior is described as:

$$p_k = g(x_{k,1}, x_{k,2}, \dots, w_{k,n}) \quad (7)$$

$$\text{With } x_{k,i} \in \hat{I}[0,1] \quad k, i, n \in \mathbb{Z}^+, i \leq n$$

Where:

π_k is the Arrival Time for Instance k ,

$x_{k,i}$ is the value state of the cell (true or false),

g is the transition function among cells $x_{k,i}$ at the Arrival Time π_k ,

i is the index of the cell,

k is the index of the Interval,

n is the number of cells per Interval.

Results

An example of modeling RTT uses cellular automata, a Periodic RTT with an Arrival Reference Time of 0.5 Temporal Units (T. U.)

The transition function for this example is rule 30 as is shown in table 1.

$x_{k,i-1}$	$x_{k,i}$	$x_{k,i+1}$	$x_{k+1,i}$
0	0	1	0
0	0	0	0
0	1	1	0
0	1	0	0
1	0	1	0
1	0	0	1
1	1	1	0
1	1	0	1

Table 1.- Transition function, rule 30.

The arrival time π_k is described by:

$$\pi_k = \sum \frac{x_{k,1}}{n} + u_k, \quad (8)$$

Where:

$$x_{k,i} \in (0,1] \quad k, i, n \in \mathbb{Z}^+, i \leq n,$$

u_k is the reference Inter Arrival Time,

n is the cell number for Instance with index k .

In Fig. 4 the graph is obtained for a Periodic RTT using a C.A. described as shown. The output and its mean value can be seen. In all cases the signal describing Arrival Times is stable. The Jitter is observed as the perturbation near the main signal; this is non stochastic and stable too.

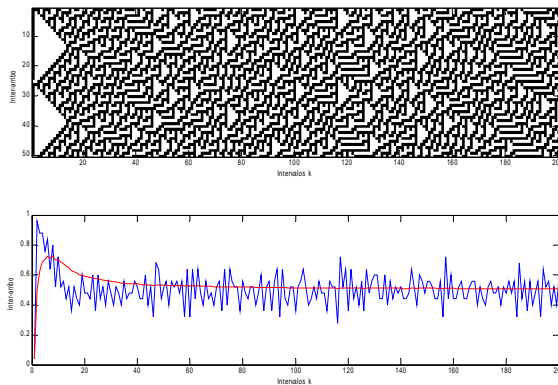


Fig. 4. Arrival times for a periodic RTT with a Cellular automaton with 50 cells, 200 evolutions, 4 neighbors and state transitions with rule 30. The Reference Arrival Time is 0.5 Temporal Units (T. U.).

In the second image of Fig. 4 the rising Transitory State can be observed in the Periodic RTT behavior, caused by the initial values of cells with $k=0$. Nevertheless the automaton evolves and converges to the Reference Value in a probability sense, with 0.5 Temporal Units (T.U.).

The statistic behavior of the automaton approaches those in [8], [9] and [10], the Jitter obtained by the simulation of the Cellular automaton, considered non stochastic perturbation and offers Gaussian behavior as observed in Fig. 5.

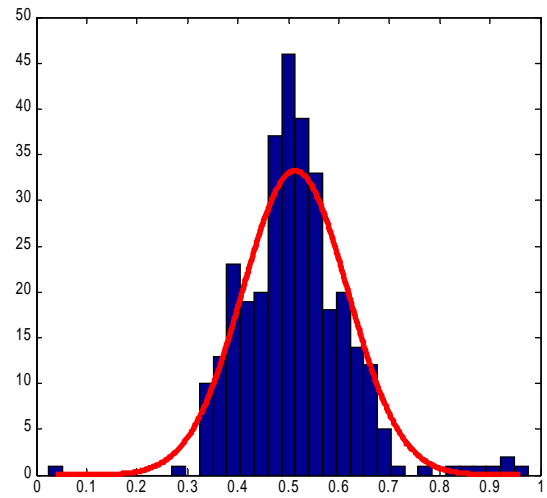


Fig. 5. Distribution Function of Arrival Times of a Periodic RTT with a Cellular automaton, 50 cells, 200 evolutions, 4 neighbors and Transition Function of rule 30. The Reference Arrival Time has 0.5 Temporal Units (T. U.). See Fig. 4.

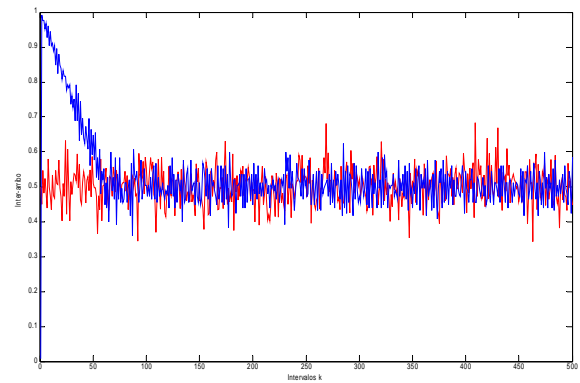


Fig. 6. Comparison Arrival Time for RTT using a Cellular Automaton and an ARMA model.

In Fig. 6 results for simulation for Arrival Times with a Cellular Automaton (CA) and an ARMA model in [8], [9] and [10] are shown together. In it, is observed that ARMA model had a main signal wrapped in stochastic noise with mean value close to the desired reference value (0.5 T. U.), while that obtained from de C.A. had variations that almost unify their initial value, and approached the desired value after the 60th evolution ($k=60$). This illustrative result showed that the Automaton system output was very sensitive to initial cell values. Therefore the system stability was guaranteed

Conclusions

Cellular Automaton represents complex deterministic behaviors with similar simulation results from equal

initial conditions, transition rules, and evolution rules. The initial values of cells $k=1$ intervene directly in the first iteration of the automaton behavior. The Inter Arrival Times of the Modeled RTT with a CA will always be stable because its maximum and minimum values will be known, with finite and bounded values. This behavior could be changed or arranged in size and time so that it could represent several tasks.

References

- Liu C., Layland J. (1973). Scheduling algorithms for multiprogramming in hard-real-time environment. *Journal of the ACM*, Vol. 20, No. 4, (1973), pp273-250.
- Mok A., Chen D. (1997). A general model for real-time tasks. Technical report, University of Texas at Austin.
- Ramanathan P., Kang D. (1994). A generalized guarantee model for servicing sporadic tasks with firm deadlines. *Real-time Systems Journal* May 1994.
- Choi S., Agrawala A (1997). Scheduling aperiodic and sporadic tasks in hard real-time systems. Technical report University of Maryland.
- Jeffay K., Stanat D., Martel C. (1991). On non-preemptive scheduling of periodic and sporadic tasks. *Proceedings of the Twelfth IEEE Real-Time Systems Symposium*, San Antonio Texas.
- Spuri M. & Buttazzo G. (1996). Scheduling aperiodic tasks in dynamic priority systems. *Journal of real-time systems*.
- J. P. Lehoczky. (1996), "Real Time Queueing Theory". 17th IEEE Real-Time Systems Symposium (RTSS '96) December 04 - 06, 1996 Washington D.C.
- Pedro Guevara López, José de Jesús Medel Juárez, Alberto Flores rueda. "Un Modelo Dinámico para el Arribo de Tareas en Tiempo Real". Congreso Argentino de Ciencias de la Computación CACIC 2003, Rio de la Plata Argentina, Oct. 2003.
- P. Guevara, J. J. Medel, D. Cruz. "Modelo Dinámico para una Tarea en Tiempo Real". Magazine *Computación y Sistemas*, ISSN 1405-5546, Vol. 8 No. 1, Págs. 61-73, México, Sept. 2004.
- Cruz Pérez, Daniel, Modelo para tiempos de arribo de tareas en tiempo real concurrentes, doctoral thesis, CICATA. I.P.N. México, 2007.

Estimating the Fundamental Tone of continuous voice in real-time

Ismael Díaz Rangel¹; Sergio Suárez Guerra¹; Josué Rangel González¹

¹ Centro de Investigación en Computación, Instituto Politécnico Nacional,

Juan de Dios Batiz esq Miguel Othon de Mendizabal s/n, P.O. 07038, México

ssuarez@cic.ipn.mx, idra06@sagitario.cic.ipn.mx, joshuab09@sagitario.cic.ipn.mx

Abstract. An important element to produce the characteristic sound of the voice is caused by the vibration mode of the vocal cords and their folds. The fundamental tone (F0) or fundamental frequency represents the excitation frequency of the vocal cords when a voiced sound is produced. In the F0 generation there are two main parameters taken into account to establish diagnostic performance of speech production: the variability of the frequency and F0 amplitude. This information, in speech synthesis systems based on rules, is data that is provided to the block that generates the excitation signal. People who become deaf after a time, lose control of their voice; for them, a tool that continuously shows the behavior of its fundamental tone, helps to improve or maintain control of their voice. This paper presents a methodology to measure and graph the fundamental tone of voice in real-time.

Key words: Fundamental Tone, Sounded Voice, Implantation Cochlear, Filtering, Preprocessing, Auto-Correlation.

1. Introduction

Frequency or Fundamental Tone (F0), also known as Pitch, is the measure of excitement that occurs on the vocal cords when speech Sound is produced [1].

The pitch is a very important parameter to consider in the analysis of voice and speech, as from this there are sounds that characterize the voiced segments in phonation. Any disturbance in the fundamental tone alters the proper diction [2] [3].

In turn, the perception of fundamental tone is important for assessment of the voice, as it provides useful information for the identification of speakers, allows the extraction of prosodic information, and is used to emphasize key words in sentences.

Furthermore, in the case of tonal languages it has a characteristic intonation phonetic value, so that in these cases the perception and tone generation provides important suprasegmental information [4].

For patients with hearing loss who have received cochlear implants, the technical limitations associated with the procedure of stimulation of the auditory nerve, determine the mechanisms of fundamental tone perception [4].

This paper presents a method for estimating the continuous voice pitch in real time. The graphical representation of the fundamental tone can be used for people who have lost their hearing ability to compare the production of their speech (in terms of F0) for recording (of the same sentence or word) obtained from a normal person so they can correct mistakes, that aims to maintain or improve the quality of the voice. It's also possible using graphing Pitch to teach oral communication to deaf people who cannot speak, but have a healthy vocal tract. In some ways, it has the advantage of "seeing what is said."

2. Preprocessing of the voice signal

The extraction and calculation of parameters of variability of F0 is implemented in different forms and has been analyzed by different signal processing techniques [5].

This well known and most widely used technique to calculate F0, is the partial autocorrelation function. The same applies directly to the voice signal or the result of a type of preprocessing.

Many authors propose techniques that allow having a voice signal in the range of F0 with results that translate into a clean and clear signal, which allows greater fidelity in the calculation of F0. The proposal used here is simple and provides very positive results when the sound signal is clearly captured.

Given that the most important information of the voice is below 4 KHz [6]. It's recommended before digitizing the voice signal, using a filter Antialiasing with a frequency of cut of 8 KHz. Since F0 is band limited between 80-250 Hz, it's Convenient to apply a low pass filter with cutoff frequency of 300 Hz up, to remove from the speech signal frequencies corresponding to the formant frequencies produced in the vocal tract, so that the response of the autocorrelation function is cleaner, see Figure 1.

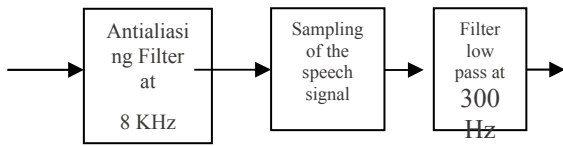


Fig.1. Block diagram of preprocessing of voice signal.

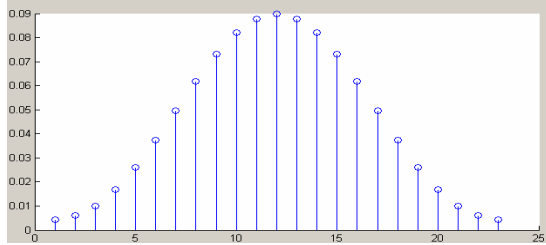


Fig.2. Impulsive response of a FIR filter at 300 Hz with 23 coefficients.

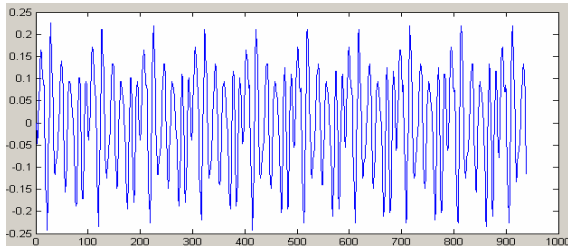


Fig.3. Segment of signal to process.

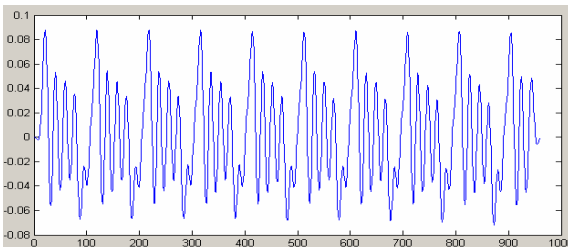


Fig.4. Segment of signal after being filtered

NOTE: There are people who have a higher fundamental tone at 300 Hz, which is not typical; in that case you can consider increasing the cutoff frequency of low pass filtering.

The partial autocorrelation

Partial autocorrelation is the convolution of the signal itself displacing in each new calculation one sample of the signal, and limiting computing environment segment of N samples. It is expressed as:

$$C_{xx}[n] = \frac{1}{N} \sum_{m=0}^{N-1-|n|} x[m]x[m+|n|] \quad (1)$$

Where N is the total data processed in a segment.

In this case, the response of the estimated autocorrelation function is positive definite, and the higher value always corresponds to the source. Example:

For: $x[n] = 2, 1, 2$,

$$C_{xx}[0] = \frac{1}{3} [2^2 + 1^2 + 2] = 3,$$

$$C_{xx}[1] = \frac{1}{3} [(2)(1) + (1)(2)] = \frac{4}{3},$$

$$C_{xx}[2] = \frac{1}{3} [(2)(2)] = \frac{4}{3}.$$

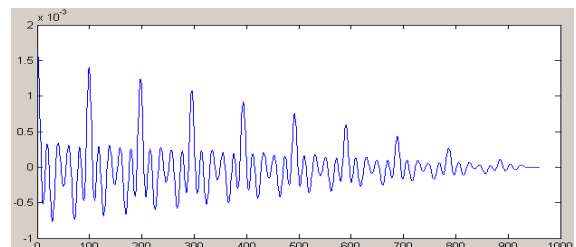


Fig.5. Autocorrelation of the segment of signal to evaluate

Method for calculating F0:

Since the speech and fundamental tone constantly change over time, the calculation of the fundamental tone must be made in segments.

Calculation of F0 on a cycle

The following describes the proposed method for calculating the fundamental tone in a segment of the speech signal:

1. It needs to take a segment of voice in which there are at least three periods of F0. If you consider the minimum frequency is 80 Hz, the segment that meets this requirement is $(3 / 80)$ vo second, 37.5 msec. This is chosen by 40 msec.
2. Partial autocorrelation is applied to the segment. The result is a set of values that depend on the sampling frequency (f_m), with which the speech signal was sampled. If $f_m = 12000$ Hz, 40 msec for 480 samples are taken and therefore a maximum of 480 values of autocorrelation.
3. The first value of autocorrelation the highest of all, corresponds to the value of the average energy of the segment. IMPORTANT: If the value of energy is very low, we must decide whether to calculate or not the fundamental tone for this interval, which can obtain no real value of F0 in the calculation.
4. It looks for the next maximum value of autocorrelation values that meets the following: it is greater than 60% of the initial value it is between the heights of the period between 250 Hz and 80 Hz. For example, if $f_m = 12000$, $N_{250} = n_{80} = 48$ and 150. This restricts the search to a bounded area and it unnecessary to calculate all the autocorrelation values. IMPORTANT: If there is more than that meets the bounds imposed conditions, there are two possibilities:
 - a. There is no fundamental tone in the segment.
 - b. It is necessary to decrease the threshold of 60% to a minimum of 30%.
5. The distance from the origin of the graph to the peak found is the fundamental tone period $T_0 = nT_0 / f_m$, then its inverse is the fundamental frequency $F_0 = f_m / nT_0$.
6. If there is no fundamental tone, saving the values of F0 for analysis by segments, provides that $F_0 = 0$, for the segment under analysis.

7. It applies the procedure made since the beginning (1) all consecutive segments, until the last possible information under analysis which yields the behavior of F0 for all the segments studied sound.

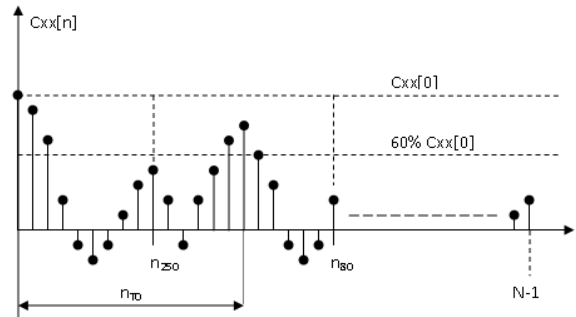


Fig.6. F0 calculation from the autocorrelation of the entrance signal.

Interesting observations:

- You should consider that the estimated F0 in this interval of time, is influenced by the values of all samples in the segment used, although there is little affected.
- If you want to calculate one seconds F0 on the basis of the distance between the 1st. peak and its successor, the 2nd is possible, but it is likely that the values are different.
- The sampling frequency determines the accuracy of the estimated F0; higher FM, better precision.
- If you want a graph of the behavior of F0 for consecutive segments, it is desirable to overlap segments by 50%, and the answer graph improves the variation of F0. Ideally, the calculation is cycle to cycle.

4.2 Calculation of F0 cycle to cycle

The calculation cycle to cycle F0 to get information allows us to determine the fundamental tone in continuous speech, and is performed based on the method of calculating F0 presented above. To extent 5, everything is equal, and then you must do the following:

6. New point is taken as F0 to find the segment that starts in additional samples to the place where F0 calculation performed above. If $F0 = 0$, then it is possible to admit that F0 does not exist for the whole segment under analysis. Then set the new point to find F0 to 40 msec. beyond the place where It started the calculation.
7. Repeat the procedure from the beginning (a) until the last possible section of the information under analysis. Thus we obtain all values in a row, cycle to cycle, from F0.

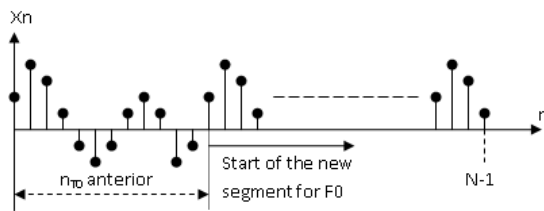


Fig. 7. Calculation of the new $nT0$.

Interesting observations:

- The number of F0 values found in this case exceeds the amount of values in the previous case, since the early segment of the calculation of each new value of F0 starts at points in addition to the starting point of the previous calculation rather than at the end of the segment of 40 msec. employee.
- In determining the calculation of F0 points depending on the period, the graph of consecutive values of F0 is not homogeneous, that is, depends on the number of times F0 was found and of course for a voice production with a higher frequency F0, the graph will be larger. MORE VALUES ARE FOR THE SAME INTERVAL F0.
- Points where there is no F0 ($F0 = 0$), corresponding to a time interval of 40 msec.

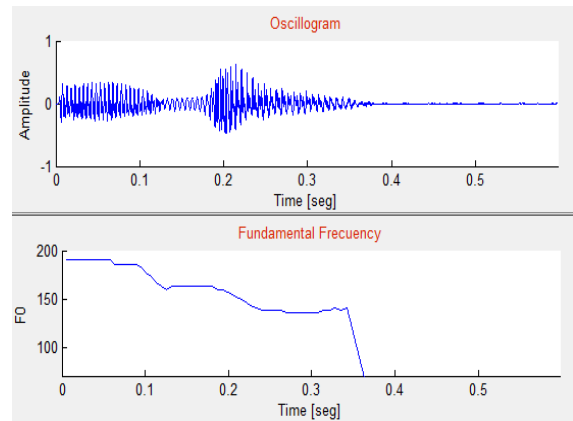


Fig.8. Oscillogram of the word “UVA” and the estimating of their fundamental tone cycle to cycle.

Conclusions and Future Work

Since the pitch is a key parameter in the production of voiced sounds and these sounds are what allow us to identify speakers, prosody and emphasis on articulate speech, the estimation and graphing in the production of continuous speech is presented as a tool that can be useful for those who, due to loss of hearing, gradually degrade the quality of their voice, because this technique allows them to "watch the talk", and compared to a speech pattern produced by a normal person, could help to maintain or improve speech quality. This model also can be utilized to teach oral communication to people who are speechless because they cannot hear, but have a healthy vocal tract.

Pitch estimation is also critical in speech synthesis systems based on rules, as it is a fact that must be supplied to the excitation generation block sound.

Future work aims to complement Pitch plotting the spectrogram, although its interpretation is more complex and gives very detailed information on the frequency domain with respect to the time of sounds produced by the vocal tract.

The authors would like to thank the following institutions for their economical support while developing this work; CONACyT, SNI, and National Polytechnic Institute, OCFAA (Grant 20090807, tools for voice recognition, translation and emotion classification (Herramientas para el reconocimiento y traducción de voz y clasificación de emociones)).

References

1. Donald G. Childers: Speech Processing and Synthesis Toolboxes. John Wiley & Sons, Inc. 2000.
2. Gonzáles, J.; Cervera, T.; Miralles, J. L.: Análisis acústico de la voz: fiabilidad de un conjunto de parámetros multidimensionales. Acta Otorrinolaringología Esp. 2002.
3. Kreiman, J.; Gerratt, B.; Gabelman, B.; Jitter, shimmer y ruido en la percepción de la calidad de la voz patológica. Bureau of Glotal Affaire UCLA School of Medicine. First Pan-American/Iberian Meeting on Acoustics, Cancún, México. 2002.
4. De la Torre, A.; Roldan, C.; Rosales, P.; Sainz, M.: Percepción del Tono Fundamental en pacientes con implante coclear. 2das Jornadas en Tecnología del Habla, Granada. Universidad de Granada. 2002.
5. Hernández Díaz, M.E., “Algoritmos para la extracción del período fundamental de la voz. Desarrollo y evaluación”. Tesis doctoral. UCLV. Cuba 1996.
6. Rabiner, L.; Juang, B.H., Fundamentals of Speech Recognition. Prentice Hall. 1993.

Implementing free software on computer equipment frequently an option for reducing electricity consumption

Alejandro Jiménez León¹, María Graciela Gutiérrez Vallejo²

¹ Dirección General de Servicios de Cómputo Académico, UNAM, Carlos B Zetina 9-3, Col Hipódromo Condesa, Del. Cuauhtemoc, 06170, México, D. F.

² CECyT 9 Juan de Dios Batíz Paredes, IPN, Del. Miguel Hidalgo, C.P. 14380, México, D. F.

¹ajleon@servidor.unam.mx,

²gragutierrez@yahoo.com.mx

Resumen. Today, educational institutions have implemented a number of computer labs, the problem is that most of them there is a consumption phantom power because the following equipment DSL modem, PCs, printers, remain connected to the mains or remain in one of the following two ways: lighted without any action, or remain in standby mode, waste energy unnecessarily. In response, the paper proposes a series of measures to reduce energy consumption, and implement free software and freeware for the time when computers are turned on but not used to decrease energy consumption

Keywords: Energy Conservation, Consumption Phantom, Freeware, Free Software

1 Objective

Design and implement policies that will optimize energy consumption in existing computers in the computer labs of schools.

2 Introduction

The energy performance of computer equipment, is a common feature of all systems by the fact of being connected to the mains power even without making consumed any activity. Therefore be sought alternatives that save energy and use of free applications accomplishes this goal by reducing energy consumption as a result lowers the cost of the electricity bill and improve the productivity of resources.

3 Methodology

When academic staff coming to school the first thing it does is turn your computer equipment, but that does not mean all day working directly in it, will often seek information or attend to other activities away from using the computer but energy consuming computers can be made in any of the following four ways:

- 1.-Off (energy consumed by the mere fact of being connected to mains)
- 2.-Stand-by (sleep, standby)
- 3.-Power on standby (does not perform any activity)
- 4.-Power to maximum efficiency.

From these arrangements, the paper analyzes how to reduce energy consumption.

For the second and third mode, there is the possibility of reducing nergy consumption through the implementation of free software applications, which will be described in terms of how they work, technical requirements and which can be obtained for the user to install the application that best suits your needs and computing environment.

To demonstrate the power consumption, the test contains a series of paintings, which reflects the energy consumption in each of the methods most commonly used for equipment such as computers, printers, routers, monitors, LCD screens , external hard drives, Ethernet hubs and other peripherals.

The following lines explain the opportunities offered by the use of appli-free to reduce consumption enrgía when computers are turned on but not used and their characteristics, how people work and technical requirements.

Edison Developed by Verdiem improves energy efficiency of personal computers, allows the user to schedule when you enter low consumption, it may indicate that you turn off the monitor and / or hard drive before entering Stand-mode By. There are two versions for Windows XP (Edison_Installer_XP.exe) and Windows Vista (Edison_Installer_vista.exe) for this system to make changes manually in the following way: To activate the power management in Windows Vista, you must enter the Control Panel> click System and Maintenance> Enter now power options> Now select a preset plan, modify a customized preset plans or create a new plan. If you edit, the system lets you adjust the monitor and the stand-by mode, to make further adjustments must click Advanced Settings

EZ Wizard. EZ Wizard a free program to manage the energy consumed by the monitor and the computer: It is available for Windows 2000 and Windows XP. (PMWiz-XP.exe).

PowerTOP. Software that reports energy consumption for applications under Linux is ideal for notebooks and which identifies energy consumption at the application level, so you can lengthen the battery life. For its implementation requires a 2.6.21 kernel, which allows operation as a "tickless" if you have the option NO_HZ activated. This program develops better on Intel Mobile, is now available the latest version 1.11. (PowerTOP-1.11.tar.gz).

Snap.com. Manages the energy used by the monitor and hard drive when the CPU is idle, generating energy savings, is compatible with Windows XP and Windows Vista. It is activated by default when the user stops using the CPU for about 30 minutes and have the system permanently how much CO2 will be sending has stopped broadcasting. (SnapCO2Saver18.exe)

Witricity Power. It is a calculator that allows users to calculate energy consumption of devices such as lap tops, cell phones, Ipod chargers, etc., used in the office. The program works as follows: the user selects the device to monitor, enter the total time of use and the program displays a series of reports containing information on hourly, monthly, and monthly consumption among other data. (Witricity.exe)

WatchOverEnergy. Application designed for operating systems Windows 9x, 2000, XP, NT. Manage energy consumption in standby mode. Monitors the monitor power. The application is activated when the PC is not being used or when no important programs are running as WatchOverEnergy can be configured for these programs or when certain files are opened, the manufacturer states that this application would reduce energy costs monitor 20 percent. WatchOverEnergy only works when you are not using the computer. (Watch_energy_setup.exe)

Local Cooling. It is a freeware application makes the hard drive to sleep when not in use or when the user does not use the PC. (LocalCooling-1.03.exe)

ShutDownOnTime. Lets turn off, hibernate, send Stand-by state or restart the computer, as determined by the user. It is suitable for work areas where they keep their computer on at night and on weekends it does not require extra care when staff retires. (ShutDownOnTime_v3.00.exe)

4 Have implications for connected equipment in-bay or just stand on

Many teams spend countless days on and the power consumption has no utility. The operating mode called Stand by, makes it possible to turn on the television with remote control, turn the computer with a phone call, etc. To better understand this situation and how it affects the electricity bill financially, expressed in kWh (kilowatt hour), it is necessary to perform the following operation:

- Divide consumption that is expressed in Watts back in the team between 1000;
- The result will be multiplied by the number of hours the equipment is working, or to obtain this value multiplied by the current price of kWh.

Example in an institution or home stays on a computer that consumes 200 Watts / hour, the result will be: $(200/1000 = 0.1 \text{ kWh})$, and $0.1 \times 24 \text{ hours} = 2.4 \text{ kWh}$. If the price per kWh for a household with average power contract in 2009 was 941 the total cost of having this device for 1 full day would be \$ 2.2584 pesos. At the end of the month the amount would be \$ 70.01 pesos. When in reality the team was only used two hours daily would cost \$ 0.1882 and at the end of the month the bill would have been \$ 5.8342 pesos. In consequence, the user pay a surplus of \$ 64.1758 pesos.

This cost varies depending on the mode that is running the computer and stays connected even when turned off.

It is therefore important to analyze the consumption shown in table 1, which highlights the power consumption when the computer is off, on standby (no activity) and on to maximum performance (number of processes are running concurrently)

5 Results

As can be seen both in Table 1 and 2, show that consumption will depend on the manner in which the team is working: waiting, running a simple program (like a Web browser), or developing complex tasks (running the defragmenter, performing calculations, etc.). Another factor that affects the configuration that has a basic computer-type office, facing a high performance model that requires twice as much energy to stay on or on standby. Apple computers use less energy in fact the iMac Desktop with 20 "display requires about 35% less energy to operate a computer with similar characteristics. In case something happens like laptops, power savings compared to

similar laptops equipped with processors and similar settings. That is why, at least talking about the residential environment and personal use Apple computers are more energy efficient than its counterparts.

With regard to LCD monitors, these are more but connected to the mains will approximately 0.20 pesos per month, and 2.4 dollars per year on electricity bills cost. With respect to laser printers, these are less efficient than inkjet because their processes requires subjecting the toner to a temperature of 200 ° C to be fixed on the paper. That is to print a single page laser printer takes almost 300 watts more than the inkjet. Multifunction printers are more efficient because it generates consumption pending a desktop scanner is similar to an inkjet printer in the same factual situation is virtually the same power in these conditions remains a multifunction printer with inkjet technology ink, capable of printing, scanning and copying. Thus one multifunction will do the same to a printer and a scanner, but both off and on hold consumes the equivalent of one of them. It would be advisable to install an ADSL Router with integrated WiFi and consumption of a WiFi ADSL Router is very similar to another device that is exclusively for WiFi access point. In many homes, where once installed a wireless ADSL router, have chosen to add a wireless access point connected to the router to provide this functionality. But if we take into account that prices are very similar, save energy and space by buying a single computer acting as a DSL modem and wireless access point at a time. This would highlight the issue of downloading Internet information campaign, which must be added the cost for the broadband connection plus the cost of energy required to keep a computer running a P2P program, and the ADSL router. This month can cost us about \$ 135.00 dollars and a year would be \$ 1.620 pesos. It is obvious that the downloading of information permanently and increase the electricity bill is unnecessary and reduces efficiency.

efficient than the CRT, in fact a classic monitor CRT (cathode ray tube) 17 "inch consumes nearly twice that of LCD 19 or 22 inches. It should be noted that the increased inch LCD does not necessarily lead to increased electricity consumption. 22-inch models even consume something less than 19 inches. Due to the fact that increased consumption of an LCD is its backlight and often necessary for backlight lamp models closer in size is almost the same. It is clear that all electronic equipment consume a small amount of energy to maintain minimal functions that allow you to light up when you press the power button. This is extended to the portable power supplies which are also consuming even with the laptop off and loaded. To get an idea, keep a desktop computer off

TABLE I ENERGY CONSUMPTION ACCORDING TO THE INSTRUCTIONS FOR USE *

	Off	Standby Power	Power at maximum performance
Basic office desktop PC (tower only)	9	59	101
High-performance desktop PC (tower only)	13	124	160
Apple iMac - built-in LCD 20 "	9	69	94
Next-generation notebook (15.4 LCD)	4	43	64
Ultra previous generation (LCD 12.1 ")	9	62	69
Appel Macbook Intel Core 2 Duo	6	27	40

* Measured consumption watts / hour

6 Saving energy from the Windows settings

Avoid having many windows or open programs, as this causes the damaging slows PC performance. It is recommended that the user to increase the RAM because this action helps the processor and hard drive to run applications or open programs. And to use wallpaper and screen saver with images of funds or dark colors because they lessen the intensity of light, especially in the case of CRT monitors, this recommendation would also apply to LCD and TFT screens. In this regard in recent months have pointed out that if black Google would save 3000 megawatts per year, this according to the following calculation "a white page requires 74 watts to spread, and a dark need only 59 watts" and Google is the number one engine on the Internet. Continuing with Windows, XP specific case, this system consumes many resources for your graphical environment and visual effects. One way to reduce consumption is: right click on My Computer> Properties, and leave a context menu with several options we click on "System Properties"> Now we click "Advanced"> A window, there is section that says "Performance, Visual effects, processor scheduling ..." if we click on the Settings button (the first button) there is another

window called Performance Options in the top of the range of options there are 4 items Customizing choose: after this action is a series of options pigeons, let alone all of them active at the option Animate windows when minimizing and maximizing, Smooth edges of screen fonts, Use visual styles on windows and buttons (important) Use common tasks in folders (important) is good to have the same options enabled otherwise it will affect the Windows XP graphical environment, where all would be clear as if the user works with Windows 98.

Another recommendation to reduce the power consumption is kept clean and orderly hard drive files, delete temporary files, cookies, history, recycle bin keep clean, these actions will improve the performance.

There are programs that perform these activities easily as in the case of Ccleaner (<http://www.ccleaner.com>) or Disk Cleanup (located in System Tools). After removing the debris of the equipment is recommended to defragment your hard drive and compressing old files and order and improve hard disk performance. This should be done before installing a new application to be in recorded in continuous segments.

7 Conclusions

The computer labs and computers installed in schools ill spend the energy to make an incorrect use of information appliances that remain on standby or switched on without any action or simply connected to the mains. It is therefore recommended the implementation of free applications to control the energy consumption of computers.

We recommend turning off computers that are not used by surge suppressors, thereby facilitating the disconnection to the mains.

Detecting peripherals that are not being used to be unplugged.

Establish electrical control panels that allow cutting the flow of energy at the end of the workday and monitor the physical condition of the electrical connections.

Give preventive and corrective maintenance of equipment, as well as keeping off the monitor, hard drives and other devices when not used.

Preferably use LCDs to reduce power consumption in half.

All these actions should be a permanent practice to reduce costs in our schools would thus helping to create awareness on the importance of avoiding energy waste and reduce the emission of millions of tons of carbon dioxide into the atmosphere by an unnecessary action as having a computer turned on without using.

TABLE II PERIPHERALS CONSUMPTION

	Off	Standby Power	Power at maximum performance
Display LCD 19"	4	43	43
Display LCD 22"	4	38	38
Monitor CRT 17"	4	74	74
Color inkjet printer	13	15	44
Color Laser Printer	2	48	335
Duplex Desktop Scanner	11	26	35
External disc USB 250 Gbytes 6.35"	6	20	37
Concentrator USB 7 puertos	4	6	6
Concentrator Ethernet 16 puertos	4	9	9
Router ADSL WiFi	4	9	9
Access point WiFi 802.11n	4	6	6
Fuente http://nova.alc.upv.es/joomla/index.php?option=com_content&task=view&id=205&Itemid=2 Institute for Energy Diversification and Saving of Energy (IDAE)			

OF THE COMMONLY USED IN COMPUTER WORK *

* Measured consumption watts / hour

8 Bibliography

DirFile.com the freeware recourse. (8 de mayo de 2006). Freeware WatchOverEnergy at DirFile. Recuperado el 15 de enero de 2009, de <http://www.dirfile.com/watchoverenergy.htm>

Energy Star. (2009). Ez Wizard : Energy Star. Recuperado el 21 de marzo de 2009, de http://www.energystar.gov/index.cfm?c=power_mgt.pr_power_mgt_ez_wiz

Filesland.com. (12 de junio de 2004). ShutDownOnTime Software Download and Review. Recuperado el 25 de febrero de 2009, de <http://www.filesland.com/companies/WindSolutions/ShutDownOnTime.html>

Free Download Manager. (2009). Descargar Witricity Power (Witricity Power). Recuperado el 25 de marzo de 2009, de http://www.freedownloadmanager.org/es/downloads/Poder_de_Witricity_49836_p/free.htm

LessWatts.org. (2009). LessWatts.org - Saving Power on Intel systems wiht linux. Recuperado el 28 de febrero de 2009, de <http://www.lesswatts.org/projects/powertop/download.php>

Lobosoft.es. (28 de marzo de 2009). Lobosoft Blog sobre desarrollo de software y seguridad informática. Recuperado el 5 de abril de 2009, de <http://www.lobosoft.es>

Saver. (2008). CO2 Saver. Recuperado el 4 de marzo de 2009, de <http://co2saver.snap.com/>

Verdiem. (2009). Verdiem: Edison Start saving energy today! Recuperado el 15 de febrero de 2009, de <http://www.verdiem.com/edison.aspx>

Three Dimensional hair model by means particles using Blender

1Jesús Antonio Álvarez-Cedillo, 2Roberto Almanza-Nieto, 3Juan Carlos Herrera-Lozada
1,2,3CIDETEC IPN, U. P. Adolfo López Mateos, Av. Juan de Dios Bátiz s/n casi esq. Miguel Othón de Mendizábal, Edif. del CIDETEC, Col. Nva. Industrial Vallejo, Del. Gustavo A. Madero, 07700, México, 1jaalvarez@ipn.mx, 2ralmanzan9700@ipn.mx, 3jlozada@ipn.mx

Abstract. The simulation and modeling of human hair is a process whose computational complexity is very large, this due to the large number of factors that must be calculated to give a realistic appearance. Generally, the method used in the film industry to simulate hair is based on particle handling graphics. In this paper we present a simple approximation of how to model human hair using particles in Blender.

Keywords: Blender, Human Hair Simulation, 3D modeling, rendering, particles

8. Introduction

3D Three-dimensional modeling of hair is considered a process of high computational cost. In modeling hair, we are faced with a complex geometry. The approximate number of hairs on a human head is of 130,000 items, a redhead has about 90,000 items, a blond-haired person can have 150.000 and, in the case of animals, we are talking about millions of items on your skin. Besides that each hair may have a special geometric shape which is not trivial in their simulation and calculation.

The diameter of a hair is very thin, it is 70 microns and may be as long as we want, this can cause a major problem of sampling, and thus making a correct sample is essential for any practice of hair rendering.

The property of reflection of light received by each hair not only blocks the light from a source in a scene, in general, each hair affects the amount of illumination, such as a single hair can cause shadows on other hair transmitted light as well as receive other, the amount of light reflected and scattered could be different and depending on the direction of growth.

The above points make the three-dimensional modeling is a computationally demanding task, therefore rendering software than a hardware parallelized graphics require considerable computing time, luckily the advance of hardware currently provides processing units graph. In these units is more likely to perform this task, even in real time. But keep in mind that not all graphics cards are designed for small items such as event or hair.

9. Graphically human hair

A human hair fiber can be represented by a curved cylinder; this is made up of particles and triangles. See Figure 1.

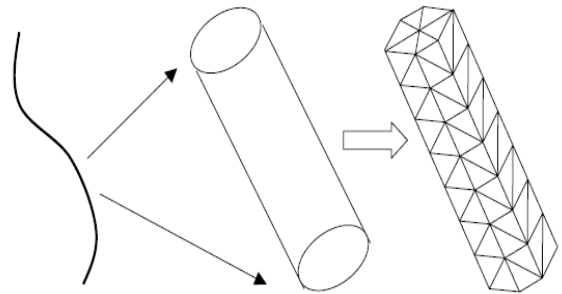


Figure 1. Graphical representation of an individual hair

This model would be valid if we were in a microscopic world where we see a few hairs together, for the case study, we have a large sample of hair, where the naive approach would generate too many triangles; otherwise, the hair is so fine that the curves is rarely significant. An alternative solution would be to bring the hair to a flat ribbon always look at the camera, as shown in Figure 2.

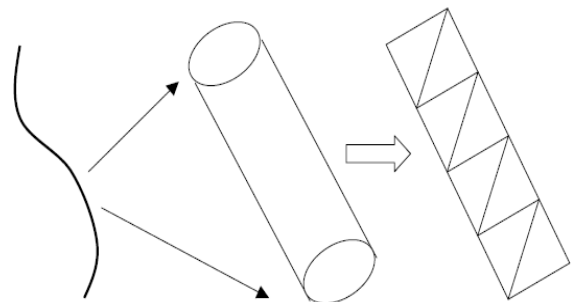


Figure 2. Representation of a flat ribbon.

Another way to simplify the geometry and obtain the appearance of hair is by means of interconnecting

lines, which are associated with an artificial thickness value (typically one pixel wide), see Figure 3.

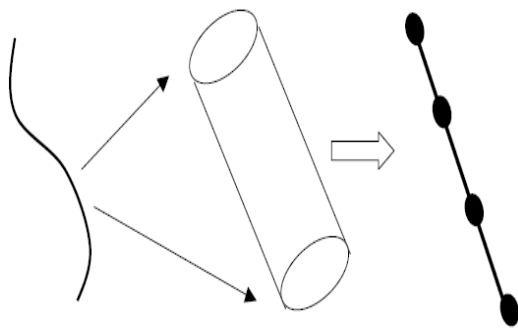


Figure 3. Hair modeling with interconnection lines.

3. The method using particles

There are several methods for working with hair as an object in the modeling of three-dimensional images, which can be found in different sources of information, including: the rigid bodies method, the particle system method and the continuous approach method [4].

The term particle system refers to a computer graphics method to simulate diffuse phenomena that are difficult to reproduce; this method allows for modeling solid objects with weak characteristics such as: fire, water and clouds, as well as hair, the result is capable of playing movements, changes dynamically, through classical representations for surfaces.

The modeling of diffuse objects is called Particles System [5,6]. The representation of particle systems is different from the normal representation of images in three key points. First, an object is not represented by a set of geometric primitives that define the boundaries of the surface such as polygons or triangles, but as a great accumulation of primitive particles that define its volume. Second point, a particle system is not a static entity as the particles change shape and move with the passage of time. The new particles are "born" and old particles "die."

Third point, an object represented by a particle system is not deterministic because its shape and appearance are not completely defined, however stochastic processes are used to create and change the shape and appearance of the object.

The particle system technique has significant advantages over classical techniques designed to surface, with respect to the modeling of diffuse objects.

For example, a particle (a point in three dimensional space) is a very simple primitive polygon, and is the base area of the surface representations. Therefore, in the same amount of processing time is possible to calculate basic and most primitive to produce a photorealistic image. Due to the simplicity of the particle distribution is also easy to apply motion (Motion-blur) [7], which is the diffuse effect caused by the rapid movement of an object in the scene. Many classical techniques ignore this step causing diffuse effect (aliasing) of the edges of objects that move quickly on the scene, like a train or plane. In addition, particle systems model objects that are "alive" (change over time), which is quite difficult to model with surface-based techniques due to the difficulty of incorporating complex dynamics.

A particle system is specified by a system of absolute position in three dimensional space and a set of particles. Each individual particle is defined by its position, speed, color and size.

The lifetime of particles is developed in three phases described below:

1. In the light particles entering the space in relation to the position of the system and according to one form of generation that defines the volume that can generate new particles.
2. During its lifetime, each particle changes and moves according to a set of rules, for example a function of renovation.
3. Each particle dies and is removed from the system when its lifetime has expired.

Particle effects are divided into classes for two main reasons:

1. User Convenience.
2. Performance.

The effects can be highly dependent on certain variables and are not affected by other variables. For performance reasons, it is not unlikely to evolve all possible variables of the particle at the same time.

Five types of systems are applied to the particle theory to facilitate the evolution of these.

- The generic system can generate models of effects like fire, smoke and explosions. Each particle has a location, speed, color and size.
- The aircraft system generates individual particles in different forms of flashes of light, reflections and effects of engine exhaust. A single particle in the planar system is represented by four items, each with the position, speed and color.
- The beam system generates laser models, effects and electricity using Bezier curves. Every particle in the beam system is a control point for the Bezier curve, including its position, speed and color attributes.
- The rotor system is applied to models of effects, whose main orbital rotation behavior is common in many applications. Each particle in a rotating system has rotation, position and color attributes.
- The trail system that behaves similarly to the generic system, but generates a static particle trail behind each particle moving. By offering a wide range of classes of particle system allows designers to develop a considerable variety of effects in practice that limit the search space for a specified period.

Under the physical aspect of control of each particle, each frame of animation and speed of each particle is determined by the outputs. To animate a particle each frame (for example the particle moves through space) a linear motion model calculates the position of the particle at time t depends on the time τ elapsed since the last frame of animation:

$$P_t = P_{t-1} + \tau V_s, \quad (1)$$

Where P_t is the vector of the particle new position, P_{t-1} is the vector of the particle in the previous animation frame, V is the vector of particle velocity, s is a scaling value to adjust the speed of animation.

Particle System Benefits

The particle system technique has significant advantages over classical techniques guide surface with respect to the modeling of diffuse objects. First, a particle (a point in three dimensional space) is much simpler than original polygon, the simplest of surface representations. Therefore, in the same amount of computing time to process more basic primitives and produce a more complex picture. Due to the simplicity of the particle distribution is also easy to apply motion, (Motion-Blur), which is the diffuse effect caused by the rapid movement of an object in the scene. Many classical techniques ignore this step causing diffuse effect (aliasing) of the edges of objects that move quickly on the scene, like a train or plane. Third, particle systems model objects that are "alive" (change over time), which is quite difficult to model with techniques based on surface due to the difficulty of incorporating complex dynamics [1]

4. USE OF PARTICLES IN BLENDER

What is Blender?

Blender is an environment that integrates a number of tools for creating a wide range of 3D content, with the added benefits of a multi-platform.

Aimed at media professionals and artists, Blender can be used to create 3D visualizations, both static images as high quality video, while the addition of a 3D engine in real time allows the creation of interactive content that can be reproduced independently. Originally developed by the company 'Not a Number' (NaN), Blender is now developed as 'Free Software', with the source code available under the GNU GPL.

The Blender particle system is fast, flexible and powerful. Each mesh object can serve as an emitter of particles; these can be influenced by global forces to simulate physical effects like gravity or wind. With these possibilities can generate effects such as: smoke, fire, explosions, fireworks or even flocks of birds.

The use of static particles can generate hair, skin, grass or plants, to apply various modeling techniques. An example of hair in Blender can be observed in Figure 4.

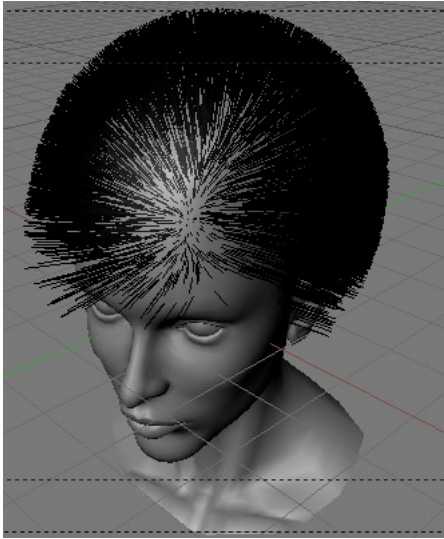


Figure 4. Hair generated using Blender

In general the flow of particles in space out of the grid, its movement can be affected by various situations, such as:

4. The initial velocity from the grid.
5. The movement of the emitter (vertex, face or object).
6. The movement according to the gravity or air resistance.
7. Influence of the force fields such as wind, vortices or guided through a curve.
8. Interaction with other objects such as collisions.
9. Slow motion physics "softbody" (only in systems of hair particles) [8].
10. Or even the manual processing.

The particles can be represented as:

5. Halos (for the preparation of flame, smoke, clouds)
6. Strands (used in the development of hair, skin, grass), the full form of a string will be displayed as a string or filaments, these filaments can be manipulated (comb, cut, move, etc..) directly in Blender.

Each object made in Blender can contain multiple particle systems, where each system can have up to 100,000 particles; we must remember that it is possible that we can have multiple sets of systems of particles within Blender associated with a single object. The following will describe the process in a simple way to work with a system of particles using Blender.

The creation and definition of a grid, serves as the basis for issuing the particle system, this system manifold in combination for each particle, develops the desired effect simulation.

After creating a Blender particle system allows you to configure your environment to choose one of three different types of particle systems [9], which are:

- **Emitter:** Particles are emitted by the selected object and have a fixed life.
- **Reactor:** It is very useful for most older particle effects.
- **Hair:** This type of system is represented as wires and such special properties can be edited in real-time 3D.

The procedure for creating Blender particle system consists of the following topics:

- We must put a base object, the modeling of hair, this object can be imported, the model used was developed in Zbrush. Of pixelogic company
- We need to change as a thick paint (Weigh Paint), to select an area where the algorithm will work.
- We must create a new set of vertices with a common name. The selected area will be affected by the algorithm. The result of the above steps are shown in Figure 5.
- Create a new particle system type HAIR "flee" the panel "Physics" enable this task.
- We increase the value, is noted that the hair grows in all of our object (Figure 6). This is a problem that is solved by placing the hair in the area to be established, so it is necessary to activate the "Extra" in the group of vertices. Figure 6a shows the solution applied.

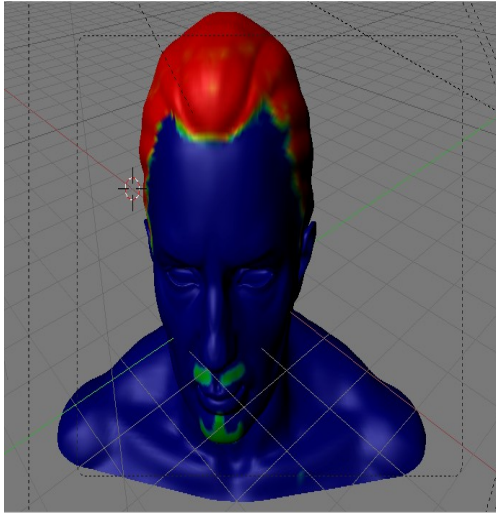


Figure 5. Area where we want to grow hair

- Create a new particle system type HAIR "flee" the panel "Physics" enable this task.
- We increase the value, is noted that the hair grows in all of our object (Figure 6). This is a problem that is solved by placing the hair in the area to be established, so it is necessary to activate the "Extra" in the group of vertices. Figure 6a shows the solution applied.

As can be seen, have been obtained only, some strands of hair, still not achieved the desired density for a photo realistic model, to achieve a more realistic simulation will need to change some parameters. Within the offspring panel "Children" can configure two options: Particle and face. See Figure 7.

At this point, the model is nearing completion, in case modeling long hair, you will need to modify some parameters in collisions.

Finally, it is necessary to add the type of material to our model, for it is given two different types of materials, one will be used by our object-based and one for the system of particles in the panel "Link and Material" by changing the corresponding parameter achieves the desired effect, then in edit mode will need to deselect all vertices of our base (See Figure 8). This will create a new material which will be used in the system of particles, the light finally be added to the model to obtain the result shown in Figure 9.

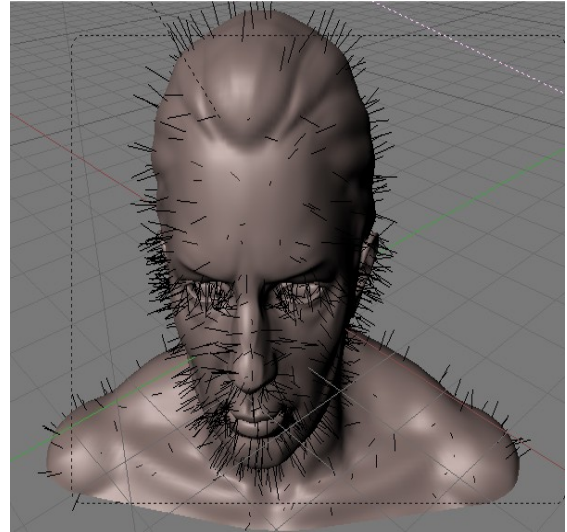


Figure 6. Filaments generated by the particle system in Blender

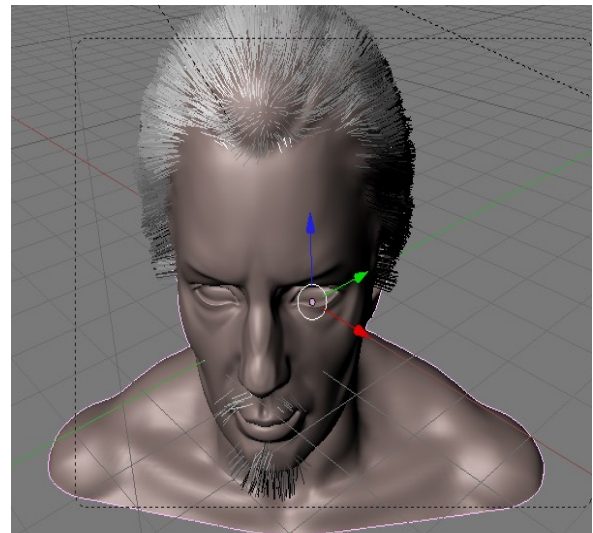
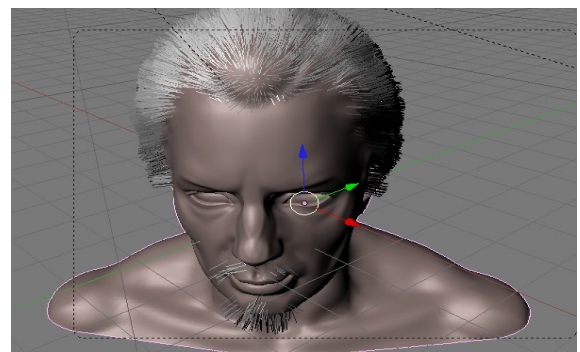


Figure 6a. Filaments grouped in the corresponding area using Blender



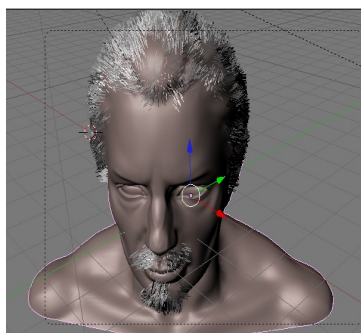


Figure 7. Blender provides different densities for the system of particles in the hair model

At this point, the model is nearing completion, in case modeling long hair, you will need to modify some parameters in collisions.

Finally, it is necessary to add the type of material to our model, for it is given two different types of materials, one will be used by our object-based and one for the system of particles in the panel "Link and Material" by changing the corresponding parameter achieves the desired effect, then in edit mode will need to deselect all vertices of our base (See Figure 8). This will create a new material which will be used in the system of particles, the light finally be added to the model to obtain the result shown in Figure 9.

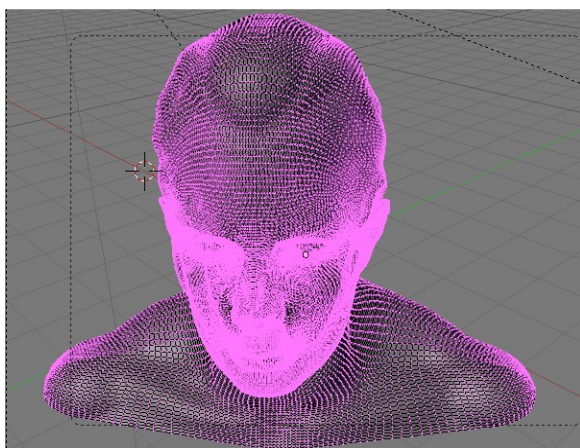


Figure 8. Having the model in edit mode in Blender

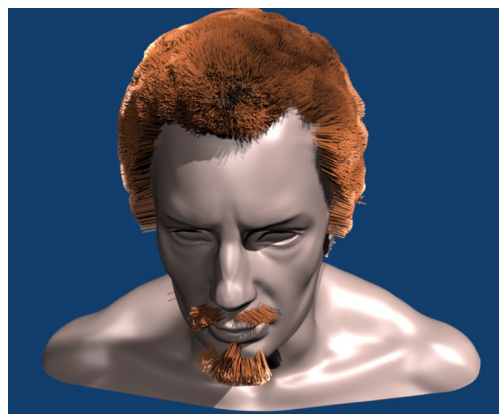


Figure 9. Final result using the particle system that provides Blender.

5. Conclusions and future work

Hair modeling is a nontrivial work for the high computational complexity required for processing. There are different techniques which aim to model the human hair sacrificing the quality of the resulting images. The particle system for modeling of hair is the most simple and fast since it uses a simple structure for each element and that simplifies the interaction that takes the system with physical phenomena, unlike other modeling such as modeling mesh-based hair where realism and interaction can be a bit more limited.

Blender provides the tools necessary to work semi professional modeling hair using a particle system, provides a variety of specialized tools and ways of rendering textures, it is also free software. Given the facilities will be developed in a Blender future work, an algorithm in Python to model hair using a particle system.

References

- [1] ERNESTO COTON, Introducción a los Sistemas de Partículas. Universidad Central de Venezuela. Facultad de Ciencias. Escuela de Computación. Laboratorio de Computación Gráfica (2004).
- [2] JOHNNY T. CHANG, JINGYI JIN, YIZHOU YU, A Practical Model for Hair Mutual Interactions. Department of Computer Science University of Illinois at Urbana Champaign (2002).
- [3] SUNIL HADAP ADOBE SYSTEMS, MARIE-PAULE CANI INP GRENOBLE, Ming Lin University of North Carolina, Tae-Yong Kim Rhythm&Hues Studio, Florence Bertails INRIA Rhone-Alpes, Steve Marschner Cornell University, Kelly Ward Walt Disney Animation Studios, Zoran Kačič-Alesić Kelly, REALISTIC HAIR SIMULATION ANIMATION AND

RENDERING, SIGGRAPH 2008 Course Notes, May 19, 2008.

- [4] ALEKA MCADAMS, ANDREW SELLE, KELLY WARD, EFTYCHIOS SIFAKIS, JOSEPH TERAN, Detail Preserving Continuum Simulation of Straight Hair, ACM Transactions on Graphics, Vol. 28, No. 3, Article 62, Publication date: August 2009.
- [5] ABRAHAM, R., AND SHAW, C. DYNAMICS The Geometry of Behavior. City on the Hill Press, Santa Cruz, Calif., 1981.
- [6] BADLER, N. I., O'ROURKE, J., AND TOLTZIS, H. A spherical human body model for visualizing movement. Proc. IEEE 67, 10 (Oct. 1979).
- [7] BLINN, J. F. Light reflection functions for simulation of clouds and dusty surfaces. Proc. SIGGRAPH '82. In Comput. Gr. 16, 3, (July 1982), 21-29.
- [8] CSUR, C., HACKATHORN, R., PARENT, R., CARLSON, W., AND HOWARD, M. Towards an interactive high visual complexity animation system. Proc. SIGGRAPH 79. In Comput. Gr. 13, 2 (Aug. 1979), 289-299.
- [9] FOURNIER, i., FUSSEL, D., AND CARPENTER, i. Computer rendering of stochastic models. Commun. ACM 25, 6, (June 1982), 371-384.

Digit recognition using Static Hidden Markov Models and Vector Quantization for Nahuatl language

José Luis Oropeza Rodríguez¹; Sergio Suárez Guerra¹

¹ Center for Computing Research, National Polytechnic Institute,
Juan de Dios Batiz esq Miguel Othon de Mendizabal s/n, P.O. 07038, Mexico
joropeza@cic.ipn.mx, ssuarez@cic.ipn.mx

Abstract. The goal of automatic speech recognition (ASR) is to develop techniques and systems that enable computer to accept speech input. The digit task has been so much employed to contribute the effort in ASR. Since 1950's, Automatic Speech Recognition Systems (ASRs) has been studied by so much researchers. In our country, universities have inverted a lot of time creating speech recognition systems (UNAM, IPN, ITESM, UAM, UDLA; among others). The performance of well-trained speech recognizers using high quality full bandwidth speech data is usually degraded when used in real world environments. In this paper, vector quantization was used in an Automatic Speech Recognition System (ASRs), which employed a dictionary conformed by eighteen command words (digits specifying from Nahuatl language). After that the results obtained were compared with other ASRs that used Discrete Hidden Markov Models. In first experiment we obtained a performance of 98.33% and 90% in the second case. Experimental results on digit task corpora showed that the performance of the proposed methods is benefits to be used in a system that decide to speech recognition with Nahuatl language. Only one speaker was analyzed but the results obtained can be expanded integrating to much speakers also.

Keywords. Automatic Speech Recognition, speaker recognition, Discrete Hidden Markov Models, Viterbi Training, and dependent-independent speaker automatic speech recognition systems.

1 Introduction

A vector quantization is a system for mapping sequence of continuous or discrete vectors into a digital sequence suitable for communication over or storage in a digital channel. The goal of such a system is data compression: to reduce the bit rate so as to minimize communication channel capacity or digital storage memory requirements while maintaining the necessary fidelity of the data.

Hidden Markov Models (HMMs) have dominated automatic speech recognition for at least the last decade. The model's success lies in its mathematical simplicity; efficient and robust algorithms have been developed to facilitate its practical implementation.

Nahuatl characteristics are following described [e1]:

- ❖ It is an agglutinant language. Words and phrases are constructed by joining prefixes, root words and suffixes to form an idea.
- ❖ It is a flexive language. The morphology of words may change (flex) according to their function in a phrase.
- ❖ It uses mostly reverential forms of speech that gives a respectful frame to human relations.

Nahuatl is an Uto-Aztecan language spoken by about 1.5 million people in Mexico. The majority of speakers live in central Mexico, particularly in Puebla, Veracruz, Hidalgo, San Luis Potosi, Guerrero, Mexico DF, Tlaxcala, Morelos and Oaxaca, and also in El Salvador.

There are numerous dialects of Nahuatl, some of which are mutually unintelligible. Most Nahuatl speakers also speak Spanish, with the exception of some of most elderly.

Classical Nahuatl was the language of the Aztec empire and was used as a lingua franca in much of Mesoamerica from the 7th century AD until the Spanish conquest in the 16th century. The modern dialects of Nahuatl spoken in the Valley of Mexico are closest to Classical Nahuatl. Nahuatl was originally written with a pictographic script which was not a full writing system but instead served as a mnemonic to remind readers of texts they had learnt orally. The script appeared in inscriptions carved in stone and in picture books, many of which the Spanish destroyed [e1].

Sounds

The consonants of classical Nahuatl

	Labial	Alveolar	Post-alveolar	Palatal	Velar	Labio-velar	Glottal
Plosive	p	t			k	k ^w	ʔ (h)*
Affricate		tʃ / tʃs	tʃ				
Fricative		s	ʃ				
Nasal	m	n					
Approximant		l		j		w	

Table 1. Phonetic of the Nahuatl language

2 Characteristics and Generalities

“The schools of thought in speech recognition” describe four different approach researched at today, they are [Kirschning 1998]:

- approach
- approach
- approach and,
- approach
- template-based
- knowledge-based
- stochastic
- connectionist

In the template-based approach, the units of speech (usually words, like in this work), are represented by templates in the same form as the speech input itself. Distance metrics are used to compare templates to find the best match, and dynamic programming is used to resolve the problem of temporal variability. Template-based approaches have been successful, particularly for simple applications requiring minimal overhead.

The stochastic approach, which is similar to the template-based approach has been using in the recent developments of ASR. One major difference is that the probabilistic models (typically Hidden Markov Models –HMM-) are used. HMM are based on a sound probabilistic framework, which can model the uncertainty inherent in speech recognition. HMM have an integral framework for simultaneously solving the segmentation and the classification problem, which makes them particularly suitable for continuous-speech recognition. One characteristic of HMM is that they make certain assumptions about the structure of speech recognition, and then estimate system parameters as though the structures were correct.

Nahuatl number system is completely vigesimal (base 20) even for numbers bigger than 100.

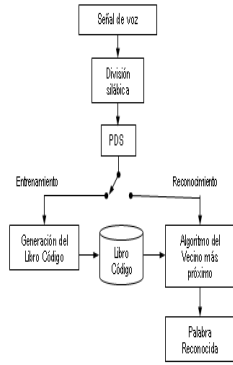
Table 2 List of the words employed in the corpus in this experiment

Number	Reading	Meaning
0	ʔ	-
1	cē	1
2	ōme	2
3	ēyi	3
4	nāhui	4
5	mācuilli	5
6	chicuacē	5 [†] + 1
7	chicōme	5 [†] + 2
8	chicuēyi	5 [†] + 3
9	chiucnāhui	5 [†] + 4
10	mahtlactli	10
11	mahtlactli-on-cē	10 and 1
12	mahtlactli-om-ōme	10 and 2
13	mahtlactli-om-ēyi	10 and 3
14	mahtlactli-on-nāhui	10 and 4
15	caxtōlli	15
16	caxtōlli-on-cē	15 and 1
17	caxtōlli-om-ōme	15 and 2
18	caxtōlli-om-ēyi	15 and 3

3 Automatic Speech Recognition Systems

The frequency bandwidth of a speech signal is about 16 KHz. A telephonic lower quality signal is obtained when ever a signal does not have energy out of the band 300-3400 Hz [Bechetti and Prina 1999]. Therefore, digital speech processing is usually performed by a frequency sampling ranging between 8000 samples/sec and 32000 samples/sec. These values correspond to a bandwidth of 4KHz and 16KHz respectively. In this work, we use a frequency sampling 16000 samples/sec and 16 bits. Figure 1 shows the scheme used for Vector Quantization method reported in this work.

Vector Quantization



Discrete Hidden Markov Models

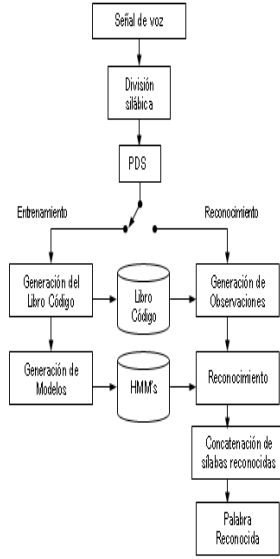


Fig 1 Schematic Diagram for Vector Quantization and Discrete Hidden Markov Models employed in this paper

3.1 Signal preprocessing

A preemphasis of high frequencies is therefore required to obtain similar amplitude for all formants. Such processing is usually obtained by filtering the speech signal with a first order FIR filter whose transfer function in the z-domain is [Oppenheim 89]:

$$H(z) = 1 - az^{-1} \quad [1]$$

A typical value for a is 0.95, which gives rise to a more than 20 dB amplification of the high frequency spectrum.

3.2 Windowing

In ASR, the most-used window shape is the Hamming window, whose impulse response is a raised cosine impulse [DeFatta et al. 1988]:

$$0.54 - 0.46 \cos\left(\frac{2\pi n}{N-1}\right) \quad n=0, \dots, N-1$$

$$0 \quad \text{otherwise}$$

$$w(n) = \{ \}$$

[2]

3.3 Unsupervised algorithms for clustering word data

Following the development in Levinson et al. [Levinson et al. 1979], we assume that we are given a finite set Ω of N observations

$$\Omega = \{x_1, x_2, \dots, x_N\} \quad [3]$$

where each observation x_i is a pattern representing a replication of one specific spoken word. Each pattern has an inherent duration (e.g. x_i is n_i frames *log*), and each frame of the pattern is some measured set of features. For the recognition system we use, the feature set is the set of (p+1) autocorrelation coefficients (p=12) [Markel and Grayu 1976] [Itakura 1975].

Since it is intended that the clustering of the N observations be based entirely on distance (similarity) data, a distance $d(x_i, x_j)$ between patterns x_i and x_j is defined as:

$$d(x_i, x_j) = \frac{x_i^t R_x x_i}{x_j R_x x_j} \quad [4]$$

Where the local frame distance $d(x_i, x_j)$ is the log likelihood distance proposed by Itakura [Itakura 1975] between the k th frame of x_i and the $w(k)$ th frame of x_j , i.e.,

Where x_i is the vector of LPC coefficients of the k th frame of pattern i , R_x is the matrix of correlation coefficients of the k th frame of pattern I , and x_ℓ^t denotes ℓ -vector transpose.

The purpose of the clustering is to represent the set Ω as the union of M disjoint clusters $\{\lambda_i, i=1, 2, \dots, M\}$ such as:

$$\lambda_i \hat{c} \quad [5]$$

The total number of clusters M need not be known or specified a priori. We denote the center or prototype of cluster ω_i as $c(\lambda_i)$ and we note that $c(\lambda_i)$ need not be a member of ω_i , then the expression that relation both elements is given by:

$$(X_k)_{k=1}^M \quad \Delta = \frac{1}{M} \sum_{k=1}^M d(C_k, a_k) \quad [6]$$

where C_k is the centroid vector, $d(C_k, a_k)$ represents the Itakura-Saito distance modified, that is a consequence of the nearest neighbor algorithm.

Table I Example of vector code distribution into a codebook

	1	2	3	4	5	6	7	8	9	10	11	12	13	14	15	16	17	18	19	20	21	22	23	24	25	26	27	28	29	30	31	32
CE	53	24	232	259	6	5	2	8	10	8	7	24	25	29	12	15	9	8	10	12	11	6	22	25	25	25	11	11	20	13	33	27
ONE	172	144	0	1	4	20	11	9	10	23	11	0	16	10	14	22	14	15	16	20	9	10	11	17	10	11	15	11	15	1	10	
YEL	57	8	182	63	14	9	21	10	12	21	25	36	29	47	30	36	8	7	11	4	14	4	5	2	13	20	25	14	21	12	9	13
NAHU	95	245	3	1	72	13	9	10	11	6	15	10	11	8	14	12	13	57	14	4	24	10	20	11	16	14	22	17	10	10	22	10
MACUHALLI	15	10	25	19	7	14	11	13	51	27	5	11	7	12	13	22	1	295	29	24	13	7	21	9	37	15	21	13	6	8	6	4
CHOCUACE	152	166	2	1	32	20	37	24	14	9	15	3	12	3	3	9	74	21	46	14	29	17	30	17	12	10	15	14	12	11	11	7
CHOCUONE	1	122	34	6	7	11	15	15	12	8	11	5	8	16	11	25	30	24	46	7	34	25	43	16	9	19	14	26	5	11	10	17
CHOCUEY	79	21	103	100	4	54	19	12	13	10	11	8	11	5	13	22	32	20	12	5	5	5	5	10	14	14	20	47	23	14	16	
CHICHNAHU	145	203	41	17	14	9	6	9	16	29	19	22	29	18	17	23	24	15	21	6	11	2	3	4	10	7	6	4	10	6	12	10
MATLAHTLE	307	21	27	10	3	8	12	8	10	12	7	6	13	10	23	21	11	12	10	10	15	15	25	24	46	44	16	15	9	10	20	20

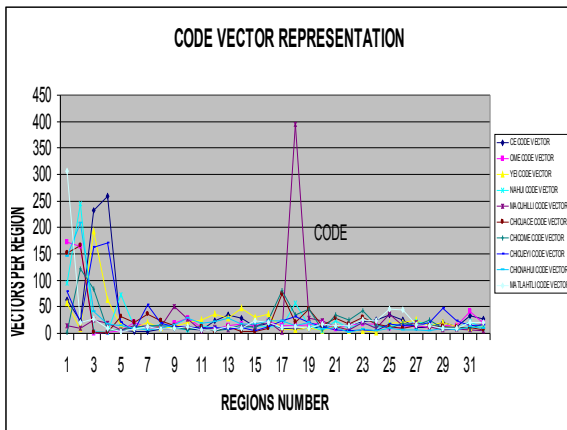


Fig 2 code book representation

4 Hidden Markov Models and Experimental Methodology

Now, we are going to show the algorithms employed for Automatic Speech Recognition using Hidden Markov Models (HMMs). Like we know, HMMs mathematical tool applied for speech recognition presents three basic problems [Rabiner and Biing-Hwang, 1993] y [Zhang 1999]:

Problem 1. Given the observation sequence $O=O_1O_2\dots O_T$, and a model $\lambda=(A,B,\pi)$, how do we efficiently compute $P(O|\lambda)$, the probability of the observation sequence, given the model?

1. Initialization

$$\alpha_1(i) = \pi_i b_i(O_1) \quad 1 \leq i \leq N \quad [7]$$

2. Induction

$$\alpha_{t+1}(j) = b_j(O_{t+1}) \sum_{i=1}^N \alpha_t(i) a_{ij} \quad 1 \leq j \leq N, 1 \leq t \leq T-1 \quad [8]$$

3. Termination

$$P(O|\lambda) = \sum_{i=1}^N \alpha_T(i) \quad [9]$$

Problem 2. Given the observation sequence $O=O_1O_2\dots O_T$ and the model λ , how do we choose a corresponding state sequence $Q=q_1q_2\dots q_T$ which is optimal in some meaningful sense?

1. Initialization

$$\delta_1(i) = \pi_i b_i(O_1) \quad 1 \leq i \leq N \quad [10]$$

2. Recursion

$$\delta_t(i) a_{ij} \hat{c} \hat{c} \hat{c} \quad 1 \leq j \leq N, 1 \leq t \leq T-1 \quad [11]$$

3. Termination

$$p = \max_{i=1}^N [\delta_T(i)] \quad [12]$$

$$q = \operatorname{argmax}_{i=1}^N [\delta_T(i)] \quad [13]$$

Problem 3. How do we adjust the model parameters

$\lambda=(A,B,\pi)$ to maximize $P(O|\lambda)$?

$$= \text{expected} \frac{\text{number of times from state } s_1 \text{ to } s_2}{\text{expected number of transitions from } s_1} \quad [14]$$

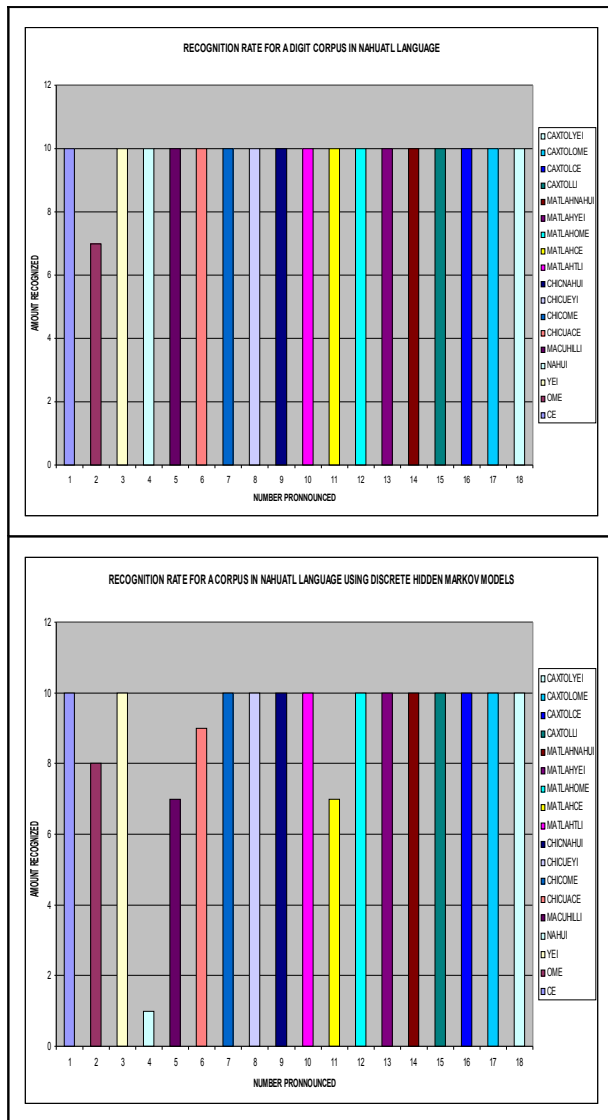


Fig. 5 Performance obtained in a graphical representation

At respect, we obtain a 99% of successful recognition and 1% of error rate and 90% of successful recognition and 10% of error rate for vector Quantization and Discrete Hidden Markov Models respectively.

6 Conclusions and future works

The main purpose of this paper was to develop a fully ASR system using vector Quantization and Discrete Hidden Markov Models. We included 200 sentences of speech recorded by one speaker; it was because we constructed an ASR system dependent of speaker. The results obtained demonstrated that ASR has a high performance independently of model employed, but vector quantization demonstrated to be better than Discrete Hidden Markov Models for sentences recorded from Nahuatl language.

One of the most important aspects to consider when we created an Automatic Speech Recognition that involves a specific language is analyze its properties, specifically walking about Nahuatl language; it has a set of properties perfectly established. In this paper we used two techniques broadly knowing: Vector Quantization and Discrete Hidden Markov Models. The interest of this work was study the results founded in using each one of these techniques.

For future works we are going to use the results obtained here to integrate the Automatic Speech Recognition for a system that will has not only speech recognition wheatear more synthesis in an application that is going to interactively it will respond to anybody people. For that, we must to work in increase the number of the speakers and programming another splitting algorithm, and we will probably obtain better results. Though the results reported demonstrated a good and better performance.

References

- [Bechetti and Prina 1999] Bechetti Claudio and Prina Ricoti Lucio, "Speech Recognition Theory and C++ Implementation", Fondazione Ugo Bordón, Rome, Italy, John Wiley and Sons, Ltd, 1999.
- [DeFatta et al. 1988] DeFatta J. David, Lucas G. Joseph and Hodgkiss S. William, Digital Signal Processing, A system design approach, John Wiley & Sons, 1988.
- [Itakura 1975] Itakura F., "Minimum prediction residual applied to speech recognition" IEEE Trans, Acous., Speech, Signal Processing, vol. 26, pp 575-582, Feb. 1975.
- [Kirschning 1998] Kirschning Albers Ingrid, "Automatic Speech Recognition with the parallel Cacade Neural network", PhD Thesis, Tokyo Japan, March 1998.
- [Levinson et al. 1979] Levinson S. E., Rabiner L. R., Rosenberg J. G. and Wilpon J. G. "Interactive clustering techniques for selecting speaker independent reference templates for isolated word recognition", "IEEE Trans. Acoust. Speech, Signal Processing, vol ASSP-27, pp.134-141, 1979.
- [Markel and Gray 1976] Markel J. D. and Gray A. H. "Linear Prediction for speech". New York: Springer-Verlag, 1976.
- [Oppenheim 89] Oppenheim A. V., Shafer R. W., Digital Dignal Processing, Prentice Hall (1989).
- [Rabiner and Biing-Hwang 1993] RABINER Lawrence and Biing-Hwang Juang, "Fundamentals of Speech Recognition", Prentice Hall, 1993.
- [Zhang 1999]. ZHANG Jialu, "On the syllable structures of Chinese relating to speech recognition",

Institute of Acoustics, Academia Sinica Beijing,
China, 1999.

[e1]

http://en.wikipedia.org/wiki/Classical_Nahuatl_language

Speech recognition based in Vector Quantization in a virtual environment

José Luis Oropeza Rodríguez¹
Juan Uriel Quezada¹

joropeza@cic.ipn.mx, cquezadab08@sagitario.cic.ipn.mx

Abstract

The goal of automatic speech recognition is to develop techniques and systems that enable computer to accept speech input. Since 1950's, the problem of the Automatic Speech Recognition (ASR) has been studied by so much researchers. In our country, universities have inverted a lot of time creating speech recognition systems (UNAM, IPN, ITESM, UAM, UDLA, etc.). The ASR is a very rich field for both practical and intellectual reasons. Practically, Speech Recognition will solve problems, improve productivity, and change the way we run our lives. Intellectually, speech recognition holds considerable promises as well as challenges in the years to come for scientist and product developers alike. This paper treats about the implementation of an ASR using the template-based approach employing a database of isolated words to control the movements into virtual environment. We supposed that are immersed into labyrinth and with our speech we selected the direction to take.

1. Introduction

Speech and language are perhaps the most evident expression of human thought and intelligence –the creation of machines that fully emulate this ability poses challenge that reach far beyond the present state of the art.

The speech recognition field has been fruitfully and productively benefited from sciences as diverse as computer science, electrical engineering, biology, psychology, linguistics, statistics, philosophy, physics and mathematics among others. The interplay between different intellectual concerns, scientific approaches, and models, and its potential impact in society make speech recognition one of the most challenging, stimulating, and exciting fields today.

As early as 1950s, simple recognizers have been built, yielding credible performance. But it was soon found that the techniques used in these systems were not easily extensible to more sophisticated systems. In particular, several dimensions emerged that

introduce serious design difficulties or significantly degrade recognition performance.

Most notably, these dimensions include:

- Isolated, connected, and continuous speech
- Vocabulary size
- Task and language constraints
- Speaker dependence or independence
- Acoustic ambiguity, confusability
- Environmental noise

The first question one should ask about a recognizer or a task is: is the speech connected or spoken one word at a time? Continuous speech recognition (CSR) is considerably more difficult than isolated word recognition (IWR) that is because at first, word boundaries are typically not detectable in continuous speech, at second, there is much greater variability in continuous speech due to stronger coarticulation (or inter-phoneme effects) and poorer articulation (“El ave es grande” becomes “la vez”).

A second dimension is the size of the vocabulary. Exhaustive search in very large vocabularies is typically unmanageable. Instead, one must turn to smaller sub-word units (phonemes, syllables, triphonemes, etc.), which may be more ambiguous and harder to detect and recognize.

A system with a semantic component may eliminate such sentences from consideration. A system with a probabilistic language model can effectively use this knowledge to rank sentences.

These knowledge sources or language models can reduce an impossible task to a trivial one. The challenge in language modeling is to derive a language model that provides maximum constraint while allowing maximum freedom of input. The constraining power of a model language can be measured by perplexity, roughly the average number of words that can occur at any decision point.

The different sources of variability that can affect speech determine most of difficulties of speech

recognition. During speech production the movements of different articulators overlap in time for consecutive phonetic segments and interact with each other. As a consequence, the vocal tract configuration at any time is influenced by more than one phonetic segment. This phenomenon is known as coarticulation mentioned above. The principal effect of the coarticulation is that the same phoneme can have very different acoustic characteristics depending on the context in which it is uttered [Farnetani 97].

The most prominent issue is that of Speaker dependence as opposed to speaker independence. A speaker dependent system uses speech from the target speaker to learn its model parameters. On the other hand, a speaker-independent system is trained once and for all, and must model a variety of speaker's voice.

Speech recognition-system performance is also significantly affected by the acoustic confusability or ambiguity of the vocabulary to be recognized. A confusable vocabulary requires detailed high performance acoustic pattern analysis. Another source of recognition-system performance degradation can be described as variability and noise.

Finally, the applications of the ASR are vast, for example: Credit-card numbers, telephone numbers, and zip codes, require only a small vocabulary.

2. Characteristics y Generalities

“The schools of thought in speech recognition” describe four different approach researched at today, they are [Kirschning 1998]:

- template-based approach
- knowledge-based approach
- stochastic approach and,
- connectionist approach

Before continuing described the characteristics of them, we must to say that ASR has implemented one stage called “speech analysis”. The applications that need voice processing (such as coding, synthesis, and recognition) require specific representations of speech information. For instance, the main requirement for speech recognition is the extraction of voice features, which may distinguish different phonemes of a language.

To decrease vocal message ambiguity, speech is therefore filtered before is arrives at the automatic recognizer. Hence, the filtering procedure can be considered as the first stage of speech analysis. Filtering is performed on discrete time quantized speech signals. Hence, the first procedure consists of an analog to digital signal conversion. Then, the extraction procedure of the significance features of speech signal is performed.

In the template-based approach, the units of speech (usually words, like in this work), are represented by templates in the same form as the speech input itself. Distance metrics are used to compare templates to find the best match, and dynamic programming is used to resolve the problem of temporal variability. Template-based approaches have been successful, particularly for simple applications requiring minimal overhead.

In the knowledge-based approach, proposed in the 1970s and early 1980s. The pure knowledge-based approach emulates human speech knowledge using expert systems. Rule-based systems have had only limited success. The addition of knowledge was found to improve other approaches substantially. Recently, in the Spanish language a new approach using the rules of the syllabic units has showed the utility of these units in the ASR.

The stochastic approach, which is similar to the template-based approach has been using in the recent developments of ASR. One major difference is that the probabilistic models (typically Hidden Markov Models –HMM-) are used. HMM are based on a sound probabilistic framework, which can model the uncertainty inherent in speech recognition. HMM have an integral framework for simultaneously solving the segmentation and the classification problem, which makes them particularly suitable for continuous-speech recognition.

One characteristic of HMM is that they make certain assumptions about the structure of speech recognition, and then estimate system parameters as though the structures were correct.

The connectionist approach use distributed representations of many simple nodes, whose connections are trained to recognize speech. Connectionist approach is a most recent development in speech recognition. While no fully integrated large-scale connectionist systems have been demonstrated yet, recent research efforts have shown considerable promise. Some of the problems that remain to be overcome include reducing time training and better modeling of sequential constraints.

The virtual reality is a representation of the things through electronic objects that the sensation gives us to be in a real situation in which we can interact.

OpenGL Performer is an extensible software toolkit for creating real-time 3D graphics and we can use it for build visual applications and virtual reality environments, Render on-air broadcast and virtual set applications quickly and maximize the graphics performance of applications

3. Template-based approach

The frequency bandwidth of a speech signal is about 16 KHz. However, most of speech energy is under 7 KHz. Speech bandwidth is generally reduced in recording. A speech signal is called orthophonic if all the spectral components over 16 KHz are discarded. A telephonic lower quality signal is obtained when ever a signal does not have energy out of the band 300-3400 Hz. Therefore, digital speech processing is usually performed by a frequency sampling ranging between 8000 samples/sec and 32000 samples/sec. These values correspond to a bandwidth of 4KHz and 16KHz respectively. In this work, we use a frequency sampling 11025 samples/sec [Bechetti and Prina 1999].

The excitation signal is assume periodic with a period equal to the pitch for vowels and other voice sounds, while for unvoiced consonants, the excitation is assumed white noise, i.e. a random signal without dominant frequencies. The excitation signal is subject to spectral modifications while it passes through the vocal tract that has an acoustic effect equivalent to linear time invariant filtering. These modifications give to the final sound the characteristic features of the different phonemes of a language. The model is relevant, for each type of excitation; a phoneme is identified mainly by considering the shape of the vocal

tract configuration can be estimated by identifying the filtering performed by the vocal tract on the excitation. Introducing the power spectrum of the signal $P_x(\omega)$, of the excitation $P_y(\omega)$ and the spectrum of the vocal tract filter $P_h(\omega)$, we have:

$$P_x(\omega) = P_y(\omega) P_h(\omega) \quad [1]$$

Where ω is the frequency of the discrete time signal. The spectrum of the filter can be obtained

from the power spectrum of the speech $P_x(\omega)$ the contribution of the excitation power $P_y(\omega)$.

3.1 Signal preprocessing

The characteristics of the vocal tract define the current uttered phoneme. Such characteristics are evidenced in the frequency domain by the location of the formants, i.e. the peaks given the resonances of the vocal tract. Although possessing relevant information, high frequency formants have smaller amplitude with respect to low frequency formants. A preemphasis of high frequencies is therefore required to obtain similar amplitude for all formants. Such processing is usually obtained by filtering the speech signal with a first order FIR filter whose transfer function in the z-domain is [Oppenheim 89]:

$$H(z) = 1 - az^{-1} \quad [2]$$

a being the preemphasis parameter. In essence, in the time domain, the preemphasized signal is related to the input signal by the relation:

$$x'(n) = x(n) - ax(n-1) \quad [3]$$

A typical value for a is 0.95, which gives rise to a more than 20 dB amplification of the high frequency spectrum.

3.2 Windowing

Traditional methods for spectral evaluation are reliable in the case of a stationary signal (i.e. a signal whose statistical characteristics are invariant with respect to time). For voice, this holds only within the short time intervals of articulatory stability, during which a short time analysis can be performed by “windowing” a signal $x'(n)$ into a sequence of windowed sequences $x_t'(n), t=1, 2, \dots, T$ called frames, which are then individually processed:

$$x_t'(n) \equiv x'(n-t \cdot Q), \quad 0 \leq n < N, \quad 1 \leq t \leq T \quad [4]$$

$$x_i(n) \equiv w(n) \cdot x'_i(n) \quad [5]$$

Where $w(n)$ is the impulse response of the window. Each frame is shifted by a temporal length Q . If $Q=N$, frames do not temporally overlap while if $Q < N$, $N-Q$ samples at the end of a frame $x'_i(n)$ are duplicated at the beginning of the following frame.

In ASR, the most-used window shape is the Hamming window, whose impulse response is a raised cosine impulse [DeFatta et al. 1988]:

$$w(n) = \begin{cases} 0.54 - 0.46 \cos\left(\frac{2\pi n}{N-1}\right) & n=0, \dots, N-1 \\ 0 & \text{otherwise} \end{cases} \quad [6]$$

3.3 Unsupervised algorithms for clustering word data

Following the development in Levinson et al. [Levinson et al. 1979], we assume that we are given a finite set Ω of N observations

$$\Omega = \{x_1, x_2, \dots, x_N\} \quad [7]$$

where each observation x_i is a pattern representing a replication of one specific spoken word. Each pattern has an inherent duration (e.g. x_i is n_i frames *log*), and each frame of the pattern is some measured set of features. For the recognition system we use, the feature set is the set of (p+1) autocorrelation coefficients (p=12) [Markel and Grayu 1976] [Itakura 1975].

Since it is intended that the clustering of the N observations be based entirely on distance (similarity) data, a distance $d(x_i, x_j)$ between patterns x_i and x_j is defined as:

$$d(x_i, x_j) = \frac{x_i^t R_x x_i}{x_j^t R_x x_j} \quad [8]$$

Where the local frame distance $d(x_i, x_j)$ is the log likelihood distance proposed by Itakura [Itakura 1975] between the k th frame of x_i and the $w(k)$ th frame of x_j , i.e.,

Where x_i is the vector of LPC coefficients of the k th frame of pattern i , R_x is the matrix of correlation coefficients of the k th frame of pattern I , and x_ℓ^t denotes ℓ -vector transpose.

The purpose of the clustering is to represent the set as the union of M disjoint clusters $\{\lambda_i, i=1, 2, \dots, M\}$ such as:

$$\lambda_i \cup \quad [9]$$

The total number of clusters M need not be known or specified a priori. We denote the center or prototype of cluster ω_i as $c(\lambda_i)$ and we note that $c(\lambda_i)$ need not be a member of ω_i , then the expression that relation both elements is given by:

$$\Delta = \frac{1}{M} \sum_{k=1}^M d(C_k, a_k) \quad [10]$$

where C_k is the centroid vector, $d(C_k, a_k)$ represents the Itakura-Saito distance modified, that is a consequence of the nearest neighbor algorithm.

4. Results

Table 1 shows distribution that we founded related with code vectors distributed into each word, also figure 1 represents the same.

Table 1 code vector distribution for each isolated word

	1	2	3	4	5	6	7	8	9	10	11	12	13	14	15	16	17	18	19	20	21	22	23	24	25	26	27	28	29	30	31	32
forward	137	16	6	2	273	102	41	25	25	11	11	26	37	65	15	40	9	23	10	7	13	6	14	6	8	18	30	54	5	15	10	17
backward	373	209	80	27	27	12	3	9	222	57	29	25	23	12	14	9	9	1	6	9	44	25	13	43	4	4	2	4	26	15	13	5
left	11	81	9	23	16	16	11	17	17	5	12	4	6	11	28	7	281	460	77	35	14	52	18	4	15	4	9	12	6	8	11	7
right	197	255	38	233	15	31	15	1	13	7	5	8	7	3	4	5	12	44	10	8	11	23	19	26	22	5	13	13	6	7	11	3
stop	13	2	689	143	10	2	90	5	9	2	50	8	10	13	1	1	5	12	6	11	3	6	2	4	3	8	16	10	9	14	14	47

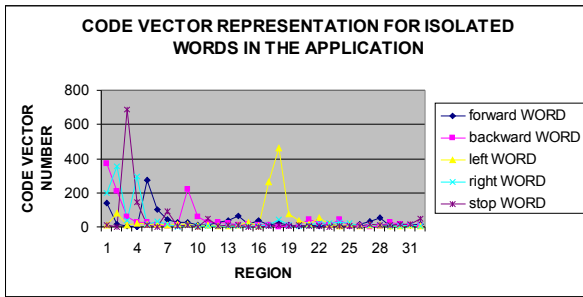


Fig 1 Code vector representation

As we can see, table 1 shows a significance difference between code vectors of isolated words. Figure 1, shows a schematic representation and we can see the principle of classification involved into vector quantization.

For this experiment we used a virtual environment created with OpenGL, figure 2 shows that.

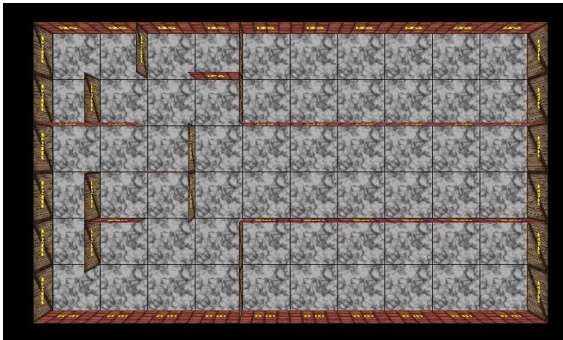


Fig 1 labyrinth virtual developed with OpenGL

Also, we used OpenAL to interact with speech; we recorded 20 sentences by word in our corpus (left, right, forward, backward and stop), 100 in a total. This application is constantly waiting a request for voice processing and decision making. After that we pronounced each isolated word and the results are showed in figure 2 to 3.

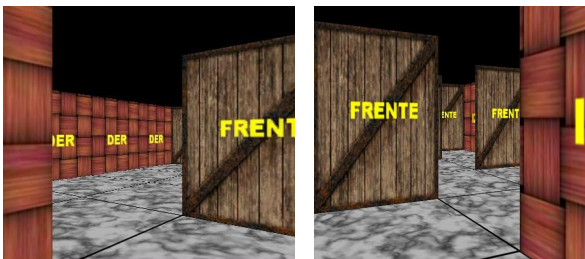


Figure 2 Direction taken after left or right command was pronounced.

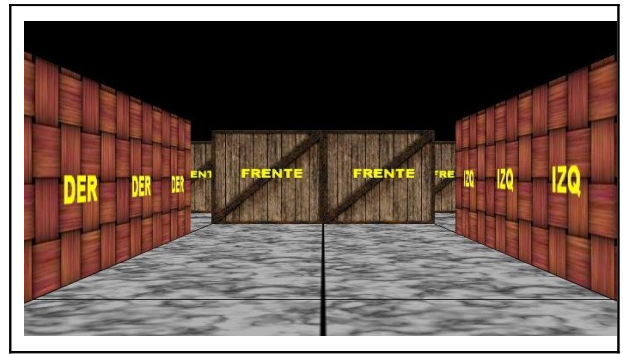


Figure 3 Direction taken after forward command was pronounced.

The evaluation of the algorithm proposed involved clustering a set of speech data consisting of 50 isolated patterns from 5 words that consists the vocabulary. The training patterns (and a subsequent set of another 50 independent testing pattern) were recorded in a room free of noise. Only one speaker provided the training and testing data. All training and test recordings were made under identical conditions (noise, laboratory, etc.).

Table I shows the distribution of the training and testing patterns amongst the 5 digits. Clustering was performed the algorithm mentioned above. Templates were generated without problems, 5 in total. The recognition system used was the LPC-based isolated word recognition system developed in our laboratory.

Table I. Number of tokens for each digit used in the training and testing phases for evaluating the VQ method proposed.

Number	DIGITS	Training Set	Testing Set
1	“adelante”-forward	10	10
2	“atrás”-backward	10	10
3	“izquierda”-left	10	10
4	“derecha”-right	10	10
5	“alto”-stop	10	10
	TOTAL	50	50

The results of a set of recognition runs in which the 100 test digits were recognized using the template according are given in the Table II. This representation is also called “Confusion matrix”.

Table II. Confusion Matrix obtained after to execute the experiment.

	1	2	3	4	5
1	10				
2		10			
3			10		
4				10	
5					10

Like we know, the Confusion matrix contains information about actual predicted classifications done by a classification speech recognition proposed above.

At respect, we obtain a 100% of successful recognition and 0% of error rate. Given in this table are results for several values of the K-nearest neighbor decision rule in which the recognition is based on the best K distances for each word (rather than the best single distance as is conventionally the case for a nearest neighbor recognizer).

5. Conclusions

The main purpose of this paper was to develop a fully automatic word clustering procedure based on the highly successful K-means iteration used in VQ (Vector Quantization) codebook design and other related areas. On the surface the resulting algorithm appears to be a trivial application of known technology. However, the successful adaptation of the K-means iteration to word clustering required solving some small but important practical problems such as how to obtain cluster center (centroids) at each stage of the iteration so that the computation would not be prohibitive, how to split clusters to advance from one size solution to the next, and finally how to create the final cluster representation, i.e., the word templates from patterns within the cluster. The application developed shows that is possible interact with virtual environment with speech recognition without problem.

The success of the algorithm has been demonstrated via solution on one set of isolated digit data.

6. References

[Farnetani 97] Farnetani E., “Coarticulation and connected speech processes”, in the Handbook of Phonetic Sciences, W. Hardcastle and J. Laver, Eds., Blackwell, pp. 371-404 (1997).

[Kirschning 1998] Kirschning Albers Ingrid, “Automatic Speech Recognition with the parallel Cascade Neural network”, PhD Thesis, Tokyo Japan, March 1998.

[Bechetti and Prina 1999] Bechetti Claudio and Prina Ricoti Lucio, “Speech Recognition Theory and C++ Implementation”, Fondazione Ugo Bordón, Rome, Italy, John Wiley and Sons, Ltd, 1999.

[Oppenheim 89] Oppenheim A. V., Shafer R. W., Digital Signal Processing, Prentice Hall (1989).

[DeFatta et al. 1988] DeFatta J. David, Lucas G. Joseph and Hodgkiss S. William, Digital Signal Processing, A system design approach, John Wiley & Sons, 1988.

[Levinson et al. 1979] Levinson S. E., Rabiner L. R., Rosenberg J. G. and Wilpon J. G. ”Interactive clustering techniques for selecting speaker independent reference templates for isolated word recognition”, “IEEE Trans. Acoust. Speech, Signal Processing, vol ASSP-27, pp.134-141, 1979.

[Markel and Gray 1976] Markel J. D. and Gray A. H. “Linear Prediction for speech”. New York: Springer-Verlag, 1976.

[Itakura 1975] Itakura F., “Minimum prediction residual applied to speech recognition” IEEE Trans, Acous., Speech, Signal Processing, vol. 26, pp 575-582, Feb. 1975.

Spatially Photoluminescence of InAs/InGaAs quantum dots

Erick. Velázquez-Lozada¹, Cirilo Leon-Vega¹, J. Álvarez-Cedillo²

¹Instituto Politécnico Nacional. ESIME, Av. Instituto Politécnico Nacional S/N. UPALM Col. Lindavista. México D. F. 07738. México.

²Instituto Politécnico Nacional, CIDETEC, Av. Juan de Dios Bátiz s/n casi esq. Miguel Othón de Mendizábal, México D.F. 07700. México.

e-mail: evlozada5@yahoo.com.mx;
cleonv@ipn.mx, jaalvarez@ipn.mx

Abstract.

Spatially-resolved photoluminescence (PL) spectroscopy was performed at different temperatures on self-assembled quantum dots embedded (Qds) into Molecular Beam Epitaxy MBE-grown in In_{0.15}Ga_{0.85}As / GaAs multi-quantum-well heterostructures. This type of heterostructures currently is used for creation of new generation lasers for optical fiber communication. Strong inhomogeneity of the PL intensity is observed by mapping samples with different In/Ga composition of the layers covered the quantum dots in the quantum well. Two different behaviors in the quantum dot PL maps are clearly observed and identified: (1) a reduction of the PL intensity is accompanied with a monotonous “blue” shift of the luminescence maximum at room temperature, and (2) the PL intensity degradation matches a stable peak position of the PL maximum.

1. Introduction.

Formation of quantum dots (QDs) as a result of Stranskiy-Krastanow growth of strained heterostructures is now widely used for the formation of semiconductor laser structures [1].

The semiconductor lasers, based on QDs structures, exhibit many advantages such as low threshold current densities, high gain and high quantum efficiency [2]. The inhomogeneity of individual QD parameters across the wafer (size,

chemical components, stress) leads to broadening of the emission spectra resulting in loss of efficiency. This type of problems in QD structures are resolved using scanning PL study performed with sub-micron resolution [3] or by high-spatial resolution transmission electron microscopy techniques [4].

To develop mechanisms responsible for variation of the PL characteristics across the wafer, we report here a complementary scanning PL study performed at room temperature on QDs grown with various technological routines.

2. Samples and Results.

The samples were created using molecular beam epitaxy technique; the samples were composed of three InAs self organized QD layers embedded into In_{0.15}Ga_{0.85}As/GaAs multilayer hetero-structure [5].

The variable parameter in the set was In-composition in the In_xGa_{1-x}As layers covered the InAs Qds.

Two different compositions were studied with $x = 0.1$ (structure ID #1361) and $x = 0.15$ (#1360). Using atomic force microscopy on a sister samples with opened QD layers, we found that the individual dots were of 15 nm in base diameter and approximately 7 nm in height. The In-plane dot density was 7 to $10 \times 10^{11} \text{ cm}^{-2}$.

The scanning PL spectroscopy was performed at room temperature, using the CW HeCd laser (325 nm, 55 mW) as the excitation source. The laser spot of 1.4 mm diameter could be focused down to 12 microns for high-resolution mapping using UV beam expander and aberration free lenses. Samples were mounted on PC controlled X – Y moving stage.

Typical mapping area was 5 mm x 15 mm rectangle with the step of 0.5 mm. The PL spectrum was dispersed by SPEX 500M spectrometer and recorded by liquid-nitrogen cooled Ge-detector coupled with a lock-in amplifier. PL maps were obtained by the consecutive measurements of the PL spectrum at individual sample spots.

Figures 1 and 2 present the room temperature PL spectra measured along the PL intensity decreasing line-scans in both samples, which show quite different features. Specifically, in 1360 sample, a principal PL maximum maintains the

spectral position at 1.020 eV within the band of 10 meV, while reducing the PL intensity by more than a factor of two.

On the contrary, the sample #1361 exhibits a gradual “blue” energy shift of the maximum starting at the wafer’s center at 1.044 eV and approaching 1.11 eV at the periphery, which matches a three-fold degradation of the PL intensity.

These observations are statistically approved by mapping the PL maximum across the whole samples for a set of 115 data points measured in the scanning mode; in Fig. 3 are shown these observations.

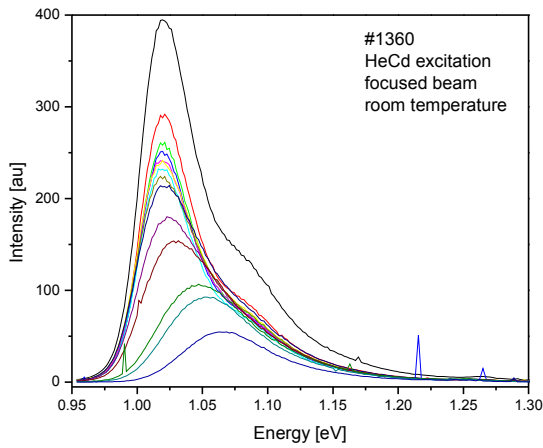


Fig. 1. Spatially resolved PL spectra at 300K on the sample #1360.

We have also noticed that the luminescence in the #1360 has at room temperature the highest intensity averaged across the wafer compared to #1361 3.2 times. Sample #1360 shows also a narrowest half width of the PL maximum in the set of three samples. It exhibits an additional peak at 1.08 eV, which was previously observed on high-quality QD samples and attributed to the luminescence through the excited states of the holes in the QD [5]. These facts indicate that electronic quality of the QD structure is superior in the sample #1360 with $x = 0.15$ composition of the covered layer. It is worth noticing, that the #1360 sample also shows partially features of the #1361 at the low PL intensity region. We can interpret the spectroscopic PL mapping results on the InAs/InGaAs QDs grown with different composition of covered InGaAs layer, as two different physical mechanisms taking place in various samples.

In #1361, a size of the dots is decreased gradually from the center of the wafer toward the sample periphery. This is exhibited as the “blue” shift of the PL maximum at room temperature.

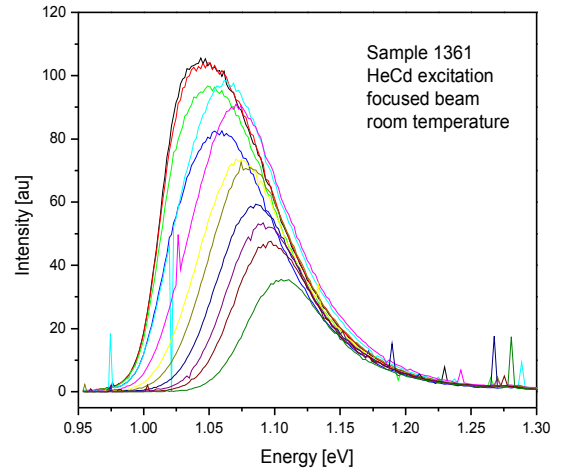


Fig.2. Spatially resolved PL spectra at 300K on the sample #1361.

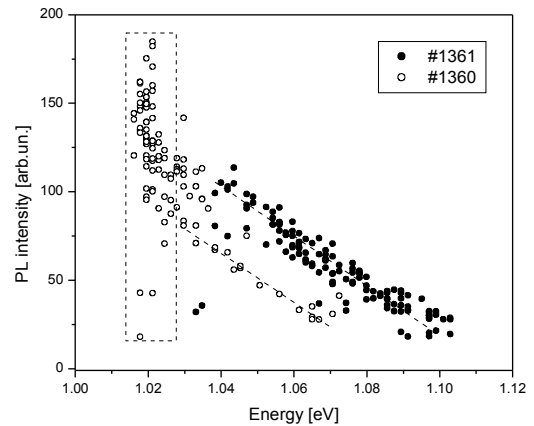


Figure 3. PL intensity versus PL peak maximum position extracted from the 115 data points on both samples.

This effect leads at the wafer periphery to shallower QD localized states (i.e. smallest electron and hole binding energy), poorer carrier localization and, as consequence, a higher probability of the carrier thermal ionization, which reduce room-temperature PL intensity. Regarding #1360 sample, the maximum position of the 1.02 eV PL band is maintained, and drop of the PL intensity can be related to inhomogeneous distribution of Non-Radiative centers, competing with QD luminescent transitions. We notice again that first mechanism is also contributed in this sample in areas with low PL intensity. Interesting is that maximum versus intensity slopes are very close in both samples.

3. Conclusions.

In this study has been observed that InAs/InGaAs QD structures have inhomogeneity of QD parameters in laser structures for optical fiber communication. Scanning PL spectroscopy suggests two distinctive mechanisms for such inhomogeneity. The first is variation of the QD size across the wafer and the second uneven spatial distribution of non-radiative defects. Both cases can be tailored by careful selection of the QD structure parameters and growth regimes.

4. References.

[1] D. Bimberg, M. Grundman, N.N. Ledentsov, Quantum Dot Heterostructures, Wiley&Sons, 2001. pp. 328 - 340.

[2] M G. T. Liu, A. Stintz, H. Li, K. J. Malloy, and L. F. Lester, Electron. Lett. Vol. 35. 1999. pp. 1163 - 1165.

[3] Sang-Kee Eah, Wonho Jhe, Yasuhiko Arakawa, Applied Physics Letters. Vol. 80. 2002. pp. 2779 – 2781.

[4] M. Catalano, A. Taurino, M. Lomescolo, L. Vasanelli, M.De Giorgi, A. Passasco, R. Rinaldi, R. Cingolani. J. Appl. Phys. Vol. 87. 2000. pp. 2261-2264.

[5] T.V. Torchynska, J.L. Casas Espinola, E. Velazquez Lozada, P.G. Eliseev, A. Stintz, K.J. Malloy and R. Pena Sierra. *Surface Scienc.* 2003. pp. 848-851.

Automatización y supervisión de un proceso neumático usando herramientas alternativas aplicadas al aprendizaje y la enseñanza

Edgar Roberto Ramos Silvestre^{1,2}

¹ Dpto. de Posgrado, CIDETEC IPN, U. P. Adolfo López Mateos, Av. Juan de Dios Bátiz s/n casi esq. Miguel Othón de Mendizábal, Edif. del CIDETEC, Col. Nva. Industrial Vallejo, Del. Gustavo A. Madero, 07700, México, D. F.

² Universidad Nacional Siglo XX, Área de Tecnología, Carrera de Ingeniería Electromecánica, C. Campero No. 36, Tel/Fax (591) 02-5820115 / 5820222, Norte de Potosí-Bolivia

Resumen. Tener un proceso automatizado y que cuente con un sistema de supervisión conlleva generalmente a una gran inversión económica, debido a que tanto el hardware como el software para realizar esto son relativamente costosos. Una alternativa de solución para bajar los costos en la automatización y supervisión de procesos es utilizar herramientas alternativas como son las tarjetas electrónicas diseñadas e implementadas con dispositivos comerciales, así como el uso de lenguajes de programación para implementar sistemas de supervisión que sean capaces de realizar intercambio dinámico de datos con el controlador lógico programable (PLC). En el presente artículo se realiza, en una primera parte, la automatización de un proceso neumático para aplicaciones didácticas en la cual se reemplaza el PLC de la marca Siemens por un PLC hecho con un microcontrolador. Luego en una segunda parte, se implementa un sistema de supervisión utilizando Visual Basic para posteriormente comunicarlo con el PLC.

Palabras Clave: Automatización, supervisión, proceso neumático, controlador lógico programable, microcontrolador.

9 Introducción

Realizar la automatización de un proceso de cualquier tipo (mecánico, neumático, hidráulico etc.) generalmente se hace con la finalidad de sustituir al operador humano por un operador artificial en la realización de una tarea física previamente

programada utilizando para ello métodos y procedimiento. Por lo tanto tener un proceso automatizado beneficia en gran manera permitiendo:

- Mejorar la productividad de la empresa, reduciendo los costos de producción y mejorando la calidad de la misma.
- Mejorar las condiciones de trabajo del personal, suprimiendo los trabajos pesados e incrementando la seguridad.
- Realizar operaciones imposibles de controlar intelectual o manualmente.
- Mejorar la disponibilidad de los productos, pudiendo proveer las cantidades necesarias en el momento preciso.
- Simplificar el mantenimiento, de forma que el operario no requiera grandes conocimientos para la manipulación del proceso productivo.
- Integrar la gestión y la producción.

Un proceso neumático es aquel que utiliza el aire comprimido como energía para mover sus actuadores. La neumática admite infinidad de aplicaciones en el campo de máquinas, herramientas, así como casi una totalidad de procesos industriales. Entre las aplicaciones más comunes y sencillas están las selladoras y envasadoras, debido a que requieren pocos cilindros para realizar el proceso, el desarrollo del presente artículo está enfocado a una de estas aplicaciones. Para adquirir el conocimiento en neumática y automatización generalmente se cuentan con un panel didáctico en el que se puede armar circuitos neumáticos para luego ser gobernados por un PLC, esto es llamado comúnmente “banco neumático”. Actualmente las universidades desarrollan cursos que se dedican a la enseñanza de la neumática, implementando herramientas y estrategias de aprendizaje y enseñanza en esta área [1,2,3].

Por otro lado también es necesario contar con un sistema de supervisión que permita monitorear los sensores y actuadores involucrados con el proceso neumático, para lo cual los fabricantes de PLC's ofrecen tanto hardware como software adicional para realizar esta tarea, sin embargo adquirirlos tiene un costo muy alto que muchas veces no es rentable implementarlo por las características que conlleva el proceso. En la búsqueda de bajar los costos de implementar sistemas de automatización y supervisión generalmente se recurre a herramientas alternativas como el uso de microcontroladores y lenguas de programación que permitirán realizar tareas programadas por el usuario [4,5]. Una gran limitación es que el uso de estas herramientas solo es aplicable a procesos medianos y pequeños que no involucren un alto grado de seguridad en el desarrollo del mismo.

El objetivo de este artículo es presentar una alternativa de solución de bajo costo para la

automatización y supervisión de un proceso neumático aplicado al aprendizaje y enseñanza, utilizando para ello herramientas alternativas que replazaran el hardware o software que el proceso requiera.

Este artículo está dividido en las siguientes secciones. En la sección II, se realiza la caracterización de la planta mostrando características de los sensores, actuadores y del PLC, así también la descripción del banco neumático. En la sección III, se realiza la automatización del proceso para lo cual replazamos el PLC de la marca Siemens por uno hecho con PICAXE-18A se presenta una comparación entre ambos controladores. En la sección IV, se realiza la supervisión del proceso utilizando un programa realizado en Visual Basic que permite utilizar los drivers OPC (Oler for Porcces Control) y DDE (Dinamic Data Exchange). En la sección V, se presentan los resultados obtenidos del desempeño que tuvo el usar una herramienta alternativa como es un microcontrolador de bajo costo. Finalmente, en la sección V, se presentan las conclusiones y trabajos a futuro.

II. Caracterización del banco neumático

En esta sección identificaremos las características físicas y dinámicas de los sensores, actuadores y el controlador lógico programable S7-200 de la marca Siemens mediante observación y análisis de sus componentes, así también describiremos el proceso secuencial del modulo de control según el principio de funcionamiento de los componentes que lo integran. Cabe mencionar que el presente trabajo está orientado a controlar actuadores neumáticos sin importar la fuerza que genera todo el sistema neumático o el comportamiento dinámico del mismo [6].

A. Parte operativa:

La parte operativa la conforman los sensores y actuadores que se usaron en el proceso. En cuanto a los sensores se tiene interruptores finales de carrera que detectan la posición de un elemento móvil mediante accionamiento mecánico, existe una gran diversidad de estos dispositivos que se suelen distinguir por el elemento móvil que genera la señal eléctrica de salida, son muy utilizados en aplicaciones industriales por su simplicidad y bajo costo. El banco neumático cuenta con diez interruptores de finales de

carrera que se los utilizan para verificar si el pistón del cilindro (actuador) esta expandido o contraído.

Los actuadores reciben la presión neumática y la transforman en fuerza de accionamiento y según su tipo de movimiento se los puede agrupar en dos grandes familias: Los que realizan la fuerza en movimiento lineal que es el caso de los cilindros, y los que aplican la fuerza en un giro y realizando un movimiento rotativo, por ejemplo los motores, actuadores de paleta y pinzas. Los cilindros son los actuadores más utilizados en aplicaciones neumáticas permitiendo realizar desplazamientos lineales de avance y retroceso de un mecanismo o dispositivo acoplado a su pistón existiendo una variedad de estos. El banco neumático cuenta con solo cinco cilindros de simple y siete de doble efecto. En la Figura 1, se muestra los sensores y actuadores utilizados en el banco neumático.

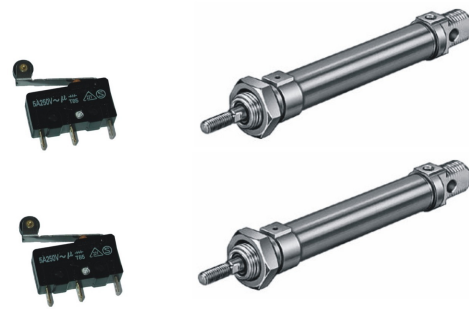


Fig. 2. Finales de carrera utilizados como sensores y los cilindros de doble efecto que son los actuadores del banco neumático.

B. Parte de mando:

Para el control de los actuadores se realizo la instrumentación de un tablero de mando [9] el cual contiene un PLC S7-200 de la marca Siemmens, 8 relés de 10 A, una fuente de alimentación de 24 VDC, un termo magnético de 10 A y fusibles de protección. En la Figura 2, se muestra la descripción de las partes que componen el tablero eléctrico.

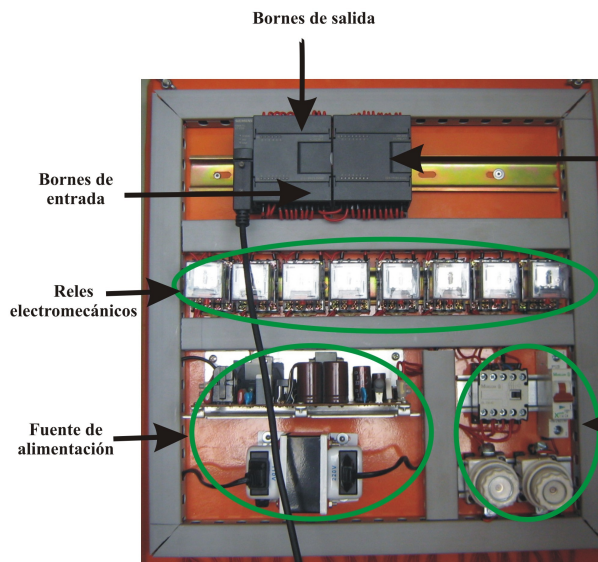


Fig. 2. Descripción del tablero eléctrico donde está instalado el PLC Simatic S7-200 de la marca Siemens.

A continuación se presenta una descripción de su arquitectura que cuenta con elementos esenciales que son:

Sección de entradas y salidas: Contiene las líneas de entrada y salida, las cuales pueden ser digitales o analógicas donde se conectarán sensores y actuadores. El PLC que se usó cuenta con 8 entradas y 6 salidas digitales en el primer módulo, y adicionalmente tiene otro módulo que cuenta con 8 entradas y 8 salidas digitales, teniendo un total de 14 entradas y 16 salidas digitales para su uso. En cuanto a entradas y salidas analógicas, no se tiene ninguna pudiendo adquirir un módulo extra para tener entradas y salidas analógicas si la aplicación lo requiere. Todas las entradas son de 24 VDC y las salidas son de relés a 10A.

Unidad central de proceso (CPU 222): Se encarga de procesar el programa que el usuario introduce, tomando una a una las instrucciones y ejecutándolas y cuando se llega al final de la secuencia vuelve al principio y sigue ejecutándolas de manera cíclica.

Unidad de alimentación: El modelo S7-200 ya cuenta con una fuente de alimentación incluida, por lo tanto se alimenta a 220 VAC a 50 Hz.

Consola de programación: Permite introducir y supervisar el programa de usuario. En la actualidad esto se lo hace por un software que el fabricante lo proporciona que para el S7-200 es el STEP 7-

Micro/WIN V4.0 SP4. Los lenguajes que acepta para la programación son:

- Esquema de contactos (KOP): Es el más utilizado ya que tiene una similitud con el utilizado por un electricista al elaborar cuadros de automatismo.
- Lenguaje por lista de instrucciones (AWL): Consiste en una lista de instrucciones que es elaborada en modo texto. El software también permite exportar de KOP a AWL.

Interfaces: Todo PLC posee la capacidad de comunicarse con otros dispositivos como una computadora u otro PLC. Lo común es del tipo RS-232 puerto serie y a través de esta línea se puede manejar todas las características internas del PLC, incluida la programación del mismo. También se puede conectar un módulo ethernet para comunicarse con el PLC mediante la red de datos.

C. Banco neumático:

El banco neumático resulta de la integración de la parte operativa y la parte de mando, de tal forma que se cuenta con un panel principal donde se pueden realizar el montaje de diversos circuitos neumáticos que representen un proceso. En la parte superior cuenta con un panel de conexiones que facilita el cableado de la parte eléctrica y se divide en tres bloques: Panel de acondicionamiento PLC - Banco neumático, panel de acondicionamiento electro neumático y panel de alimentación. El primero nos permite conectarnos con las entradas y salidas del PLC S7-200 y así controlar el proceso, el segundo panel permite conectar las válvulas solenoides a interruptores que se encuentran en el mismo panel esto con el fin de realizar una activación manual de los actuadores y por último el panel de alimentación se encarga de energizar los diferentes actuadores que conforman el circuito. El banco neumático cuenta también con un compresor que es el encargado de proveer el aire comprimido para activar los diferentes cilindros que estén conectados. En la Figura 3, se muestra el banco neumático ensamblado y listo para realizar pruebas.



Fig. 3. Banco neumático que resulta de la integración de la parte operativa y la de mando, y otros accesorios adicionales.

III. Automatización del proceso

En esta sección se realiza la automatización de un proceso secuencial [7,8] sencillo para efectos de demostración, para lo cual se abordara el problema de dos formas, la primera utilizando un PLC de la marca Siemens modelo Simatic S7-200 y la segunda utilizando un PLC construido a partir de un microcontrolador PICAXE-18A.

Para automatizar un proceso, primero se debe conocer el orden de las operaciones en que suceden y así realizar el control del mecanismo. Para el presente artículo el proceso a controlar estará orientado una aplicación de una selladora neumática muy utilizado en la industria, a continuación describiremos el algoritmo de operación:

1. Al inicio los actuadores se encuentran en su posición de reposo, es decir los pistones de los cilindros de doble efecto están contraídos.
2. Se oprime el botón de inicio y el cilindro 1 pasa a su estado expandido, y después de unos segundos pasa a su estado contraído.
3. Cuando el cilindro 1, llega a su posición de reposo (posición inicial), activa el cilindro 2 y este pasa al estado expandido y después de unos segundos pasa a un estado contraído.
4. El proceso es secuencial y se repite los pasos 2 y 3 hasta que se oprima el botón de parada y los cilindros vuelven a su posición de reposo.

A. Utilizando el Simatic S7-200

La realización del programa para automatizar este proceso se realizo en el STEP 7-MicroWIN 32 V3.1, que es el software que el fabricante vende con el PLC Simatic S7-200. Cabe mencionar que todo el cableado para los sensores, actuadores y pulsadores ya están montados en el tablero de mando como se explico en la caracterización del banco neumático. En el algoritmo 1, se muestra el programa en formato AWL que controla el proceso neumático.

Algoritmo 1. Ejemplo de programa desarrollado MicroWIN 32 V3.1 que controla el proceso neumático, elaboración propia.

```
Network 1
LD      I0.0
O       Q0.0
AN      M0.0
=       Q0.0
Network 2
LD      Q0.0
TON     T37, 200
Network 3
LD      T37
O       Q0.1
AN      M0.1
=       Q0.1
Network 4
LD      T37
=       M0.0
Network 5
LD      Q0.1
TON     T38, 200
Network 6
LD      T38
O       Q0.2
AN      M0.2
=       Q0.2
Network 7
LD      T38
=       M0.1
Network 8
LD      Q0.2
TON     T39, 200
Network 9
LD      T39
O       Q0.3
AN      M0.3
=       Q0.3
Network 10
LD      T39
=       M0.2
Network 11
LD      Q0.3
TON     T40, 200
Network 12
LD      T40
=       I0.0
Network 13
LD      T40
=       M0.3
Network 14
LD      I0.0
O       Q0.4
=       Q0.4
END_ORGANIZATION_BLOCK
SUBROUTINE_BLOCK SBR_0:SBR0
```

B. Utilizando el PLC con PICAXE-18A

Una alternativa para automatizar este proceso secuencial es utilizar un PLC construido con un microcontrolador PICAXE-18A, este tiene la característica de poder cargarlo con un programa sin tener que sacarlo de la tarjeta, también la programación de este se la realiza en lenguaje Basic resultando relativamente más sencilla de programar comparado con los otros microcontroladores. El PLC con PICAXE-18A cuenta con 5 entradas optoacopladas, 8 salidas a través de relés de 7 A de contacto para tensiones hasta de 250 VAC y se alimenta con una fuente de 12 VDC. En la Figura 4, se muestra el esquema de conexión del PLC con PICAXE y los actuadores.

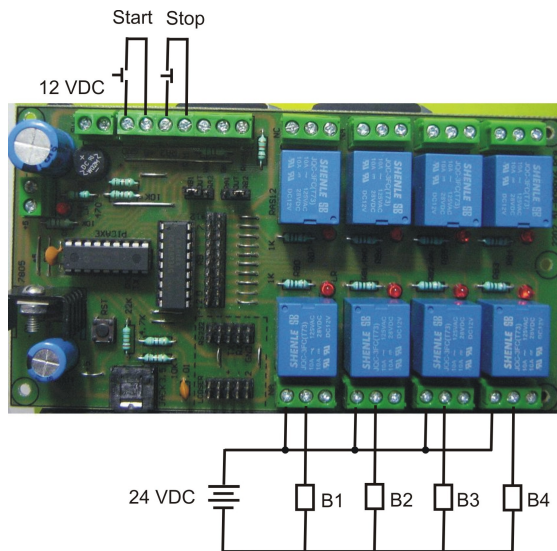


Fig. 4. PLC construido con un microcontrolador PICAXE-18A, esquema de conexión con los actuadores y los pulsadores de inicio y stop.

En cuanto a la programación del PLC se utilizó el “Programming Editor”, que es un software de distribución gratuita utilizado para aplicaciones didácticas permitiendo simular y luego descargar el programa en el microcontrolador PICAXE. La ventaja de este software es que permite programar en diagrama de flujo o Basic y acepta todos los tipos de PICAXE. En el algoritmo 2, se muestra el programa en lenguaje Basic que permite controlar el proceso neumático.

Algoritmo 2. Ejemplo de programa desarrollado en Basic que controla el proceso neumático, elaboración propia.

```
main:
label_6:  if pin0=1 then label_11
          goto label_6
label_11: high 0
          pause 1000
```

```
low 0
high 1
pause 1000
low 1
high 2
pause 1000
low 2
high 3
pause 1000
low 3
goto label_11
```

IV. Supervisión del proceso

Se puede definir a supervisión como “un conjunto de acciones desempeñadas con el propósito de asegurar el correcto funcionamiento del proceso incluso en situaciones anómalas”. El sistema de supervisión debe ser capaz de monitorear las diferentes variables del proceso, realizar el control de los actuadores, posibilidad de crear paneles de alarma con registro de incidencias y generación de históricos de las señales de planta. En la actualidad los sistemas SCADA (Supervisory Control and Data Acquisition) son los encargados de realizar la supervisión de la planta, generalmente cada fabricante de PLC’s tiene a la oferta software para realizar estos sistemas pero generalmente son costosos [10].

El sistema de supervisión es el último nivel en la pirámide de la automatización como se muestra en la Figura 5, el nivel de dispositivos comprenden los bloques de entradas y salidas de todo el sistema teniendo entre ellos a bloques I/O, actuadores e interfaces hombre maquina (HMI). El nivel de control comprende a los autómatas programables como los PLC’s, los cuales son encargados, mediante un programa introducido por usuario, de controlar las variables del proceso y de esta forma contar con un sistema automático. El nivel de información comprende equipos de computo y monitoreo los cuales tienen un software adecuado que permite realizar la supervisión de los niveles anteriores, permitiendo tener un monitoreo y control de los dispositivos del sistema.

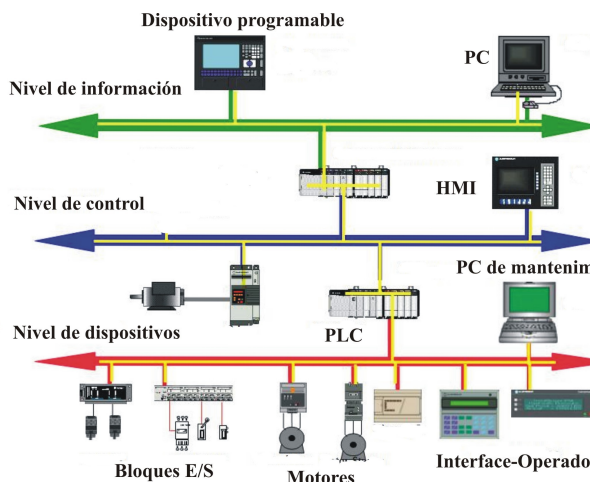


Fig. 5. Pirámide de la automatización donde se muestra los diferentes niveles. El sistema SCADA se encuentra en el nivel de información.

Un SCADA, es un sistema multitarea y está basado en bases de datos de tiempo real localizadas en uno o más servidores. Estos servidores son responsables por la adquisición y manipulación de datos de un conjunto de parámetros de los dispositivos conectados a él. Los sistemas de supervisión de procesos industriales utilizan programas especiales que permiten enlazar las variables de proceso con los objetos gráficos o mímicos que visualiza el operador en pantalla. Estos programas son llamados frecuentemente drivers y permiten leer datos de un dispositivo electrónico tal como un PLC y llevarlos a un sistema de supervisión para ser visualizados, analizados o almacenados. Los dos tipos de tecnologías más utilizados para crear este tipo de enlaces son: *Dynamic Data Exchange (DDE)* y *OLE For Process Control (OPC)*.

En el presente artículo se presenta una alternativa para diseñar un programa que se asemeje a un sistema SCADA utilizando lenguajes de programación que permitan el intercambio de datos en forma dinámica entre el PLC y la computadora. Para realizar esto se utilizara el servidor DDE de Siemens y se comunicara con Visual Basic para el intercambio de datos como se muestra en la Figura 6.

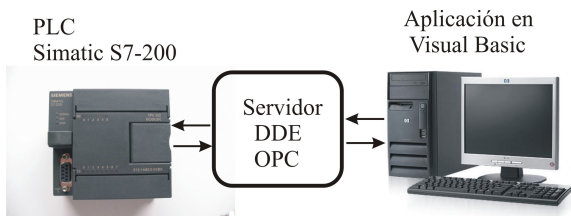


Fig. 6. Comunicación del PLC Simatic S7-200 con una aplicación desarrollada en Visual Basic utilizando un servidor DDE/OPC.

En el sistema SCADA que se diseño presenta una arquitectura que presenta dos capas:

- La capa cliente: Se ocupa de la interacción entre el ser humano y la máquina.
- La capa servidor de datos: Esta capa es responsable de comunicarse con los dispositivos de campo mediante los PLC's, y de enviar la información a otras estaciones cliente mediante la red de datos.

Visual Basic tiene la capacidad de comunicarse con servidores DDE y poder intercambiar datos, esto fue aprovechado y se realizo un programa para comunicarlo con el PLC y de esa forma leer y escribir en sus variables internas dentro del mismo. Dentro las propiedades de un objeto los parámetros a cambiar son los siguientes: LinkItem, LinkMode, LinkTimeout y LinkTopic, en el primero se especifica el nombre de la variable que se usara en común para el intercambio de datos, el segundo permite que una aplicación destino inicie una conversación DDE con el formulario, en el tercero se configura el tiempo en milisegundos que se espera para la comunicación y por último el cuarto establece el tema al que este formulario va a responder a una conversación DDE, cuando funciona como origen. En la figura 7, se muestra la configuración que se realizo en Visual Basic para tener una comunicación con el servidor DDE. Estos parámetros solo están disponibles en algunos objetos como en los cuadros de texto (TextBox), pero no así en los botones (CommandButton).

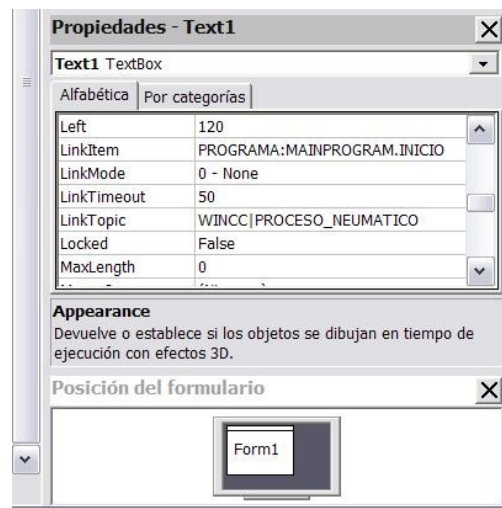


Fig. 7. Parámetros a configurar en Visual Basic para la comunicación con el servidor DDE.

V. Resultados obtenidos

Luego de sustituir el PLC Simatic S7-200 por otro construido con un microcontrolador PICAXE se pudo ver que el desempeño de los actuadores era el mismo, y realiza un buen control del proceso neumático. Teniendo como limitación el número de salidas con

las que cuenta el microcontrolador ya que esto limita el número de actuadores que se pueden controlar. En cuanto al sistema de supervisión se realizó un programa en Visual Basic que permitió comunicarse con el Simatic S7-200 mediante un servidor DDE y realizar la transferencia de datos para monitorear las variables y activar los actuadores. También se comparó el desempeño del sistema desarrollado con el PC_SIMU que es un software que el fabricante provee para la simulación de un sistema de supervisión. En la Figura 8, se muestra la interface que se desarrolló para la supervisión de este proceso.

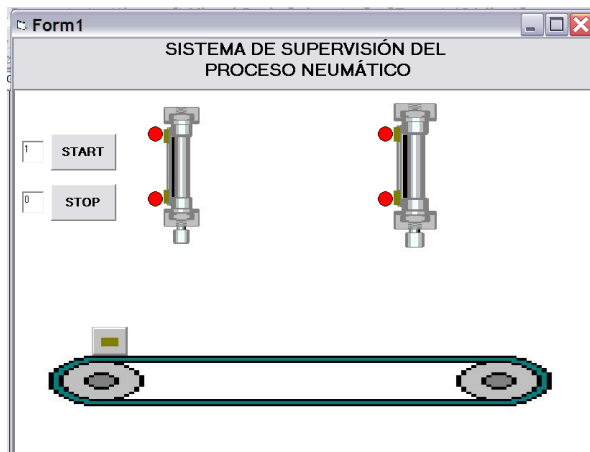


Fig. 8. Sistema de supervisión desarrollado en Visual Basic para el monitoreo y control de un proceso neumático.

VI. Conclusiones y trabajos a futuro

La automatización y supervisión de procesos como materia de estudio es bastante amplia y contar con un banco de pruebas para realizar pruebas ayuda en gran manera a entender cómo funciona cada dispositivo. En la actualidad se cuenta con herramientas de software que permiten simular procesos neumáticos como el Automation Studio™, también se puede encontrar software para simular PLC's de las diferentes marcas existentes en el mercado

En este trabajo se ha realizado la automatización de un proceso secuencial neumático, abordando el problema de dos formas: La primera utilizando un PLC comercial de la marca Siemens y la segunda utilizando un PLC alternativo construido con un microcontrolador PICAXE. Se pudo observar que ambos PLC's controlan al proceso en forma similar y que es posible sustituir un PLC costoso por otro que utilice un microcontrolador relativamente económico. Es necesario mencionar que esto solo será posible si el proceso no es muy complejo y no requiera mayor número de entradas o salidas que el PICAXE puede suministrar.

En lo relativo a la supervisión del proceso neumático se diseñó una interface grafica en Visual Basic que emula un sistema SCADA permitiendo intercambiar datos en forma dinámica entre el PLC y la computadora. El servidor que se utilizó fue el DDE Server que también lo provee el fabricante. Es importante mencionar que con esto se logra sustituir un sistema de supervisión, generalmente es costoso incluso más que el mismo PLC, por una aplicación alternativa desarrollada con un lenguaje de programación de alto nivel.

El desarrollo del presente artículo se limitó a automatizar y supervisar un proceso sencillo que cuenta con solo dos actuadores neumáticos, pudiendo aumentar el número de estos e incluir sensores dependiendo los requerimientos del proceso neumático.

Dentro las perspectivas futuras de trabajo, utilizando este banco neumático de pruebas, se planea realizar la automatización y supervisión de procesos más complejos que requieran mayor número de actuadores y sensores.

Agradecimientos. E. R. Ramos-Silvestre agradece el soporte económico recibido mediante una beca de estudios por parte Secretaría de Relaciones Exteriores – Dirección General de Asuntos Culturales – Dirección de Intercambio Académico de México.

Referencias

1. Rodrigues, G.; Torres, J.: Modelo de enseñanza neumática y automatización para ingenieros. *Proceedings of the 7th Latin American and Caribbean Conference for Engineering and Technology*, (2009).
2. Horacio, G, et al.: Implementación de herramientas didácticas interactivas para la enseñanza de ingeniería. <http://ing.unne.edu.ar/gd/menu.htm>, Accedido el 20 de Marzo de 2008.
3. Ocampo, J. R.: Implementación de estrategias de aprendizaje Combinado a la Enseñanza de Cursos de Ingeniería en UNITEC. *Procedente del VI International American and Caribbean Conference for Engineering and Technology*, Tegucigalpa, Honduras, pp. 1-8 (2008).
4. Torres, J.; Redondo, J.: Reparación y Automatización de una Máquina Universal de Ensayos. *Procedente del VI congreso nacional de ingeniería mecánica*, Universidad de Los Andes, Mérida, Venezuela, pp 1-8, (2006)
5. Zorzano, L.; Zorzano, A.; Zorzano, J.: Sistema de bajo coste para el aprendizaje y la enseñanza de los sistemas de adquisición de señales basados en microcontroladores,

Procedente del congreso Tecnología Aplicadas a la Enseñanza de la Electrónica TAAE, Zaragoza, (2008).

6. Tressler J. M.; Clement T.; Kazerooni H. And Lim M.: Dynamic behavior of pneumatic systems for lower extremity extenders. *Proceedings of the 2002 IEEE International Conference on Robotics & Automatio*, Washington DC., pp. 3248-3253 (2002).
7. Garcia, E.: *Automatización de Procesos Industrial*, Alfaomega grupo editor, México (2001).
8. Ogata, K.: *Ingeniería de Control Moderno*, Prentice Hall Hispanoamericana, Tercera Edición, Mexico (1998).
9. Bolton, W.: *Instrumentation and Control Systems*, Elsevier Science & Technology Books, USA (2004).
10. Rodrigues, A.: *Sistemas SCADA*, Alfaomega grupo editor, México (2007).

Diseño de una Antena Concentradora de Señal para Laptop

Area: comunicaciones

1Carlos Aquino Ruiz caquino@ipn.mx, 2Israel
Rivera Zárate irivera@ipn.mx,

1Juan Antonio Ríos Chávez jriosc0500@ipn.mx

1 ESCUELA SUPERIOR DE INGENIERÍA
MECÁNICA Y ELÉCTRICA UNIDAD
CULHUACAN Av.Santa Ana #1000 Col. San
Francisco Culhuacan,

Deleg. Coyoacán C.P. 04430, México D.F Tel.
56242000 ext. 73100

2 CENTRO DE INNOVACION Y
DESARROLLO TECNOLÓGICO. Unidad

Profesional Adolfo López Mateos
Av. Juan de Dios Bátiz S/N y Miguel Othón de
Mendizabal Tel. 56242000 ext. 52535

Resumen: El uso de redes inalámbricas actualmente nos ofrece una gran cantidad de servicios que operan a través de Internet y para conectarse a una de ellas se tiene que estar en una zona delimitada para que haya una óptima recepción de señal, pero no siempre se puede estar inmóvil en un solo sitio, y la movilidad provoca una disminución en la intensidad de señal, por lo tanto, en este trabajo se pretende diseñar una antena que capture, concentre y redirecciones la señal hacia la tarjeta de red de una laptop mejorando la recepción y el aumento de la intensidad de señal.

Palabras Clave: antena, fractal, laptop, intensidad de señal, tarjeta de red, acoplamiento.

Introducción

Actualmente el uso de redes inalámbricas es muy común en casi todo el mundo, pero existe un gran problema que afecta directamente a la intensidad de la señal; específicamente en una laptop, las redes inalámbricas funcionan por radiofrecuencia las cuales pueden verse afectadas por objetos, elementos de construcción, algunas otras fuentes de radiofrecuencia, por cambios climáticos, superficies que disminuyan la cobertura o por el simple hecho de moverse de un lugar a otro. Para esto es necesario acoplar un complemento a la tarjeta de red con la finalidad de que concentre una mayor cantidad de señal y la redireccione para que sea aprovechada por la tarjeta, aumentando la intensidad de señal en la laptop evitando que disminuya a un punto tal que se pierda la conexión.

La antena aquí propuesta se diseñó como si fuese una calcomanía para que sea adherible a la laptop, además se utilizó la tecnología de antenas de parche con acoplamiento por proximidad.

Definición de Antena

Una antena [1][5] es un dispositivo transductor formado por un conjunto de conductores que, unido a un generador, permite la emisión de ondas de radiofrecuencia por el espacio libre, o que, conectado a una impedancia, sirve para captar las ondas emitidas por una fuente lejana.

Antenas de Microcinta

Una microcinta [3][6][2] es un conductor eléctrico fino separado de un plano a tierra por una capa de aislamiento (substrato dieléctrico). Las microcintas se utilizan en los diseños de circuitos impresos donde las señales de alta frecuencia necesitan ser encaminadas a la aplicación requerida.

Las antenas de microcinta pueden usarse como transmisores o receptores basando su funcionamiento en las microondas identificadas en el rango de frecuencias comprendido entre 1GHz y 300GHz y denominadas también ondas milimétricas por su longitud de onda del orden de los milímetros[4].

Este tipo de antenas son muy prácticas por su fácil manejo y manipulación, pueden usarse técnicas litográficas o alguna otra técnica que convenga al diseñador. La forma básica de construcción de una antena de microcinta se describe en los siguientes puntos:

- Una superficie conductora muy delgada llamada parche
- Un substrato dieléctrico
- Si es antena transmisora, una alimentación, la cual suministra la potencia de RF al elemento.



Fig. 1 Representación de una antena fractal de microcinta.

Podemos decir que una antena fractal posee las siguientes características principales:

- Un gran ancho de banda y comportamiento multibanda
- En la mayoría de los casos tienen una ganancia considerable dependiente del rango de frecuencias que abarque

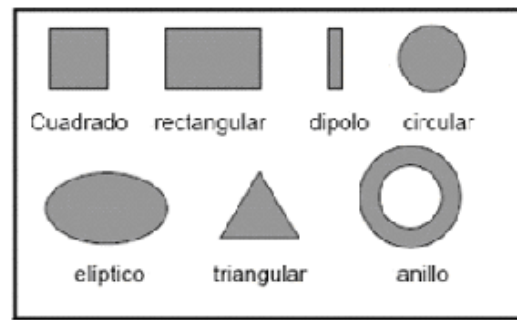
Topología de parches

El parche conductor [7] puede ser variable dependiendo de una gran cantidad existente de topologías para simplificar el análisis y la predicción de su desempeño. Ver figura 2

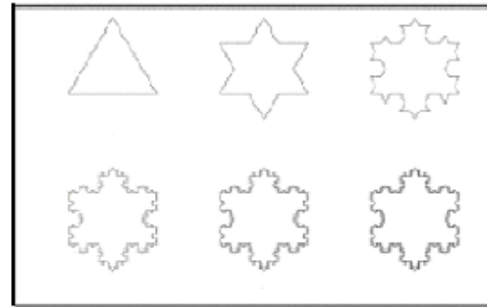
Ventajas y Desventajas de las Antenas de Microcinta [7]

Ventajas

- Son livianas y ocupan poco volumen
- Tienen un perfil plano, lo cual las vuelve fáciles de adaptar a cualquier superficie
- Bajos costos de fabricación y facilidad para fabricarlas en serie
- Pueden diseñarse para trabajar a distintas frecuencias



a)



b)

Fig. 2 Topologías de parche conductor

Desventajas

- Tienen limitada potencia
- Trabajan específicamente a una frecuencia de diseño

Técnicas de Acoplamiento

Existen varios métodos para acoplar a las antenas de microcinta. Estos métodos se clasifican en dos categorías:

- De contacto
- De contacto nulo

En los métodos de contacto, la potencia de radiofrecuencia es traspasada directamente al parche usando elementos conectivos tales como líneas de microcinta.

Los métodos de contacto nulo están basados en la transferencia de potencia a través del acoplamiento de campos.

Para el diseño de nuestra antena se usó uno de los métodos de contacto nulo: el acoplamiento por proximidad

En el acoplamiento por proximidad se integra el transductor cerca del dispositivo al cual se pretende complementar pero sin que exista alguna conexión física entre ellos. Esta técnica tiene la ventaja de eliminar radiaciones indeseadas provenientes de la alimentación y a la vez proporciona un amplio ancho de banda.

Diseño del Parche Conductor

Para diseñar la antena es necesario tener clara la aplicación para la cual queremos implementar, aunado a esto la frecuencia de operación a la cual se va a operar, el material dieléctrico que se va a usar, la constante dieléctrica de dicho material y el grosor del mismo para así poder calcular las dimensiones del parche.

Métodos de Cálculo y Análisis

El análisis de las antenas de microcinta para su posterior diseño se hace a través de modelos que simulan su comportamiento. Los modelos más populares son:

- Modelo por línea de transmisión
- Modelo de cavidades
- Modelo de onda completa

El modelo usado para el diseño de esta antena fue el modelo por línea de transmisión ya que es simple y da buena interpretación física de lo que ocurre.

Largo y Ancho del Parche

El ancho del parche conductor está dado por la siguiente ecuación:

$$W = \frac{c}{2f_0 \sqrt{\frac{\epsilon_r + 1}{2}}} \quad (1)$$

Donde c es la velocidad de la luz, ϵ_r es la constante dieléctrica del material utilizado y f_0 es la frecuencia de operación.

Para calcular ϵ_{eff} que es la constante dieléctrica efectiva del material, usamos la ecuación 2

$$\epsilon_{eff} = \frac{\epsilon_r + 1}{2} + \frac{\epsilon_r - 1}{2} \left[1 + 12 \left(\frac{h}{W} \right) \right]^{-0.5} \quad (2)$$

Para calcular L_{eff} que es el largo efectivo del parche ocupamos la ecuación 3

$$L_{eff} = \frac{c}{2f_0 \sqrt{\epsilon_{eff}}} \quad (3)$$

A través de resultados empíricos se determinó una extensión del parche ΔL . Esta extensión está dada por:

$$\Delta L = 0.412h \left[\frac{(\epsilon_{eff} + 0.3) \left(\frac{W}{h} + 2.64 \right)}{(\epsilon_{eff} - 0.258) \left(\frac{W}{h} + 0.8 \right)} \right] \quad (4)$$

Para calcular el largo real de construcción del parche está dado por la ecuación 5

$$L = L_{eff} - 2\Delta L \quad (5)$$

Finalmente se calculan las dimensiones del substrato dieléctrico que es el material en el cual reposa el parche conductor, para esto aplicamos las ecuaciones (6) y (7)

$$L_g = 6h + L \quad (6)$$

$$W_g = 6h + W \quad (7)$$

A continuación se muestra la forma del parche previamente obteniendo las dimensiones:

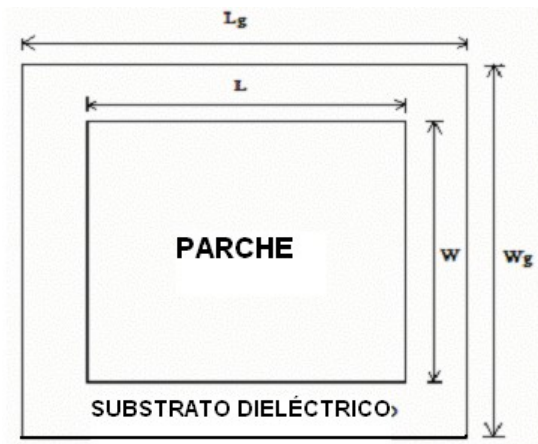


Fig. 3 Medidas del parche conductor

Para el diseño de la antena propuesta se realizaron algunas iteraciones de dos tipos de antenas fractales, basándonos en el largo y ancho obtenido anteriormente, estas serán: triángulo de Sierpinski y Curva de Koch.

Para construir ambas propuestas se construye un triángulo como el mostrado en la figura 4

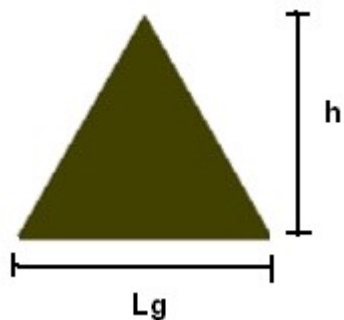


Fig. 4 Triángulo base para ambos tipos de antenas

Para calcular la altura h del triángulo seguimos la ecuación 8

$$h = \frac{L_g + 2}{2} = \frac{L_g}{2} + 1 \quad (8)$$

Después del triángulo equilátero obtenido se extrae el triángulo formado al unir los puntos medios del original como se muestra en la figura 5

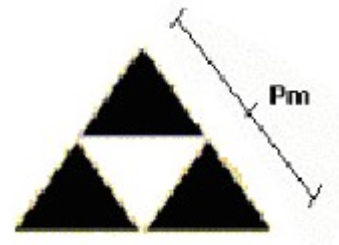


Fig. 5 Iteración del triángulo de Sierpinski

Para calcular el punto medio de cada lado del triángulo equilátero se utiliza la ecuación 9

$$P_m = \frac{L_g}{2} \quad (9)$$

Para diseñar la Curva de Koch es necesario agregar un triángulo equilátero de igual dimensión que el primero de acuerdo a como se visualiza en la figura 6

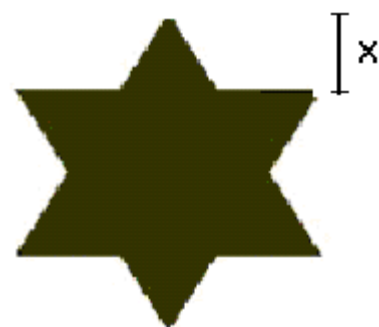


Fig. 6 Iteración de la curva de Koch

Por último para calcular el espacio “ x ” entre triángulos se utiliza la ecuación 10

$$X = \frac{h}{2.875} \quad (10)$$

Diseño Físico de la Antena

Partimos de los datos iniciales para realizar los cálculos. Primero se establece la frecuencia de operación de la tarjeta de red de una laptop la cual es 2.4GHz, el sustrato a utilizar es la mica ya que es un material fácil de conseguir y económico, por lo tanto, su constante dieléctrica es 5.4, y por último la medición del grosor del material dieléctrico (mica) fue de 0.2mm.

Aplicando las ecuaciones antes mencionadas se obtuvieron los siguientes resultados:

$$\text{Resultados Obtenidos} \left\{ \begin{array}{l} W = 34.9385 \text{ mm} \approx 35 \text{ mm} \\ L = 26.34332 \text{ mm} \approx 26 \text{ mm} \\ L_g = 27.54332 \text{ mm} \approx 28 \text{ mm} \\ W_g = 36.13856 \text{ mm} \approx 36 \text{ mm} \end{array} \right.$$

Para las Iteraciones del triángulo de Sierpinski y la Curva de Koch se obtuvieron las siguientes medidas:

$$\text{Resultados Obtenidos} \left\{ \begin{array}{l} h = 2.4 \text{ cm} \\ P_m = 14 \text{ mm} \\ X = 0.8 \text{ cm} \end{array} \right.$$

Implementación

La tarjeta de red antes mencionada se encuentra cerca de la tapa de la laptop y de la batería de la misma al igual que la guía de onda de la tarjeta, por lo tanto se implemento la antena propuesta cerca de estas partes de la laptop.



Fig. 7 Fotografía de la tarjeta de red y la guía de onda de una laptop

Como habíamos mencionado anteriormente el lugar más óptimo para implementar la antena fue dentro de la batería de la laptop como se muestra en la figura 8.

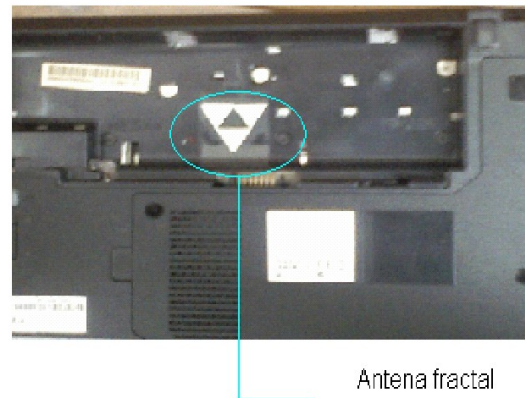


Fig. 8 Fotografía de la antena fractal implementada en la laptop

Pruebas y Resultados

Antes de realizar las pruebas correspondientes con las antenas diseñadas, se propuso una distancia de alejamiento del access point de aproximadamente 15m que es la distancia donde se hacía notable la disminución de la intensidad de señal. A continuación se muestra la curva característica de dicha disminución:

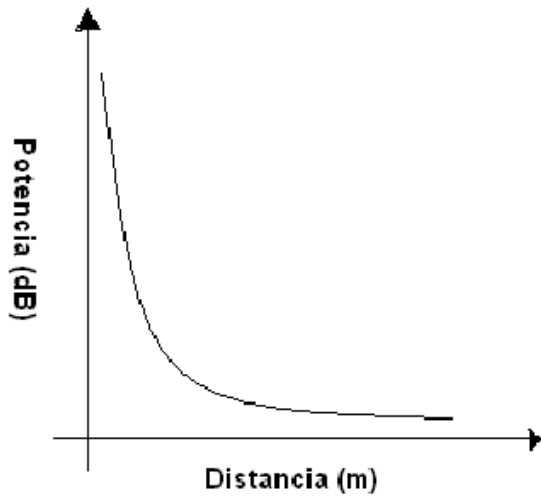


Fig. 9 Disminución de la potencia conforma a la distancia

Además cabe mencionar el clima de la Ciudad de México el día de las pruebas ya que como sabemos entre mas nublado se encuentre mayor será la atenuación de la señal



Fig. 10 Clima de la Ciudad de México en el día de la prueba

Después se midió la intensidad de señal de la red inalámbrica que lleva por nombre “Antonio” sin implementarle el complemento diseñado y los resultados obtenidos se muestran en la figura 10

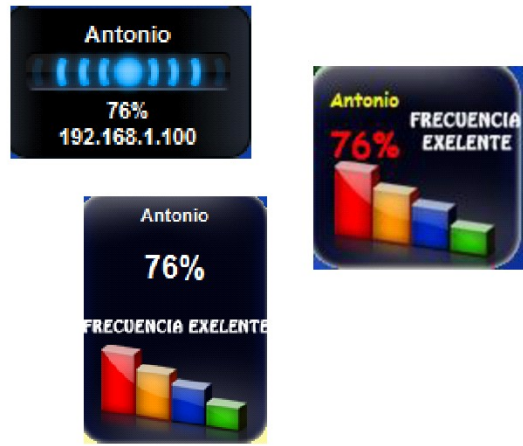


Fig. 11 Intensidad de señal de la red “Antonio” sin la antena

Por último se midieron los resultados con las antenas fractales diseñadas y esto fue lo que se obtuvo:



Fig. 12 Intensidad de señal de la red “Antonio” con la antena fractal implementada

Resultados Obtenidos

La siguiente tabla muestra la comparación de los resultados obtenidos.

Tipo de Antena	Porcentaje de señal antes de implementarla	Porcentaje de señal después de implementarla
Triángulo de Sierspinki	76%	87%
Curva de Koch	76%	87%

Conclusiones

El diseño de la antena es relativamente sencillo en cuanto a la realización de los cálculos, sólo que al momento de realizar el diseño físicamente es necesario ser muy precisos en las mediciones y en los cortes ya que tienen que ser lo más exactos posibles.

En ambos diseños el aumento fue considerable e igual. Una antena de microcinta tiene demasiadas ventajas en comparación con otros tipos de antenas que trabajan a la misma frecuencia, ya que son livianas y de poco volumen, además de fácil instalación y un diseño atractivo.

Antes de implementar la antena se deben limpiar las impurezas de la laptop con un trapo húmedo y procurar no tocar con la yema de los dedos el dieléctrico de la antena, ya que esto podría obstaculizar el desempeño de la misma.

Referencias

- [1] WAYNE, Tomasi, *Sistemas de comunicaciones electrónicas*, Prentice Hall, México, 1996
- [2] KRAUS, Jhon, *Antenas*, Mc Graw Hill
- [3] CARDAMA, COFRE, RIUS, ROMEU, BLANCH, BATALLER, *Antenas*, Alfaomega, México, 2004, pp. 110-112, 334-335
- [4] MIRANDA, José Miguel, *Ingeniería de Microondas Técnicas Experimentales*, Prentice Hall, 2002, pp. 243-250
- [5] SOSA Pedroza, Jorge Roberto, *Radiación Electromagnética y Antenas*, Limusa, pp. 107-124
- [6] SAUNDERS R., Simon, *Antenas and Propagation for Wireless Communication Systems*, Wiley, 1999, pp. 83-84
- [7]<http://antenared.com/2009/02/antenasmicrocinta-o-patch-caracteristicasbasicas/>

Classification of diabetic retinopathy using digital image treatment, HU moments and associative memories.

Maribel Bustos Mejía¹, Benjamín Luna Benoso¹,
Rolando Flores Carapía², Rosa Eunice Echeverría
Portillo², José Cruz Martínez Perales¹

¹Escuela Superior de Cómputo del IPN

²Centro de Innovación y Desarrollo Tecnológico en
Cómputo del IPN

Telephone (55) 57296000, Ext. 52031 E-mail:
jmartinezp@ipn.mx

Abstract — *This investigation shows the implementation of a system capable of identify if a patient suffers diabetic retinopathy. We used a bank of images of the vascular network retinian of patients provided by the hospital of specialties medical center La Raza of the Instituto Mexicano del Seguro Social (IMSS). Each image of the bank images were applied digital treatment of images to them, later the characteristics were extracted by means of the Hu moments and finally for the process of classification the associative memories alpha-beta were used.*

Keywords — associative memories, digital treatment of images, Hu moments.

INTRODUCTION

The diabetic retinopathy (DR) is an illness caused by the prolong exposition to the diabetic that deteriorates the sight and it can lead to total lose [1].

The DR is difficult to diagnose when it is in the first stage because the damages present in the eye are very small to perceive with the naked that is way the ophthalmology specialist used different techniques, one of this is the angiography with fluorescein [2]. The angiography fluorescein consists in inject to the patient a substance calls fluorescein and trace his trajectory into the eye through a succession photographs to take the net of vascular retinian using a digital angiograph.

The flourescein used in this study for detection DR can be provoked secondary effects on the patients [3], that way in this job we developed a system capable of detects if a patient have diabetic retinopathy through the analysis of the image of retinian vascular net to the patient this avoid the use of flourescein.

This document is organized in the next way: the section II presents the methodology with its basic concepts required to the development this job, the section III shows the experiments and results obtained and the section IV presents the conclusions

METHODOLOGY

Basic concepts

Immediately we presents a necessities definitions series to develop to this work.

Digital Treatment of Images

The digital treatment of images is responsible of manipulate two-dimensional images taking in a count the colors or shapes, it focus in images that have a set measures o values that are located in a two-dimensional space.

A digital image is a two-dimensional function $f(x, y)$ of the intensity of the light (brightness) in a point of the space, being (x, y) the coordinates of that point [4], of this way a digital image can be treated as a matrix (fig. 1)

Fig. 1 Digital image and its representation matrix

therefore it can be redefine a digital image $F_{ij} = [f_{ij}]_{m \times n}$ where $f_{ij} = f(x_i, x_j)$ for each (x_i, x_j) pixel of the image [4].

Inside the digital treatment of images it can be found the *processing and segmentation* of the images [5]. The processing of images is charge of giving them best quality of the image analyzing the density of the gray, the noise level, the brightness, the contrast, etc., between the improvement techniques of the images can be found in the *spatial filtering*. The Spatial filtering has the objective of accentuates or diminishes the features of the image, the input of this process is an image on gray scale and the output is the modify image, resulting of this operation made with the image and the filter. The filter is a representation for a spatial mask. Inside the filters we find the *Laplaciano of the Gaussiano* filters and the *Median filter*. In the other hand the segmentation of the image is a process that is in charge of the divide in small parts taking parts of a similar attributes.

Laplaciano of the Gaussiano Filter (LoG)

The *Laplaciano of the Gaussiano* filter allow detecting edges softening the image applying the second derivative on the Gaussiano filter equation, to reduce the noise sensitivity that usually LoG is applied. The following equation defines the *Laplaciano of the Gaussiano* is [4]:

$$\nabla^2 f = [f(x+1, y) + f(x-1, y) + f(x, y+1) + f(x, y-1) - 4f(x, y)] \quad (1)$$

Median Filter

The median filter replaced each pixel of the image by the pixels median of the mask, contains nearby neighbors [4]. For example if considering the fig. 2, in ascending order, the pixel values covered by the mask are: 115, 119, 120, 123, 124, 125, 126 and 150 where the median value is 124.

Fig. 2 Example of a particular case of the median filter

Hu Moments

Definition: if $r, s \in \mathbb{N}$ defined the **statistical moments as:**

$$m_{rs} = \sum_{i,j \in REG} i^r j^s \quad (2)$$

Where REG is the set of pixels within the region.

The region of a *center gravity* is defined by coordinates (\bar{i}, \bar{j}) , where

$$\bar{i} = \frac{m_{10}}{m_{00}} \quad \bar{j} = \frac{m_{01}}{m_{00}} \quad (3)$$

From the center of gravity, *central moments* are defined as:

$$\mu_{rs} = \sum_{i,j \in REG} (i - \bar{i})^r (j - \bar{j})^s \quad (4)$$

The 7 *Hu moments* are defined as follows [6]:

$$\Phi_1 = \eta_{20} + \eta_{02}$$

$$\Phi_2 = (\eta_{20} - \eta_{02})^2 + 4\eta_{11}^2$$

$$\Phi_3 = (\eta_{30} - 3\eta_{12})^2 + (3\eta_{21} - \eta_{03})^2$$

$$\Phi_4 = (\eta_{30} + \eta_{12})^2 + (\eta_{21} + \eta_{03})^2$$

$$\Phi_5 = (\eta_{30} - 3\eta_{12})(\eta_{30} + \eta_{12}) \left[(\eta_{30} + \eta_{12})^2 - 3(\eta_{21} + \eta_{03})^2 \right] + (3\eta_{21} - \eta_{03})(\eta_{21} + \eta_{03}) \left[(\eta_{30} + \eta_{12})^2 - 3(\eta_{21} + \eta_{03})^2 \right]$$

$$\Phi_6 = (\eta_{20} - \eta_{02}) \left[(\eta_{30} + \eta_{12})^2 - (\eta_{21} + \eta_{03})^2 \right] + 4\eta_{11}(\eta_{30} + \eta_{12})(\eta_{21} + \eta_{03})$$

$$\Phi_7 = (3\eta_{21} - \eta_{03})(\eta_{30} + \eta_{12}) \left[(\eta_{30} + \eta_{12})^2 - 3(\eta_{21} + \eta_{03})^2 \right] - (\eta_{30} - 3\eta_{12})(\eta_{21} + \eta_{03}) \left[(\eta_{30} + \eta_{12})^2 - 3(\eta_{21} + \eta_{03})^2 \right]$$

where:

$$\eta_{rs} = \frac{\mu_{rs}}{\mu_{00}} \quad y \quad t = \frac{r+s}{2} + 1$$

(5)

That it knows the *Hu moments* are invariant to translations, rotations and scaling.

Associative Memories

An associative memory has a primary purpose, successfully recover complete patterns from input patterns, which may be altered with ear noise, subtractive or combined [7].

x	y	$\beta(x, y)$
0	0	0
0	1	0
1	0	0
1	1	1
2	0	1
2	1	1

The associative memories operation is divided in two phases: learning phase (generation of memory) and recovery phase (memory operation). Input pattern is represented by a vector \bar{x} column and output vector by a vector \bar{y} column. Each input

pattern \bar{x} is a correspondence with a output pattern \bar{y} , the annotation for this association is similar that of an ordered pair, namely (\bar{x}, \bar{y}) [8].

The associative memory M is represented by a matrix generated of a finite set of association are known in advance and is called the *fundamental set*. If p is the cardinality of the *fundamental set*, then this is represented as [7, 8]:

$$\left\{ (\bar{x}^\mu, \bar{y}^\mu) \mid 1, 2, \dots, p \right\} \quad (6)$$

Definition: An associative memory is called auto-associative if it meets $\bar{x}^\mu = \bar{y}^\mu$ for each $\mu = 1, 2, \dots, p$. Otherwise is said to be a *hetero-associative* memory.

Definition: Are $A = \{0, 1\}$ y $B = \{0, 1, 2\}$, operators α y β are defined as follows:

$$\alpha : A \times A \rightarrow B$$

$$\beta : B \times A \rightarrow A$$

x	y	$\alpha(x, y)$
0	0	1
0	1	0
1	0	2
1	1	1

The associative memories *alfa-beta* makes use of operators α y β . The associative memories *alfa-beta max* in learning phase is defined as follows:

1. For each $\mu = 1, 2, \dots, p$ the matrix is constructed

$$[\bar{x}_\mu \vee \bar{x}_\mu] = [a_{ij}] \quad \text{with} \quad a_{ij} = \alpha(x_i^\mu, y_j^\mu) \quad (7)$$

2. Operator binary max is applied each of the matrices obtained in section

$$M = \max_{\alpha} [\bar{x}_{\mu} \vee \bar{x}_{\mu}], \quad \text{namely,}$$

$$m_{ij} = \max_{\mu=1}^p (\alpha(x_i^{\mu}, y_j^{\mu}))$$

(8)

For the recovery phase, shows a pattern \bar{x}^{ω} and operated with the memory M as follows:

$$M \min_{\beta} \bar{x}^{\omega} = [t_{ij}], \quad \text{where}$$

$$t_{ij} = \min_{j=1}^n \beta(m_{ij}, x_j^{\omega})$$

(9)

RESULTS

A. Experiments

The experiments were worked on a bank of images of the retinal vascular network of patients *provided by the hospital of specialties medical center La Raza Gaudencio González Garza of the Instituto Mexicano del Seguro Social (IMSS)*. First, each RGB image was worked in grayscales through the green plane (G) (fig. 3).

Fig. 3 Original image and grayscales

Every image was applied the *Laplaciano of the Gaussiano* filter, with edges were detected applying the second derivative on the *Gaussiano* equation filter considering the filter shown in the figure 4.

Fig. 4 Laplaciano of the Gaussiano filter

Immediately the image was segmented binarized by the threshold 50-255, leaving the segmented image as the fig.5.

Fig. 5 Segmented image through binarization 50.255

Then applied the median filter to remove unnecessary points leaving only with the required information (fig. 6).

Fig. 6 Application of the median filter

Each segmented image as in fig. 6, were derived *Hu moments* so that in this way gets the pattern that represents each image, where each input pattern represents one of the *Hu moments*. From the set of patterns obtained for each image, was built auto-associative memory *alfa-beta max*. To validate the method, we used the method of cross validation which consists in partitioning the set of known patterns in k identical blocks, of which one is for test and the $k-1$ remaining is to build the associative memory, this is repeated for each permutation of test blocks.

The result yielded by the system shows performance success rate of 95%.

The final system is to introducing the retinal vascular network image of a patient, then the system detects if the patient have o no retinopathy, in case of disease, shows a report with all patient data and hospitals where they can be attended.

CONCLUSIONS

We have been shown the theoretical fundament development of a system capable to detect if a patient suffer diabetic retinopathy. For that was made using the *digital treatment of images, Hu moments and associative alfa-beta memories*. **The proposed system shows effectiveness of performance of 95% using the method of cross validation.**

References

- M. A. Santiago, S. J. García, I. Gómez, (2008). Protocolo de Detección y Seguimiento de la Retinopatía Diabética. Medicine - Programa de Formación Médica Continuada Acreditado, Elsevier, Volumen 10, Issue 17, p. 1169-1174.
- M. Trento, M. Bajardi, E. Borgo, P. Passera, M. Maurino, R. Gibbins, (2002). Perceptions of Diabetic Retinopathy and Screening Procedures Among Diabetic People. Diabetic Medicine: a journal of the British Diabetic Association, 19 (10), p. 810-813.

- P. C. Hernández, J. J. Giralt, C. R. Simo, (2008). Treatment of diabetic retinopathy. Endocrinología y Nutrición, Elsevier, 55, p.92-98.
- R. C. González, R. E. Woods, (2002). Digital Image Processing. Segunda edición. Prentice Hall.
- R. J. Winder, P. J. Morrow, I. N. McRitchie, J. R. Bailie, P. M. Hart, (2009). Algorithms for digital image processing in diabetic retinopathy. Computerized Medical Imaging and Graphics, Volume 33, Issue 8, p. 608-622.
- J. A. Muñoz-Rodríguez, A. Asundi, R. Rodríguez-Vera, (2005). Recognition of a Light Line Pattern by Hu Moments for 3-D Reconstruction of a Rotated Object. Optics & Laser Technology, Volume 37, Issue 2, p. 131-138.
- C. Yañez-Márquez, L. P. Sánchez-Fernández, I. López-Yañez, (2006). Alpha-Beta Associative Memories for Gray Level Patterns. Lecture Notes in Computer Science, Springer Heidelberg, LNCS 3971, p. 818-823.
- [8]M. E. Acevedo-Mosqueda, C. Yañez-Márquez, I. López-Yañez, (2007). Alpha-Beta Bidirectional Associative Memories: Theory and Applications. Neural Processing Letters, 26(1), p. 1-40

Implementación de la Huella digital para el encendido de automóvil

¹Celedonio Enrique Aguilar Meza
jriosc0500@ipn.mx, ²Israel Rivera Zárate
irivera@ipn.mx,
¹ José Alahín Estrada Diego
chegue_6@hotmail.com

Resumen: Una de las preocupaciones de los habitantes de nuestro país (México) es el creciente índice de robo de automóviles, los medios actualmente de seguridad que incluyen los autos, que van desde las tradicionales llaves y bastones, hasta las llaves con código y las alarmas comunes no son suficientes para disminuir en cierta medida el problema; Por ello en el presente trabajo pretende diseñar e implementar un sistema de encendido de automóvil basado en un medio de identificación biométrica “Huella Dactilar”, que permita el uso del auto por el propietario y las personas que el autorice, con lo anterior se pretende brindar mayor seguridad para los ciudadanos y sus pertenencias.

Palabras Clave: inseguridad, automóvil, biométrica, dactilar, encendido, base de datos.

Introducción

Un impacto muy fuerte en nuestra sociedad es la inseguridad en particular el robo de automóviles de modelos recientes, las compañías productoras de esto han implementado sistemas de seguridad tradicionales basados en llaves y sistemas de alarma. Las nuevas tendencia en seguridad en los autos es la inclusión de sistemas biométricos basados en huella digita; específicamente en el sistema de encendido de el automóvil por medio de huella digital, sin tener que meter una llave o una tarjeta, logrando con ello que el dueño del automóvil (o quien el autorice) posean el único medio de arranque del móvil. El diseño de este sistema de encendido será por huella digital que trabaja por medio de escaneo y comparación de huella.

Para el arranque c motor del automóvil se usa un motor de corriente continua (conocido como marcha) que se alimenta desde la batería de acumuladores a través de de un relevador, este relevador a su vez es accionado desde el interruptor de encendido de automóvil, que para nuestro caso dicho interruptor ser controlado por el sistema de escaneo y validación de huella.

1 ESCUELA SUPERIOR DE INGENIERÍA
MECÁNICA Y ELÉCTRICA UNIDAD
CULHUACAN Av.Santa Ana #1000 Col. San
Francisco Culhuacan,
Deleg. Coyoacán C.P. 04430, México D.F Tel.
56242000 ext. 73100
2 CENTRO DE INNOVACION Y
DESARROLLO TECNOLÓGICO. Unidad
Profesional Adolfo López Mateos
Av. Juan de Dios Bátiz S/N y Miguel Othón de
Mendizabal Tel. 56242000 ext. 52535

El sistema de encendido por medio de huella propuesto, se planea par ser montado en los automóviles de modelos recientes como un aditamento extra en el panel del conductor.

Fundamentos de la Huella Digital

Los seres humanos poseen medios de identificación integrados únicos e irrepetibles, por citar algunos se tiene la huella digital, el iris del ojo, el ADN; el mas accesible y económico es el de huella. Las personas tienen “valles y crestas” de piel en la punta de los dedos, estos valles y crestas se forman por una combinación de factores genéticos y ambientales aleatorios, lo que define una huella única e irrepetible. El principal uso de la huella digital es identificar de manera exacta y única a una persona; certificando la autenticidad de la persona de manera única e inconfundible mediante un dispositivo electrónico de captura de huella y de un programa que realiza la verificación.



Figura no. 1

Tipos los Lectores de Huella Digital.

El lector de huella digital lleva a cabo dos tareas, la primera es obtener una imagen de la huella y

segundo comparar el patrón de valles y crestas de dicha imagen, con los patrones de las huellas que se tienen almacenadas. Los métodos principales de obtener una imagen de huella digital son por lectura óptica o lectura de capacitancia.

El Lector Óptico funciona con un dispositivo CCD (Charged Coupled Device), que tiene un arreglo de diodos sensibles a la luz que genera una señal eléctrica en respuesta a fotones de luz que es reflejada, cada diodo graba un píxel o un pequeño punto que representa la luz que es reflejada y colectivamente la luz y perfiles oscuros forman una imagen de la huella leída. El CCD genera una imagen invertida del dedo, con aéreas mas oscuras que representan mas luz reflejada (los valles entre las crestas). Antes de comparar la información obtenida contra la almacenada el procesador del lector se asegura que el CCD ha capturado una imagen clara, verificando la oscuridad promedio de los pixeles, o los valores generales en una pequeña muestra, y rechaza la lectura si la imagen general es demasiado oscura o demasiado clara.

El Lector de Capacitancia de huella digital, como los ópticos, genera una imagen de las crestas y valles que conforman la huella, pero en vez de hacerlo con luz, los capacitores utilizan corriente eléctrica.

El sensor capacitivo (figura no. 2) está hecho de uno o más chips que contienen un arreglo de pequeñas celdas. Cada celda incluye dos placas conductoras, cubiertas con una capa aislante.

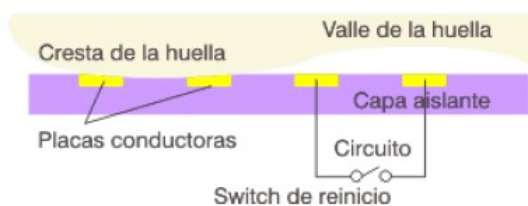


Figura no. 2 Sensor Capacitivo.

Las celdas son más pequeñas que el ancho de una cresta del dedo. El sensor es conectado a un integrador, un circuito eléctrico construido sobre la base de un amplificador operacional inversor que altera un flujo de corriente. La alteración se basa en el voltaje relativo de dos fuentes, llamado la terminal inversora y el terminal no-inversora es conectada a tierra, y la terminal inversora es conectada a una fuente de voltaje de referencia y un bucle de retroalimentación que incluye las dos placas conductoras, que

funcionan como un capacitor, esto es, un componente que puede almacenar una carga. La superficie del dedo actúa como una tercera placa capacitadora, se para por las capas aislantes en la estructura de la celda y, en el caso de los valles de la huella, una bolsa de aire.

Al variar la distancia entre las placas capacitadoras (moviendo el dedo mas cerca o mas lejos de las placas conductoras), se cambia la capacitancia (o habilidad para almacenar una carga) total del capacitor. Gracias a esta cualidad, el capacitor en una celda bajo una cresta tendrá una capacitancia más grande que el capacitor en una celda bajo un valle. Ya que la distancia al dedo altera la capacitancia, la cresta del dedo resultara en una salida de voltaje diferente a la del valle de un dedo.

El procesador de lector lee esta salida del voltaje y determina si es característico de una cresta o un valle. Al leer cada celda en el arreglo de sensores, el procesador puede construir una imagen de la huella, similar a la imagen capturada por el óptico. Las ventajas de un lector capacitivo es que requiere una verdadera forma de huella digital y no solo un patrón de luz y oscuridad que haga la impresión visual de una huella digital. Esto hace que el sistema sea más difícil de engañar. Adicionalmente, al usar unos chips semiconductor en vez de una unidad CCD, los lectores capacitivos tienden hacer mas compacto que los ópticos.

Análisis de la Huella

La pantalla de los lectores de huella digital típicamente empalma varias imágenes de huellas digitales para encontrar una que corresponda. En realidad, este no es un modo practico para encontrar las huellas digitales,. Una imagen borrosa puede hacer que don imágenes de la misma huella se vean bastante diferentes, así que raramente se podrá obtener un empalme perfecto. Adicionalmente, utilizar la imagen completa de la huella digital en un análisis comparativo utiliza muchos recursos del procesador, y además hace más sencillo robar los datos impresos de la huella de alguien.

En vez de esto, la mayoría de los lectores comparan rasgos específicos de las huellas digitales, generalmente conocidos como minutiae. Típicamente, los investigadores humanos y computadoras se concentran en puntos donde las líneas de las crestas terminan o donde se separan en dos (bifurcaciones).

Colectivamente estos y otros rasgos distintivos se llaman típicos.

El software del sistema de lector utiliza algoritmo complejos para reconocer y analizar estas minutiae. La idea básica es medir las posiciones relativas de la minutiae. Una manera simple de pensar en esto es considerar las figuras que varios minutiae forman cuando dibuja líneas rectas entre ellas. Si dos imágenes tienen tres terminaciones de crestas y dos bifurcaciones formando la misma figura dentro de la misma dimensión, hay una gran posibilidad de que sean de la misma persona.

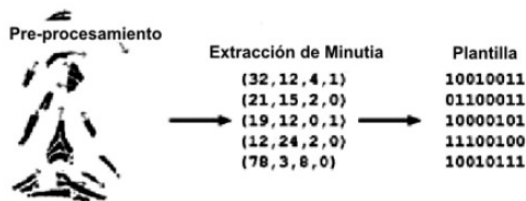


Figura no. 3 Procesamiento de la Señal

Para obtener una coincidencia, el sistema del lector no necesita encontrar el patrón entero de minutiae en la muestra y en la imagen almacenada simplemente debe encontrar un número suficiente de patrones de minutiae que ambas imágenes tengan en común. El número exacto varía de acuerdo a la programación de lector.

Ventaja y Desventajas de la Huella Digital.

Ventajas generales.

Las ventajas de un sistema biométrico de huella digital son que los atributos físicos de una persona suelen ser difíciles de facilitar, uno no puede adivinar una huella digital como adivina un password, no puede perder sus huellas digitales como pierde una llave y no puede olvidar sus huellas digitales, como puede olvidar un password.

Para hacer los sistemas de seguridad más confiables, es una buena idea combinar el análisis biométrico con un medio convencional de identificación, como un password o una tarjeta. Existen lectores de huella que además pueden verificar una tarjeta inteligente, en donde se almacena la huella digital del usuario. El lector corteja que la huella codificada en la tarjeta sea la misma que se este poniendo sobre

el lector, proporcionando un grado mayor de seguridad y eliminando las limitaciones de espacio de almacenamiento de huellas en un servidor, pues se pueden emitir credenciales con huellas codificadas de manera infinita.

Cada día se implementan mas y mas nuevas soluciones con lectores de huella digital, por lo que un futuro cercano será una tecnología utilizada por una gran proporción de la gente. Esto sin duda hará que el intento de robo de algún bien o suplantación de un individuo sea muy difícil de lograr, Al ser usado varios factores para la identificación de una persona.

Desventajas.

El proceso de autenticación requiere de una clave y de una huella digital.

La huella capturada se compara con la que este registrada en la base de datos para saber si es "autentica" o igual.

El proceso de identificación de huella digital solo requiere de la huella digital que es identificada de entre otras directamente de una base de datos, aunque podemos preguntarnos, si tiene limite la huella digital para identificar personal.

¡Realmente existen personas sin huellas digitales; estas personas generalmente trabajan con materiales abrasivos como es el caso del personal de construcción que esta en contacto directo con cemento, arena, etc. O personas que utilizan químicos muy fuertes.

Introducción al Relevador

En la figura no. 4 se muestra de una forma mas abstracta un relevador. Un símbolo de un circuito, con el cual podemos realizar distintas operaciones,

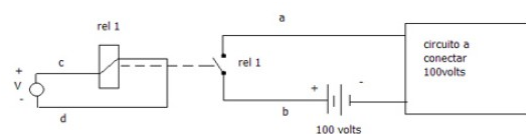


Figura no. 4 Circuito Eléctrico del Relevador.

Como la de conectar una batería de 100 volts a un sistema, por ejemplo un motor, que hace circular una corriente de un ampere, por ejemplo por los contactos A y B si el relevador actúa con seis volts y por la bobina del mismo circula 0.1 ampere, estamos obteniendo una ganancia de potencia de $100 \text{ watts} / 0.6 \text{ watts} = 166.6$, esta ganancia es grande, pero tiene la limitación que la transferencia es no lineal, la misma operación realizada con algún sistema lineal, hace que el mismo tenga dimensiones mas grandes en comparación con un relevador, además de ser mas complejo y caro pero a veces no tenemos mas opción que instalar en nuestro sistema un elemento que tenga una transferencia lineal.

Encendido del Automóvil

Para el encendido del motor del automóvil se usa un motor eléctrico de corriente continua (conocido como alternador) que se alimenta desde la batería de acumuladores a través de un relevador, Este relevador a su vez se acciona desde el interruptor de encendido del automóvil.

Cuando se acciona el interruptor de arranque se alimenta con electricidad proveniente de la batería a la bobina del relevador, y este a su vez cierra dos grandes contactos en su interior alimentando el motor de arranque directamente desde la batería a través de un grueso conductor (representado con color rojo).

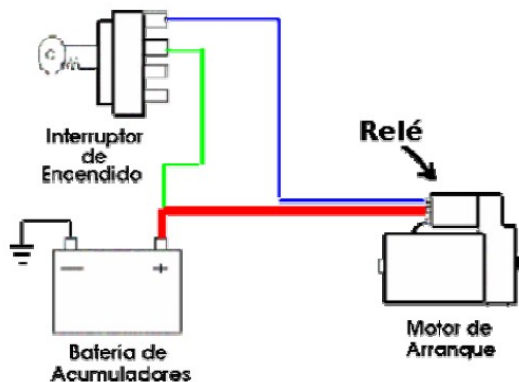


Figura no. 5 Esquema del Sistema de Encendido.

Diseño e Implementación

En la figura no. 6 se muestra el diagrama a bloques del sistema de arranque del automóvil; el cual el general inicia con la lectura y autenticación de la huella, luego se activa el relevador de pulso, que ha su vez prende los relevadores de paso de corriente; lo cual permite el paso de alimentación para el motor de cc (marcha), que finalmente enciende el auto.

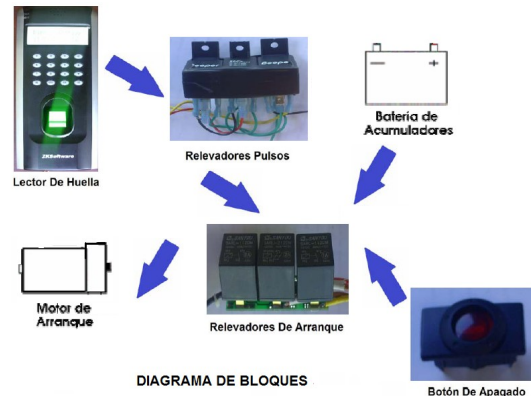


Figura no. 6 Diagrama a Bloques.

En la figura no. 7 se muestra la lógica de control del sistema de arranque del auto.

Pruebas y Resultados

Las pruebas inician con la identificación de las líneas de corriente, tierra y control, en el interruptor de encendido del automóvil (figura no. 8).

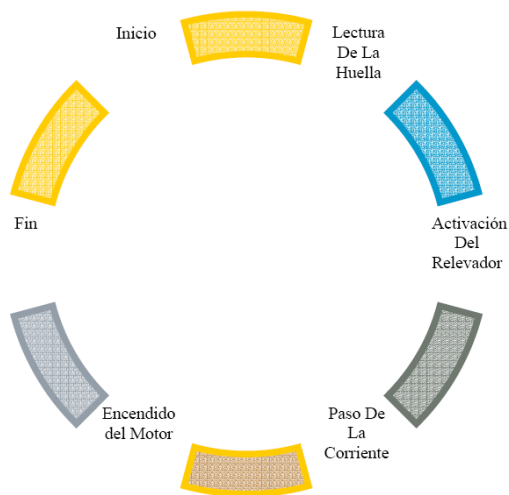


Figura no. 7 Diagrama de flujo.

Como segunda prueba se alimento el automóvil con el módulo de relevadores, que se intercala entre el interruptor de encendido y motor de cc de arranque, los cuales se activarán una vez que el lector detecte y valide la huella digital, como es mostrado en la Figura no. 9.



Figura no. 9 Conexión y alimentación de los Relevadores.

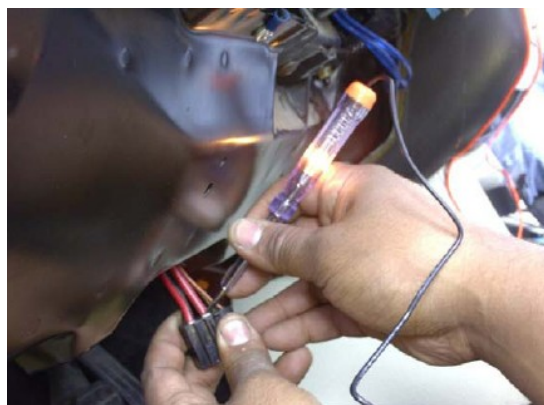


Figura no. 8 Identificación de las Líneas de Control.

Para comprobar el funcionamiento de los instrumentos de medición del auto y el sistema de encendido con el módulo implementado, se ve en la figura no. 10, donde en la parte inferior del velocímetro se ven los indicadores de encendido.



Figura no. 10 Activación del Automóvil.

Como ultimo paso, se hizo la integración de de todo el sistema, como se muestra en la Figura no. 11, la prueba consistió en alimentar el sistema eléctrico y arrancar el automóvil, los problemas que se encontraron fueron: el pulso que viene del lector de huella tarda mucho, provocando que la marcha trabaje mas tiempo de lo normal, lo cual con el tiempo puede averiar el sistema. El segundo problema fue el apagado del auto, lo cuál se solucionó agregando un botón, para el corte de alimentación del motor de cc.

Conclusiones

Durante el desarrollo de este proyecto se conocieron el funcionamiento y aplicación de los nuevos elementos como: el lector de huella digital, relevadores, diodos, etc.

Por otro lado al implementar sistema de arranque del automóvil, se logró hacerlo funcionar adecuadamente; Encontrándose el

problema del puso que viene del lector de huella tarda demasiado, provocando que la marcha trabaje mas tiempo de lo normal que al tiempo puede dañarla, otro problema es el apagado del automóvil, que para el caso se resolvió con un interruptor de apagado.



Figura no. 11. Sistema de Encendido Completo.

ITS

Intelligent Transport Systems

Sistemas Inteligentes de Transporte

Ing. Gabriel E. Gómez Cruz
Irgo Innovación
ernestogomezacruz@gmail.com

Descripción, importancia y desarrollo de los sistemas inteligentes de transporte en el mundo. Situación, beneficios y aplicaciones en México.

Definición.

[Wikipedia] El concepto de Sistemas Inteligentes de Transporte (Inglés: Intelligent Transportation Systems (ITS)) es un conjunto de soluciones tecnológicas de las telecomunicaciones y la informática (conocida como telemática) diseñadas para mejorar la operación y seguridad del transporte terrestre, tanto para carreteras urbanas y rurales, como para ferrocarriles. Este conjunto de soluciones telemáticas también pueden utilizarse en otros modos de transporte, pero su principal desarrollo ha sido orientado al transporte terrestre. Existen varias definiciones, y como es una disciplina joven, evoluciona rápidamente, lo que dificulta el consenso en una definición única.

[Sociedad Americana de Transporte Inteligente ITSA] se define a sí misma como "gente usando tecnología en transportes para salvar vidas, tiempo y dinero".

[El Departamento de Transporte de los EUA] en 1999 definió formalmente ITS: "Los sistemas inteligentes de transporte recolectan, almacenan, procesan y distribuyen información relacionada al movimiento de personas y bienes. Ejemplos incluyen los sistemas para la gestión de tránsito, la gestión del transporte público, el manejo de emergencias, la información a los usuarios, la seguridad y el control avanzado de los vehículos, las operaciones de vehículos comerciales, el pago electrónico y el cruce seguro a nivel de las líneas de ferrocarril".

[Instituto Mexicano de Transporte] "ITS es la aplicación de tecnología avanzada de captura y proceso de información, comunicaciones y control para mejorar la eficiencia y seguridad en un sistema de transporte".

[Universidad de Praga] Es una amplia variedad de tecnologías aplicadas a la transportación para hacer los sistemas más seguros, eficientes, confiables y amigables con el ambiente, sin que se tenga que, necesariamente, cambiar físicamente la infraestructura existente. Las tecnologías involucradas incluyen desde sensores y tecnologías de control, comunicaciones e informática, hasta la inclusión de sistemas de transporte, ingeniería, telecomunicaciones, computación, finanzas, e-commerce, y manufactura de automóviles, convirtiendo a los ITS en un fenómeno global emergente que beneficia a la esfera pública y privada.

Algunos ejemplos de beneficio:

Sector Público

- Control de Tráfico
- Aumento de Seguridad en el proceso de transportación
- Control de Aduanas (Contenedores, seguridad, administración, etc.)
- Control de Inmigración
- Sistemas de Peaje en Transporte Público
- Sistemas de Peaje en Carreteras.

Sector Privado

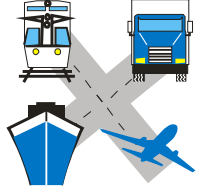
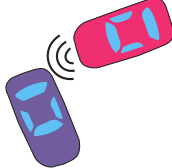

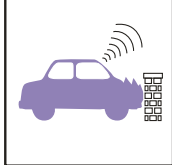
- Optimización de cadenas logísticas en el transporte multimodal
- Mayor confiabilidad
- Menores consumos de energía
- Mayor seguridad

Principales líneas de desarrollo

Para fines de simplificación, usaremos el esquema planteado en los EUA por la Administración de Investigación e Innovación en Tecnología para los Sistemas Inteligentes de Transporte (RITA):



Infraestructura Inteligente	
Control de Tránsito 	Control de Autopistas 
Seguridad Vial 	Meteorología en Caminos 
Mto. y construcción de Caminos 	Transporte Público 
Incidentes de Tránsito 	Administración de Emergencias 
Pago electrónico de peajes 	Información para viajeros 
Administración de Bases de Datos 	Distribución Física 

Transporte Multimodal	
	
Vehículos Inteligentes	
Prevención de Accidentes 	Asistencia al Conductor 
Notificación de Accidentes 	

Organizaciones Principales en el Mundo

EUA (ITSA)



Unión Europea (ERTICO)



Asia-Pacífico



ITS en México

Principales Líneas de Acción planteadas en el ámbito federal

1. **Arquitectura Nacional de Sistemas Inteligentes de Transporte.** Determinar las políticas en el sector transporte (cuya cabeza de sector es la SCT, Secretaría de Comunicaciones y Transportes) para coordinar e integrar los esfuerzos para la mejora del desempeño, a través de dotar a la infraestructura presente y futura de los elementos tecnológicos necesarios.

(Instituto Mexicano de Transporte, IMT)

Una arquitectura ITS para México deberá definir los elementos y su interrelación para asegurar que los sistemas, equipos y servicios relacionados con ITS que se desarrollen en México sean compatibles, y que puedan utilizarse en las distintas regiones del país. La arquitectura buscará coordinar las acciones de los sectores público y privado para la adecuada implantación de las tecnologías ITS en México.

Sin embargo, habrá que buscar que la arquitectura ITS sea lo suficientemente flexible para que no limite las opciones de los oferentes de servicios a los usuarios.

Una arquitectura nacional de ITS no deberá ser el diseño de un sistema. Su papel será definir el marco en el cual se desarrollen diferentes diseños de sistemas que busquen satisfacer las necesidades particulares, presentes y futuras de los usuarios, pero sin dejar de lado los conceptos de compatibilidad e interoperabilidad.

Una arquitectura ITS para México deberá definir las funciones que deben llevarse a cabo para implantar un servicio al usuario, el equipo o entidades físicas en donde llevar a cabo estas funciones, los flujos de información e interfaces entre los diferentes componentes físicos y los requerimientos de comunicación para que los flujos de información puedan realizarse. Además, definir los estándares necesarios para lograr la interoperabilidad a nivel regional, nacional e incluso internacional.

- Actores a nivel nacional
- Secretaría de Comunicaciones y Transportes (SCT)
 - Dirección General de Autotransporte Federal (DGAFF)
 - Unidad de Autopistas de Cuota (UAC)
 - Dirección General de Servicios Técnicos

- Dirección General de Carreteras Federales
- Dirección General de Conservación de Carreteras
- Dirección General de Planeación y Centros
- Aeropuertos y Servicios Auxiliares
- Dirección General de Puertos y Marina Mercante
- Dirección General de Tarifas, Transporte Ferroviario y Multimodal
- Caminos y Puentes Federales/FARAC/AMICO
- Cámara Nacional del Autotransporte de Carga (CANACAR)
- Cámara Nacional del Autotransporte de Pasajeros y Turismo (CANAPAT)
- Asociación Nacional del Transporte Privado (ANTP)
- Policía Federal
- SHCP, SAT, Administración General de Aduanas

Tabla 1

Servicios al usuario de la arquitectura ITS México listados por orden de importancia

- Servicio al usuario
- Administración del transporte público
- Información de servicios al viajero
- Información previa al viaje (peatones, conductores)
- Administración de vehículos de emergencia
- Monitoreo de seguridad a bordo del vehículo
- Procesos de administración de vehículos comerciales
- Inspección al lado del camino
- Control de tránsito
- Proveer información de ocurrencia de restricciones al tránsito
- Seguridad para el usuario del transporte público
- Servicios de pago electrónico
- Administración de flotillas comerciales
- Administración de condiciones ambientales (clima y medio ambiente)
- Administración de la demanda de viajes
- Respuesta a incidentes con materiales peligrosos

- Verificación y reducción de emisiones
 - Activación de restricciones al movimiento antes de impactos
 - Liberación electrónica de vehículos comerciales
 - Administración de carga intermodal
 - Eliminación de colisiones basada en los vehículos
 - Selección de rutas
 - Administración de incidentes y desastres
 - Apoyo al viajero en tránsito (navegación)
 - Operaciones de mantenimiento y construcción
 - Operaciones y mantenimiento
 - Reservaciones y vehículos compartidos
 - Seguridad basada en infraestructura
 - Mejoras a la seguridad basada en sensores
 - Notificación automática de emergencias y personal de seguridad
 - Transporte público personalizado
 - Sistemas de carreteras automáticas
 - Funciones de información almacenada
 - Operación automática de vehículos
2. **Automatización de cruces fronterizos.** Relacionados con sistemas inteligentes de revisión (Rayos X, Cromatógrafo de gases, Revisión en infrarrojo, sistemas aleatorios de revisión), así como sistemas de peaje.
 3. **Grupo de armonización de comunicación aplicada de corto alcance en Norteamérica.** Determinación de los estándares de radiocomunicación y telefonía en telemática para ITS.
 4. **Sistemas de peaje.** Automatización del pago en los cruces de casetas de peaje a través de sistemas de transreceptores activos en los vehículos y el uso de antenas de radio en las posiciones de peaje capaces de realizar interacción con las bases de datos bancarias.
 5. **Carretera inteligente** (interacción de la infraestructura por medio de sensores y radiocomunicación ubicados sobre la vía y los equipos ubicados en los vehículos inteligentes).
 6. **Sistemas de localización vehicular vía satélite (GPS).** Equipos de localización e información vía satélite capaces de proporcionar a los usuarios información detallada sobre la infraestructura y las facilidades disponibles vía GIS (Sistemas de Información Geográfica, asimismo brinda a los operadores del GPS, información del vehículo, la trayectoria y características de la misma.
7. **Optimización de cadenas logísticas en el transporte multimodal.** Operación de flotas vehiculares de distribución física, obteniéndose datos como tiempos de recorrido, paradas, trayectoria, velocidad y ubicación momento a momento de vehículos, y mercancías.
 8. **Centro de verificación de pesos (dinámico).** Equipos capaces de realizar la aplicación de las normas de peso y medidas en vehículos de carga, mediante el pesaje de los mismos sin detenerse.
 9. **Control de vehículos extranjeros.** Mediante un documento inteligente de ingreso de los mismos (calcomanía o tarjeta) que cuenta con un transreceptor activo o pasivo capaz de proporcionar y guardar información dirigida hacia las bases de datos de las Policías, Controles de Inmigración y Fiscales correspondientes.
 10. **Control de tránsito.** Tratar de dotar a cada una de las autoridades de tránsito de las ciudades del país de los instrumentos jurídicos, tecnológicos y de infraestructura para el mejor desempeño del tránsito vehicular en su jurisdicción.
- Principales Líneas de Acción planteadas en la Ciudad de México*
1. Sistemas Masivos de Transporte de Pasajeros
 - Sistema de Transporte Colectivo Metro
 - Metrobús
 - RTP
 2. Subsecretaría de Información e Inteligencia Policial
 - Centro Computarizado de Control Vial
 - Video Centro de Control de Seguridad y Tránsito
 - Sistema de Control de Semaforización
 - Vías de sentido horario reversible
 - Ejes Viales 5 y 6 Sur
 - Radial Río San Joaquín
 - Control de límites de velocidad vía remota a través de radar
 - Emisión y pago de infracciones vía remota con terminal portátil inteligente de agentes de tránsito
 - Consulta de infracciones vía internet
 3. Secretaría de Transporte y Vialidad
 - Sistema de emisión y control de Licencias para conducir, incluido sistema de puntaje.

- Sistema de verificación vehicular de emisiones
- Prevención de Robo de Vehículos vía GPS
- Tarjeta de circulación con transpondedor integrado.

Conclusiones.

Los ITS en el mundo marcan una nueva tendencia, globalizadora, creciente y están dando lugar al nacimiento de un nuevo enfoque y, más aún, una nueva industria. Los esfuerzos existentes tienden a integrarse y generar un bloque integrador de soluciones.

La Industria de ITS en México es incipiente y los esfuerzos existentes son aislados e insuficientes, sin embargo crean un nicho de oportunidad para la industria y tecnólogos capaces de innovar integrando soluciones existentes, y de nueva creación para adaptarse a la realidad nacional.

Referencias.

1. Wikipedia, Sistemas Inteligentes de Transporte, septiembre 18, 2010. http://es.wikipedia.org/wiki/Sistemas_inteligentes_de_transporte
2. Universidad de Praga, Checoslovaquia, Programa de Maestría en ITS 2009. Acceso septiembre 18, 2010. www.technikum-wien.at/index.php?download=8324.pdf
3. Moxa industrial system integrators, Ejemplos de sistemas remotos de its. acceso septiembre 18, 2010. http://www.moxa.com/Zones/Serial_Communication/Typical_Applications/Transportation.htm, <http://www.moxa-jp.com/modules/news/article.php?storyid=9>
4. Canada Government, Transport, Infrastructure an Communities Portfolio, *Intelligent Transportation Systems in 98 B-Line Rapid Bus Service: Advanced Technology at Work*. acceso sept 18, 2010. <http://www.tc.gc.ca/eng/programs/environment-utsp-intelligenttransportationsystems-945.htm>
5. Frost&Sullivan industrial systems, Angielina Tay, *Shanghai Demonstrating a Platform for DYNAMIC Traffic Information Services for the Beijing DYNASTY*. acceso sept 18, 2010. <http://www.frost.com/prod/servlet/market-insight-top.pag?docid=88270839>
6. United States of America, Department of Transport, Research and Innovative Technology Administration RITA, ITS overview, acceso septiembre 18, 2010. <http://www.itsoverview.its.dot.gov/>
7. Intelligent Transport Systems America, acceso septiembre 18, 2010. <http://www.itsa.org/>
8. Intelligent Transport Systems Europe acceso septiembre 18, 2010. <http://www.ertico.com/>
9. Traffic Tech is a total solutions provider of integrated systems in traffic management, intelligent transportation, parking management, security, communications and truck weigh stations, *Description of ITS services* acceso septiembre 18, 2010 http://www.traffic-tech.com/intelligent_transportation_systems.php
10. Kanagawa, Japan Police Prefecture, *Traffic Control Center*, acceso septiembre 18, 2010 <http://www.police.pref.kanagawa.jp/eng/emes/engf3001.htm>
11. RoadTraffic-Technology, The website for the road traffic industry, *Tunnels USA*, acceso septiembre 18, 2010 <http://www.roadtraffic-technology.com/>
12. Dellaware Valley Regional Planning Commission, *Transportation Operations and ITS Planning* acceso septiembre 18, 2010 <http://www.dvrpc.org/Operations/ITS.htm>
13. Red Social de ITS, acceso septiembre 18, 2010. <http://itsworld.ning.com/>
14. The United Nations University, 1996 Alan Gilbert, *The mega-city in Latin America*, acceso septiembre 18, 2010 <http://www.unu.edu/unupress/unupbooks/uu23me/uu23me00.htm#Contents>
15. Asian Development Bank, Kenzo HIROKI, Director for Infrastructure and Exploration, Cabinet Office, Japan *Using Intelligent Transport System (ITS) for Sustainable Development of Asia* acceso septiembre 18, 2010. <http://www.adb.org/Documents/Events/2009/Transport-Community-Practice/Transport-System/Intelligent-Transport-System.pdf>
16. Secretaría de Comunicaciones y Transportes, Instituto Mexicano de Transporte, Jorge A Acha Daza, Juan Carlos Espinosa Rescala *Hacia Una Arquitectura Nacional Para Los Sistemas Inteligentes De Transporte*, Sanfandila, Querétaro 2004. www.imt.mx/archivos/Publicaciones/PublicacionTecnica/pt251.pdf
17. Aldona Jarasuniene Vilnius Gediminas Technical University, Transport Research Institute, The 7th International Conference "Reliability and STATISTICS in Transportation and communication 2007" *The Estimation of Current Position Of Intelligent Transport systems (ITS) and their implementation In lithuanian road system*, acceso septiembre 18, 2010. www.tsi.lv/Research/Conference/RelStat_07.../Session_3_07.pdf
18. Gobierno del Distrito Federal, Secretaría de Seguridad Pública *Consulta de infracciones*

- de tránsito* acceso septiembre 18, 2010.
<http://www.setravi.df.gob.mx/index.jsp>
<http://www.infracciones.ssp.df.gob.mx/>
19. Gobierno del Distrito Federal, Secretaría de Seguridad Pública *Consulta de infracciones por exceso de velocidad* acceso septiembre 18, 2010
<http://www.setravi.df.gob.mx/index.jsp>
<http://portal.ssp.df.gob.mx/Portal/Radares/P-lacasDetectadoslist.aspx?>
 20. Gobierno del Distrito Federal, Secretaría de Transporte y Vialidad *Consulta de puntos en Licencia de Manejo* acceso septiembre 18, 2010.
<http://www.setravi.df.gob.mx/index.jsp>
 21. Gobierno del Distrito Federal, Secretaría de Seguridad Pública *Consulta de alerta vial*, acceso septiembre 18, 2010.
<http://www.setravi.df.gob.mx/index.jsp>

CINEMATICA Y DINÁMICA DE LA MARCHA HUMANA

Sánchez Cristo A. F.1 ,Velasco Toledo N. F.2 ,
Niño Suarez P. A.3

1 Investigador Universidad Militar Nueva Granada,
Colombia, afelipesc@gmail.com

2 Docente Universidad Militar Nueva Granada,
Colombia

3 Docente Universidad Militar Nueva Granada,
Colombia

INTRODUCCIÓN

Llevar a cabo ciertas actividades laborales exige la manipulación y transporte de cargas pesadas por parte de los operarios, un ejemplo particular de esta situación aparece en las operaciones militares donde el equipo de campaña puede pesar cerca de 40 kilogramos. Esta pesada carga disminuye el rendimiento de las tropas en sus actividades operativas, además aumenta el riesgo de sufrir lesiones en el sistema musculoesquelético. Dentro del grupo de investigación Davinci de la Universidad Militar Nueva Granada, se tiene un particular interés por desarrollar un exoesqueleto que permita al operador manipular y transportar cargas de forma manual dentro de su ambiente natural de desempeño.

Para lograr este desarrollo se debe conocer como es el comportamiento de la marcha humana, cuales son los torques necesarios para lograr un movimiento suave y continuo. Además es necesario entender como evolucionan estas fuerzas a lo largo del proceso de dar un paso. Debido a que el desarrollo del exoesqueleto es para potenciar el movimiento y aliviar las cargas que en algún momento se puedan estar soportando, es evidente que se debe tener la certeza de como se ve reflejada esta carga externa sobre las diferentes articulaciones de los miembros inferiores humanos. Este trabajo entonces esta enfocado en obtener una caracterización cinemática y dinámica de la marcha humana para lograr su entendimiento, tanto estáticamente como en movimiento, sin tener en cuenta este peso extra. De esta manera se aportan datos necesarios para el diseño en tres

dimensiones del exoesqueleto, el cual el Grupo de investigación se encuentra desarrollando.

El documento está dividido en 4 partes, en la primera se comentan algunos trabajos que motivan la realización de este.

La segunda sección expone la forma como se organizó la información para iniciar el modelo y los recursos (software) utilizados, el tercer capítulo presenta los resultados obtenidos y finalmente las conclusiones del trabajo realizado.

II. MOTIVACIÓN

La marcha humana es un evento de gran complejidad que tiene su origen en el sistema nervioso central y cuenta con una amplia variedad de mecanismos de retroalimentación, el mismo sistema que permite caminar a una persona es el encargado de que esta pueda desempeñar otra serie de actividades tales como correr, saltar y transportar objetos de diferente tamaño y peso, entre otras acciones. Para cada una de las actividades mencionadas el sistema musculoesquelético es capaz de adaptarse buscando optimizar los recursos energéticos, además de minimizar el riesgo de lesionar sus delicados componentes. Gracias al aumento en la capacidad de las computadoras, muchas tareas que anteriormente podían parecer muy complejas hoy en día se pueden realizar fácilmente, este podría ser el caso del modelamiento de un sistema[1], [2].

El modelamiento de la marcha humana ha sido base para muchos avances tecnológicos, tal es el caso de los robots bípedos con forma humana, cuyo método de locomoción replica el usado por los humanos[3], [4], para esta aplicación es fundamental conocer como es el comportamiento del momento angular del cuerpo y los centros de masa, mismos que son estrictamente controlados por el sistema nervioso[5]; dicho control estricto debe replicarse en una máquina que pretenda caminar de la misma forma que lo haría una persona normal.

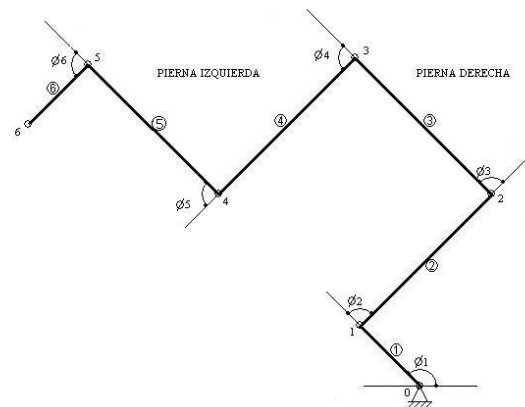
Otras aplicaciones de la simulación de la marcha incluyen la animación por computador en cinematografía[6] donde lo que interesa es el detalle minucioso de las acciones para que sean representadas fielmente por un personaje animado. La simulación de la marcha humana también es de utilidad en el estudio de anomalías

del sistema musculoesquelético[7] y el diseño de alternativas para el tratamiento de las mismas[8]. Para del diseño de un exoesqueleto es necesario conocer los movimientos que se generan durante las actividades del usuario, puesto que al tratarse de un sistema que ofrece apoyo a los movimientos del operador, el dispositivo debe ser capaz de seguir fielmente cada variación que la persona portadora haga en sus movimientos[9]. Lo anterior sugiere que antes de iniciar cualquier fase de diseño es necesario conocer de antemano el comportamiento del sistema en las diferentes situaciones a que podría ser sometido; la razón de este trabajo es iniciar una fase de modelamiento y simulación de la marcha humana, como herramienta para evaluar el desempeño de un exoesqueleto para asistencia mecánica.

III. MATERIALES Y MÉTODOS

Tradicionalmente se ha descrito el ciclo de la marcha como un proceso de dos etapas, primero está el ciclo de apoyo, el cual dura aproximadamente un 60 % del total del paso, y segundo el ciclo de balanceo, este toma un 40 %[2]. Sin embargo para este caso esta separación no es completamente útil, por lo que se decidió separar el paso en otras dos fases diferentes. La primera está determinada cuando uno de los dos pies se encuentra apoyado en el piso y mantiene la punta de los dedos fija mientras el otro pie realiza el movimiento de balanceo, esto quiere decir que es exactamente la mitad del ciclo del paso completo, la segunda es el otro medio paso. En otras palabras si en la primera fase la punta del pie derecho se encuentra fija al piso y el pie izquierdo realiza el balanceo, en la segunda la punta del pie izquierdo se encontrará fija al piso mientras que el pie derecho realizará el movimiento de balanceo.

(a) Eslabonamiento del ejemplo OpenSim



(b) Eslabonamiento del modelo propuesto

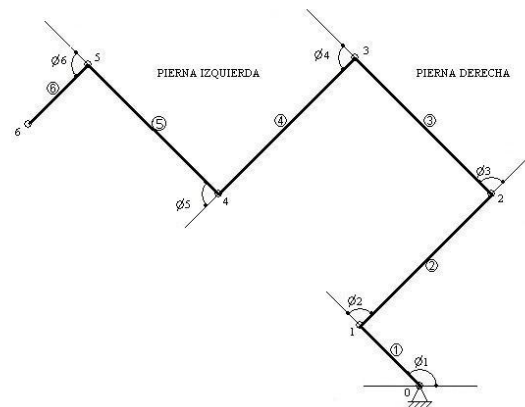


Figura 1: Eslabonamiento de los modelos

MODELO CINEMÁTICO

Esta forma de analizar el ciclo del paso se adoptó debido a que se trató a los miembros inferiores del cuerpo humano como una cadena cinemática de seis eslabones. De esta manera, se empleó la representación de Denavit-Hartenberg (D-H)[10].

Este es un método matricial que permite establecer de manera sistemática un sistema de coordenadas ligado a cada eslabón de una cadena articulada, para determinar a continuación las ecuaciones cinemáticas de la cadena completa[11], [12].

Ecuación general de la matriz de transformación homogénea

$$A_{i-1}^i = \begin{bmatrix} C\theta_i & -C\alpha_i S\theta_i & S\theta_i S\alpha_i & a_i C\theta_i \\ S\theta_i & C\alpha_i C\theta_i & -S\alpha_i C\theta_i & a_i S\theta_i \\ 0 & S\alpha_i & C\alpha_i & d_i \\ 0 & 0 & 0 & 1 \end{bmatrix} \quad (1)$$

donde θ , α , a y d son los parámetros estructurales del sistema para cada articulación.. Para la aplicación del método a este caso en particular, se definió como marco de referencia general al sistema de coordenadas con origen en la punta del pie que se encuentra fijo al piso y como eslabón final la del otro pie (ver fig 1b).

V. GENERACIÓN DE CURVAS DE MOVIMIENTO

Para realizar la simulación usando el modelo propuesto, es necesario contar con datos que indiquen la posición de los eslabones en cada instante de tiempo, para ello dichos datos se obtuvieron a partir de un ejemplo desarrollado en un software de código abierto llamado OpenSim [13], sin embargo en ese ejemplo el sistema de referencia para el origen se encuentra ubicado en la cadera (ver Fig. 1a), por tal razón fue necesario encontrar una transformación que permitió llevar los datos obtenidos del programa al modelo descrito en la sección anterior.

Una vez obtenidos los valores de posición angular para cada eslabón en cada instante de tiempo dentro del modelo cinemático propuesto, y con los datos obtenidos se elaboró un programa en MatLab para obtener las ecuaciones de estos movimientos con ayuda del ToolBox Curve Fitting y se obtuvo una función de la forma

Dichas funciones obtenidas fueron derivadas dos veces sucesivamente con respecto al tiempo, para obtener una función para la velocidad angular y otra para la aceleración angular respectivamente para cada eslabón, con estos resultados ahora es posible obtener cuantos valores se desee dentro del intervalo de tiempo bajo estudio, garantizando que se trata de curvas suaves.

VI.

MODELO DINÁMICO

Para realizar el modelo dinámico se empleó el algoritmo de Euler-Lagrange[14], el cual es una serie de pasos, que aunque

necesita de un gasto computacional considerable, y posee información redundante, conlleva a una expresión muy bien estructurada del modelo dinámico de las cadenas cinemáticas de varios eslabones. El vector de torques está definido por la siguiente ecuación

$$\tau = Dq + H + C$$

..

(3) donde D es la matriz de inercias, H es la matriz de Coriolis, C es la matriz de gravedades.

Este método es matricial y utiliza la cinemática de la cadena anteriormente expuesta, lo que resulta ser una ventaja para lograr el entendimiento completo del sistema. Para la obtención del modelo dinámico se partió de la representación D-H para el modelo propuesto, de tal forma que los datos obtenidos de manera computacional son ampliamente utilizados en esta parte del proceso. Se realizaron simulaciones en Matlab donde

se logró obtener el vector de torques para el sistema. Para encontrar los momentos de inercia se empleó una técnica muy común y es aproximar la forma del muslo y la pantorrilla a cilindros con densidad uniforme, de esta misma manera el pie se representa como una pirámide, y debido a que se está trabajando sobre un plano los centroides únicamente poseen componentes X e Y , así pues se simplifica de manera drástica el cálculo del modelo dinámico. Para obtener las masas de cada uno de los eslabones se emplearon las ecuaciones obtenidas

por [1] estas son (ver ecuaciones 4, 5 y 6)

$$M_m = 0,1032(M_t) + 12,76(L_m)(C_m)^2 - 1,023 \quad (4)$$

$$M_p = 0,026(M_t) + 31,33(L_p)(C_p)^2 + 0,016 \quad (5)$$

$$M_f = 0,0083(M_t) + 254,5(A_m)(h_f)(L_f)^2 - 0,065$$

donde

M_m corresponde a la Masa del muslo

M_p corresponde a la Masa de la pantorrilla

M_f corresponde a la Masa del pie

Mt corresponde a la Masa total del cuerpo
Lm corresponde a la Longitud del muslo
Cm corresponde a la Circunferencia del musl

$$f(x) = a_0 + \sum_{i=1}^n a_i \cos(n\omega x) + b_i \sin(n\omega x) \quad (2)$$